Human REV3L: Expression and Protein Interaction Studies

By

Gregory N. Gan

B.S. Biology, Tufts University, Boston MA, 1998

Submitted to the Graduate Faculty of

the University of Pittsburgh School of Medicine

in partial fulfillment of the requirements for the degree of

Doctor of Philosophy

University of Pittsburgh

2007

UNIVERSITY OF PITTSBURGH

FACULTY OF THE SCHOOL OF MEDICINE

This dissertation was presented

by

Gregory N. Gan

It was defended on August 14th, 2007 and approved by

Committee Chairperson: Donald B. DeFranco, Ph.D.
Professor, Department of Pharmacology

Laura Niedernhofer, M.D./Ph.D.
Assistant Professor, Department of Molecular Genetics and Biochemistry

Richard A. Steinman, M.D./Ph.D.
Associate Professor, Department of Medicine

Lin Zhang, Ph.D.
Assistant Professor, Department of Pharmacology

Dissertation Advisor: Richard D. Wood, Ph.D.
Professor, Department of Pharmacology

Forward

"Doing your Ph.D. is like playing the stock market. It has its ups and downs, but if you stick with it, in the end your investment pays off."

Dedicated to my wife and family

Christine, Grace, Anthony and Pin Pin Gan

Acknowledgements

The accomplishment of this dissertation would not have been possible without the time, assistance and support of so many individuals. First, I would like to thank my mentor, Dr. Richard Wood. I remember the excitement and the passion for science I felt from Rick when I was still searching for a thesis lab. His love for science was infectious and inspiring for a young graduate student. He has provided me with scientific guidance, mentorship and the necessary skills so that I may be successful as I begin the next phase of my training. Thanks, also, to the members of the Wood lab: Dr. Mineaki Seki, Dr. Kei-ichi Takata, Drs. Birgitte and John Wittschieben, Vera Roginskaya, Vaishali Patil, Karen Zima, Veronika Glushets, Sharon Shung, Jamie Moroco, and Jenny Kim. I want to especially thank Birgitte and John, two outstanding mentors who provided their time, training, endless scientific discussions, and friendship. To my thesis committee, Drs. Don DeFranco, Laura Niedernhofer, Richard Steinman, and Lin Zhang, for their suggestions, criticisms and support throughout this thesis. To Andria Robinson for her help with organ necropsy and to Cornelia Smith for assistance and training in regards to tissue sectioning. To my amazing friends who have helped me throughout graduate school and in particular, Jen Johnson and Fran Fletcher, for all their food, friendship and support throughout this entire dissertation. To my wife's family, John, Dorothy, Joanne, and Tony White for their endless encouragement and support. To my brother Anthony and my sister Grace for their inspiration, love and for keeping me grounded. To my late father, Dr. John Gan, who has always been a source of inner strength and a wonderful role model. To my mother, Pin Pin, who always believed in me and never once doubted that I could accomplish anything I set my mind to.

Finally, to my wife Dr. Christine Gan. She has been my best friend and confidant for so long. Her love, support (both at home and in the lab), her mind and the way she conducts herself is a constant inspiration to me and reminds me every day how lucky I am. Thanks for all your help throughout this endeavor!

Greg Gan

September 2007

Human REV3L: Expression and Protein Interaction Studies

Gregory N. Gan, Ph.D.

University of Pittsburgh, 2007

REV3L is a specialized DNA polymerase essential for DNA damage-induced mutagenesis and for the ability of cells to tolerate DNA damage. Our understanding of REV3L biochemistry stems predominantly from studies done with the budding yeast homolog, Rev3. Yeast DNA polymerase zeta consists of two proteins, Rev3, the catalytic subunit, and Rev7, an accessory factor which enhances the activity of Rev3, *in vitro*. Yeast Rev1 acts as a scaffold by associating with Polymerase zeta and enhances its translesion bypass activity on a mismatch primer template. Because of the large size of the mammalian *REV3L* cDNA (10.6 kbp) and protein (353 kDa), work in this field has focused solely on functional genetic studies associated with disruption or knockdown of the gene. Loss of REV3L causes embryonic lethality in mice and leads to progressive chromosomal instability in *Rev3L* disrupted cell lines. In the developing mouse embryo, *Rev3L* transcript is found in all tissues. However, its expression pattern at the cellular level in the adult mouse has not been examined. Determining the protein interactions of REV3L will provide a better understanding of how the protein functions at the molecular level. In addition, elucidating how Rev3L is expressed and regulated in mammalian cells will indicate what role it may play in tissues of the adult organism and why it is essential for life.

In order to study human REV3L biochemistry, this project focused on cloning, expressing, purifying and detecting full-length human REV3L protein. Human REV3L was hypothesized to interact with REV1 and/or REV7 based on knowledge about te yeast homologs. Furthermore, using a *REV3L lacZ* expression mouse model, the expression of REV3L in mouse

organs containing proliferative cells was characterized. It was hypothesized that organs with highly proliferative tissue require *REV3L*.

First, the results of immunoprecipitation studies demonstrated that full-length human REV3L interacts with REV1, but does not interact with REV7 in a DNA damage independent fashion. Preliminary analysis of deletion mutants indicates that the C-terminal domain of REV1 is required for the protein-protein interaction. Secondly, REV1 and REV3L are ubiquitinated in a DNA damage independent fashion and this covalent modification is not required for REV1-REV3L interaction. Finally, *REV3L* expression in mice is highest in testis, cardiac tissue and the smooth musculature of lung and intestines and low in lymphoid tissues. These sites of expression suggest that *REV3L* may be important for highly oxidative tissue compared to proliferative tissue.

In summary, this dissertation provides insight on human REV3L's protein-protein interaction with REV1 and REV7; their post-translational modification, and tissue-specific expression pattern in the adult mouse.

Table of Contents

TITLE i

FORWARD iii

ACKNOWLEDGEMENTS iv

ABSTRACT v

TABLE OF CONTENTS vii

LIST OF TABLES xiii

LIST OF FIGURES xiv

1.0 **INTRODUCTION** 1

1.1 PREFACE 1

1.2 MUTAGENESIS AND DNA DAMAGE BYPASS 2

1.3 THE ROLE OF RAD6-RAD18 IN DNA MUTAGENESIS 4

1.4 YEAST REV GENETICS AND PROTEIN BIOCHEMISTRY 9

1.5 FUNCTIONAL GENETICS AND BIOCHEMISTRY OF THE INVERTEBRATE REV PROTEINS .. 14

1.6 FUNCTIONAL GENETIC STUDIES REGARDING THE AVIAN REV GENES 18

1.7 MAMMALIAN REV1, REV3L AND REV7 20

1.7.1 Functional Genetic Studies Regarding the Mammalian REV Genes 20

1.7.2 Mammalian REV Protein Biochemistry 24

1.8 THE DISSERTATION 29

2.0 **GENERATING REV3L SPECIFIC ANTIBODIES** 33

2.1 INTRODUCTION 33

2.2 METHODS 35

2.2.1 Cloning the Six REV3L Fragments for Antibody Production 35
2.2.2 Small Scale Expression of the Six REV3L Fragments for Antibody Production. 38
2.2.3 Large Scale Purification of the N-terminal and Rev7 Binding Domain Fragments for Generating an Antibody Affinity Purification Column 42
2.2.4 Screening the anti-REV3L Antibodies 46
2.2.5 Tissue Culture 47
2.2.6 Screening Subcellular Fractionated Extracts for Mammalian REV3L (Small-scale) 47
2.2.7 Screening Subcellular Fractionated Extracts for Mammalian REV3L (Large-scale) 49
2.2.8 Engineering a REV3L-HF Wild-type and Active-Site Mutant Expression Cell Line 49
2.2.9 Extracting Protein from Mouse Tissue 51
2.2.10 Knockdown of Human REV3L by shRNA 51
2.3 RESULTS 53
2.3.1 Cloning and Expression of the Six REV3L Fragments for Antibody Production 53
2.3.2 Large-Scale Purification of N-terminal and yeast Rev7 Binding Domain Fragments for use on an Affinity Purification Column 61
2.3.3 Screening the REV3L-specific Antibodies 65
2.3.4 Attempts at Detecting Mammalian REV3L in Human Cell Lines and Mouse Tissue Extracts 69
2.3.5 REV3L-HF Wild-type and Active-Site Mutant Expression Cell Line 71
2.3.6 Knockdown of Human REV3L by shRNA 75

2.4 DISCUSSION 80
2.4.1 Optimization of the Anti-REV3L Specific Antibodies for the Detection of Recombinant Human Full-length REV3L 80
2.4.2 Detection of Endogenous and Recombinant Expression of Human REV3L in Cells and the Role of shRNA on REV3L Function 81
3.0 **REV3L CLONING AND PROTEIN EXPRESSION** 84
3.1 INTRODUCTION 84
3.2 METHODS 85
3.2.1 Cloning full-length recombinant human REV3L 85
3.2.2 Cloning the REV3L Polymerase Domain Active-Site Mutant 94
3.2.3 Cloning Full-length Human REV1 96
3.2.4 Cloning Full-length Human REV7 97
3.2.5 Method for Expression and Detection of Recombinant Full-Length Human REV3L, REV1 and REV7 Using RIPA Lysis Buffer 100
3.2.6 Immunoblotting Full-length Human REV3L, REV1 and REV7 104
3.2.7 Silver Stain of Full-length Human REV3L, REV1 and REV7 106
3.2.8 DNA Polymerase Activity Assay 107
3.3 RESULTS 109
3.3.1 Expression of Recombinant Full-length Human REV3L 109
3.3.2 Expression of Recombinant Full-length Human REV1 and REV7 111
3.3.3 Testing the Influence of the 5' UTR in REV3L Expression 112
3.3.4 DNA Polymerase Activity Assay 112
3.4 DISCUSSION 119

3.4.1 Expression of Human Full-length REV3L 119
3.4.2 Expression of Human Full-length REV1 and REV7 120
3.4.3 5' UTR of Human REV3L 121
3.4.4 DNA Polymerase Activity 122
4.0 **HUMAN REV1, REV3L AND REV7 EXPRESSION AND INTERACTION STUDIES** 126
4.1 INTRODUCTION 126
4.2 METHODS 128
4.2.1 Cloning the REV1 and REV3L Fragments 128
4.2.2 Freeze-Thaw Lysis Method for REV1, REV3L, REV7 Co-immunoprecipitation 132
4.2.3 Chromatin Digestion 133
4.2.4 Co-Immunoprecipitation of REV Protein Complex 134
4.2.5 Co-transfection of HA-ubiquitin and REV1, REV3L or REV7 135
4.2.6 DNA Damage and Nocodazole Treatment of Transiently Transfected 293T Cells 135
4.2.7 Proteasome Inhibitor Treatment of Transiently Transfected 293T Cells 137
4.3 RESULTS 137
4.3.1 REV1-REV3L Protein Interaction 137
4.3.2 REV1-REV7 Protein Interaction 142
4.3.3 REV3L-REV7 Protein Interaction 147
4.3.4 Expression of REV1 and REV3L Protein Fragments 148

4.3.5 REV1 and REV3L Fragment Interaction with Full-length REV1 and REV3L.. 150
4.3.6 Ubiquitination of REV1, REV3L and REV7 152
4.4 DISCUSSION 156
4.4.1 REV1-REV3L Protein Interaction 156
4.4.2 REV1-REV7 Protein Interaction 161
4.4.3 REV3L-REV7 Protein Interaction 161
4.4.4 Ubiquitination of the REV1, REV3L and REV7 Proteins 164
5.0 ***REV3L* LACZ EXPRESSION STUDIES IN MICE** 167
5.1 INTRODUCTION 167
5.2 METHODS 169
5.2.1 *Rev3L* $^{+/-}$ *lacZ* Expression Mice 169
5.2.2 Organ Harvest from Euthanized Mice 170
5.2.3 Frozen Tissue Preparation by OCT Method 170
5.2.4 Sectioning OCT Tissue Blocks 171
5.2.5 LacZ Staining OCT Tissue Sections 171
5.3 RESULTS 173
5.3.1 Expression of *Rev3L* in the Testis 173
5.3.2 Expression of Rev3L in the Pulmonary, Cardiovascular, Gastrointestinal System..
..... 173
5.3.3 Lack of *REV3L* LacZ Expression in the Hematopoeitic System 176
5.4 DISCUSSION 183
5.4.1 *REV3L* is Expressed Throughout the Testis 183

5.4.2 *REV3L* LacZ Expression in the Pulmonary, Cardiovascular and Gastrointestinal System 184
5.4.3 Lack of *REV3L* LacZ Expression in the Hematopoeitic System 186
6.0 **CONCLUSIONS** 188
6.1 NOVEL REAGENTS FOR STUDYING HUMAN FULL-LENGTH REV3L 188
6.2 TISSUE EXPRESSION STUDIES 189
6.2.1 Rev3L Expression in the Testis 189
6.2.2 *Rev3L* Expression in the Musculature 190
6.2.3 Future Direction for the *Rev3L LacZ* Expression Mice 192
6.3 THE REV3L-REV1 PROTEIN INTERACTION 193
6.3.1 Characterizing the Domains 193
6.3.2 Future Direction Regarding the REV1-REV3L Protein Interaction Studies 196
6.3.3 Covalent Modification and Possible Regulation of the Human REV Proteins 198
6.4 CONCLUSION 200
APPENDIX 202
APPENDIX A. PCR PRIMER SEQUENCES 202
APPENDIX B. PCR PROTOCOLS 207
APPENDIX C. LYSIS BUFFERS 211
APPENDIX D. GEL PURIFICATION AND PROTEIN ANALYSIS 213
APPENDIX E. BUFFERS AND MODIFIED RIPA LYSIS BUFFER FOR POLYMERASE ACTIVITY ASSAY 217
APPENDIX F. CHEMICON SOLUTIONS FOR LACZ TISSUE STAINING 218
REFERENCES 219

List of Tables

TABLE 1. THE KNOWN DNA POLYMERASES 5

TABLE 2. MASTERLIST FOR PRIMARY AND SECONDARY ANTIBODY DILUTIONS 68

TABLE 3. MASTERLIST FOR PLASMID TRANSFECTION AND PROTEIN IMMUNOPRECIPITATION 103

List of Figures

FIGURE 1.1 MODEL ILLUSTRATING YEAST REV1-POL ZETA LESION BYPASS AT A STALLED REPLICATION FORK. 7

FIGURE 1.2 MECHANISM FOR INITIATING REPLICATION BYPASS IN *SACCHAROMYCES CEREVISIAE*. 8

FIGURE 1.3 DIAGRAM OF YEAST REV1 AND HUMAN REV1. 11

FIGURE 1.4 MODEL FOR LESION BYPASS DURING G2/M. 16

FIGURE 1.5 DIAGRAM OF YEAST REV3 AND HUMAN REV3L. 25

FIGURE 2.1 DIAGRAM ILLUSTRATING THE SIX MAJOR POLYPEPTIDE DOMAINS CHOSEN FOR IMMUNIZATION INTO CHICKENS FOR PRODUCTION OF CHICKEN ANTI-HUMAN REV3L POLYCLONAL ANTIBODIES. 37

FIGURE 2.2 EXPRESSION OF N-TERMINAL, POLYMERASE DOMAIN AND CONSERVED REGION FRAGMENTS. 55

FIGURE 2.3 ILLUSTRATION DETAILING HOW EXCISION OF PROTEIN GEL FRAGMENTS FROM A TRIS-GLYCINE GEL. 56

FIGURE 2.4 EXPRESSION OF THE REV7 BINDING DOMAIN AND ALTERNATIVE SPLICE N-TERMINAL FRAGMENTS. 57

FIGURE 2.5 EXPRESSION OF SMALL AND LARGE-SCALE REV3L C-TERMINAL DOMAIN FRAGMENT. 58

FIGURE 2.6 EXPRESSION OF LARGE-SCALE REV3L N-TERMINAL, POLYMERASE DOMAIN, ALTERNATIVE SPLICE AND REV7 BINDING DOMAIN FRAGMENTS. 60

FIGURE 2.7 ELUTION OF GEL PURIFIED N-TERMINAL FRAGMENT FROM MACERATED GEL PIECES. 62

FIGURE 2.8 ELUTED PROTEIN SAMPLE FROM FIG 2.7 CONCENTRATED ON A PALL FILTRON MACROSEP 10K FILTER. 63

FIGURE 2.9 DETERMINING THE DEGREE OF N-TERMINAL POLYPEPTIDE CONJUGATION TO THE AMINO-LINK AFFINITY COLUMN. 64

FIGURE 2.10 ANTI-REV3L SPECIFIC ANTIBODIES CAN DETECT THE POLYPEPTIDE FRAGMENTS THEY WERE GENERATED AGAINST. 66

FIGURE 2.11 DIAGRAM AND FIGURE DEMONSTRATING THE LOCATION AND RESULTS FOR TWO AFFINITY PURIFIED REV3L SPECIFIC ANTIBODIES. 67

FIGURE 2.12 IMMUNOBLOTTING FOR ENDOGENOUS HUMAN REV3L IN HUMAN FORESKIN FIBROBLASTS TREATED WITH REV3L ANTI-SENSE. 70

FIGURE 2.13 IMMUNOBLOTTING FOR ENDOGENOUS HUMAN REV3L IN RAMOS AND HELA CELL LINES. 72

FIGURE 2.14 EXAMINATION OF THREE DIFFERENT CELL LYSIS PROTOCOLS ON THE RAMOS CELL LINE. 73

FIGURE 2.15 IMMUNOBLOT ANALYSIS OF INDUCIBLE 293T-REX REV3L-HF WILD TYPE AND ACTIVE-SITE MUTANT CELLS. 74

FIGURE 2.16 SCHEMATIC DIAGRAM ILLUSTRATING THE LOCATION OF WHERE THE THREE SHRNA CONSTRUCTS ANNEAL TO IN THE REV3L CDNA. 75

FIGURE 2.17 DETERMINING ENDOGENOUS REV3L EXPRESSION IN HELA CELLS SUPPRESSED USING THREE DIFFERENT REV3L SHRNA RETROVIRUSES. 78

FIGURE 2.18 IMMUNOBLOT ANALYSIS OF REV3L SHRNA TRANSDUCED INTO AN INDUCIBLE 293T-REX REV3L-HF WILD TYPE, CLONE #9 CELL LINE. 79

FIGURE 3.1 SCHEME FOR SUBCLONING HREV3L INTO PBLUESCRIPT II KS+. 87

FIGURE 3.2 DIAGNOSTIC RESTRICTION ENZYME DIGESTION OF PBLUESCRIPT II (KS+)-HREV3L (PG2-5). 88

FIGURE 3.3 MODIFICATION OF THE 5' AND 3' REGION OF HREV3L CDNA. 90

FIGURE 3.4 SUBCLONING OF THREE MODIFIED HREV3L CDNA'S FROM PENTR1A INTO THE MAMMALIAN PTSIGN EXPRESSION VECTOR. 93

FIGURE 3.5 DIAGRAM OF TWO-STEP PCR METHOD FOR GENERATING REV3L POLYMERASE DOMAIN ACTIVE SITE MUTANT. 96

FIGURE 3.6 EXPRESSION AND DETECTION OF RECOMBINANT HUMAN REV3L PROTEIN. 100

FIGURE 3.7 EXPRESSION AND DETECTION OF HUMAN REV1-V5 AND REV7-HF. 113

FIGURE 3.8 TRANSLATION WITH AND WITHOUT THE 5' UTR OF RECOMBINANT HUMAN REV3L-FLAG PROTEIN. 114

FIGURE 3.9 EXAMINING RECOMBINANT REV3L'S CATALYTIC POLYMERASE ACTIVITY WITH REV7 AND REV1 ON AN OLIGO DT:POLY DA DNA TEMPLATE. 116

FIGURE 3.10 TESTING FOR CATALYTIC DNA POLYMERASE ACTIVITY OF RECOMBINANT REV3L WITH REV7 AND REV1 ON AN ACTIVATED CALF-THYMUS DNA TEMPLATE. 117

FIGURE 3.11 EXAMINING RECOMBINANT TESTING FOR CATALYTIC DNA POLYMERASE ACTIVITY OF RECOMBINANT REV3L WITH REV7 AND REV1 ON AN ACTIVATED CALF-THYMUS DNA TEMPLATE. 118

FIGURE 4.1 DIAGRAM OF FULL-LENGTH HUMAN REV1-V5 AND CORRESPONDING REV1 G76R BRCT POINT MUTANT AND REV1 FRAGMENTS. 129

FIGURE 4.2 DIAGRAM OF FULL-LENGTH HUMAN REV3L-HIS-FLAG (REV3L-HF) AND CORRESPONDING REV3L-HF FRAGMENTS. 130

FIGURE 4.3 INTERACTION OF FULL-LENGTH HUMAN REV1 AND REV3L BY CO-IMMUNOPRECIPITATION. 140

FIGURE 4.4 FULL-LENGTH HUMAN REV3L INTERACTS WITH REV1 WT OR REV1 G76R BRCT POINT MUTANT (REV1 MUT) BY CO-IMMUNOPRECIPITATION. 142

FIGURE 4.5 DNA DAMAGE AND ITS EFFECT ON THE HUMAN REV1-REV3L COMPLEX. 143

FIGURE 4.6 THE EFFECT OF DNA DAMAGE ON RECOMBINANT FULL-LENGTH HUMAN REV1 AND REV3L. 144

FIGURE 4.7 THE EFFECT OF UV-IRRADIATION AND NOCODAZOLE ON REV1-REV3L INTERACTION. 145

FIGURE 4.8 FULL-LENGTH HUMAN REV1 WT AND G76R BRCT POINT MUTANT INTERACTS WITH REV7 BY CO-IMMUNOPRECIPITATION. 146

FIGURE 4.9 FULL-LENGTH HUMAN REV3L DOES NOT INTERACT WITH REV7 IRRESPECTIVE OF UV DAMAGE. 147

FIGURE 4.10 EXPRESSION AND DETECTION OF REV1 G76R BRCT POINT MUTANT AND REV1 CTD FRAGMENT. 149

FIGURE 4.11 THE CTD OF REV1 INTERACTS WITH FULL-LENGTH HUMAN REV3L. 151

FIGURE 4.12 THE CTD OF REV1 INTERACTS WITH FULL-LENGTH HUMAN REV7. 152

FIGURE 4.13 UBIQUITINATION OF HUMAN REV3L. 153

FIGURE 4.14 UBIQUITINATION OF HUMAN REV1. 154

FIGURE 4.15 UBIQUITINATION OF HUMAN REV7. 155

FIGURE 5.1 *REV3L*$^{+/-}$ *LACZ* EXPRESSION IN MOUSE SEMINIFEROUS TUBULE. 174

FIGURE 5.2 *REV3L*$^{+/-}$ *LACZ* EXPRESSION IN MOUSE EPIPDIDYMUS. 175

FIGURE 5.3 *REV3L*$^{+/-}$ *LACZ* EXPRESSION IN MOUSE CARDIAC TISSUE. 177

FIGURE 5.4 *REV3L*$^{+/-}$ *LACZ* EXPRESSION IN MOUSE TERMINAL BRONCHIOLE. 178

FIGURE 5.5 *REV3L*$^{+/-}$ *LACZ* EXPRESSION IN MOUSE SMALL INTESTINE. 180

FIGURE 5.6 *REV3L*$^{+/-}$ *LACZ* EXPRESSION IN MOUSE SPLEEN. 181

FIGURE 5.7 *REV3L*$^{+/-}$ *LACZ* EXPRESSION IN THE THYMUS AND PEYER'S PATCH OF THE ILIUM.... 182

Gene and Protein Nomenclature

Rev1, Rev3, Rev7	*Saccharomyces cerevisiae* gene or protein
rev1, rev3, rev7	*Saccharomyces cerevisiae* mutant gene
mus205	*Drosophila melanogaster* gene
DmRev1, DmRev3, DmRev7	*Drosophila melanogaster* protein
Rev1, Rev3L, Rev7	mouse gene
REV1, REV3L, REV7	human gene
REV1, REV3L, REV7	mouse or human protein

Commonly Used Abbreviations

4-NQO	4-Nitroquinoline 1-oxide
AP site	Apurinic/Apyrimidinic site
BPDE	Benzo[a]pyrene Diolepoxide
BRCT	BRCA 1 C-terminal
CPD	Cyclobutane Pyrimidine Dimer
CDDP/DDP	Cisplatin
IR	Gamma Irradiation
MEF	Murine Embryonic Fibroblast
MMS	Methylmethanesulfonate
MMEJ	Microhomology Mediated End Joining
NHEJ	Non-Homologous End Joining
PAD	Polymerase Associated Domain

PCNA	Proliferating Cell Nuclear Antigen
Pol zeta	Polymerase Zeta (ζ)
SCE	Sister Chromatid Exchange
shRNA	Short Hairpin RNA
SUMO	Small Ubiquitin-like Modifier
Ub	Ubiquitin
UBM	Ubiquitin Binding Motif
UVC (254 nm)	Ultraviolet radiation
mUNG	Mammalian Uracil N-glycosylase

1.0 INTRODUCTION

1.1 Preface

This dissertation begins to examine the interaction of human REV3L with other proteins involved in the process of damage tolerance and DNA mutagenesis as well as its expression in mouse tissues. It has been shown that yeast Rev3 (the yeast homolog of human REV3L) protein interacts with yeast Rev7 and Rev1 in order to help yeast cells tolerate both endogenous and exogenous DNA damage in exchange for an increase in damage-induced mutagenesis. Our biochemical knowledge of human REV3L is very limited. However, genetic analysis of human *REV3L* indicates some conservation of function with yeast, as mammalian REV3L is important for both damage tolerance and mutagenesis. This introduction will first provide a brief discussion on DNA mutagenesis, the DNA damage bypass proteins involved, and how the damage bypass process is activated in yeast. The second section will provide background on the genetics and biochemistry of the yeast, invertebrate and vertebrate REV3L, REV1 and REV7 genes and proteins. Particular attention will focus on the three *REV* genes and their role in DNA damage tolerance and mutagenesis, the observed phenotype of the anti-sense suppressed and disrupted *REV* genes in cells, the biochemical role of Rev3 as a DNA polymerase in yeast and *Drosophila*, the potential role of Rev3 in double-strand break repair, protein interaction studies involving Rev3 and Rev1, and *Rev3L* tissue expression in adult mice. The study of human

REV3L biochemistry is important in order to gain a better understanding of both damage tolerance and mutagenesis. Both oncogenesis as well as the process of somatic hypermutation in the developing immune system are two processes where DNA mutagenesis is active. Elucidation of how these proteins interact and where they are expressed will provide insight into their function as it pertains to cancer and B-cell/antibody development.

1.2 MUTAGENESIS AND DNA DAMAGE BYPASS

DNA damage itself does not itself induce mutation. Rather, mutations are a consequence of the processing of DNA damage by DNA repair (or misrepair). For example, nucleotide misincorporation by a DNA polymerase during repair or DNA replication can generate a point mutation. This describes only one way in which mutations may arise. The process of more complex types of mutagenesis is far more complex and can involve either small scale mutations (ie point mutations, insertions or deletions) or large scale mutations (ie. gene amplification, deletion, and chromosomal translocation). The consequence of these mutations are varied and may lead to benign changes having no functional consequence on gene expression (silent mutation), or to complete loss of a gene and cellular dysfunction. Therefore, the cell must maintain genome fidelity in spite of DNA being constantly damaged by a variety of endogenous and environmental agents.

Endogenous damage is associated with normal cellular function. The consequence of being an aerobic, water-based organism is that it subjects us constantly to hydrolytic and oxidative processes that are inherent to life. Every day, each human cell experiences ~19,000

depurinations and depyrimidations which lead to the formation of apurinic/apyrimidinic (AP) sites (1). If left uncorrected, these can lead to mutations and strand breakage.

Environmental damage is defined as all other chemical and radiological sources of DNA damage which cells may be exposed to as it progresses throughout its life. For example, radiologic agents like ultraviolet radiation (UV-C 254 nm) and gamma irradiation are common sources of damage. The former causes cyclobutane pyrimidine dimers and (6-4) photoproducts which can halt DNA replication. The latter generates a large number of hydroxyl radicals capable of reacting with DNA and causing double-strand breaks. Types of chemotherapeutic chemical damage include compounds like methylmethanesulphonate (MMS) and cisplatin which react with DNA bases. MMS is a potent electrophile which alkylates DNA bases. Cisplatin is capable of simultaneously generating intrastrand and interstrand DNA crosslinks as well as crosslinking DNA to protein (1,2).

Organisms evolved sophisticated DNA repair mechanisms to remove these lesions including nucleotide excision repair, mismatch repair, recombination repair and base excision repair (2). However, DNA replication can and will occur in the presence of genomic DNA lesions. When a lesion is encountered during DNA synthesis, the replication fork is stalled by prematurely halting the replicative DNA polymerases alpha (α), delta (δ), and epsilon (ε) (3-5). A stalled replication fork that remains unrepaired can lead to fork collapse and the generation of double-strand breaks (6). Unlike the repair pathways mentioned above, DNA translesion synthesis enzymes directly bypass DNA lesions thereby allowing the cell to continue DNA replication. These evolutionarily conserved, ubiquitously expressed enzymes are called DNA translesion synthesis (bypass) polymerases. The translesion synthesis DNA polymerases include the B-family polymerase, Pol zeta (ζ), the A-family polymerase, Pol theta (θ), and the Y-family

polymerases, Pol eta (η), Pol iota (ι), Pol kappa (κ) and Rev1 (Table I). These proteins are likely to play crucial roles in certain cell types and/or at specific times during an organism's development (5). The biological signficance of these translesion synthesis polymerases is evident in xeroderma pigmentosum variant individuals who lack Pol eta. Normally, Pol eta functions to bypass thymine-thymine cyclobutane pyrimidine (CPD) dimers by correctly inserting adenines across the thymine dimer lesion during replication. Loss of Pol eta in these individuals results in diminished DNA damage tolerance to CPDs, increased mutagenesis and concomitantly, a greatly increased susceptibility to sunlight-induced skin cancers (7-9). It is postulated that another translesion synthesis polymerase(s) (perhaps Rev1 and Pol zeta) is recruited in the absence of Pol eta to bypass cyclobutane pyrimidine dimers, albeit incorrectly, thereby misincorporating a nucleotide into the genome of the cell. Based on genetic and biochemical work on Rev1 and Pol zeta from yeast, Figure 1.1 illustrates the overall understanding of how these enzymes function at a stalled replication fork.

1.3 THE ROLE OF RAD6-RAD18 IN DNA MUTAGENESIS

Because of the secondary nature of this material, much of this section has been summarized based on the following reviews and selected publications (1,10-13). Rad6 is an E2-ubiquitin conjugase while Rad18 is a single-stranded DNA-binding protein that binds Rad6. This protein complex acts by mono-ubiquitinating PCNA at Lys164 and initiates three different postreplication pathways for both mutagenic and error-free bypass of DNA lesions (Figure 1.2). Two-of-the-three pathways involve both of the translesion synthesis polymerases, Pol zeta,

which is considered to be error-prone, and Pol eta, which, depending on the template, can be either mutagenic or error-free. The functional consequence of this monoubiquitination is the direct recruitment of Pol eta to monoubiquitinated-PCNA at a stalled replication fork (14). Furthermore, Pol zeta catalytic activity was also stimulated by mono-ubiquitinated PCNA when bypassing an AP site and not by the DNA damage checkpoint clamp, Rad17-Mec3-Ddc1 (15).

Table 1. The Known DNA Polymerases

Family	Polymerase		Function
A	γ	Gamma	Mitochondrial replication
	θ	Theta	Lesion bypass, SHM
	ν	Nu	Thymine glycol bypass
B	α	Alpha	DNA replication priming
	δ	Delta	DNA replication, NER, MMR
	ε	Epsilon	
	ζ	Zeta	General Lesion bypass, SHM
X	β	Beta	Base excision repair
	λ	Lambda	Possible meiosis-associated repair
	μ	Mu	NHEJ
	TdT		Ig diversity
Y	η	Eta	CPD bypass
	ι	Iota	6-4/CPD bypass
	κ	Kappa	bulky adduct bypass
	Rev1		UV mutagenesis/dCMP loading, Scaffolding Protein

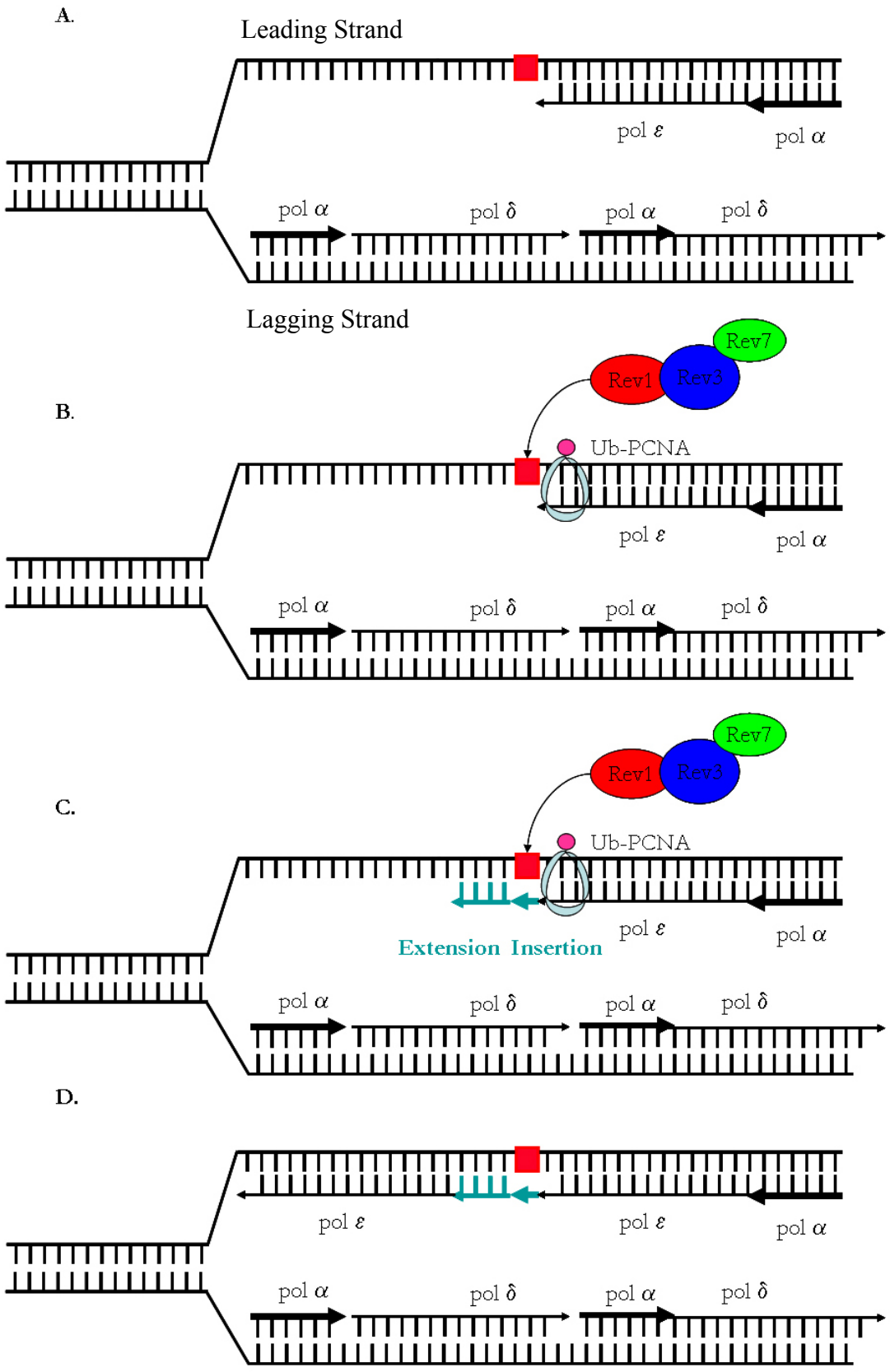
A.
Leading Strand
pol ε
pol α
pol α
pol δ
pol α
pol δ
Lagging Strand
B.
Rev7
Rev1
Rev3
Ub-PCNA
pol ε
pol α
pol α
pol δ
pol α
pol δ
C.
Rev7
Rev1
Rev3
Ub-PCNA
pol ε
pol α
Extension Insertion
pol α
pol δ
pol α
pol δ
D.
pol ε
pol ε
pol α
pol α
pol δ
pol α
pol δ

Figure 1.1 Model Illustrating Yeast Rev1-Pol Zeta Lesion Bypass at a Stalled Replication Fork.

Figures A-D represents the leading (top) and lagging (bottom) strand of a DNA replication fork during S-phase. The red square signifies a non-coding DNA lesion. A. DNA replication polymerases, Pol epsilon and delta, are responsible for replicating genomic DNA. DNA damage is often repaired before cells enter into S-phase. However, genome replication occurs in the presence of DNA damage. The DNA replication polymerases are often unable to bypass these non-coding lesions and DNA replication is halted. This stalled replication fork can potentially lead to a cytotoxic double-strand break. B. The cell responds to this stalled replication fork by activating the ubiquitin ligase, Rad6-Rad18, which mono-ubiquitinates PCNA (Ub-PCNA). Ub-PCNA presumably causes the dissociation of the DNA replication polymerases and the association of damage bypass polymerases in order to circumvent this non-coding lesion. Three proteins involved in lesion bypass are Rev1, Rev3 and Rev7. Rev3 and Rev7 heterodimerize to make the DNA polymerase, Pol zeta. Pol zeta associates with Rev1 and this trimeric complex associates to Ub-PCNA through Rev1. C. Either Rev1 or Pol zeta can *insert* a nucleotide opposite this non-coding lesion and subsequently Pol zeta can *extend* 1 – 3 nucleotides from this potentially misincorporated nucleotide functionally bypassing this damage. D. By an as yet undefined mechanism, these lesion bypass polymerases dissociate from the template, Ub-PCNA is removed and the normal DNA replication polymerases reassociate and continue genome replication. This model describes how potential mutations can become stably incorporated into an organism's genome by Rev1-Pol zeta.

Though yeast and human Pol zeta do not possess a PCNA binding domain, its binding to PCNA may be mediated through another protein – potentially a REV1-PCNA interaction (unpublished observations in human cells, Wood lab). The third pathway is considered an error-free mechanism whereby monoubiquitinated K164-PCNA becomes polyubiquitinated (Lys-63) by the ubiquitin conjugating protein complex, Rad5-Mms2-Ubc13. How the template switch pathway is error-free is poorly understood, but is presumed to utilize the newly synthesized, undamaged daughter strand as a template to bypass the lesion. Furthermore, Rad52-dependent recombinational repair is available as a potential backup mechanism in the absence of lesion bypass for error free repair of double-strand breaks. It is currently unknown what role mammalian homologous recombination plays in error free bypass, but it is predicted to function similarly to yeast. This pathway, however, is actively suppressed by both the Srs2 protein which directly inhibits Rad51-nucleoprotein filament formation and by SUMO (small-ubiquitin like modifier) modification of PCNA at Lys-164 and Lys-127 by Ubc9.

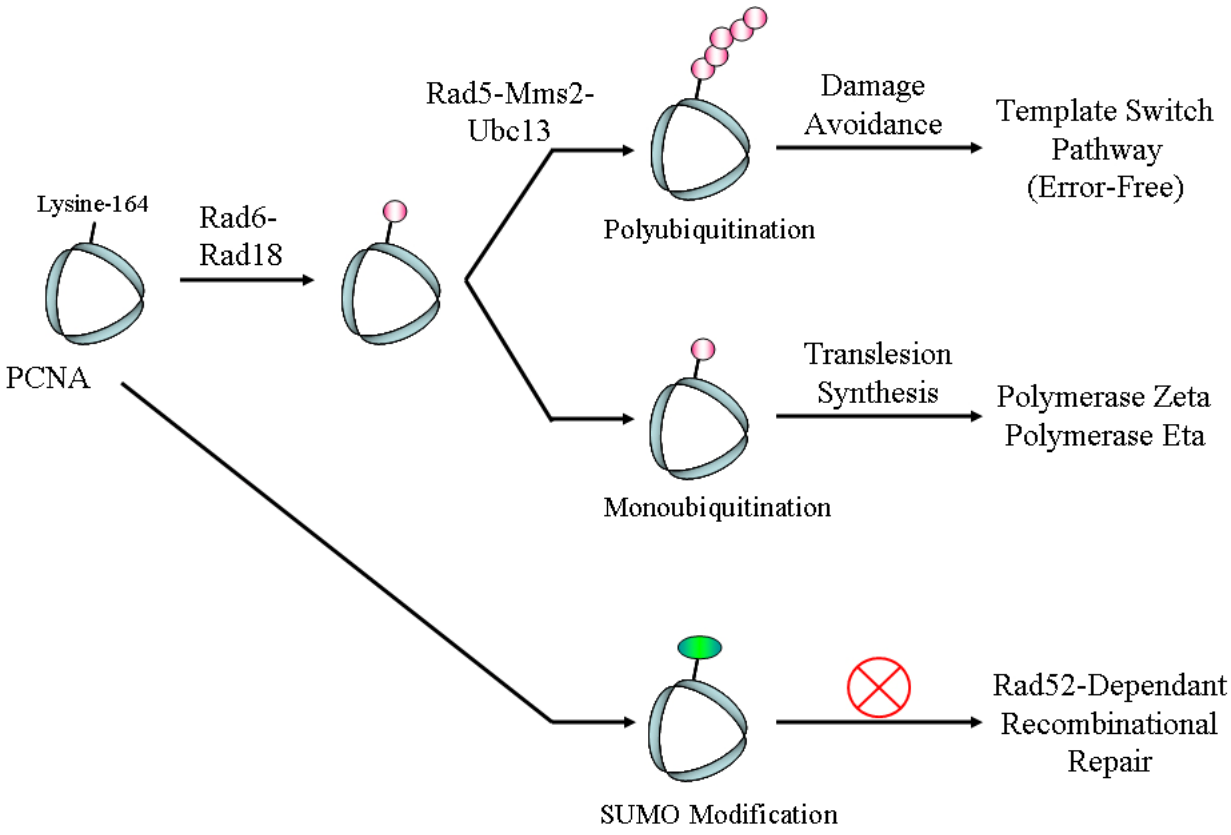

Figure 1.2 Mechanism for Initiating Replication Bypass in *Saccharomyces cerevisiae*.

The initiation of replication bypass of a non-coding lesion begins with ubiquitination of Lys-164 on PCNA by the ubiquitin ligase, Rad6-Rad18. If PCNA remains monoubiquitinated, replication bypass is directed towards translesion synthesis. Recruitment of either Polymerase zeta or eta for damage bypass (depending on the type of damage) can lead to either error prone or error free bypass of the DNA lesion. Should monoubiquitinated PCNA become further polyubiquitinated at Lys-63 of ubiquitin by the ubiquitin ligase, Rad5-Mms2-Ubc13, replication bypass is directed towards the error free template switch pathway. The error free Rad52 mediated recombinational repair pathway acts as a back-up mechanism to replication bypass. This pathway is actively inhibited in yeast by SUMO (small-ubiquitin like modifier) modification of PCNA at Lys-164 and by the Srs2 protein which directly inhibits Rad51 nucleofilament formation. This figure was adapted from the following references (11,16).

Sumoylation is thought to act as a regulatory switch on PCNA by activating it during DNA replication to prevent DNA recombination and under conditions where cells experience extreme DNA damage. In contrast, ubiquitination of PCNA is thought to occur when cells receive light to moderate damage. Generation of a K164R PCNA mutant renders Rad6-Rad18 ubiquitination

and Ubc9 sumoylation of PCNA infeasible. This mutation leads to a complete loss of damage-induced mutagenesis by Pol zeta. Interestingly though, these mutants are less sensitive to UV irradiation compared to *rad6* or *rad18* mutants. It is presumed that error-free Rad52 recombinational repair predominantly takes over in these mutants since the Rad6-Rad18 post-replication repair is inactivated.

1.4 YEAST REV GENETICS AND PROTEIN BIOCHEMISTRY

The first identification of genes associated with UV-induced mutagenesis came from studies by Lemontt and Lawrence (17-20). Their group noted that loss of the genes *rev1*, *rev3* and *rev7* conferred a "reversionless" phenotype preventing cells from undergoing UV damage-induced mutagenesis. Seminal work by Lawrence's group demonstrated that *Saccharomyces cerevisiae* (*S. cerevisiae*) DNA Polymerase zeta consisted of two subunits, Rev3, the catalytic polymerase subunit, and Rev7, an accessory protein which enhanced the polymerase's catalytic activity. Rev3 has protein homology to the B-family replicative polymerases. However, it lacks a 3' to 5' exonuclease activity. Pol zeta is not essential for viability or genomic DNA replication in yeast. Further work by Lawrence's group showed that Pol zeta was able to insert a nucleotide opposite a cyclobutane pyrimidine dimer on a synthetic oligonucleotide template and could extend from this mismatched nucleotide template by incorporating all four nucleotides into the newly synthesized strand (21). The genome replicative B-family polymerases have a significantly higher fidelity compared to Pol zeta. In comparison, Pol zeta has a higher-fidelity compared to

the Y-family polymerases. For example, Pol zeta misincorporates nucleotides opposite lesions with a frequency of 10^{-4} to 10^{-5} compared to Pol iota which misincorporates nucleotides at a much higher frequency (10^{-1} to 10^{-2}) (22). Closer examination of yeast Pol zeta's function indicated that it is capable of inserting and extending from some DNA lesions. However, in conjunction with other translesion synthesis polymerases that can insert across a DNA lesion, it was demonstrated that Pol zeta is highly efficient at extending from a mismatched primer termini *in vitro* (22-27). One protein, Rev1, has been demonstrated to interact with Pol zeta. Rev1 has been shown to insert dCMP opposite G or an AP site and Pol zeta can perform DNA extension from this potentially misincorporated nucleotide (21,26).

The two-step, two polymerase lesion bypass model suggests that two polymerases are involved in bypassing a DNA lesion – one for insertion, the other for extension. Both of the polymerases may somehow interact either directly or in conjunction with an adaptor protein. Two possible adaptor proteins include Rev1 and PCNA (proliferating cell nuclear antigen). Yeast Rev1 possesses a dCMP transferase and has been demonstrated to insert dCMP opposite G or an AP site (24) (Figure 1.3). However, its true function may be to act as a scaffolding protein and associate other translesion synthesis polymerases to DNA. PCNA is a trimeric protein ring that clamps around DNA and enhances the processivity of the genome replicative polymerases episilon and delta. This allows these polymerases to incorporate nucleotides over the large DNA template (28). It has been proposed that translesion synthesis polymerases also interact with PCNA in a "toolbelt" model; allowing for direct substitution of replicative polymerases for bypass polymerases since they share different subunits on the same PCNA (29). Error-prone or error-free postreplication repair is initiated by the mono-ubiquitination of Lys164 on PCNA by Rad6- Rad18 (30-32). It was recently discovered that the Y-family polymerases contained

conserved ubiquitin-binding motifs (UBMs) that enhanced their interaction with ubiquitinated PCNA (33,34). Loss of these UBMs not only diminished Rev1 interaction with PCNA, but also significantly diminished UV damage-induced mutagenesis and survival in yeast *in vivo* (35). Initial characterization of a yeast *rev1-1* mutant also possessed diminished UV damage-induced mutagenesis (36). Years later, the rev1-1 mutant was characterized as having a discrete point mutation at G193R which was localized to the BRCT (BRCA 1 C-terminal) domain of yeast Rev1 (37). In higher organisms, the BRCT domain was important for mediating Rev1 interaction with PCNA and the formation of nuclear foci (38,39). The G193R BRCT point mutation in Rev1 did not alter the Rev1-Pol zeta interaction (as demonstrated by immunoprecipitation). Interestingly, the Rev1 point mutant could not associate to DNA

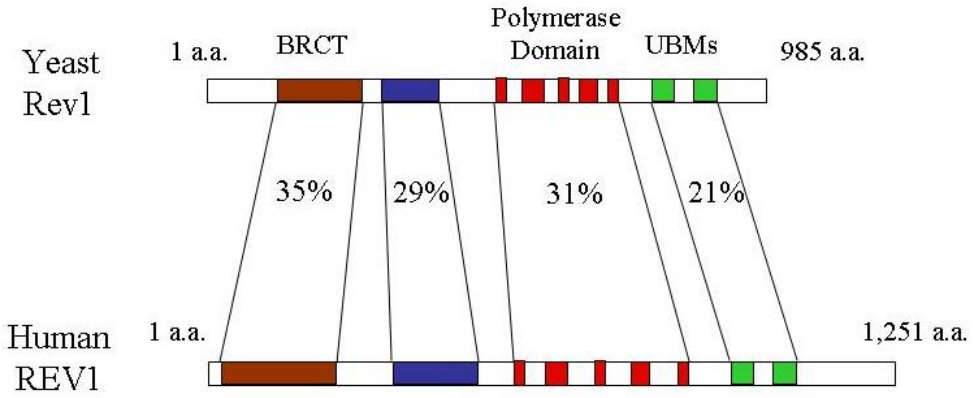

Figure 1.3 Diagram of Yeast Rev1 and Human REV1.

Four regions between the yeast and human protein share high sequence identity, the BRCT (Brca1 C-terminus) domain (35%), an internally conserved region (29%), the Polymerase Domain (31%), and the Ubiquitin Binding Motif (UBM) (21%).

double-strand breaks. Synthesizing the mammalian and yeast findings indicates that the association of Rev1 to damaged DNA is mediated through its interaction with PCNA (40). The role of the Rev1-Pol zeta complex at these double-strand breaks is under investigation. Work in yeast indicates that Rev3/Pol zeta is involved in base substitution and frame shift mutations at sites of double-strand break repair (41) and may be involved in non-homologous end-joining (NHEJ) (42) or microhomology mediated end-joining (MMEJ) (43). Findings in vertebrate cells indicate that loss of REV3 leads to diminished homologous recombination in the form of decreased sister chromatid events (44-47). Recent evidence in mammalian cells indicates that bypass of interstrand crosslink damage caused by cisplatin can be repaired either in a recombination dependent (48) or independent process (49). The recombination dependent model suggests that a double-strand break generated proximal to the interstrand crosslink enhanced homology recombinant dependant repair. A variety of proteins associated with nucleotide excision repair, mismatch repair, homologous recombination and Fanconia anemia proteins as well as REV3L were required to overcome this interstrand crosslink (48). It has been proposed that REV3L assists in the process of replicating past this bulky interstrand crosslink moiety. However, biochemical evidence to support this model is currently lacking.

Recent evidence has shown that yeast Rev1 can interact with either yeast Rev7, Rev3 or with the Pol zeta complex (Rev3-Rev7) by co-immunoprecipitation. The protein domains responsible for the Rev1-Rev3 interaction were the last 72 amino acids of the C-terminal domain of Rev1 and polymerase domain of Rev3. Rev1 can interact with Rev7 and this interaction was mediated by polymerase associated domain (PAD) of Rev1 (26,50,51). However, if Rev7 was allowed to interact with Rev1 first, this prevented later formation of a Rev1-Pol zeta complex when either Rev3 or Pol zeta was added to the mixture (26). Expression of a C-terminal domain

fragment (amino acids 747 – 985) in yeast caused a dominant-negative phenotype as demonstrated by increased sensitivity with diminished induced mutagenesis after DNA damage (51). This demonstrates the importance of the C-terminal domain of Rev1 to translesion synthesis. Therefore, the formation of this tripartite complex is likely important *in vivo*. Notably, loss of the dCMP activity of Rev1 has no functional consequence on yeast translesion synthesis (23). In contrast, the ability of yeast Rev1 to act as a scaffolding protein through interaction with Pol zeta is more important for translesion synthesis. It was shown using *in vitro* polymerase assays that the Rev1-Pol zeta complex compared to Pol zeta alone was more efficient at extension from mismatched primer termini (26). Not only does this interaction suggest a potential mechanism for how AP sites or bulky lesions could be bypassed within the cell, but it also highlights growing evidence regarding the role of Rev1 as a scaffolding protein on DNA for the translesion synthesis polymerases (52). However, whether this tripartite complex formation occurs and whether it has biological function in multi-cellular eukaryotes has yet to be determined.

Understanding how and when this tripartite complex associates may shed insight into the function of the yeast Rev1-Pol zeta complex. DNA replication polymerases that stall on a replication fork due to DNA distortions in the template or unrepaired DNA damage can lead to fork collapse and the generation of mutagenic and/or cytotoxic double-strand breaks (6). However, recent work in yeast demonstrated that replicative polymerases encountering UV lesions on the replication fork can uncouple the leading and lagging strands during DNA replication and reprime downstream of these single-strand gaps, thus allowing for continuation of DNA replication (Figure 1.4). These gaps on both strands are persistent throughout S phase and perceivably into G_2. Elimination of translesion synthesis polymerases had no effect on the

replication fork stability or resolution. Rather, it led to accumulation of more ssDNA gaps. These results indicated that translesion synthesis was occurring behind these gaps during S phase and potentially into G_2 (53). Recent work by Waters demonstrated that while yeast Rev3 and yeast Rev7 remain constituitively expressed in the cell throughout the cell cycle, yeast Rev1 was cell cycle regulated and was mostly absent throughout G1 and S and upregulated during G_2 and M. Furthermore, Rev1 protein expression was independent of DNA damage, suggesting that Rev1 function was limited predominantly to G_2/M and not S (54). Muzi-Falconi's group further demonstrated that Rev1 was phosphorylated by Mec1 in a cell cycle and DNA damage dependent fashion. However, phosphorylation independent of DNA damage and cell cycle was necessary for Rev1 to interact with chromosomes (55). The implication of these results is that formation of the yeast Rev1-Pol zeta complex may be regulated during the cell cycle by post-translational modification.

1.5 FUNCTIONAL GENETICS AND BIOCHEMISTRY OF THE INVERTEBRATE REV PROTEINS

The organism *Drosophila melanogaster* has long been used in the study of genes associated with DNA damage and repair. A search for MMS-sensitive P-insertion mutants on chromosome II revealed many candidate genes. One mutant, *mus205* closely resembled *S. cerevisiae* Rev3 by sequence homology. Lohman's group found that the *mus205* mutant was highly sensitive to UV and alkylating agents but not to ionizing radiation. They noted that treatment of *mus205* mutant

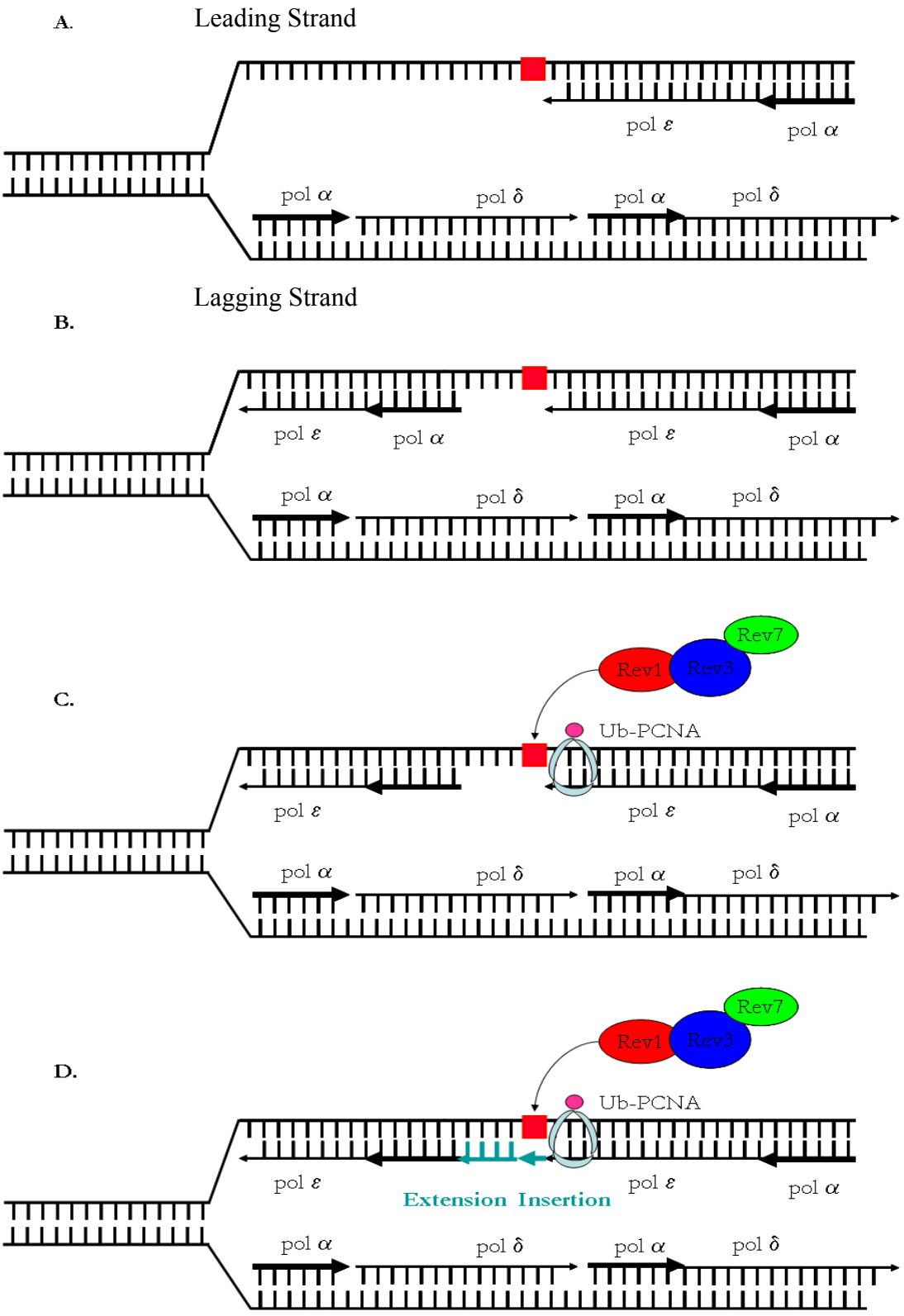
A.
Leading Strand
pol ε
pol α
pol α
pol δ
pol α
pol δ
B.
Lagging Strand
pol ε
pol α
pol ε
pol α
pol α
pol δ
pol α
pol δ
C.
Rev7
Rev1
Rev3
Ub-PCNA
pol ε
pol ε
pol α
pol α
pol δ
pol α
pol δ
D.
Rev7
Rev1
Rev3
Ub-PCNA
pol ε
Extension Insertion
pol ε
pol α
pol α
pol δ
pol α
pol δ

Figure 1.4 Model for Lesion Bypass During G2/M.

Recent evidence in yeast indicates that bypass of DNA damage may not be occurring exclusively during S-phase and may in fact be occurring during G_2/M. This figure presents an alternative model for how damage bypass can occur outside of S-phase. Figures A-D represents the leading (top) and lagging (bottom) strand of a DNA replication fork during S and G_2/M-phase. The red square signifies a non-coding DNA lesion (ie. CPD or 6-4 photoproduct). A. DNA replication polymerases, Pol epsilon and delta, are responsible for replicating genomic DNA. DNA damage is repaired before cells enter into S-phase. However, genome replication occurs in the presence of DNA damage. The DNA replication polymerases are often unable to bypass these non-coding lesions and DNA replication is temporarily halted. B. Rather than halt DNA replication, the replication machinery uncouples from the lesion and re-initiates DNA synthesis downstream of the lesion leaving a single-strand gap containing the non-coding DNA lesion behind. C. Towards the end of S-phase and at the start of G_2/M, after much of the genome has been replicated, DNA lesion bypass polymerases, Rev1 and Pol zeta are recruited to these single-strand gaps. Pol zeta-Rev1 association to this lesion is facilitated by the association of Rev1 to Ub-PCNA. D. Either Rev1 or Pol zeta inserts a nucleotide opposite the lesion. Pol zeta then extends from this misincorporated nucleotide generating a new primer from which the normal replicative polymerases can extend.

with 4-nitroquinoline 1-oxide (4-NQO), ionizing radiation or MMS resulted in no change in mutagenesic frequency. This indicates that the *Drosophila* homolog of Rev3, though highly similar in sequence identity and damage sensitivity, remained damage hypomutable (56). A possible reason for the hypomutability phenotype could be due to some cells being hypersensitive to these agents. Unable to bypass these lesions in a mutagenic fashion, sensitive cells would apoptose and be replaced by other neighboring cells (56). In order to gain a better understanding of eukaryotic Rev3 in multi-cellular organisms, Sakaguchi's group purified endogenous *D. melanogaster* (Dm)Rev3 using a DmRev1 protein-affinity column. The protein had a molecular weight of ~240 kDa and was a highly processive polymerase on a poly(dA)/oligo$(dT)_{10:1}$ template. DmRev3 had a mutation frequency comparable to Dmpol α and was almost eight times less error prone compared to rat pol β. Corresponding with the above genetic findings, DmRev3 was unable to bypass CPD's, 6-4 photoproducts or mismatched primer termini, indicating a lack of error-prone bypass activity. It was shown that yeast Rev3 interacts with yeast Rev7 to make DNA polymerase zeta. In order to determine whether DmRev3 could similarly bind DmRev7, they used a DmRev3 fragment (amino acids 858 –

1217), but not the full-length protein, and demonstrated that the DmRev3 fragment could interact with DmRev7. However, addition of DmRev7 did not enhance DmRev3's catalytic activity (57). These results corroborate Eeken's findings where DmRev3 may not be an error-prone translesion bypass polymerase involved in mismatch or bulky adduct bypass.Rather, it may play a very specialized role in *Drosophila* tolerating certain types of DNA damage, such as AP sites, in conjunction with other repair polymerases such as DmPol Beta. Sakaguchi's group further demonstrated that DmRev7 interacted with the Dm AP endonuclease 1 homologue, Rrp1, and DmRev3 to Rev7, but not Rev3 directly to Rrp1. They demonstrated that Rrp1 preferred 3'-mismatched substrates and that Rev3 could strand displace a single nucleotide gapped template. Furthermore, DmRev7 and DmRev3 mRNA levels increased in response to UV, MMS and hydrogen peroxide. They speculate that DNA damage elevates endogenous levels of Rev3 and Rev7 proteins, and that Rev7 functions by interacting with Rrp1 (and potentially Flap endonuclease 1) in order to excise an AP site via base excision repair. Rev3 would then fill the excised gap (58). In total, these results suggest that endogenously-derived *Drosophila* Rev3 is distinctly different from its yeast recombinant homolog. This functional difference between yeast and *Drosophila* Rev3 biochemistry may represent a specialized function of this protein in invertebrates. If a method could be developed to express vertebrate Rev3 protein, studies could begin to help resolve the biochemistry and cellular expression pattern of vertebrate Rev3 as well as to reconcile how these results correspond with the yeast and *Drosophila* evidence.

1.6 FUNCTIONAL GENETIC STUDIES REGARDING THE AVIAN REV GENES

When work studying avian Rev3 began, there were no reported mammalian Rev3$^{-/-}$ cell lines because disruption of mouse REV3L leads to embryonic lethality (59-62). This made it difficult to identify the essential function of REV3L in higher eukaryotes. Thus, in order to better understand the role of the vertebrate Rev genes, DT40 chicken B-cell lymphoma cells were disrupted for Rev1, Rev3 and Rev7 and their phenotype analyzed. Disruption of Rev1, Rev3, Rev7 or all three Rev genes in DT40 causes sensitivity to UV, MMS, cisplatin, ionizing radiation, tamoxifen, hydrogen peroxide and nitric oxide radicals (45,63-65). In the recombination-independent interstrand crosslink repair of psoralen and mitomycin C damage, Li's group investigated what proteins were involved in their mutagenic bypass in the absence of homologous recombination (66,67). Using Rev1 or Rev3 disrupted DT40 cells, they observed increased cell sensitivity, diminished recombination-independent interstrand crosslink repair in a luciferase reporter reactivation assay and a decreased mutational frequency at the site of bypass when REV1 and REV3L disrupted cells were treated with psoralen or mitomycin C. Although Rev1 and Rev3 may play a role in recombination independent repair of psoralen and mitomycin C interstrand crosslinks, other groups noted that agents capable of generating double-strand breaks required Rev1, Rev3 and Rev7 for repair by homologous recombination. Increases in chromosomal breaks observed during the G_2/M phase of either the single gene or triple gene disrupted DT40 cells after ionizing radiation and nitric oxide treatment indicated that Rev1, Rev3 and Rev7 were involved in double-strand break repair. In the Rev1, Rev3 and Rev7 disrupted cells, the absence of exogenous DNA damage was sufficient to increase the number of

spontaneous sister chromatid exchange events (SCE) compared to wild-type cells. However, treatment with 4-NQO almosted doubled the number of SCEs observed in all mutant cell types. However, the Rev1, Rev3 and Rev7 gene disrupted cell line displayed spontaneous SCE similar to the wild type cell line (45,65). Li's group reasoned that the lack of Rev1, Rev3 and Rev7 prevented cells from incorporating nucleotides over this large number of single-strand gaps therefore causing an increased dependence upon homologous recombination to repair these gaps. Why the Rev1, Rev3, Rev7 gene disrupted cell line does not experience more SCE events is unknown, although in this respect, it is similar to homologous recombination deficient cell lines (65). In contrast, nitric oxide treatment of Rev3 null DT40 cells leads to a minimal elevation in SCEs while a more pronounced number of SCEs are observed in wild-type cells (63). This result suggests that in DT40 cells, Rev3 and homologous recombination may both play a very important role in tolerating nitric oxide mediated damage. In summary, loss of Rev1, Rev3 and Rev7 appears to render these Rev gene-disrupted DT40 cells highly sensitive to variety of DNA damaging agents. Depending on the type of damage, Rev1 and Rev3 appear to play a role in either recombination-independent bypass with NER (psoralen or mitomycin C) or recombination dependent bypass in association with homologous recombination (ionizing radiation and 4-NQO). How the Rev proteins actually interact with these lesions and whether they interact with the NER or homologous recombination proteins need to be determined.

1.7 MAMMALIAN REV1, REV3L AND REV7

1.7.1 Functional Genetic Studies Regarding the Mammalian REV Genes

In order to understand the function of mammalian REV proteins, various anti-sense, small hairpin RNA (shRNA) and over-expressing cell lines were generated. Characterization of human REV3L anti-sense foreskin fibroblasts cells demonstrated a diminished mutation frequency after UV irradiation or benzo[*a*]pyrene diolepoxide (BPDE) compared to parental lines. Furthermore, there was no significant difference in damage sensitivity between the anti-sense and the parental lines when they were treated with either damaging agent (68). Diminished mutagenesis without a significant change in cell survival was similarly observed for a human REV1 anti-sense foreskin fibroblast cell line treated with UV irradiation (69). However, in comparison to the UV irradiated cells, cisplatin treated REV3L anti-sense cells were hypersensitive and had diminished mutagenesis compared to the parental lines (44). Notably, shRNA knockdown of REV1 and REV3L in ovarian (cell line 2008) and colorectal (HCT116) tumor cell lines yielded opposite results. These cells demonstrated more sensitivity to cisplatin as measured by clonogenic assays compared to the parental lines. Similarly, these mRNA suppressed cells had diminished spontaneous and damage-induced mutagenesis measured by development of 6-thioguanine resistance upon cisplatin treatment (46,47). Both the REV1 and REV3L knockdown cell lines demonstrate diminished extrachromosomal recombination suggesting that REV1 and REV3L play a role in homologous recombination. In contrast, overexpression of REV1 in ovarian tumor lines caused resistance to cisplatin and increased

mutagenic frequency compared to parental lines (70). These results suggest that mammalian REV3L and REV1 play a more important role in damage tolerance of certain DNA damaging agents compared to others.

Recently, a naspharyngeal carcinoma cell line expressing shRNA to suppress REV7 was developed and displayed a decrease in cisplatin induced mutagenesis, increased chromosomal instability due to diminished sister chromatid exchange, and an increase in sensitivity to cisplatin and gamma irradiation (71). The increased damage sensitivity to cisplatin and the diminished homologous recombinational repair in human REV1, REV7 and REV3L knock down cell lines suggests that all three human REV proteins are involved in the same post-replication repair pathway (44,46,71). What role these three REV proteins play in homologous recombination is currently under investigation.

Multiple groups interested in identifying the contribution of mammalian REV3L to DNA damage tolerance and somatic hypermutation attempted to generate transgenic mice. However, they discovered that disruption of the mouse *Rev3L* gene causes embryonic lethality. Embryonic death was observed between 8.5 – 12.5 days and many of the null embryos were significantly smaller compared to wild type and heterozygous embryos (59,60,72). Levels of p53 protein were elevated in response to loss of *Rev3L*,. However, disruption of *p53* was unable to rescue the *Rev3L* null embryos (73,74). These findings demonstrate that REV3L is essential for mammalian development. Compared to the wild type and heterozygous *REV3L* embryos, cells derived from the null embryos had a larger number of chromosomal aberrations (73). In order to better understand tissue distribution of Rev3L, the Wood lab engineered a knock-in to the Rev3L locus construct containing an IRES-l*acZ*-Neo^{r} cassette which enabled beta-galactosidase staining of embryonic tissue. Expression was detected throughout the developing embryo and was

particularly in the somites. Regions containing greater *lacZ* expression compared to other tissue included the ectoderm (brain), endoderm (lung) and the mesoderm (muscles) (59). The global *Rev3L lacZ* expression in embryonic mouse tissue corresponded to the Northern blot and RT-PCR expression patterns in adult mouse and human tissue (62,75,76) demonstrating the importance of *REV3L* in both embryogenesis and adult tissue maintenance.

Attempts to generate mouse embryonic fibroblasts from the *Rev3L* null fetuses proved extremely difficult even after elimination of *p53* since these cells fail to grow. However, two independent groups eventually demonstrated that mitotically active murine embryonic fibroblasts (MEF) disrupted for both *Rev3L* and *p53* could be generated. One group characterized their *Rev3L* null, *p53* null MEFs as having a slower growth rate compared to *Rev3L* wt, *p53* null MEFs, hypersensitivity to UV irradiation and cisplatin, and accumulating in S and G_2/M in response to DNA damage (77). The cell line developed in the Wood lab displayed a moderate sensitivity to a variety of DNA damaging agents (cisplatin, UV and gamma irradiation and MMS) . More striking was the widespread and spontaneous genome instability in the form of chromosomal aberrations and translocation events (78). Human fibroblast cells stably expressing a *REV3L* anti-sense construct similarly demonstrated an increased sensitivity to cisplatin as well as diminished spontaneous and damage-induced extrachromosomal homologous recombination using a two plasmid reporter system (44). This indicated that the involvement of REV3L in maintaining genome stability is potentially due to its role in homologous recombination.

Generation of a mouse expressing *Rev3L* anti-sense RNA and derivative cell lines were easier to generate since residual levels of REV3L protein allowed for the birth of viable pups (79). Of the ten *Rev3L* anti-sense founder lines generated, only one animal had a high anti-sense copy number. Cells expressing very high *Rev3L* anti-sense transcripts could lead to embryonic

lethality which may explain why only one founder line could be established. These mice were healthy with normal body weight and lifespan (the original founder lived for least 23 months). Upon immune challenge, these mice mounted a normal immune response with large germinal centers and developed memory B-cells. However, the number of B-cells in these germinal centers were fewer. Furthermore, these B-cells were unable to generate high affinity antibodies. Examination of the *Rev3L* anti-sense mouse memory B-cells indicated a decrease in somatic mutations in the Ig V_H gene compared to parental controls, suggesting the problem in affinity maturation may be due to a decrease in overall somatic hypermutation (79). These mice are no longer available because the transgenic anti-sense construct has been inactivated by methylation. The fact that this occurs indicates a high selection pressure for REV3L expression in developing embryos. Of note, when Rev1 is disrupted in chicken DT40 B-cells, it demostrated the importance of the dCMP transferase activity of Rev1 in immunoglobulin diversification. Mutational analysis of immunoglobulin light chains indicated that loss of the catalytic activity of Rev1 shifted nucleotide incorporation from C to A suggesting another translesion synthesis polymerase may be inserting opposite a UNG-mediated AP site (80). Fibroblasts generated from the anti-sense adult mice demonstrated an overall decrease in UV-induced mutagenesis at the *hprt* gene. However, there was no observed difference in sensitivity to UV irradiation between the knock down cell line and the parental controls (81). These findings corroborate the human REV3L anti-sense cell line results and imply that REV3L mediated UV-induced mutagenesis is conserved between yeast and mammalian cells.

1.7.2 Mammalian REV Protein Biochemistry

Two major cDNA forms exist for mammalian *REV3L*. Both code for transcripts greater than 10 kbp in length. One form encodes for a 3,053 amino acid protein (82) while the other encodes a 3,130 amino acid protein (75,83). The amino acid difference is based on a 128 bp insert in the mRNA caused by an alternative splice variant at +139/140 of the open reading frame leading to a premature stop codon. Initiation of translation at an alternative start site downstream (amino acid 79) from the predicted REV3L start site codes for the 3,053 amino acid protein (82). The predicted size of this B-family protein is 353 kDa. Mammalian REV3L is twice the size of yeast Rev3 (173 kDa) and much of this is due to one exon, exon 13, which encodes a 1388 amino acid piece (Figure 1.5). Aside from this large exon, the yeast and mammalian proteins share three somewhat conserved regions: an N-terminal region, a possible Rev7 binding region and a polymerase domain. Human REV3L possesses six conserved DNA polymerase motifs (84) in its C-terminal region, suggesting that REV3L is probably a DNA polymerase. The mammalian polymerase motif shares a 43% sequence identity with the yeast polymerase domain (75). The N-terminal and Rev7 binding domain regions found in the human protein correspond with studied regions in yeast and share a 29% sequence homology with each (85). Human REV3L probably belongs to the B-family of DNA polymerases based on four conserved Pol δ motifs found in the N-terminal region of both the yeast and mammalian protein (75). Despite mammalian REV3L being classified as a B-family DNA polymerase based on sequence, no biochemical DNA polymerase activity has been demonstrated.

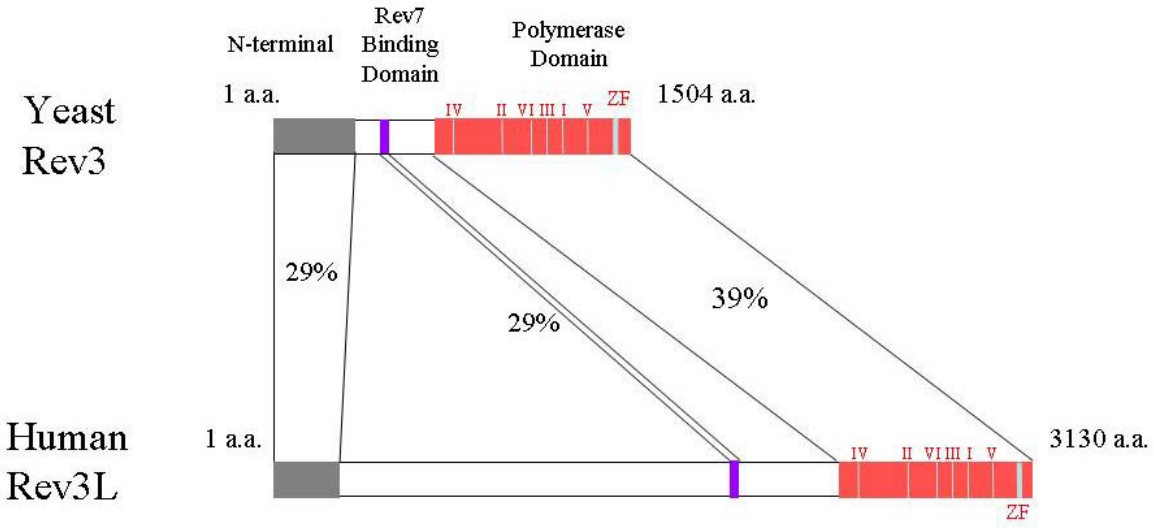

Figure 1.5 Diagram of yeast Rev3 and human REV3L.

The human protein is twice the molecular weight of its yeast homolog. Three regions between the yeast and human protein share significant sequence identity, the N-terminal Domain (29%), the Rev7 Binding Domain (29%) and the Polymerase Domain (39%). Zinc Finger (ZF)

The biochemical data on human REV3L protein is limited to a few studies of protein interactions. The interaction of human REV7 with human REV3L has been demonstrated using a fragment of human REV3L (1776 – 2044). The human REV3L fragment and full-length REV7 were shown to interact by yeast two-hybrid assays and by co-immunoprecipitation experiments using transiently co-transfected HeLa cells (86). Furthermore, Fishel's group also showed by yeast two-hybrid assays that a region of human REV7 (21 – 155 a.a.) was responsible for interaction with human REV3L (and REV1) (86). However, formal determination of whether human REV7 can bind full-length human REV3L has not been achieved because of an inability (by many lab groups) to express and purify the full-length human REV3L protein, The large size of the gene (~10.6 kbp) and the inability of most recombinant expression systems to

handle such a large protein (353 kDa) have contributed to this difficulty. Furthermore, these technical challenges also stymied the field because antibodies to REV3L and the necessary controls, such as REV3L null or REV3L overexpressing cell lines to validate this reagent, are lacking. However, several groups succeeded in expressing both of the smaller Rev proteins, human and mouse REV1 and REV7 (86-90).

Human *REV1* cDNA is 4255 bp in length and encodes for a 1251 amino acid protein with a molecular weight of 138 kDa (Figure 1.3). Similar to yeast, human REV1 possesses a dCMP transferase activity and by kinetic analysis, prefers to insert a single dCMP across template G (90,91). Furthermore, human REV1 can insert dCMP across an AP site or a uracil (90). To note, another human REV1 variant, possibly generated by alternative splicing, codes for a 1250 amino acid protein. Site-directed mutagenesis of D569 and E570 to alanine within the catalytic domain of human REV1 inactivates the 1250 amino acid dCMP transferase activity (92). These findings suggest that the 1251 and 1250 forms are functionally similar and that their translesion bypass activity is due to their dCMP transferase activity. Growing evidence, however, indicates that the dCMP transferase activity is not responsible for damage tolerance. Rather, structural domains are responsible for this. Three major regions of interest on REV1 are the BRCT domain, two ubiquitin binding domains and its extreme C-terminal domain. Embryonic stem cells derived from a *REV1* G76R BRCT point mutant mouse displayed an increased sensitivity to UV irradiation with a prolonged S and G_2/M phase. Upon damage, these cells had an increased number of chromatid aberrations without an increase in the number of sister chromatid exchanges (39). Dissection of the functional protein domains of REV1 demonstrated that the BRCT domain (amino acids 1 – 151) is important for nuclear localization. However, larger fragments corresponding to the N and C-terminal halves of the protein (1 – 730 and 730 – 1251)

were also shown to translocate into the nucleus. This suggests that other domains of the REV1 protein can facilitate nuclear localization (52). The biochemical function of the BRCT domain of REV1 is the interaction with both PCNA and Ub-PCNA. A discrete point mutation at G76R (homologous to the yeast *rev1-1* G193R point mutation) or complete deletion of the BRCT domain abolishes this PCNA-REV1 interaction in MRC5 cells as evidenced by immunoprecipitation. Both the point mutant and the deletion mutant prevent REV1 from forming constituitive nuclear foci in undamaged cells, but upon UV irradiation, these cells form fewer damage induced nuclear foci compared to cells containing wild type REV1 (38). The remnant damage-induced foci formed in the absence of a functional BRCT domain is presumably possible because of the ubiquitin-binding domains (UBM1: 933 – 962 and UBM2: 1011 – 1040). These domains have been shown to both bind ubiquitin as well as enhance the association of REV1 with Ub-PCNA. Deletion or mutation of the UBMs significantly diminished the amount of damaged-induced nuclear foci formed while the double BRCT-UBM knockout completely abolished REV1s ability to form nuclear foci (33). Another group observed that human REV1 lacking its BRCT domain localized to the nucleus and also formed foci in the absence of UV irradiation. Successive truncation fragments delineated a C-terminal portion of REV1 (amino acids 826 – 1036) required for nuclear localization and foci formation (93). Although Takahashi's group was unaware of the newly discovered UBMs, this observed interaction was most likely due to DNA-bound Ub-PCNA interacting with the REV1 ubiquitin-binding domains. In summary, the BRCT and ubiquitin binding motifs of REV1 are both required to bind PCNA and PCNA presumably interacts with DNA. Upon DNA damage, REV1 binding to PCNA is enhanced in response to ubiquitinated PCNA allowing formation of nuclear

replication foci at sites of DNA damage. Discussion of the protein-protein interaction partners associated with REV1 will be done in conjunction with mammalian REV3L and REV7.

Human *REV7* (MAD2B) cDNA is 1,163 bp and encodes a 211 amino acid protein with a predicted molecular weight of 24 kDa. Human REV7 has a sequence identity and similarity of 23% and 53%, respectively, to yeast Rev7. Notably, human REV7 has a 23% and 54% sequence identity and similarity with human MAD2, a spindle cycle checkpoint protein (88,94). Like its yeast counterpart, human REV7 possess a HORMA domain and this region is thought to mediate its potential interaction with CDC20, MAD2 and possibly REV3L. In response to DNA damage and cell stress, REV7 acted as an adaptor by binding the transcription factor, Elk-1, and the phosphorylated MAP kinase, Jnk. Jnk phosphorylates Elk-1 leading to the activation of Elk-1 responsive genes such as *egr-1* (95). These findings suggest a possible mechanism of how the damage tolerance protein REV7, at the transcription level, can respond to DNA damage. Earlier work studying cell cycle progression demonstrated that REV7/MAD2B is able to inhibit the Anaphase Promoting Complex (APC) through interactions with CDC20 and Cdh1 (96). However, these findings are probably incorrect since overexpression as well as siRNA knockdown of human *REV7/MAD2B* had no effect on cell proliferation, mitotic index or the cell cycle (71,88).

Because the yeast Rev homologs interact with one another, there has been a great deal of interest in determining whether the human homologs also interact. Using yeast two-hybrid assays and/or transient transfection, multiple groups demonstrated that full-length REV7 and a REV1 fragment (a.a. 1130 – 1251) interact *in vitro.* Mammalian REV1-REV7 interaction is mediated by the C-terminal domain of REV1 (86,87,89) The C-terminal domain of mammalian REV1 appears to be unimportant for interacting with many other translesion synthesis

polymerases. By yeast two-hybrid and transient co-transfection, mouse and human Polymerase iota, eta and kappa interacted with the C-terminus of REV1 (52,89). This supports the theory that REV1 may act as a scaffolding protein and facilitates the interchange between different DNA translesion polymerases at a site of damage. There has been no reported interaction between mammalian REV3L and REV1 fragments or full-length proteins even though this interaction has been demonstrated in yeast (26,40,86).

1.8 THE DISSERTATION

The two major aims of this work were to analyze the interaction between human REV3L and REV1 and REV7 proteins and to identify where *Rev3L* was expressed in adult mouse tissue. Because of the difficulty cloning the *REV3L* gene and expressing human REV3L protein, a great deal of technical effort was needed in order to express, purify and detect this 353 kDa protein. Therefore, in order to begin study of human REV3L, fundamental reagents such as REV3L specific antibodies (Chapter 2) and the full-length REV3L-Flag tagged protein (Chapter 3) had to be generated. Discovering how to express full-length human REV3L allowed examination of REV3L polymerase activity (Chapter 3) and its post-translational modification (Chapter 4). In order to gain insight into how REV3L may function at the tissue and cellular level, histochemical studies were initiated using a *Rev3L-lacZ* expression system driven off the endogenous mouse *Rev3L* promoter.

In Chapter 2, I discuss how REV3L specific chicken antibodies were generated against highly conserved regions of the REV3L protein. Chapter 3 details how a recombinant full-length

human REV3L-His and Flag tagged protein were expressed, Flag-purified and detected by anti-Flag immunoblot. Using this reagent, the affinity purified antibodies were screened against the full-length human REV3L protein. In order to determine the specificity of this interaction, a cell line expressing REV3L anti-sense RNA was acquired and multiple REV3L shRNA and inducible expression cell lines were generated. However, the specificity of the affinity purified REV3L specific antibodies could not be validated using these reagents. Therefore, these antibodies are currently being used only to detect the recombinant protein. The generation of full-length recombinant REV3L protein has allowed the Wood lab to begin addressing whether REV3L protein possesses polymerase activity. REV3L protein either alone or in combination with REV1 and REV7 was assayed on two different DNA templates. There was no observed REV3L polymerase activity either alone or in combination with REV1 and/or REV7 above background. An inherent problem associated with REV3L expression is the inability to generate large quantities of protein. This does not mean that REV3L does not possess polymerase activity, but that more conditions need to be assayed in order to determine optimal conditions for activity.

Chapter 4 describes how protein interaction and post-translational modifications of REV1, REV3L and REV7 were studied. Using a modified freeze-thaw lysis protocol, it was demonstrated for the first time, that full-length human REV3L interacts with full-length human REV1 by co-immunoprecipitation. Furthermore, the C-terminal domain of REV1 (1112 – 1251 a.a.), in part, mediates its interaction with REV3L and REV7. A REV3L-REV7 interaction was not observed. Potential reasons supporting interaction or lack of interaction for these two proteins are many, however, should be tempered with the consideration that the recombinant proteins may not necessarily reflect the endogenous cellular conditions. Work has also begun to

characterize the ubiquitin-mediated post-translational modification of the REV proteins. This work demonstrates that REV1 and REV7 are both mono and di-ubiquitinated. Furthermore, preliminary evidence indicates REV3L is similarly ubiquitinated. It is unknown whether this ubiquitination is associated with proteasomal degradation or damage signaling and remains to be determined.

Finally, in Chapter 5, study has been initiated into the tissue expression of *Rev3L* in mice transgenically modified with a *Rev3L-lacZ* expression cassette driven off the endogenous *Rev3L* promoter. Rev3L was observed as a function of lacZ expression and were found to be highest in mouse testis, the cardiac ventricles and the smooth muscle of the lungs and intestines. This finding challenges the current notion that REV3L is important only in proliferating cells. One possibility is that these tissues are highly metabolic and may suggest that REV3L is important for tolerating oxidative damage. Based on these observations, it can now be postulated that REV3L is important for tolerating oxidative damage. Currently, REV3L expression is not observed in the hematopoetic system which is contrary to the published literature. This could merely be a false negative which necessitates that an alternative method such as *in situ* hybridization be used to confirm the musculature results.

The significance of this dissertation provides for the first time valuable tools necessary to begin studying full-length human REV3L biochemistry. These tools have been used to initiate studies demonstrating that human REV1 and REV3L interact and that this interaction is mediated in part by the C-terminal domain of REV1. One potential model is that REV1-REV3L, perhaps in association with PCNA, can associate to sites of oxidative DNA damage in human cells. Furthermore, the discovery that the REV proteins are ubiquitinated could suggest a

mechanism for damage signaling, protein-protein interaction or protein turnover and offer exciting avenues for future study.

2.0 GENERATING REV3L SPECIFIC ANTIBODIES

2.1 INTRODUCTION

Various groups have demonstrated that *REV3L* mRNA is expressed in many human tissues and in normal and tumor cell lines (75,76). Although, *REV3L* transcript appears to be ubiquitously expressed, it provides limited information regarding how the protein is expressed, how it is regulated, and what potential function it may have in different tissue or cells. In order to understand the function of human REV3L, significant effort has been made to detect the endogenous protein. Many groups have attempted to generate monoclonal and polyclonal antibodies in mice and rabbits with no success. Two confounding factors may explain why prior attempts were unsuccessful. First, the large degree of sequence homology between full-length mouse, rabbit and human REV3L is high – mouse and human share an 89% identity and a 91% similarity and could lead to a poorly immunogenic response due to recognition of self. Specifically, the N-terminal region and yeast Rev7 Binding Domain region between mouse and human share an 89% and 93% identity, respectively. At this time, there is no published rabbit REV3L protein sequence to compare against mouse or human. It was decided to immunize chickens because prior attempts in mice and rabbits had failed to generate an adequate antibody. Furthermore, the phylogenetic difference between birds and mammals should make human REV3L more immunogenic in chickens thus allowing for the generation of a higher affinity

antibody. The second and more likely problem is the relative expression levels of endogenous REV3L. Even though Rev3 is ubiquitously expressed in various organisms and has been found to be expressed in all human tissue (75,76), its relative protein expression remains unknown. Vertebrate Rev3 protein expression is presumed to be low in cells because of its mutagenic DNA lesion bypass activity. This assumption is based on a great deal of yeast Rev3/Pol zeta work which has delineated the proteins *in vitro* DNA polymerase activity (21,22,97-99). Unfortunately, without a positive correct control, these other lab groups were unable to validate their antibodies thus complicating detection and interpretation of endogenous mammalian full-length REV3L by immunoblot. The Wood lab was in a unique position to develop these human REV3L specific antibodies because of our access to a REV3L null murine embryonic fibroblast cell line as well as to various REV3L anti-sense and shRNA constructs and cell lines. Furthermore, the ability to generate a recombinant full-length human REV3L protein (Chapter 3) would allow for screening of these antibodies against the full-length protein and would provide a valuble protein size marker when screening for endogenous human REV3L.

It is worth noting that two *REV3L* cDNA's exist; one coding for a 3130 amino acids protein (75,83) while the other for a 3053 amino acids (82). The reason for this size disparity most likely stems from cloning of different human cDNA libraries when assembling the gene. The reason for this size difference is due to an alternative splice event which introduces a 128 bp insert (exon 3). The Morelli, et al cDNA contains this 128 bp insert while the Lin, et al cDNA does not. Gibbs, et al reported only observing the 128 bp insert in some of their sequenced clones. Based on the Morelli, et al exon cDNA map, the Gibbs and Lin translation would start at exon 2 generating the 3130 amino acid REV3L protein. However, introduction of the 128 bp (exon 3) splice variant would cause a premature truncation product (47 amino acid) shortly after

initiation. An alternative ATG start site down stream of the first ATG could allow for REV3L translation generating the 3053 amino acid form. Which form predominates in the cell is currently unknown, but the 128 bp insertional splice variant may play an additional role in regulation of REV3L.

This chapter discusses the development of multiple human REV3L specific chicken antibodies based on the predicted 3,130 amino acid sequence. These antibodies were validated using the recombinant full-length human REV3L protein. Finally, REV3L shRNA was used to knock down endogenous and recombinant REV3L in order to validate potential bands thought to be REV3L specific signals.

2.2 METHODS

2.2.1 Cloning the Six REV3L Fragments for Antibody Production

Six conserved immunogenic epitopes sharing sequence homology with human and mouse REV3L protein were identified as potential regions for generating polypeptides fragments for immunization in chickens. These polypeptide motifs were chosen because of their highly immunogenic and hydrophilic profile calculated by the Parker and Welling Antigenicity and the Hopp/Woods Hydrophilicity algorithm using MacVector 7.0. The 6 identified regions correspond to the extreme 78 amino acid Alternative Splice region (amino acids 1 - 78), the 394 amino acid N-terminal region (amino acids 79 - 472), a 298 amino acid internal conserved domain region (amino acids 902 - 1199), a 70 amino acid yeast Rev7 binding domain region

(amino acids 1851 - 1920), and a 416 amino acid polymerase domain region (amino acids 2365 - 2780). Alternative Splice fragment Refer to Figure 2.1 for REV3L polypeptide epitope map. Refer to Appendix A for primer sequences. These fragments were PCR amplified using Platinum Taq Polymerase, high-fidelity (Invitrogen). Refer to Appendix B for PCR amplification protocol corresponding for each amplified region. Conserved Region, REV7 Binding Domain and Polymerase domain constructs were designed to use the vector backbone's N-terminal 6x His tag while the Alt Splice and the N-terminal fragments were generated with a 3' end 10x His tag using PCR primers. All PCR products were gel purified and eluted in 32 µl of Qiagen elution buffer. The Alternative Splice and N-terminal fragments were directionally subcloned into the pET-28a bacterial expression vector (Novagen) using NcoI (NEB) and XhoI (NEB). The Conserved Region, REV7 Binding Domain and Polymerase Domain were all directionally subcloned into the pET-15b bacterial expression vector (Novagen) using NdeI (NEB) and XhoI (NEB). A 439 amino acid C-terminal domain region (amino acids 2691 - 3130). The C-terminal domain region overlaps with a portion of the polymerase domain region. The C-terminal domain was cloned into the pET-30a bacterial expression plasmid (Novagen) by D. Winter and Gearhart (NIA). This fragment was designed to use the vector backbone's N-terminal 6x His tag.

The restriction enzyme digested, gel purified PCR inserts and the gel purified restriction enzyme digested pET vectors were ligated at 16ºC overnight using a commercial T4 DNA ligase kit (NEB). Ligated plasmids were transformed into One-shot DH5α Chemically Competent cells (Invitrogen). In brief, 1:3 and 1:5 ratio of vector to insert of ligated plasmid was mixed with 50 ul of competent bacteria on ice for 30 minutes. Cells were heat shocked at 42ºC for 55 seconds

and transferred back on ice for 2 minutes. Cells were then grown for 1 hour in 500 ul of SOC media at 37ºC at 225 RPM's. Transformed cells were then plated out on either carbenicillin

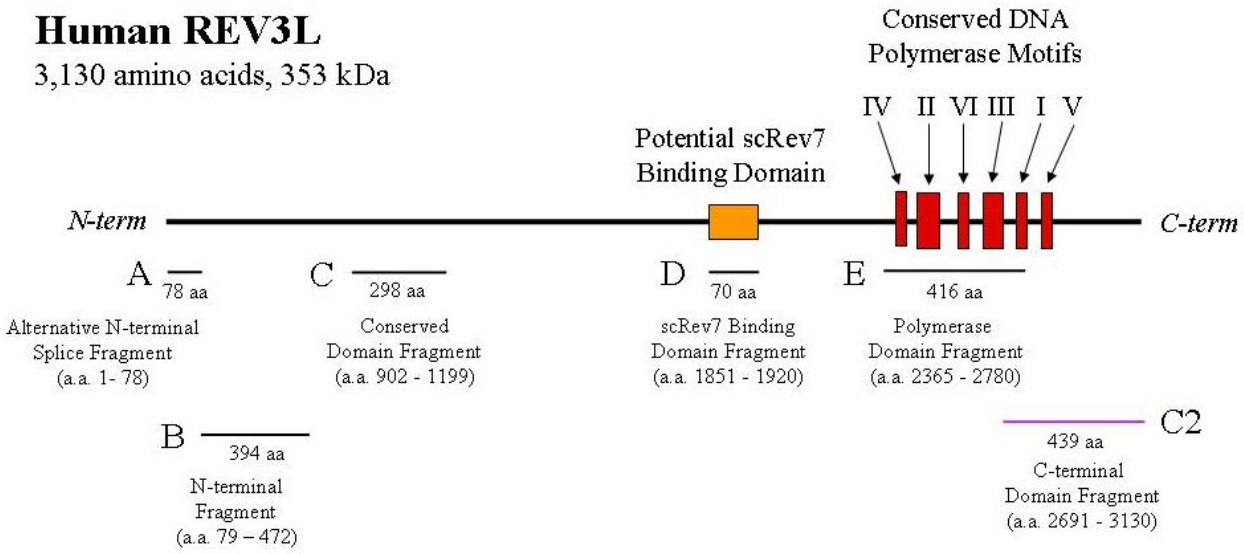

Figure 2.1 Diagram illustrating the six major polypeptide domains chosen for immunization into chickens for production of chicken anti-human REV3L polyclonal antibodies.

The regions were determined based on their aliphatic and immunogenic profiles as determined by the Parker and Welling Antigenicity and the Hopp/Woods Hydrophilicity algorithm using MacVector 7.0.

(pET-15b) or kanamycin (pET-28a and pET-30a) agar plates and grown overnight in a 37ºC incubator. Colonies were picked and grown in Luria-Bertani (LB) broth with the appropriate antibiotic for 16 hours. Minipreps were generated the next day using a standard Qiagen DNA mini prep kit (Qiagen). Potential colonies containing the desired inserts were initially screened by PCR using the established primers and amplification protocols described above. Positive colonies demonstrated by PCR amplification of the insert were further analyzed by restriction

enzyme digestion. The diagnostic digestions used for further determining potential clones were the same ones used for cloning the insert into the vector as described above. These five constructs were not sequenced.

DNA mini preps corresponding to the five potential constructs were transformed into the IPTG inducible bacterial expression cell line, BL21(DE3) (Invitrogen). 25 ng of each plasmid was added to 50 µl of bacteria on ice and incubated for 30 minutes. Cells were heat shocked at 42ºC for 40 seconds in 1.5 ml eppendorf tubes using a heat block and replaced on ice for 2 minutes. Cells were incubated in 300 µl SOC media for 1 hour at 37ºC and shaken at 225 RPMs. After 1 hour, 20 or 100 µl of bacteria were plated onto either carbenicillin or kanamycin agar plates and incubated overnight at 37ºC. The following day, 3 potential clones were picked, restreaked on to fresh agar plates with appropriate antibiotic and inoculated into 3 ml of fresh LB with appropriate antibiotic and cells were grown overnight at 37ºC and shaken at 225 RPMs. The overnight stock was used for mini-preps, protein induction and banking at -80ºC for long-term cold storage.

2.2.2 Small Scale Expression of the Six REV3L Fragments for Antibody Production

150 µl of overnight culture was added to 3 ml of fresh LB with appropriate antibiotic and grown to an OD_{600} of 0.5. Cells were induced for 4 hours with 1 mM IPTG. After 4 hours, 2 ml of bacteria were spun down in a 2.2 ml eppendorf tube at 13,000 g's for 5 minutes at 4ºC. Protein solubility was determined using a modified Qiaexpressionist protocol. 400 µl of native lysis buffer (Appendix C) was used to lyse each tube and placed on ice for 30 minutes. Cells were

then sonicated for 2 minutes at 60 mAmps in a large water-filled inverted bell jar sonication apparatus. Cells were then spun down at 13,000 g's for 20 minutes at 4ºC. The 400 µl supernatant was saved and the pellet resolubilized in 8 M Urea Lysis buffer. Uninduced samples were processed similarly without receiving IPTG induction.

In order to verify protein expression, the REV3L protein fragments were resolved using SDS-PAGE and stained with Coomassie Brilliant Blue. The N-terminal, Conserved Region, Polymerase Domain and C-terminal fragments were run on self-casted 10% and 12% SDS-PAGE with a 5% stacking column (Appendix D) while the Alt. Splice and REV7 Binding Domain fragments were run on self-casted 15% SDS-PAGE with a 5% stacking column (Appendix D). An unmarked molecular weight standard (Biorad) was run as a size control marker. For each lane, 10 µl of either soluble fraction (native lysis buffer) or insoluble fraction (urea lysis buffer) was mixed with 3x SDS loading buffer, loaded and resolved at 30 mA. Gels were stained overnight in a solution of Coomassie Brilliant Blue (Biorad) and rapidly destained by two washes in boiling ddH_2O (microwave 2 quart of water for 12 minutes). The relative amount of each protein fragment was determined by visual approximation.

At this stage, the only fragment that could not be expressed was the Conserved Region domain and was eliminated from the expression study.

As a representative example for the remaining five fragments, the large scale expression and purification for the C-terminal domain will be described in detail. Large scale protein expression was initiated by growing 1 – 4 liters of the appropriate bacteria and induced with 1 mM IPTG for 4 hours. 1 liter of the C-terminal fragment expressing bacteria was IPTG induced and harvested for protein. Because the protein of interest is predominantly within the insoluble pellet, the bacterial cytoplasmic fraction was pre-cleared from the pellet by lysing the bacteria in

256 ml (8 ml TEDM/50 ml pellet) of TEDM buffer (supplemented with 256 µl of 1 M DTT, 18 µl of 14 M β-mercaptoethanol, 5.12 mg lysozyme, 192 µl of 100 mM AEBSF). The pellet was mixed using a stir bar for 30 minutes. While on ice, 64 µl of 100 mM AEBSF (final concentration is now 100 µM) and 12.8 ml of 1% sodium deoxycholate was added and allowed to solubilize the cell pellet for 20 minutes. Then, the cell lysate was sonciated on ice with a large tip sonicator (10 sec burst with 10 sec pause in between – repeat six times). The cell pellet was spun down at 8500 RPM's at 4ºC for 20 minutes. The pellet fraction was washed with the remaining TE medium (without DM) and the cell pellet spun down again at 8500 RPM's at 4ºC for 10 minutes. The pellet was then resuspended in GuHCl extraction buffer (1.5 ml/50 ml pellet) and then transferred to a 50 ml Falcon tube and mixed for 2 hours on a head-to-toe rotator. This resuspended material was then spun down in an ultracentrifuge (Sorvall T645.5) at 30,000 g's for 30 minutes. The gentle lysis, GuHCl extracted C-terminal fragment was stored at 4ºC for later analysis. The C-terminal domain fragment was purified and concentrated using the protein's 6x-His tag on Ni^{2+}-NTA agarose (Qiagen). Because of difficulty with eluting the protein from the resin, it was decided to elute the protein from the beads by SDS-PAGE and excise the protein of interest directly from the gel. Resin bounds C-terminal domain protein was boiled in 3x SDS Loading Buffer for 5 minutes and loaded onto a large self-casted 10% SDS-PAGE gel with a 5% stacking column (Appendix D). Protein was resolved through the stacking gel at 25 mAmps; once it entered the separating gel, the current was increased to 35 mAmps. In order to determine migration and orientation of protein of interest, two methods were used to determine approximate protein migration in the gel. First, SeeBlue Plus Molecular Weight Marker from Pierce was used because the protein of interest migrated at 50 kDa. Second, the ends of the gel were cut vertically (refer figure 2.3), stained with Coomassie Brilliant Blue for 1

hour, rapidly destained in boiling water and reassembled with the unstained portion. Based on stained gel portions, the predicted region where the protein of interest had migrated on the gel was cut with a clean razor blade into 5 pieces. Four of these five fragments were transferred to a cryostat vial. The fifth fragment was cut into four pieces and added to each cryostat tube. This entire procedure was repeated twice in order to achieve an approximate concentration of 0.5 mg/ml for each tube – the minimum required for AvesLab to immunize two hens. 1 ml of sterile PBS was added to each tube and these samples were stored at -80ºC until they were ready to be shipped to AvesLabs.

Similar conditions were used for large scale expression, purification and gel fragment isolation of N-terminal and Polymerase Domain protein fragments. Of the two polypeptide fragments, the Polymerase Domain was the only protein that bound Ni^{2+}-NTA agarose (Qiagen) appreciably. The other fragment was TCA precipitated, concentrated and resuspended in 8 M Urea lysis buffer in order to load a sufficient amount of protein for gel fragment isolation. Both samples were resolved on a large-scale, self-cast 15% SDS-PAGE gel with a 5% stacking column. Protein bands of interest were excised and stored at -80ºC until they were ready to ship to AvesLabs.

For the Alternative Splice and REV7 Binding Domain fragment large scale protein expression, 1 liter of 1 mM IPTG-induced bacteria was grown. Because of the large quantity of soluble protein produced by the Alternative Splice and REV7 Binding Domain expression bacteria, cells were resuspended in a native lysis buffer supplemented with various protease inhibitors and 1 mg/ml of lysozyme. The cells were allowed to sit on ice for 30 minutes before sonicating at 60 mAmps for 10x 10 seconds bursts with a 10 second rest in between. Cell lysates were spun down at 9500 RPM's at 4ºC for 20 minutes and TCA precipitated, concentrated and

resuspended in 8 M Urea lysis buffer in order to load a sufficient amount of protein for gel fragment isolation. Both samples were resolved on a large scale, self-cast 15% SDS-PAGE gel with a 5% stacking column. Protein bands of interest were excised and stored at -80ºC until ready for shipment to AvesLabs.

2.2.3 Large Scale Purification of the N-terminal and Rev7 Binding Domain Fragments for Generating an Antibody Affinity Purification Column

In order to generate the N-terminal fragment, an overnight culture of 110 ml of LB/Kanamycin with Clone #7 (pET28a-N-term) was grow at 37ºC, shaking at 225 RPM. Next day, 100 ml of bacteria was added to 2 L of fresh LB/Kanamycin and incubated at 37ºC, shaking at 225 RPM for ~ 1 hour (want OD_{600}: 0.5 – 0.7). A master mix was made of bacteria in order to ensure uniform culture conditions before starting. 525 ml of mixed bacteria was aliquoted to 4x 2 L Erlenmeyer flasks. Once the desired OD_{600} was reached, 0.52 ml 1 M IPTG was added to each flask. Bacteria was induced for 6 hours at 37ºC, shaking at 225 RPM. Cultures were spun down at 5600 RPM for 15 minutes and frozen at -80ºC.

The bacteria were lysed in 40 ml of 8M Urea Lysis buffer for each 1 L of bacteria. The lysis material was incubated on ice for 10 minutes. The bacterial slurry was sonicated 8x in 10 sec (amplitude: 60%) bursts with 8x 10 sec rest/pauses. The bacteria solution remained on ice to ensure that the solution did not warm up too quickly. After sonication, the lysed material was spun down at 9,500 RPMs for 30 minutes at 4ºC. The material was resuspended in 40 ml total of 6M GuHCl and placed on a stationary rotator and rotate for 2 hours at RT. The GuHCl

resuspended material was spun down at 9500 RPMs for 30 minutes at 4ºC. This clarified resuspension extract was removed taking care not to disturb the pellet – protein should be enriched in this extract. This material was stored at 4ºC.

40 ml 10% TCA was added to 40 ml GuHCl-protein material and incubated on ice for 15 minutes. The material was spun down in 2.2 ml eppendorf tubes for 20 minutes at 13,000 g's at 4ºC. The material was washed once in 2 ml of 75% EtOH for 10 minutes at 13,000 g's at 4ºC followed by a second wash using 1 ml of 75% EtOH for 5 minutes at 13,000 g's at 4ºC. The protein pellet was gently dried and then 1 ml of 8 M Urea lysis buffer was used to resuspend four protein pellet tubes. The pellet was broken up using the pipette tip between each tube resuspension and allowed 10 minutes between each resuspension for protein to dissolve. After all tubes were resuspended, all the material was pooled together into 1x 15 ml Falcon and an appropriate amount of 4x SDS L Bf was added to each tube (ie. 8 ml urea lysis buffer = 2.5 ml of 4x SDS loading buffer. Samples were aliquoted into 1.5 ml screw cap tube – 1 ml/tube and boiled at 95ºC for 10 minutes and stored at 4ºC until ready to use.

Because the N-terminal fragment can not be purified using Ni-NTA or Talon, it was decided to gel purify and elute the protein of interest. A large scale 10% Tris-Glycine SDS-PAGE gel/5% stacking column was cast. Follow the protocol from original experiment already detailed. The material was run at 60 mA (two gels/container) for ~8 – 10 hours, the gel section of interest cut out (N-term is just below 50 kDa – 2 bands, lower band relevant; this is identified using See Blue Plus 2 MWM) with a clean razor and put into 1.5 ml eppendorf tubes. Samples were frozen at -20ºC until ready to be processed. On the day of processing, gel fragments were allowed to warm to room temperature before starting. Gel fragments were mascerated using a Kontes 1.5 ml tissue homogenizer with a rubber tipped policeman. 400 – 500 µl of sodium

phosphate (pH 7.0) were added to each tube and incubate at 55ºC for 5 hours. Tubes were spun down for 30 minutes at max speed – the elution buffer was pooled into a collection tube (1st elution). Another 500 µl of sodium phosphate was added to each tube and incubated at 55ºC for another 5 hours or overnight. Pooled 1st and 2nd elutions were stored at 4ºC with 0.01% NaN_3. Each fraction was checked by Coomassie and Western to get a baseline protein amount before proceeding to concentrate the material. Material was transferred to a fresh tube – NOTE: must remove/eliminate as much of the contaminating SDS-PAGE because it contains Tris-Glycine, a contaminant for the Pierce Affinity columns.

In order to concentrate the N-terminal polypeptide, a Macrosep 10K concentrator (Pal Filtron) was used. Pooled material was spun down at 5000 g's for 2 hours (used a SA-600). After the initial spin, fresh sodium phosphate solution was slowly added to the top chamber in order to further dilute or eliminate any Tris-Glycine material from the PAGE material that may have contaminated the initial protein elution. The material was respun at 5000 g's for another 2 hours and continued to spin as needed until the final volume was around 2 ml. Samples were rechecked by Coomassie and Western blot to verify material purity and concentration before conjugating to the affinity column. 0.05% NaN_3 was added and refrigerated until ready to use.

Because the Rev7 Binding Domain protein was soluble and expressed in robust quantities, 60 ml of inoculated culture was grown overnight and 50 ml of overnight culture was added to 950 ml of fresh LB/carbenicillin. Cultures were prepared, grown and spun down similarly as described above. The REV7 Binding Domain was processed using a large-scale native lysis buffer preparation. Clarified bacterial lysate was subjected to two concentration columns in order to purify the abundant Rev7 Binding Domain polypeptide. 45 ml of the bacterial lysate divided into three 15 ml portions were placed onto three Macrosep 50 K

concentrators (Pall Filtron) and spun at 6800 g's for 2 hours (used SA-600). Material was spun down until there was ~2 ml of concentrate remaining. Another 8 ml of phosphate buffer was slowly added to the concentrate and respun again. All the filtrate from both spins were collected and placed on three Macrosep 10K concentrator and spun down at 6800 g's for 2 hours cycles until all but 1 ml of material had been passed through. The buffer was exchanged with a total of 14 ml of sodium phosphate buffer and respun until there was 1 ml of concentrate left in each (3x) concentrator. Samples (~3 ml) were pooled and further concentrated in a single Macrosep 10K concentrator using the above spin conditions. A final 470 ml concentrate was collected and rechecked by Coomassie and Western blot to verify material purity and concentration before conjugating to the affinity column. 0.05% NaN_3 was added and refrigerated until ready to use.

Because both of these polypeptides were eluted in sodium phosphate buffer, they could be directly coupled to the Amino Link Affinity Column (Pierce). In brief, polypeptide fragments of interest were covalently coupled to a 4% cross-linked agarose matrix containing an aldehyde functional group. The aldehyde spontaneously reacts with the primary amines of lysine or of the N-terminal end of a protein and this secondary amide linkage is stabilized using the reductant, sodium cyanoborohydride. The resultant REV3L polypeptide fragment covalently conjugated to agarose is then packed on a column, washed extensively to remove unbound polypeptide fragments and chemicals and was then used for affinity purification of the anti-REV3L antibodies.

2.2.4 Screening the anti-REV3L Antibodies

The ten chicken anti-human REV3L antibodies (2 antibodies for each group) from AvesLab were screened in three major parts. First, the polypeptide fragments were used to pre-screen the new chicken antibodies. Second, potential antibodies were then screened against the recombinant full-length human REV3L-Flag tag protein (described in Chapter 3). Third, potential antibody candidates able to detect the full-length were affinity purified against the polypeptide epitopes and then screened against the recombinant full-length human REV3L-Flag protein (described in Chapter 3).

For the first screen, the small scale polypeptide fragment expression procedure described above was used. 5 µl of clarified uninduced and induced extracts were loaded onto Biorad self-cast 10% (for Pol domain, C-terminal, and N-terminal fragments) or self-cast 15% (for Alt splice and REV7 binding domain) Tris-glycine-SDS gels with a 5% stacking column and run at 20 mAmps using a Biorad gel apparatus. SeeBlue2 Plus molecular weight standard (Invitrogen) was used as a sizing control for each gel. Protein fragments were transferred at 30 V onto 0.45 µm PVDF membranes (Millipore) overnight using a Biorad gel transfer apparatus. Polypeptide fragments were immunoblotted with their respective antibodies at a primary antibody concentration of 1:5000 and a secondary goat anti-chicken HRP antibody (Aveslab) concentration of 1:100,000. For the second screen, 15 µl of Flag immunoprecipitated REV3L-Flag tag protein was used to screen all ten antibodies. The full-length human REV3L-Flag protein was resolved on a 3-8% Tris-acetate gel using the NuPAGE gel system (Invitrogen). Refer to Chapter 3 for Protein Expression. In the third round, candidate antibodies able to recognize the full-length protein were affinity purified and re-screened against the

immunoprecipitated full-length REV3L-Flag tag protein. Affinity purified antibody conditions were optimized using the recombinant REV3L protein.

2.2.5 Tissue Culture

HeLa (Wood lab), and 293T (ATCC) cells were grown in Dulbecco's modified essential (DMEM) media supplemented with 10% fetal bovine serum and 1% penicillin/streptomycin (P/S) at 37°C in a 5% humidified CO_2 incubator. A Burkitt's lymphoma cell line, Ramos (Wood lab), was a suspension cell line grown in RPMI 1640 media supplemented with 5% fetal bovine serum and 1% penicillin/streptomycin. The cell lines 9N (parental) and 6I (anti-sense REV3L) was a generous gift from Dr. V. Maher (Li Z 2002). These cells were originally derived from human foreskin fibroblasts and were grown in DMEM supplemented with 10% FBS, 1% P/S, 0.2 mM L-aspartate, 0.2 mM L-serine, 1 mM sodium pyruvate. An additional 1 mg/ml of puromycin was added to the media for maintaining the anti-sense REV3L 6I cells.

2.2.6 Screening Subcellular Fractionated Extracts for Mammalian REV3L (Small-scale)

This protocol was originally developed by Dr. Birgitte Wittschieben of the Wood lab and members of the Rapic-Otrin Lab and has been subsequently modified by the author. Approximately 2 x 10^7 cells were detached from 10 cm plates using 1 ml of 1x trypsin/EDTA and inactivated in 4 ml media. Cells were collected in a 15 ml Falcon tube and the plate was

rewashed with 5 ml of 1x PBS. This PBS was added to the 15 ml Falcon tube and this cell solution was spun down at 2000 rpm for 2 minutes at room temperature. Cells were resuspended and washed in 10 ml of fresh, cold 1x PBS and spun down at 2000 rpm for 2 minutes at room temperature. Cells were resuspended in 1 ml of 1x PBS and spun down in a 1.5 ml eppendorf tube at 2000 g's for 2 min at 4ºC. Cells were put on ice and briefly washed with 850 µl of Hypotonic lysis buffer, spun down for 1 minute and the lysis buffer carefully decanted from the cells. Another 850 µl of Hypotonic lysis buffer was added and cells were incubated on ice for 10 minutes. Cells were pushed through an insulin needle ~10 times in order to achieve a minimal amount of cell lysis; degree of lysis was determined under a microscope and using trypan blue. Extreme care needed to be taken in order to prevent overlysis and opening the nuclear membrane. The cells were spun down at 2000 RPM for10 minutes at 4°C. The supernatant was saved as the cytosolic fraction. The pellet was resuspended in 300 µl of Nuclear Extraction buffer and a spin vane magnet was added to the solution and mixed for 1 hour in a 4°C cold room. After 1 hour, the magnet was removed and the material was spun down at 5000 rpm for 10 minutes at 4°C. This supernatant was saved as the nuclear extract fraction. This remaining pellet was resuspended in 200 µl of room temperature Chromatin Extraction buffer. 50 U of micrococcal nuclease (Roche) was added to digest the chromatin into mononucleosomes. This buffer solution was incubated at 37°C for 10 – 15 minutes and every 3 minutes the solution was pipetted up and down in order to break up the pellet. The digested material was then spun down for 10 minutes at 4°C. The supernatant was saved as the insoluble chromatin extract fraction. The pellet was solubilized in 200 µl of 2x SDS Loading buffer to pellet and boil for 3 minutes. All samples were frozen in liquid nitrogen.

2.2.7 Screening Subcellular Fractionated Extracts for Mammalian REV3L (Large-scale)

The large-scale subcellular fraction protocol was initially developed by the author and Dr. Birgitte Wittschieben and this most recent protocol was optimized by Dr. Birgitte Wittshieben. In principle, the large-scale protocol is similar to the small-scale protocol described above except 1 billion cells were harvested at one time and the outer cell membrane was disrupted using a Dounce Homogenizer B (Kontes) and the Nuclear membrane was disrupted using a Dounce Homogenizer A (Kontes).

2.2.8 Engineering a REV3L-HF Wild-type and Active-Site Mutant Expression Cell Line

The REV3L-HF WT or ASM cDNA was subcloned into the pcDNA5/FRT/TO Flp-In vector (Invitrogen). Refer to Chapter 3 for the full-length WT and ASM cDNAs. This project was a collaborative effort between Dr. Birgitte Wittschieben and the author where plasmids were constructed by the author in exchange for homemade Danish cakes. pG^2-25 was restriction enzyme digested with KpnI (NEB) and NotI (NEB), gel purified and ligated overnight at 16ºC using T4 DNA ligase (NEB) into the KpnI-NotI, dephosphorylated, gel purified vector and transformed into Stbl2 high efficiency, chemically competent bacteria (Invitrogen). Bacteria was plated on LB agar/carbenicillin plates and grown overnight at 30ºC, colonies picked, restreaked and inoculated into fresh LB/carbenicillin and grown overnight at 30ºC for DNA mini preps the next day. Mini-preps were processed using the Wizard SV DNA mini-prep kit (Promega). DNA

was digested with the restriction enzymes used to subclone the cDNA into pcDNA5/FRT/TO. Potential clones were DNA sequence verified. In order to generate the active-site mutant (polymerase domain mutant), the plasmid, pTSIGN-REV3L-HF ASM, was restriction enzyme digested with BstXI and NotI and this gel purified fragment was subcloned into the newly constructed pcDNA5/FRT/TO-REV3L-HF WT plasmid. Potential clones were screened digesting with HaeII. Potential clones were sent for DNA sequence confirmation.

The pcDNA5/FRT/TO-REV3L-HF WT or ASM plasmid was co-transfected with pOG44 plasmid into the Flp-in 293T-Rex expression cell line (Invitrogen). In brief, the technology utilizes yeast Flp Recombination Target (FRT) sequence present in both the plasmid and within the cell line. The gene of interest is recombined into a specific genomic site in the 293T-Rex cells using Flp Recombinase (generated by pOG44). The integration allows for expression of a single copy of human REV3L-HF WT or ASM driven by a CMV promoter regulated by a tetracycline-inducible response element in each cell. Cells were selected for integrants using 0.5% Hygromycin supplemented into the media. Protein induction was done by plating 2 -3 x106 cells per 10 cm dish and allowing them to plate down for 2 days before inducing 18 hours prior to harvest with 0.1 μg/ml tetracycline. Pooled and individual clones were screened for protein expression from Flag M2 agarose immunoprecipitated lysates by resolving on a 3-8% Tris-acetate gel (refer to Chpt 3 for details) and immunoblotting with αFlag M2 mAb.

2.2.9 Extracting Protein from Mouse Tissue

Add 500 µl of hi-salt RIPA buffer with Calbiochem IC3 protease inhibitor (50 µl/g tissue) to 0.5 g tissue. Sonicate samples on ice, 3 sec/bursts until sample is not chunky. Avoid foaming by leaving sonicator tip in sample and then turning off sonicator. Once complete, take 50 µl of concentrate and further dilute in 450 µl lysis buffer (and more protease inhibitor – 5 µl) and mix diluted lysis mixture thoroughly using a P200 pipetteman. Sample 50 ml from concentrate and diluted concentrate and clarify extract by spinning sample at 13,000 g's for 10 minutes to remove insoluble material. Protein was measured from both clarified and non-clarified extracts by Bradford Assay (Biorad). 60 and 100 µg of total protein was loaded per lane and run out on a 3 – 8% Tris Acetate gel (protocol described in Chapter 3) and immunoblotted for endogenous mouse REV3L using the affinity purified chicken anti-human REV3L specific antibodies.

2.2.10 Knockdown of Human REV3L by shRNA

Endogenous human REV3L was suppressed in human cell lines using two different methods. The first method used a retroviral REV3L shRNA system (Systems Bioscience, Inc) to knockdown endogenous REV3L in HeLa, Maher's parental and 6I cell lines, and the 293T-Rex REV3L-HF WT inducible cell line, Clone #9 (68). Three shRNA constructs designed using a proprietary algorithm for predicting optimal shRNA sequences was generated by the company. The company subcloned the three shRNA sequences into expression plasmids. Using a 293FT breeder cell line, the shRNA expression plasmid was co-transfected along with two other

plasmids necessary for assembling three different replication incompetent FIV retrovirus containing the REV3L shRNA (designated shRNA REV3L #1, #2 and #3). In order to transduce the cells, 1 ml of concentrated virus was mixed with 1 ml of DMEM (no FBS) and 2 µl of polybrene (Sigma). Cells were incubated in this 2 ml transduction media in a 5% CO_2 incubator at 32ºC overnight. Next day, the transduction media was removed and replaced with fresh media and allowed to grow for the remaining time. Successfully transduced cells were green (independent eGFP sequence cloned into shRNA plasmid). Positive pooled cells were banked as well as FACsorted for individual clones. Clones established after 3 weeks were also banked. In order to verify that endogenous REV3L transcript was knocked down, cellular mRNA was measured by RT-PCR in HeLa cells and endogenous and recombinant REV3L expression was examined in both HeLa and in the inducible REV3L-HF expression cell line by immunoprecipitation and immunoblot. For RT-PCR, 8000 cells were processed using the Superscript III CellsDirect cDNA Synthesis System kit in order to generate cDNA from mRNA following the protocol explicitly. REV3L PCR product was amplified using 2 Units of Platinum Taq (Invitrogen), 0.6 µM of both the forward and reverse primer, and 400 µM dNTP in a 25 µl volume. Primers were designed to span over intronic sequences in order to limit amplification of cDNA and prevent non-specific amplification of genomic DNA. GAPDH control fragment was amplified using the same reaction conditions with the only difference being the forward and reverse primers sequences and the number cycles used to amplify GAPDH (25 cycles). PCR amplified samples were run out on a 1.2% agarose gel in Tris-acetate EDTA buffer supplemented with 130 ng/ml of ethidium bromide. The predicted PCR product size of REV3L was 326 bp and 788 bp for GAPDH. Refer to Appendix B for RT-PCR protocol. For immunoblot, both cell lines were lysed using the hi-salt RIPA lysis protocol and extracts were

generated from 20 million cells. 60 μg of HeLa total protein cell extract was resolved using a 3-8% Tris-acetate SDS-PAGE gel, transferred onto 0.45 μm PVDF membrane and immunoblotted using the affinity-purified anti-Rev7 Binding Domain antibody.

The second method used a published REV3L shRNA plasmid demonstrated to knockdown endogenous REV3L transcript by 70% (47). Parental HeLa and 293T-Rex Inducible REV3L-HF and previously transduced (described above) HeLa and 293T-Rex Inducible REV3L-HF clones were transiently transfected with the shRNA plasmid and after two days treated with 1 μg/ml puromycin in order to initiate clonal selection. Cells that survived puromycin selection (designated as pooled cells) were banked as well as FACsorted for individual clones. Clones established after 6 weeks were also banked. In order to verify that endogenous REV3L transcript was knocked down, cellular mRNA was measured by RT-PCR in HeLa cells and recombinant REV3L-HF expression was examined in the inducible REV3L expression cell line by immunoprecipitation and immunoblot.

2.3 RESULTS

2.3.1 Cloning and Expression of the Six REV3L Fragments for Antibody Production

The six human REV3L fragments were successfully cloned and five-of-the-six were able to be expressed in bacteria using IPTG. This was demonstrated by Coomassie stain (Figure 2.2 and 2.3) and anti-His tag mAb (Novagen) immunoblot (data not shown) of the proteins resolved using SDS-PAGE. The pET22b-N-terminal plasmid was not used in any further protein

purification. The pET22b vector allowed for expression and localization of the recombinant protein into the periplasmic space, a region between the bacterial membrane and its cell wall. The predicted molecular weights for the Polymerase domain fragment, N-terminal fragment and C-terminal fragment were around 50 kDa. The Conserved Region fragment was 38 kDa, the alternative splice fragment was 10 kDa and the REV7 Binding Domain fragment was 9.4 kDa. None of the six fragments were sequence confirmed. The Conserved Region fragment could not be expressed optimally at the small-scale level and work on this fragment was stopped. The remaining five fragments were expressed and the yeast Rev7 Binding Domain and Alternative splice fragments were found to be very soluble (Figure 2.4) while the N-terminal, C-terminal and Polymerase Domain fragments were insoluble and concentrated within inclusion bodies found in the cell pellet (Figure 2.2). The large C-terminal domain fragment was similarly concentrated in the insoluble fraction (data not shown) and was highly expressed upon IPTG induction (Figure 2.5A). Initial purification of the fragments using Ni-NTA proved difficult as some fragments bound very well (Polymerase Domain and C-terminal) while others did not (N-terminal, Alt. Splice and REV7 Binding Domain). Aveslab recommended that the polypeptides gel purified fragments be sent to them for injection into chickens. Proteins unable to bind Ni-NTA were concentrated using a 10% Trichloroacetic acid solution and resuspended in 8 M Urea lysis buffer (4:1 or 5:1, original protein volume to new 8M Urea lysis buffer resuspended volume). Proteins able to bind Ni-NTA were bound and electroeluted from the beads by SDS-PAGE.

Large scale bacterial preps were grown and purified for the recombinant fragments as described in the methods. A representative example of the calculations for each fragment is described as followed. For the C-terminal domain fragment, the amount of protein predicted by visualization of the gel was approximately 3 μg/3.5 μl of lysate per lane. Protein analysis as

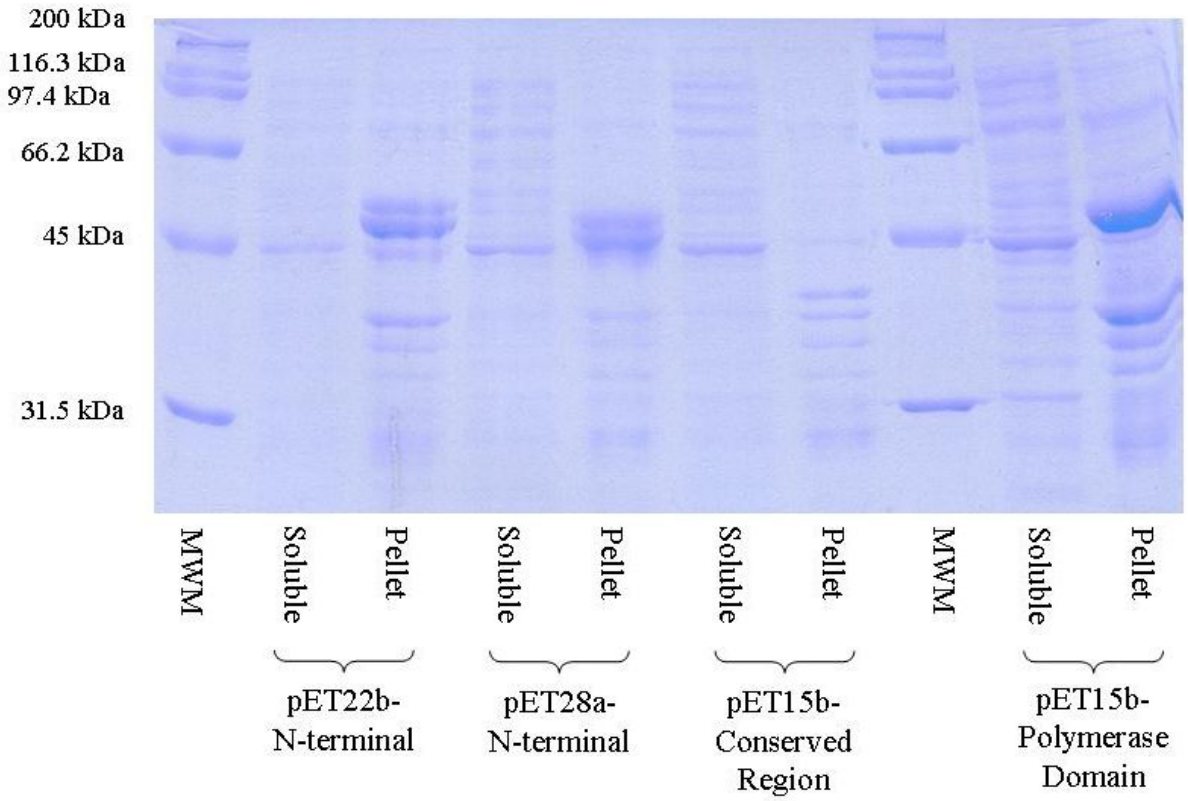

Figure 2.2 Expression of N-terminal, Polymerase Domain and Conserved Region fragments.

These fragments were subcloned into the pET bacterial expression vector and transformed into BL21(DE3). Bacteria were IPTG induced for protein expression. Protein was harvested from cells using a native lysis solution and a soluble cytoplasmic fraction and an insoluble pellet fraction (resuspended in 8M Urea lysis buffer) was generated. 10 μl of protein was resolved using a 10% Tris-glycine SDS-PAGE gel followed by staining with Coomassie Brilliant Blue. Both soluble and pellet derived samples were examined..

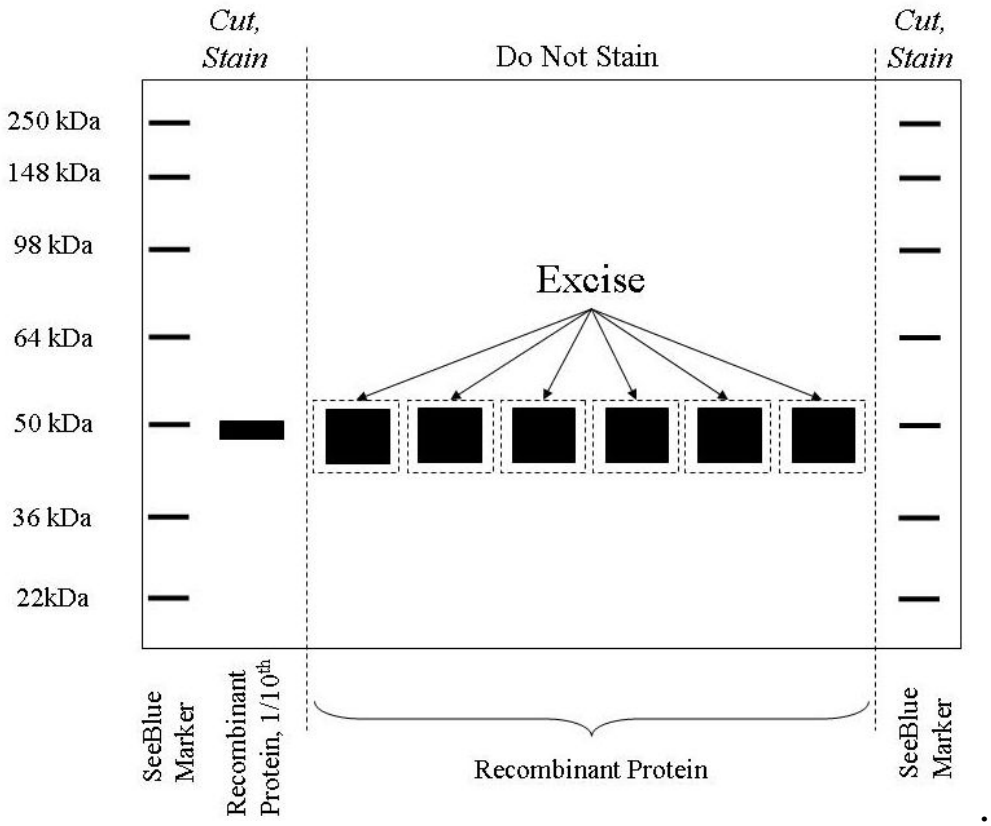

Figure 2.3 Illustration detailing how excision of protein gel fragments from a Tris-glycine gel.

Descriptive cartoon detailing how the large-scale Tris-glycine SDS-PAGE gels were cut, stained, destained and reassembled in order to approximate the gel migration pattern of all five polypeptides purified this way**.**

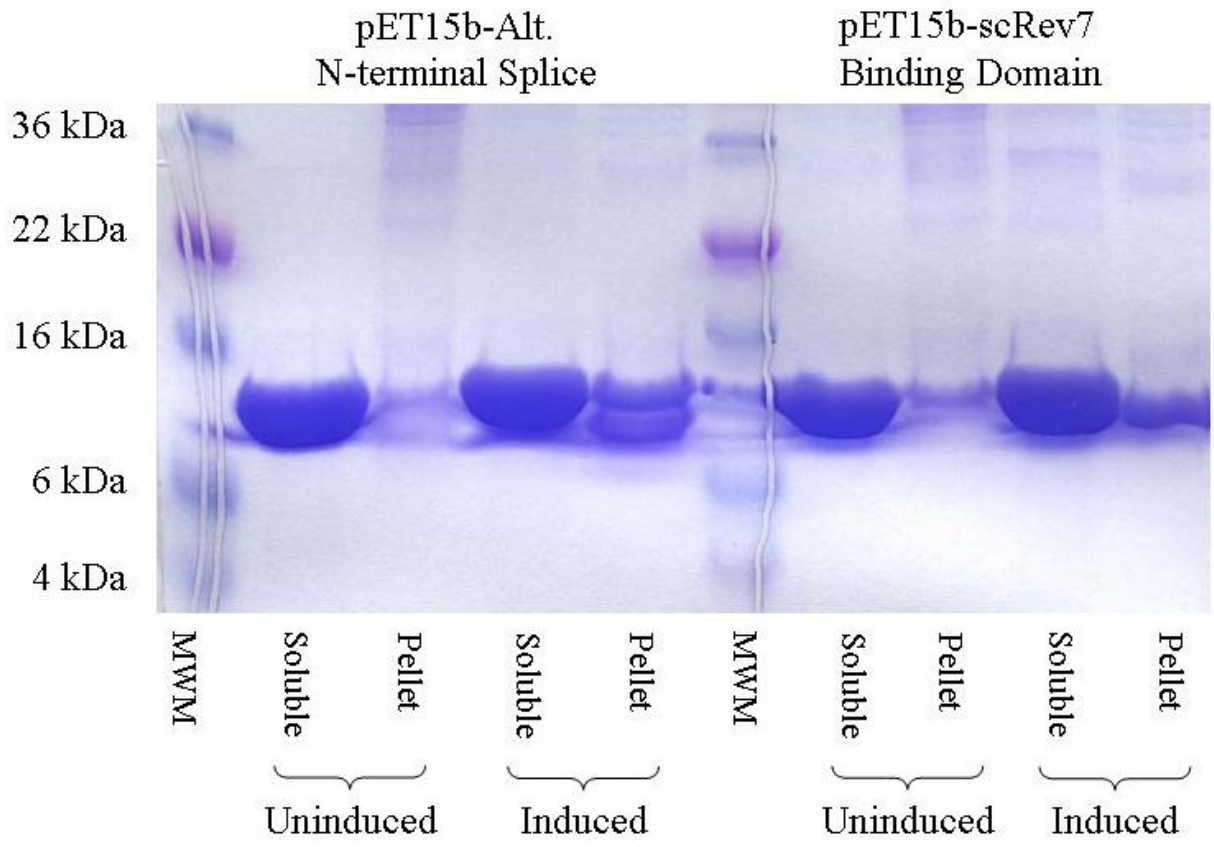

Figure 2.4 Expression of the Rev7 Binding Domain and Alternative Splice N-terminal fragments.

These fragments were subcloned into the pET bacterial expression vector and transformed into BL21(DE3). Bacteria were IPTG induced for protein expression. Protein was harvested from cells using a native lysis solution and a soluble cytoplasmic fraction and an insoluble pellet fraction (resuspended in 8M Urea lysis buffer) was generated. 10 µl of protein was resolved using a 15% Tris-glycine SDS-PAGE gel followed by staining with Coomassie Brilliant Blue. Uninduced and induced bacteria and both soluble and pellet derived samples were examined.

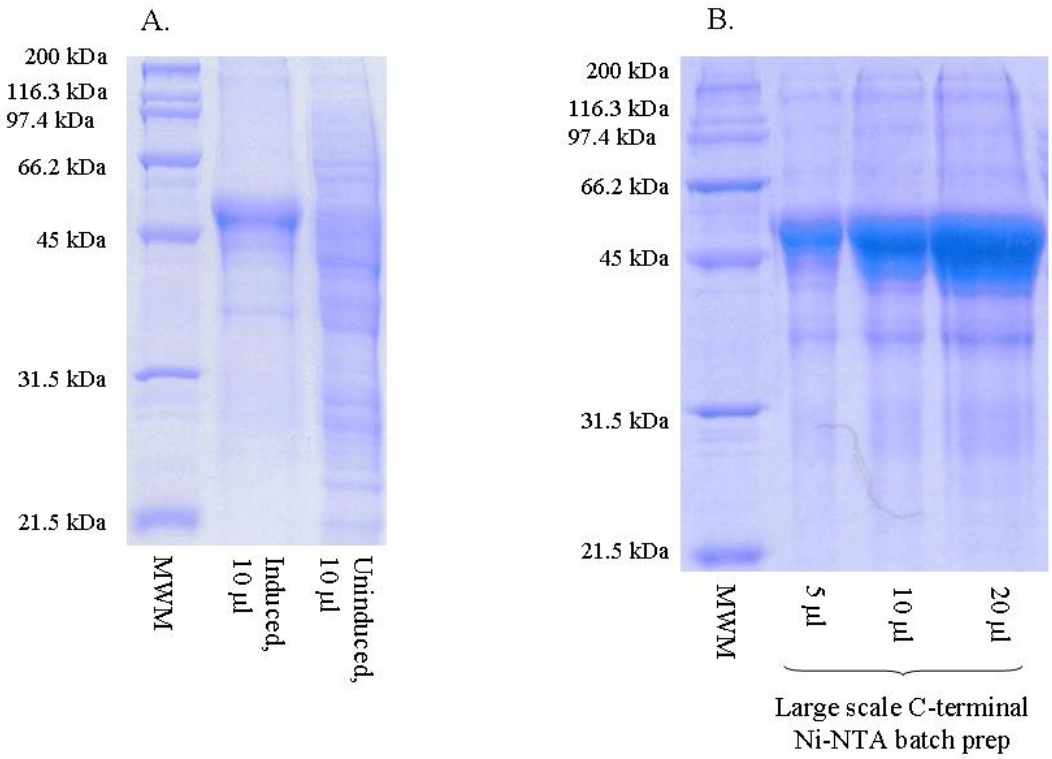

Figure 2.5 Expression of small and large-scale REV3L C-terminal domain fragment.

The fragment was subcloned into the pET bacterial expression vector and transformed into BL21(DE3). Bacteria was IPTG induced for protein expression. Protein was harvested from cells lysed in a GuHCl lysis solution in order to extract the insoluble protein contained in inclusion bodies. Protein extract was batch purified using Ni-NTA and resolved using a 10% Tris-glycine SDS-PAGE gel followed by staining with Coomassie Brilliant Blue. A. Small-scale lysis preparation. B. Large-scale lysis preparation of material bound to Ni-NTA, resolved on a large-scale SDS-PAGE gel and gel fragments excised for submission to Aveslabs for antibody production. Re-verification of predicted protein concentration from prepared material.

measured by Bradford assay indicated 4.9 µg per 3.5 µl of lysate measured. However, only 60 – 70% of this total protein was the recombinant protein, the rest was non-specific bacterial or pieces of degraded REV3L protein fragments. Therefore, the approximate final protein concentration was determined to be ~3.4 µg/3.5 µl. Assume ~1 – 0.8 mg/ml of recombinant

protein. 10 ml of the recombinant protein was bound to 1 ml of Ni-NTA beads (10 – 8 mg/ml). Assumed there would be a 20% loss of protein to the sides of the tube (8 – 6.4 mg/ml) and another 10% would remain tightly bound to the Ni-NTA (7.2 – 5.8 mg/ml). Based on these approximations, an average of 6.5 mg of protein was resuspended in 2.6 ml of 2x SDS loading buffer and 250 μl was added to each lane. Excised gel fragments were ~500 – 650 μg/tube – four tubes total. Remnant, unloaded protein solubilized in loading buffer was resolved on a mini-gel in order to confirm predicted protein concentrations (Figure 2.5B). There is approximately 5 μg of protein in the lane receiving 5 μl of large-scale protein extract (~1 mg/ml).

In brief, the N-terminal domain fragment had a concentration of 1.5 – 2 μg/μl and each gel fragment contained 450 – 600 μg/tube (Figure 2.6A). The polymerase domain fragment had a concentration of 2 μg/μl and each gel fragment contained about 500 μg/tube (Figure 2.6B). The Alternative Splice fragment had a concentration around 1 – 1.5 μg/μl and each gel fragment contained about 300 – 400 μg/tube (Figure 2.6C). The Rev7 Binding Domain had a concentration of 1.5 – 2 μg/μl and each gel fragment contained about 400 – 500 μg/tube (Figure 2.6D). These gel fragments were submitted to Aveslabs for injection into two hens in order to generate the various chicken anti-human REV3L polyclonal antibodies.

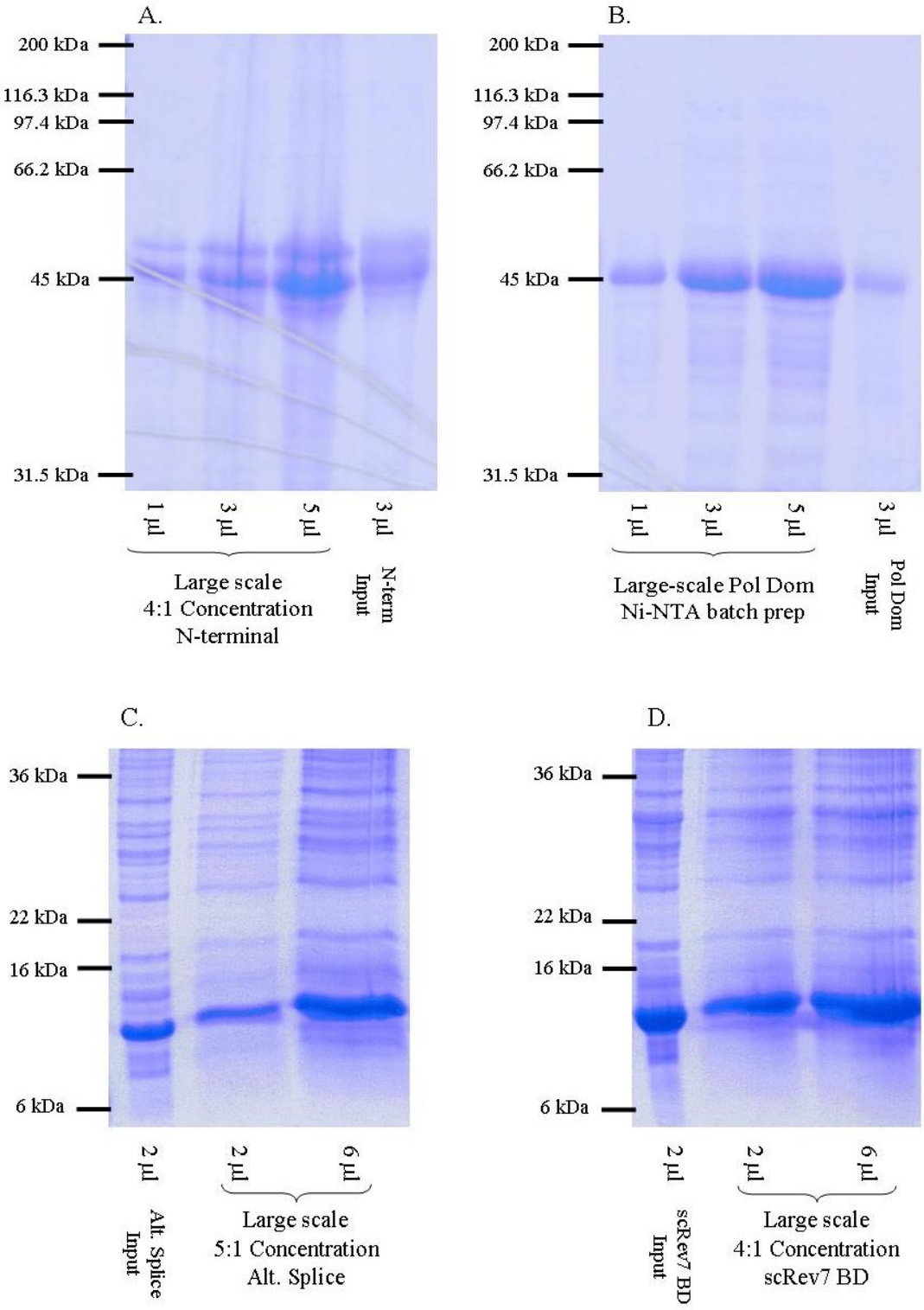

Figure 2.6 Expression of large-scale REV3L N-terminal, Polymerase Domain, Alternative Splice and Rev7 Binding Domain fragments.

The fragments were subcloned into the pET bacterial expression vector and transformed into BL21(DE3). Bacteria were IPTG induced for protein expression. N-terminal and Polymerase Domain fragments were harvested from

cells lysed in a GuHCl lysis solution in order to extract the insoluble protein contained in inclusion bodies. Alternative Splice and yeast Rev7 Binding Domain fragments were harvested from cells using a native lysis solution. The Polymerase Domain fragment was bound to Ni-NTA and electroeluted off the beads by resolving on a Tris-glycine SDS-PAGE gel. The N-terminal, Alternative Splice and yeast Rev7 Binding Domain fragments were concentrated using trichloroacetic acid and resuspended in 8M Urea lysis buffer and resolved on a Tris-glycine SDS-PAGE gel. Figures A-D were all re-verifications of predicted protein concentrations from the prepared material.

2.3.2 Large-Scale Purification of N-terminal and yeast Rev7 Binding Domain Fragments for use on an Affinity Purification Column

The polypeptide fragments were prepared the same way as when the fragments were generated for chicken immunization. The N-terminal fragment was gel purified from protein resolved on a large-scale Tris-glycine SDS-PAGE gel. In order to release the protein from the SDS-PAGE gel fragments, the gel pieces had to be macerated in order to increase its surface area, eluted in phosphate buffered saline while being heated at 55°C, and the eluted protein concentrated using a Macrosep 10K Concentration filter (Pall Filtron). Multiple samples were re-examined after gel elution to determine protein amount by Coomassie (Figure 2.7) and by immunoblot (data not shown). The eluted protein was then pooled together and concentrated using the Macrosep 10K concentrators and relative concentrating capacity was analyzed by SDS-PAGE and staining by Coomassie (Figure 2.8). None of the N-terminal fragment passed into the filtrate, all of the protein remained in the concentrate fraction. By visual interpretation of the Coomassie stained gel, approximately 4 – 5 μg/μl of N-terminal protein was predicted. In the pre-coupled fraction (2 ml total), approximately 6 mg of total N-terminal protein (~1.2 μg/μl) was cross-linked with the agarose matrix. Analysis of the post-coupled fraction (2 ml total), approximately 2 mg total protein (~0.4 μg/μl) did not bind to the column. Washing of the column (5 ml) indicates that

another 1 mg of total protein (~0.2 μg/μl) did not bind to the column. Subsequent washes do not indicate significant loss of anymore N-terminal polypeptide fragment. Based off of these rough approximations, it was predicted that 2 - 3 mg of total protein was successfully conjugated onto the agarose affinity column (Figure 2.9).

In brief, the C-terminal domain fragment was similarly expressed, purified, eluted and concentrated like the N-terminal domain fragment. Approximately, 5 mg was successfully conjugated to the agarose matrix.

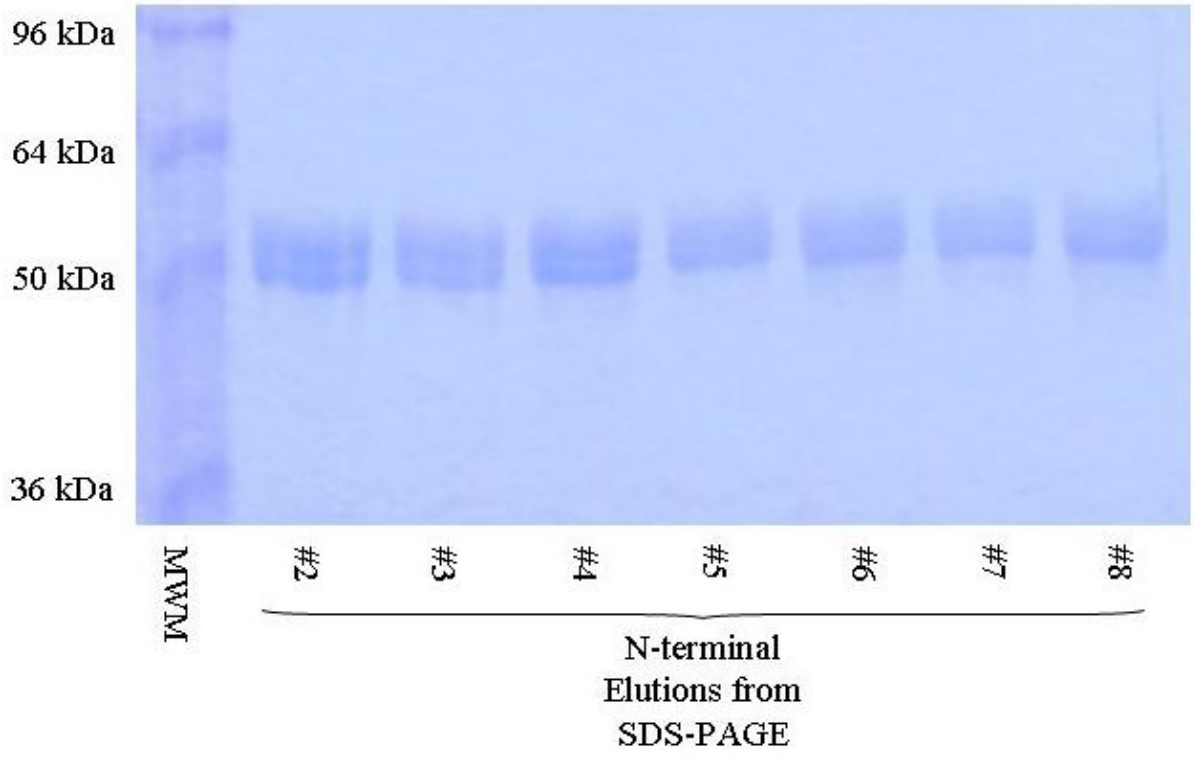

Figure 2.7 Elution of gel purified N-terminal fragment from macerated gel pieces.

The N-terminal fragments were expressed in BL21(DE3) cells. The bacteria was gently lysed in 8M Urea lysis buffer and the inclusion body pellet containing the N-terminal protein was extracted in a 6M GuHCl lysis buffer. The protein material was TCA precipitated, resuspended in 8M Urea lysis buffer and resolved on a 10% Tris-glycine SDS-PAGE gel. Gel fragments were cut out corresponding to the predicted migration distance of the protein on the gel. The gel pieces were macerated and protein eluted using a sodium phosphate buffer from the crushed gel at 55°C. The eluted protein was then examined by SDS-PAGE gel in order to determine amount of protein recovered.

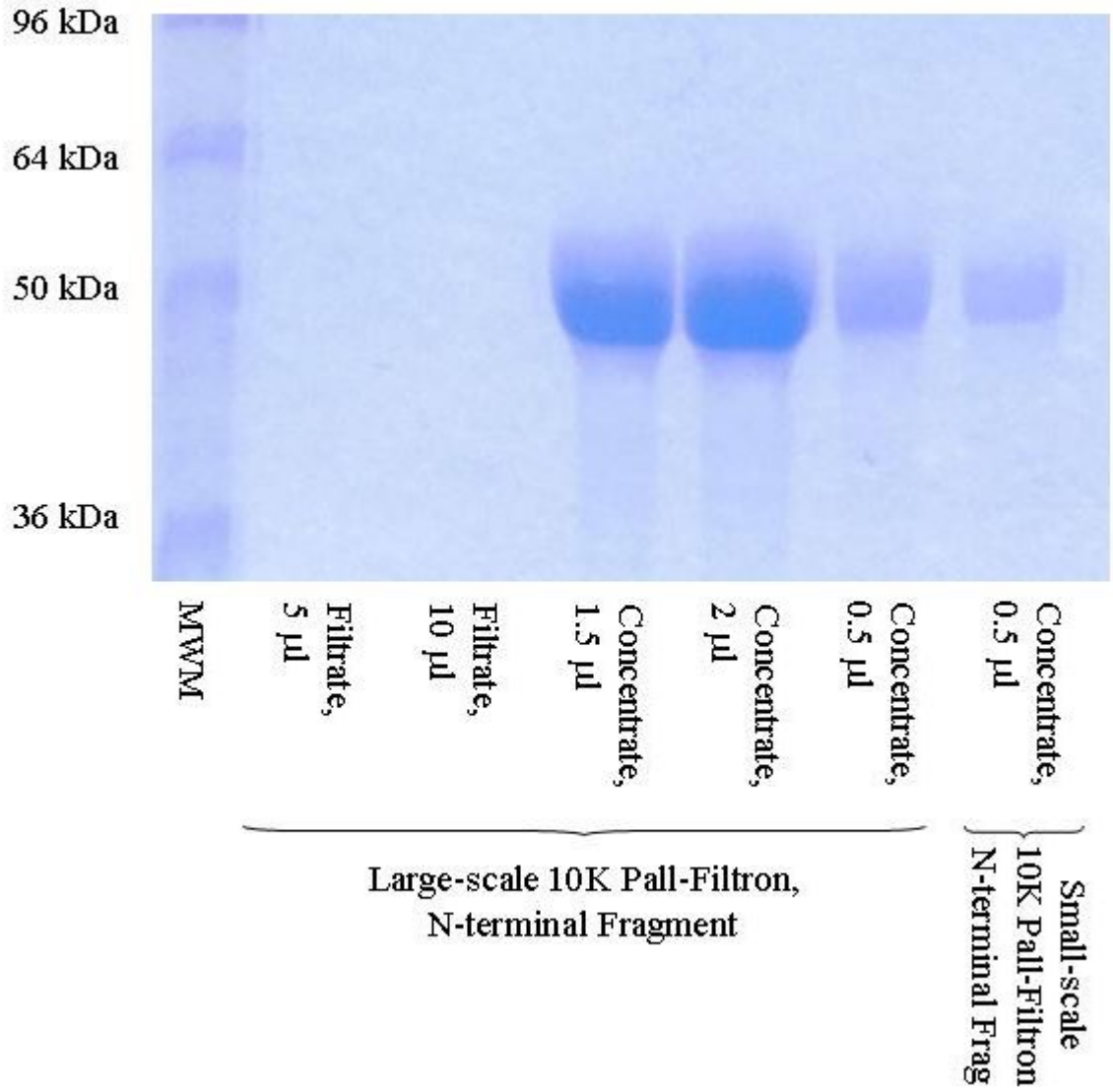

Figure 2.8 Eluted Protein Sample from Fig 2.7 Concentrated on a Pall Filtron Macrosep 10k Filter.

Material was spun down at 5000 g's in 2 hours cycles until the desired volume of 2 ml was achieved. The protein from both the filtrate and the concentrate was examined for relative amount of concentration in order to determine amount of N-terminal protein available for conjugating to the activated agarose matrix.

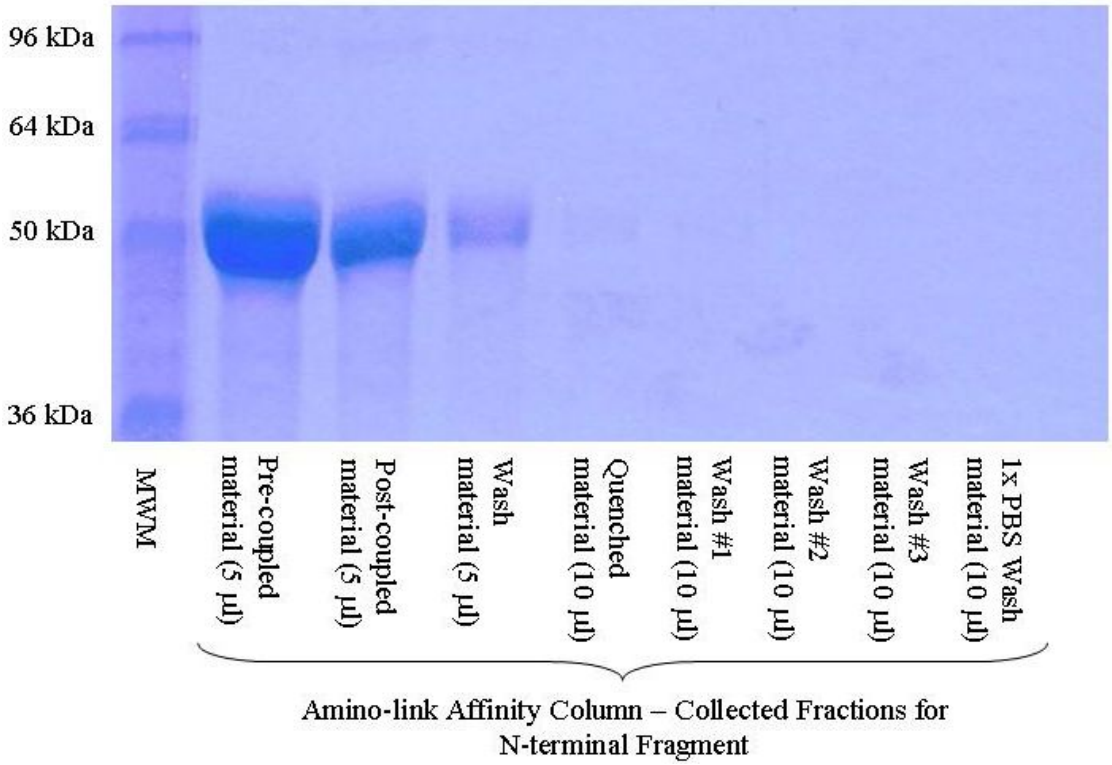

Figure 2.9 Determining the Degree of N-Terminal Polypeptide Conjugation to the Amino-link Affinity Column. Because the protein was eluted in phosphate buffered saline, there was no further need to add coupling buffer. 2 ml of N-terminal polypeptide was added directly to the activated agarose for conjugation. Different fractions were collected pre and post conjugation and with all the appropriate washes in order to determine amount of protein conjugated to the column.

Purification and concentration of the yeast Rev7 Binding Domain fragment using two different Pall Filtron concentrators was a success. Because of the small size of this fragment (~9.4 kDa), a majority of the material was able to be pushed through a 50K filter while retaining much of the higher molecular weight contaminants. The fragment was then concentrated using a 10K filter. Examination of a Coomassie stained gel indicated some faint higher molecular weight contaminants, however, a significant majority of the enriched protein was the yeast Rev7 Binding Domain fragment. The final concentration of this protein was around 22 – 24 µg/µl (final volume of 470 µl) (data not shown). Similar analysis of pre-coupled, post-coupled and

washed column material indicated that ~8 – 9 mg of Rev7 Binding Domain fragment was successfully conjugated to the agarose matrix (data not shown).

2.3.3 Screening the REV3L-specific Antibodies

The antibodies were initially screened against the polypeptide fragments they were generated against. For both the N-terminal (4359 and 4360) and Rev7 Binding Domain (4357 and 4358) antibodies, a primary antibody dilutions of 1:5000 and a secondary dilution of 1:100,000 were optimal conditions for observing the recombinant polypeptide with minimal background (Figure 2.10A, B). The Polymerase Domain, C-terminal Domain, and Alternative Splice fragments were able to be visualized at a 1:1000 and 1:5000 primary antibody dilution. However, because of their high background on film, it was impossible to scan and incorporate these results into this document. The second round of screening involved immunoblotting the ten REV3L specific antibodies against the full-length recombinant human REV3L-Flag tagged protein. However, due to severe background issues, none of the film could be adequately scanned and included in this document. Refer to Chapter 3 for the protocol used for resolving full-length human REV3L using the NuPAGE system (Invitrogen). The two best antibody groups able to detect the full-length protein were the N-terminal (4359, 4360) and Rev7 Binding Domain (4357, 4358) pAbs. The C-terminal antibodies showed some promise with detecting the full-length protein and were also affinity purified. The final screening involved using the affinity purified antibodies against the full-length REV3L-Flag tagged proteins. Of the three groups of antibodies, only the Rev7 Binding Domain (4358) and the N-terminal Domain (4359) affinity purified antibodies had the

cleanest and best detection of the full length protein (Figure 2.11). Immunoblotting and detection conditions for both these affinity purified antibodies were optimized using the full-length human REV3L-Flag tagged protein. Final conditions for both antibodies were determined: primary antibody 1:500 and for secondary 1:20,000 – 25,000 (Table 2). The C-terminal Domain affinity purified antibody even after multiple attempts at optimization surprisingly lost its ability to detect the full-length protein as well as had an increase in the amount of background contaminations in each blot. Therefore, work on this antibody stopped.

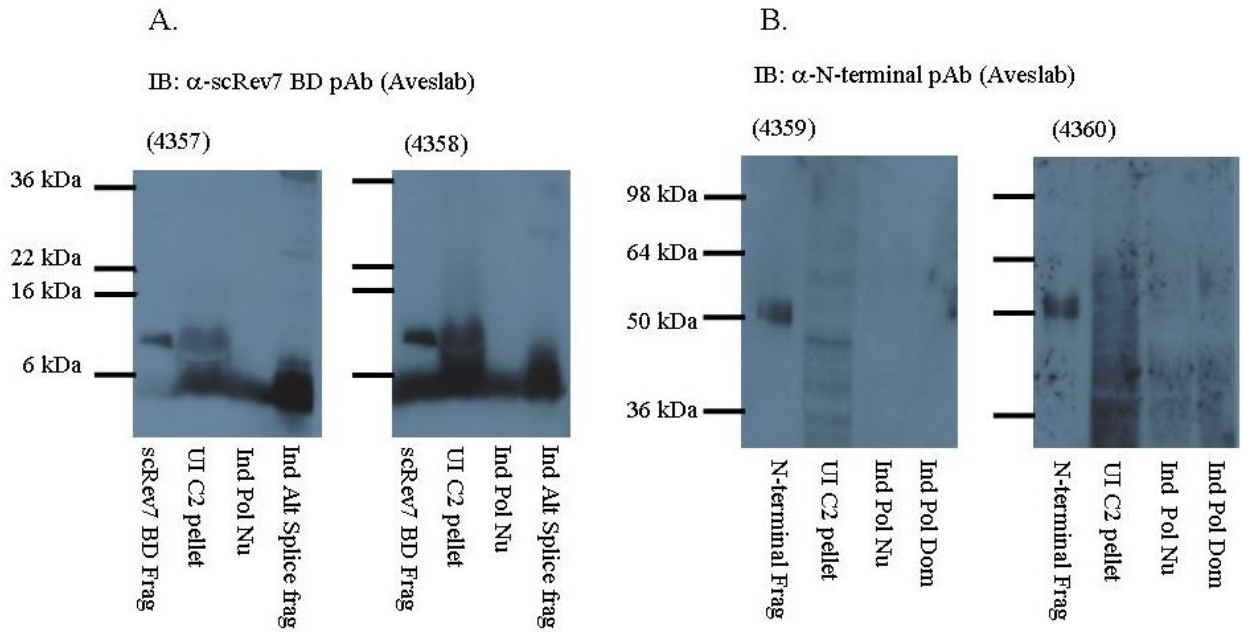

Figure 2.10 Anti-REV3L specific antibodies can detect the polypeptide fragments they were generated against.

5 µl of the recombinant polypeptide fragment was resolved on either a 15% or 10% Tris-glycine SDS-PAGE gel and immunoblotted testing both non-affinity purified antibodies against the recombinant polypeptide fragment. Control fragments were run in conjunction with the recombinant fragment of interest. These included an uninduced (UI) C-terminal domain (C2) pellet, an induced Pol Nu polymerase domain fragment, and an induced Alternative Splice fragment. These fragments were sampled from crude lysate and 5 µl was resolved by SDS-PAGE.

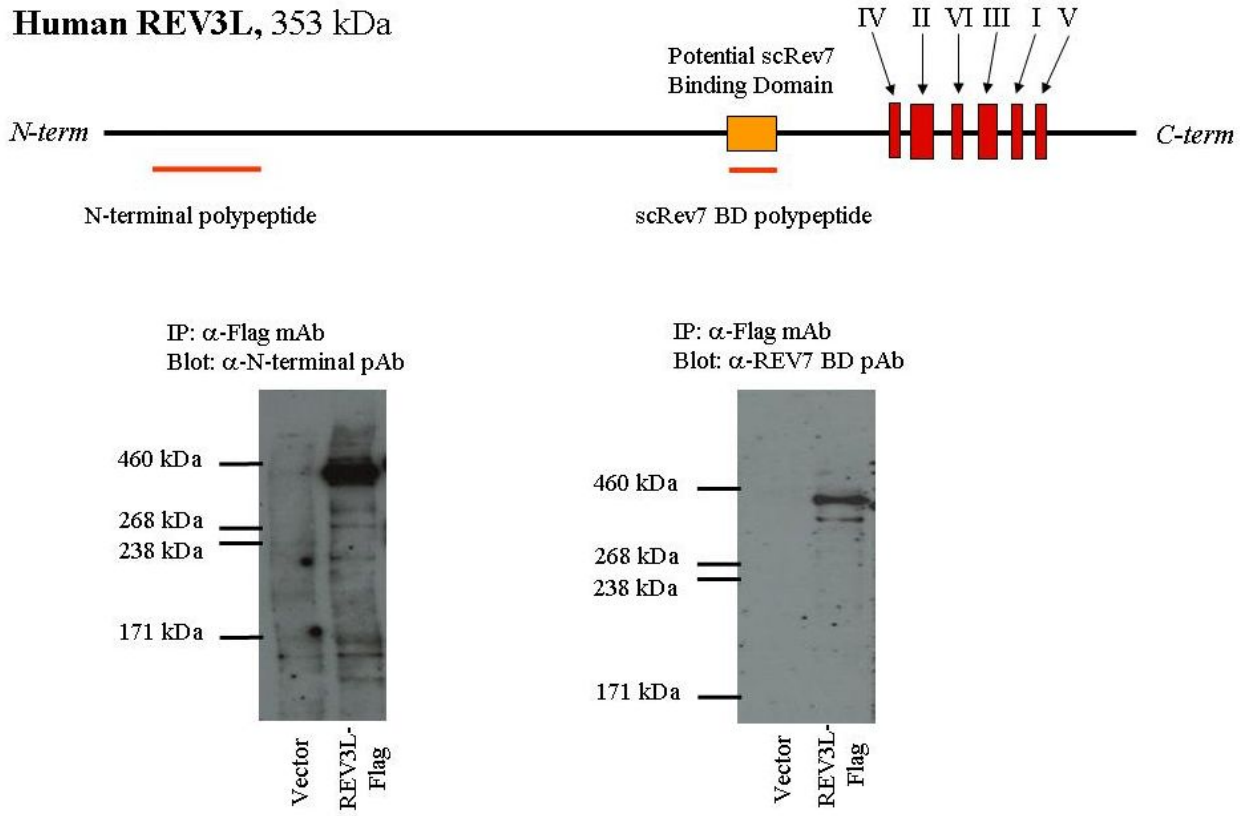

Figure 2.11 Diagram and figure demonstrating the location and results for two affinity purified REV3L specific antibodies.

Affinity purified antibodies were blotted using a primary antibody dilution of 1:500 to detect full-length human REV3L-Flag tag resolved on a 3-8% Tris-acetate gel and transferred onto 0.45 μm PVDF. Secondary antibody was diluted 1:20,000 using a Promega rabbit anti-chicken IgG HRP. Protein was detected using a commercial chemiluminescence reagent kit (Pierce).

Table 2. Masterlist for Primary and Secondary Antibody Dilutions

Protein of Interest	Antibody	1º Dil	Type	App	Company	2º Dil	Company	Dilution Buffer
rhREV3L	mouse α-Flag M2	1:5000	monoclonal	IB	Sigma	1:70,000	Sigma	10% milk/1x PBS Tween20 (0.1%); 5% goat serum/1x PBS Tween20 (0.1%)
	chicken α-N-Terminal	1:500	affinity-purified polyclonal	IB	Wood lab and AvesLab	1:20,000	Promega	10% milk/1x PBS Tween20 (0.1%); 5% goat serum/1x PBS Tween20 (0.1%)
	chicken α-REV7 Binding Domain	1:500	affinity-purified polyclonal	IB	Wood lab and AvesLab	1:20,000	Promega	10% milk/1x PBS Tween20 (0.1%); 5% goat serum/1x PBS Tween20 (0.1%)
rhREV1	mouse α-V5	1:5000 or 1:10,000	monoclonal	IB, IF	Invitrogen	1:70,000	Sigma	10% milk/1x PBS Tween20 (0.1%)
	goat α-REV1	1:500	polyclonal	IB	Santa Cruz	1:50,000		10% milk/1x PBS Tween20 (0.1%)
rhREV7 or REV7	mouse α-Flag M2	1:5000	monoclonal	IB	Sigma	1:70,000	Sigma	10% milk/1x PBS Tween20 (0.1%)
	mouse α-HA	1:10,000	monoclonal	IB, IP	ICRF	1:70,000	Sigma	10% milk/1x PBS Tween20 (0.1%)
	rabbit α-REV7	1:5000	polyclonal	IB	Abcam	1:50,000	Sigma	10% milk/1x PBS Tween20 (0.1%)
PCNA	mouse α-PC-18	1:2000	monoclonal	IB, IP	Santa Cruz	1:70,000	Sigma	10% milk/1x PBS Tween20 (0.1%)
ATM	mouse α-ATM-2C1	1:1000	monoclonal	IB	GeneTex, Inc	1:50,000	Sigma	10% milk/1x PBS Tween20 (0.1%); 5% goat serum/1x PBS Tween20 (0.1%)
Tubulin	mouse a-tubulin	1:1000	monoclonal	IB	Santa Cruz	1:50,000	Sigma	10% milk/1x PBS Tween20 (0.1%)
Ubiquitin	mouse α-HA	1:10,000	monoclonal	IB, IP	ICRF	1:70,000	Sigma	10% milk/1x PBS Tween20 (0.1%)

2.3.4 Attempts at Detecting Mammalian REV3L in Human Cell Lines and Mouse Tissue Extracts

The two affinity purified human REV3L specific antibodies were first tested on mouse tissue extracts presumed to contain abundant *Rev3L* transcript. Two lines of evidence encouraged this investigation. First,the *REV3L* LacZ tissue expression results demonstrated that mouse testis, heart and brain stained blue compared to other tissue suggesting a large amount of REV3L transcript production (refer to Chapter 5). Second, various groups had demonstrated by northern blot and RT-PCR that REV3L transcript is present in the brain, heart and testis. Therefore, heart, brain and testis tissue were harvested from mice, processed for protein, and immunoblotted using both the affinity-purified REV3L specific antibodies. Neither antibody could detect a high-molecular weight protein signal corresponding to the positive control (data not shown). An inability to detect any large specific band in these mouse tissue corroborated prior results examining cellular extracts generated from Dr. John Wittschieben's REV3L wild-type and null cell lines. Therefore, efforts were focused on human cell lines. Dr. Maher's REV3L anti-sense human foreskin fibroblast cell line was acquired in order to help determine whether the affinity-purified anti-REV3L antibodies could detect endogenous human REV3L protein (68). From the parental and anti-sense knock-down cell lines, a small-scale set of subcellular fractionated extracts were generated in order to determine where REV3L could be localizing. Analysis of the subcellular fractions from the Maher cell lines were inconclusive for detecting a putative REV3L band with both the affinity purified anti-Rev7 Binding Domain pAb (Figure 2.12) or the affinity purified anti-N-terminal pAb (data not shown). However, a large-scale subcellular fractionated chromatin extract generated from HeLa cells indicated a prominent band which corresponded to the approximate migration distance of recombinant REV3L-HF (Figure 2.12).

In order to verify whether this band was present in other tumor lines, large-scale subcellular fractionated protein extracts generated by Dr. Birgitte Wittschieben were analyzed. A similar band at approximately 360 – 400 kDa was observed in the nuclear and chromatin extract fractions of Ramos and HeLa (Figure 2.13A) and in a bladder and a lymphoma cell line (data not shown). Silver stain of Ramos and HeLa indicates two prominent bands observed around

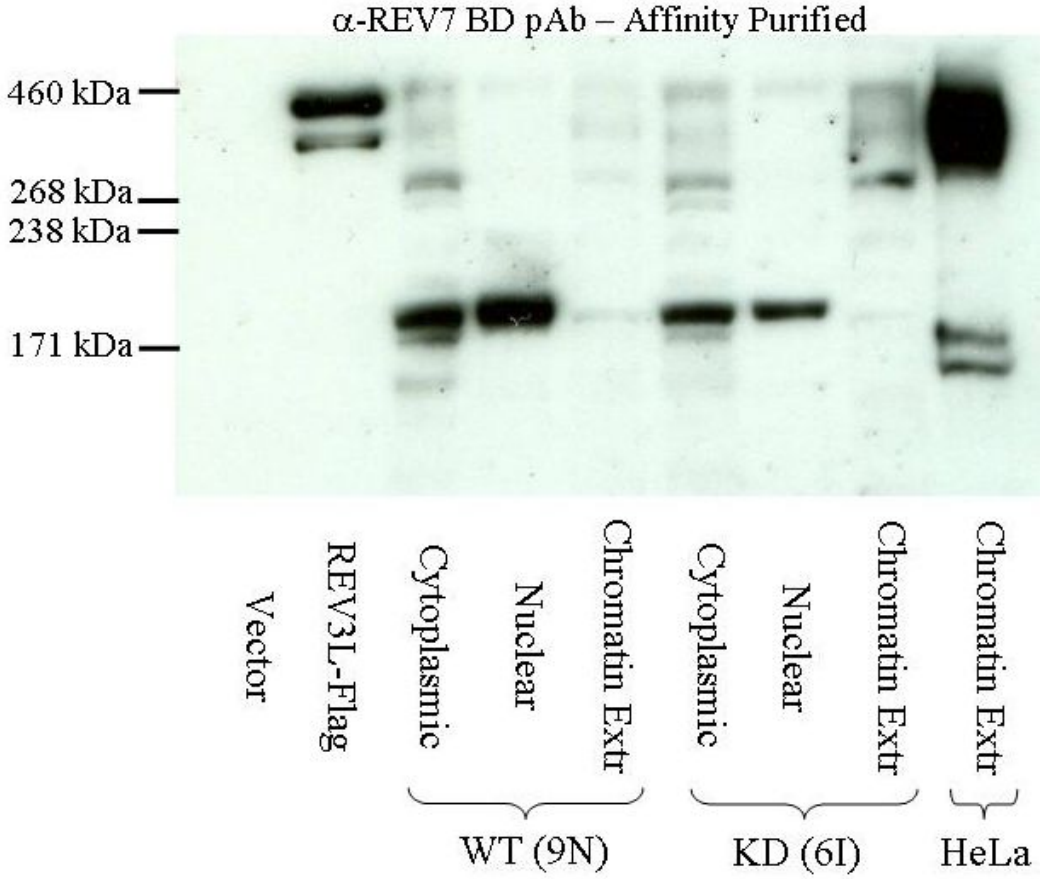

Figure 2.12 Immunoblotting for endogenous human REV3L in human foreskin fibroblasts treated with REV3L anti-sense.

2 x10^7 cells were processed using a small-scale subcellular fractionation protocol. 60 μg of each protein extract was resolved on a 3-8% Tris-acetate SDS-PAGE gel, transferred onto 0.45 μm PVDF and immunoblotted using the affinity-purified anti-Rev7 Binding Domain antibody. The positive and negative control lane consisted of 10 μl of Flag immunoprecipitated REV3L-HF protein or vector control protein loaded as a sizing control.

400 and 460 kDa in the nuclear and chromatin extracts of both cells. These correspond to two similar high molecular weight bands observed in Flag immunoprecipitated REV3L-HF samples (Figure 2.13B). In order to verify the observed band was due to extract preparation, I examined three different large-scale Ramos cell extracts prepared using three different methods. In all three methods, the same high molecular weight band was detected in 60 μg protein extracts using the affinity purified anti-Rev7 Binding Domain antibody. However, analysis of those same extracts using the anti-N-terminal Domain antibody did not yield a similar high molecular weight banding pattern (Figure 2.14). In order to determine whether the high molecular weight band observed was REV3L, *REV3L* shRNA retroviral constructs were generated in order to knock down endogenous and exogenous REV3L expression in HeLa and in a REV3L conditional overexpression cell line.

2.3.5 REV3L-HF Wild-type and Active-Site Mutant Expression Cell Line

Attempts by various labs as well as our own to generate a full-length REV3L expression cell line have been largely unsuccessful. An attempt trying to engineer a constituitively expressed REV3L in a variant Flp-in 293T mammalian expression cell line (Invitrogen) proved unable to express full-length REV3L (data not shown). Promising resultswere finally achieved using the Flp-in 293T-Rex inducible mammalian expression cell line (Invitrogen). The number of individual clonal REV3L cells was limited as well as their ability to attach to their tissue culture dishes was worse compared to the vector control cell lines. Low plating density (1 x10^6 cells) proved disadvantageous for overall cell fitness and growth compared to plating higher cell

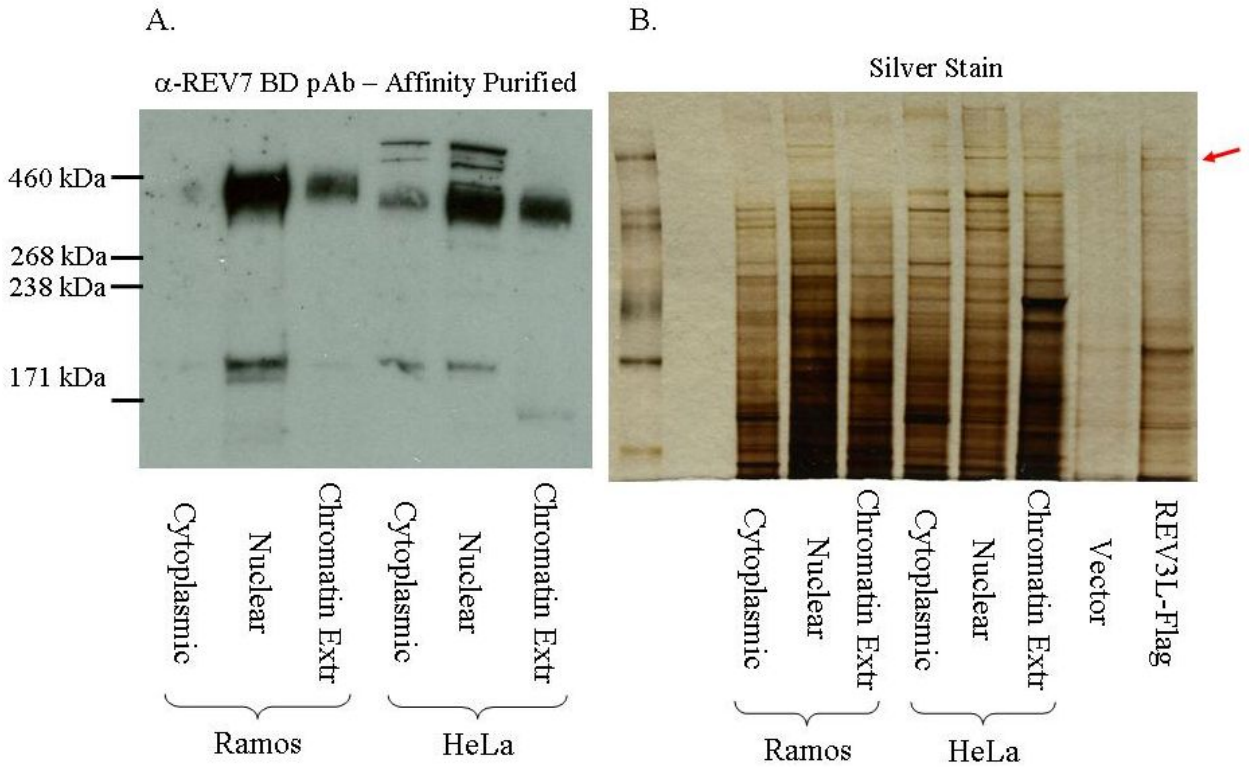

Figure 2.13 Immunoblotting for endogenous human REV3L in Ramos and HeLa cell lines.

1 x10^9 cells were processed for each cell line using a large-scale, subcellular fractionation extract protocol. 60 µg of each protein extract was resolved on a 3-8% Tris-acetate SDS-PAGE gel, transferred onto 0.45 µm PVDF and immunoblotted using the affinity-purified anti-Rev7 Binding Domain antibody. On another gel, the same amount of protein was resolved on an SDS-PAGE gel and subjected to silver stain analysis. The positive and negative control lane consisted of 10 µl of Flag immunoprecipitated REV3L-HF protein or vector control protein loaded as a sizing control.

densities. This phenomenon was not as prevalent with the vector control plasmids. When screening the initial pooled population of cells by immunoblot, a weak signal was detected for full-length REV3L-HF in the pooled sample of cells. Screening the available wild-type and active-site mutant clones demonstrated that very few clones could express either protein to any

appreciable level. However three potential clones – 2 wild-type and 1 active-site mutant – were isolated for further analysis (Figure 2.15).

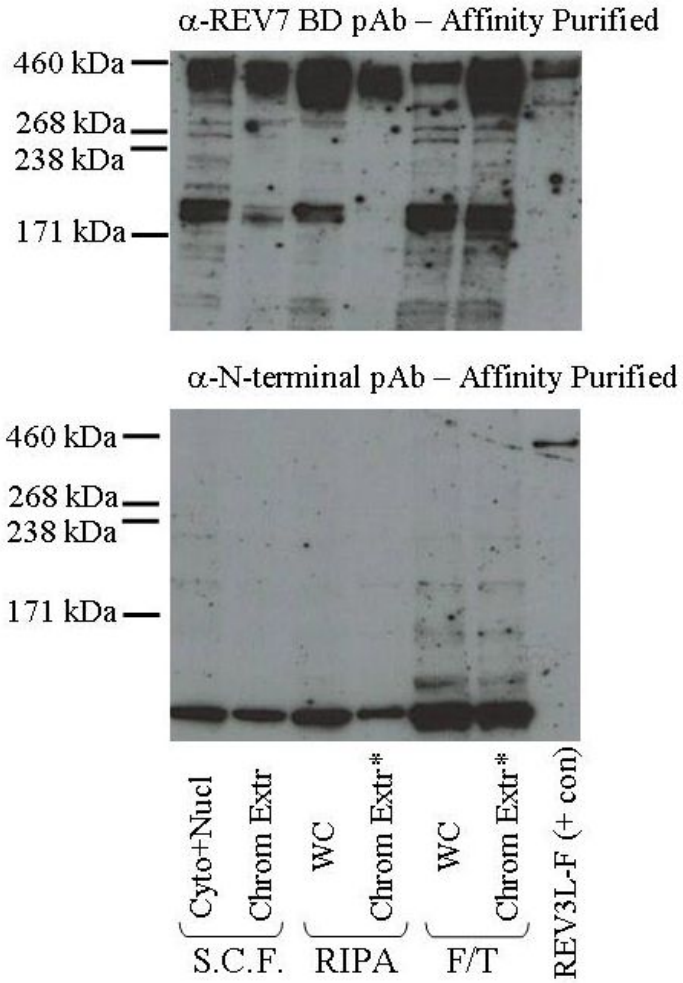

Figure 2.14 Examination of three different cell lysis protocols on the Ramos cell line.

1 x10^9 cell were lysed using three different methods. The first method involved subcellular fraction as previously described (Chapter 2). The second method involved a standard RIPA lysis buffer as described elsewhere(Chapter 3). The final method involved a Freeze-thaw lysis buffer as described elsewhere (Chapter 4). 60 µg of total protein was resolved on a 3-8% Tris-acetate SDS-PAGE gel, protein was transferred onto a 0.45 µm PVDF membrane and the membrane was blotted with either the affinity purified anti-Rev7 Binding Domain antibody or the anti-N-terminal Domain antibody. The positive control lane consisted of 10 µl of Flag immunoprecipitated REV3L-HF protein or vector control protein loaded as a sizing control.

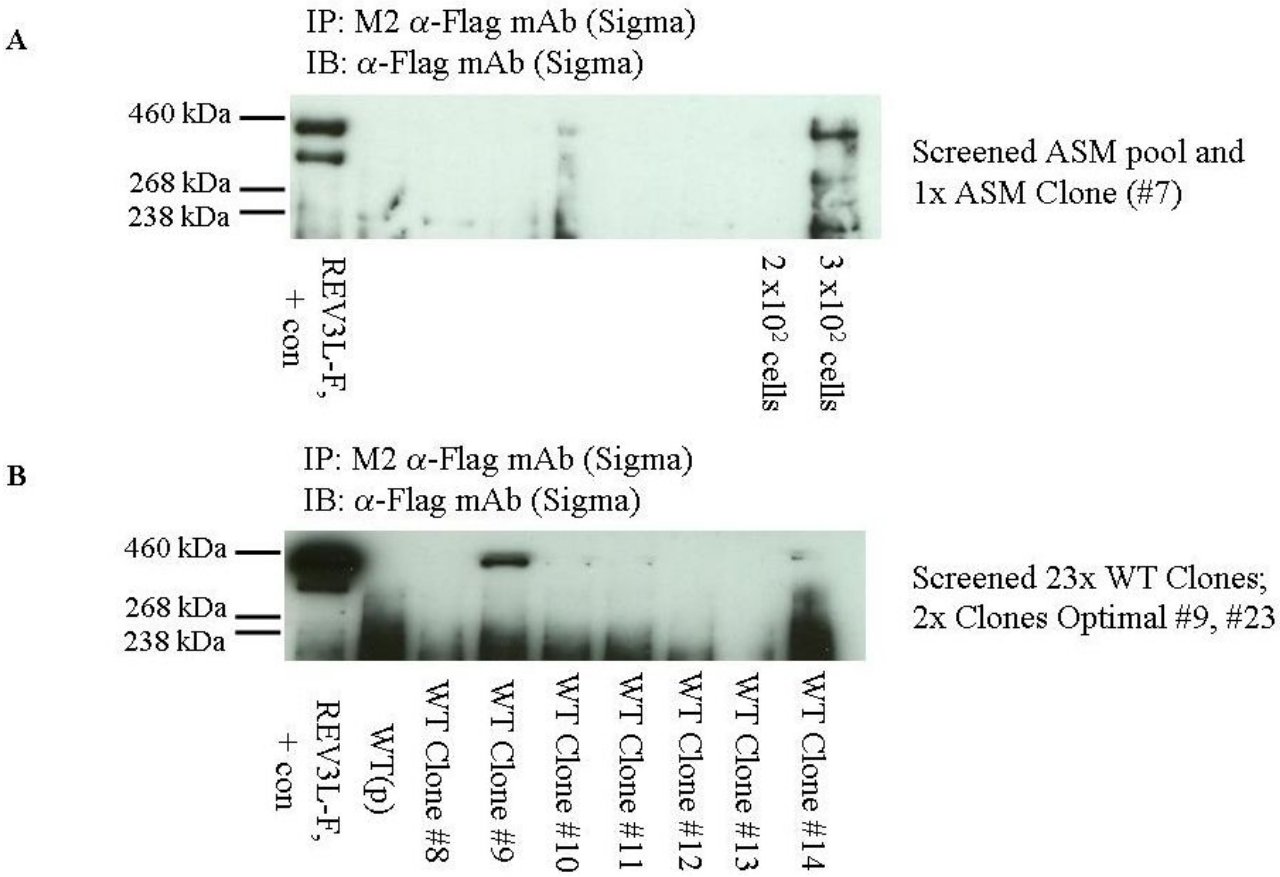

Figure 2.15 Immunoblot analysis of inducible 293T-Rex REV3L-HF wild type and active-site mutant cells.

3 x10^6 cells corresponding to each clone were seeded and given 48 hours to plate down on 2x 10 cm dishes. By 48 hours, the cells were induced with 0.1 μg/ml of doxycycline and given 18 hours to express REV3L-HF protein. Cells were lysed using RIPA buffer and immunoprecipitated using Flag M2 agarose. All of the immunoprecipitated protein was resolved on a 3-8% Tris-acetate SDS-PAGE gel, transferred on 0.45 μm PVDF membrane and immunoblotted using a αFlag M2 antibody. The positive control lane consisted of 10 μl of Flag immunoprecipitated REV3L-HF protein or vector control protein loaded as a sizing control.

2.3.6 Knockdown of Human REV3L by shRNA

Systems Bioscience Inc, constructed three potential shRNA sequences using a proprietary shRNA determination algorithm. Two of the sequences specifically targeted the region I of the polymerase domain and one at the C-terminal end of the REV3L gene (Figure 2.16). All three shRNA plasmids (#1, #2 and #3) were intended to be co-transfected with two other assembly plasmids into 293FT cells enabling generation of a replication incompetent shRNA retrovirus. Initial transduction results indicated that the Maher cell line and the 293T-Rex inducible REV3L-HF WT Cl#9 inducible cell line were highly transducible as observed by eGFP

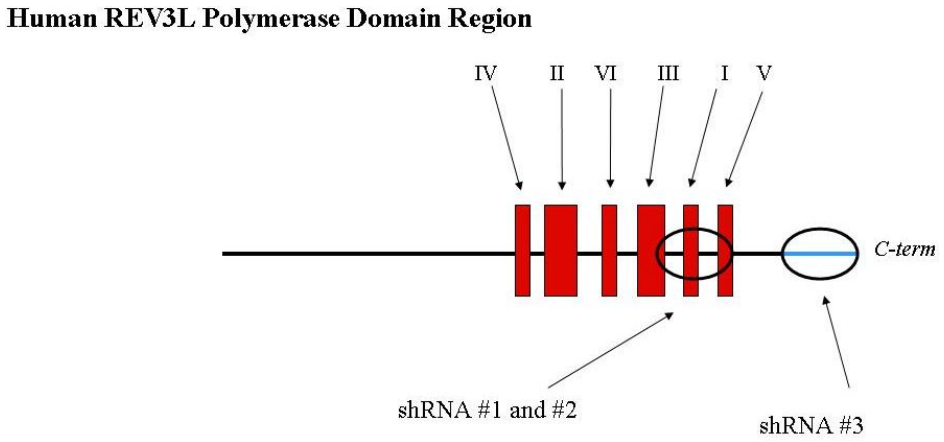

Lentiviral FIV retroviral system (System Bioscience, Inc)

Figure 2.16 Schematic diagram illustrating the location of where the three shRNA constructs anneal to in the REV3L cDNA.

shRNA #1 anneals just upstream of Region I of the polymerase domain. shRNA #2 anneals just downstream of Region I of the polymerase domain. shRNA #3 anneals at the C-terminal end. These plasmids were 1 of 3 needed to generate the three REV3L shRNA retroviral vectors.

fluorescence. HeLa however was more difficult to infect. Both the Maher and 293T expression cell line underwent two rounds and were ~70 – 80% green by the second round of transduction while the HeLa required three rounds of transduction and were only 20% green. All cell populations were FACSorted inorder to enrich for a pooled population of green, retrovirally infected, shRNA integrated cells. HeLa pooled knock down cells were examined both by RT-PCR and by immunoblotting with affinity-purified anti-Rev7 Binding Domain antibody. Results by RT-PCR indicated that the REV3L shRNA #2 retrovirus could diminish the amount of endogenous REV3L mRNA (Figure 2.17A). Those same cells were harvested using a RIPA lysis buffer protocol. Similarly, two high molecular weight bands (greater than 460 kDa) are diminished in band intensity for the shRNA#2 transduced cells compared to vector control or shRNA #1 or #3 (Figure 2.17B). One method used to validate whether the shRNA's could knock down REV3L expression was to transduce the inducible 293T-Rex REV3L-HF WT Cl#9 cell line. RT-PCR was not performed on these cell lines because we were interested in the final outcome of the REV3L gene product. Therefore, protein expression was the final endpoint which would indicate whether the REV3L shRNA retroviruses were effective. Comparison of all three shRNAs in these cells treated with doxycycline indicated that the overexpressing REV3L could not be suppressed using any of the shRNA retroviruses (Figure 2.18). Individual clones although isolated were not individually examined for REV3L knockdown in protein. Having acquired another shRNA construct (shREV3-PIG) which supposedly demonstrated an ability to knock down REV3L mRNA by 70% (47), this plasmid was transfected into either REV3L shRNA retrovirally transduced HeLa and 293T-Rex REV3L cells or the non-transduced parental controls. Results similarly demonstrated that successful selection using puromycin of pooled cells transfected with this plasmid were unable to knockdown REV3L protein expression

when cells were induced with doxycycline (data not shown). At this moment, further work on the REV3L shRNA plasmids have been halted and attempts at trying to verify whether the bands observed in HeLa are REV3L specific bands have also been stopped. The REV3L specific antibodies will be used to detect recombinant expressed full-length human REV3L.

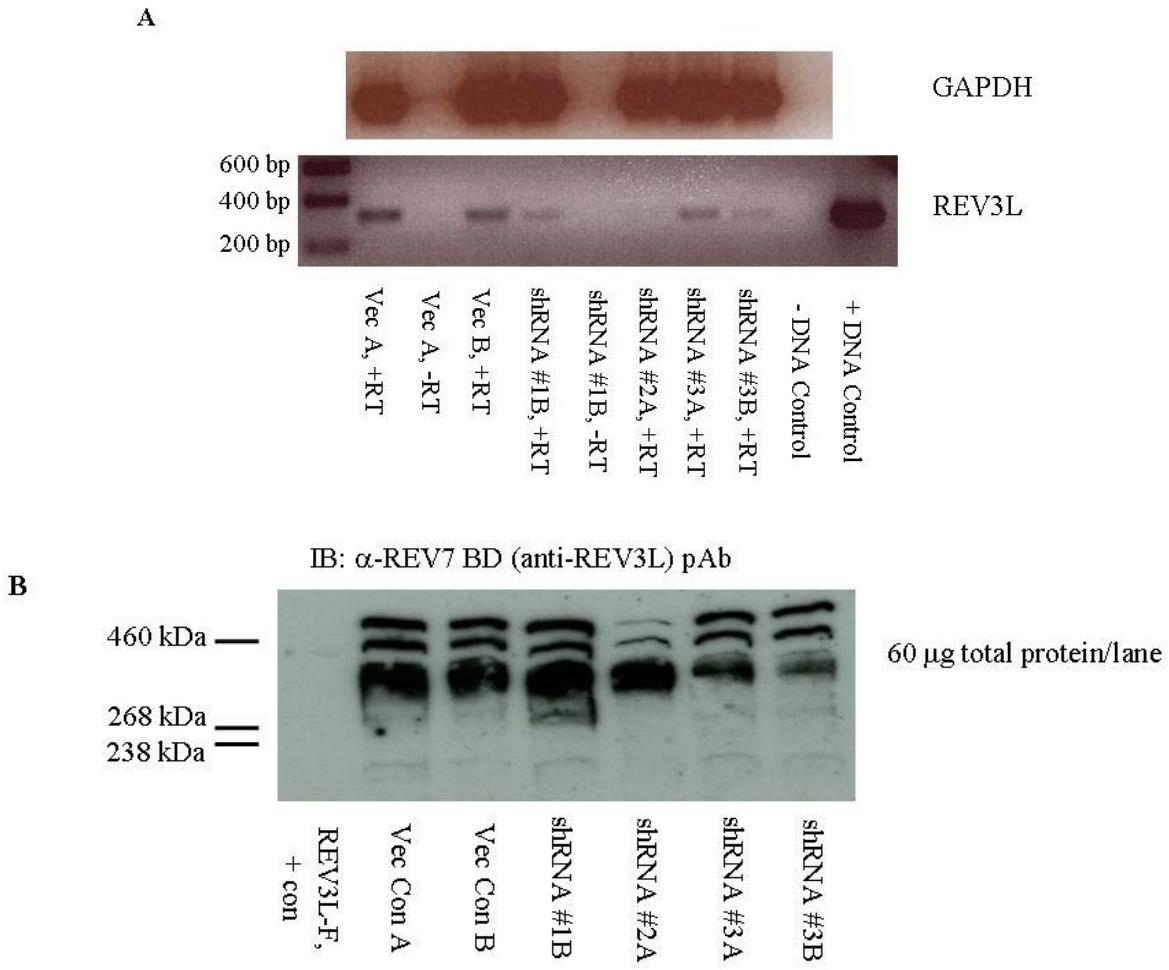

Figure 2.17 Determining endogenous REV3L expression in HeLa cells suppressed using three different REV3L shRNA retroviruses.

A. 8000 cell were processed in order to generate cDNA using a commercial kit for RT-PCR analysis of REV3L and the control gene, GAPDH. Endogenous REV3L and GAPDH were amplified using Platinum Taq and 0.6 µM Forward and Reverse primers which span intronic segments. B. 2 x10^7 HeLa cells were lysed using a hi-salt RIPA lysis buffer and 60 µg of protein extract was resolved using a 3-8% Tris-acetate SDS-PAGE gel. Protein was transferred onto a 0.45 µm PVDF membrane and blotted using an affinity purified anti-Rev7 Binding Domain antibody.

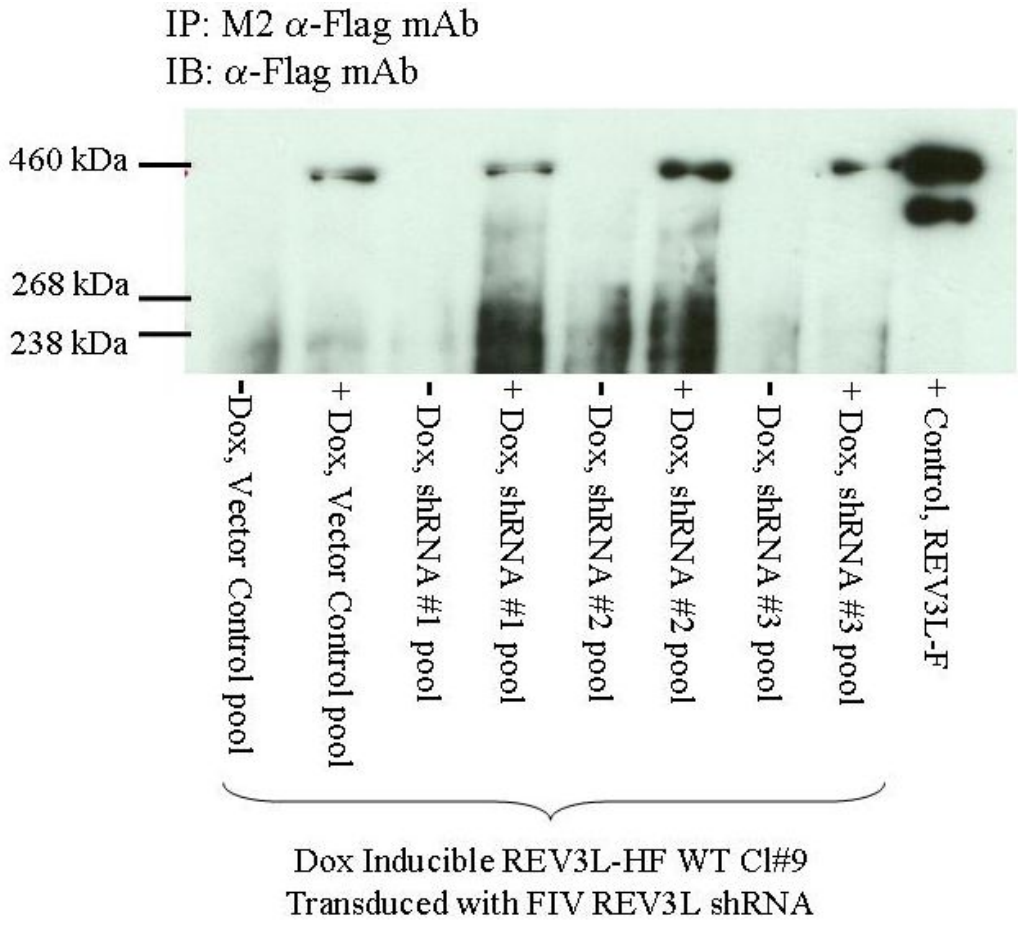

Figure 2.18 Immunoblot analysis of REV3L shRNA transduced into an inducible 293T-Rex REV3L-HF wild type, Clone #9 cell line.

3 x10^6 cells corresponding to each clone were seeded and given 48 hours to plate down on 2x 10 cm dishes. By 48 hours, the cells were induced with 0.1 μg/ml of doxycycline and given 18 hours to express REV3L-HF protein. Cells were lysed using a hi-salt RIPA buffer and immunoprecipitated using Flag M2 agarose. All of the immunoprecipitated protein was resolved on a 3-8% Tris-acetate SDS-PAGE gel, transferred onto 0.45 μm PVDF membrane and immunoblotted using a αFlag M2 antibody.

2.4 DISCUSSION

2.4.1 Optimization of the Anti-REV3L Specific Antibodies for the Detection of Recombinant Human Full-length REV3L

The work contributed in this thesis is the generation of two (potentially four) affinity-purified anti-REV3L specific antibodies able to detect the full-length human REV3L protein. Other labs and commercial entities (100,101) claim to have developed specific anti-human REV3L antibodies generated against small REV3L polypeptide fragments. However, the antibodies generated for this dissertation are unique because they have demonstrated interaction with both the polypeptide fragments they were generated against as well as the full-length protein. Furthermore, these antibodies demonstrate an ability to bind to a potential endogenous REV3L protein in HeLa that is partially decreased when using a REV3L shRNA retrovirus. These results are potentially exciting but will need to be further confirmed using an alternative method to validate that the detected band is indeed human REV3L.

The potential applications of these antibodies have not been fully explored. These antibodies have predominantly been used for immunoblot. However, they should also be examined for potential application in ELISA, immunofluorescence and immunoprecipitation. For immunofluorescence, only basic work has been done using the N-terminal antibody. Although the first experiment yielded negative results, the full spectrum of conditions have yet to be examined. Therefore, further work with the REV3L antibody project is merited.

2.4.2 Detection of Endogenous and Recombinant Expression of Human REV3L in Cells and the Role of shRNA on REV3L Function

Further speculation as to why mammalian REV3L levels may be low are based on a 5' untranslated region in the mRNA coding for a stem-hairpin loop presumed to potentially inhibit expression of the protein (75). Furthermore, splice variants have been found coding for a 128 bp insert early in the mRNA which introduces a premature stop codon terminating potential REV3L protein translation (76,83). Having high levels of Rev3 protein could be problematic in normal DNA synthesis leading to increased cellular mutagenesis. The obvious consequence of this in higher vertebrates is oncogenesis. One way in which a cell could get around this problem is compartmentalization of the protein away from DNA and recruitment only during specific times. Another way in which a cell could regulate Rev3 expression would be to upregulate the protein during times of genotoxic stress or post-translational modification activating the protein in response to DNA damage. Recent work in yeast indicates that Rev3 and Rev7 are constitutively expressed (correspondence with G. Walker) while Rev1 is upregulated during G_2/M (54). Furthermore, work has demonstrated that Rev1 interacts with Rev3 and yeast Pol Zeta (40,99). This would suggest that Rev3 is incapable of engaging with DNA without Rev1 and may suggest a compartmentalization model rather than need for upregulation in yeast. However, if this model were true in higher eukaryotes, then the various groups who had developed REV3L specific antibodies and were studying mammalian full-length REV3L would have reported detection of the full-length protein much sooner. This would argue in favor of the possibility that mammalian REV3L is expressed at very low levels in cells but does not rule out the possibility that REV3L is still compartmentalized.

Our work both with the two affinity purified REV3L specific antibodies, the recombinant REV3L protein and the various REV3L overexpression and knockdown cell lines demonstrates three things. First, a majority of recombinant REV3L remains trapped in the gel with only a small amount transferring onto the PVDF membrane (data not shown). Studies examining the amount of REV3L protein transferred by silver stain pre and post-transfer onto a 0.45 μm PVDF membrane indicate that ~99% of the protein remains trapped within the gel. The reason why recombinant REV3L remains trapped in the gel is probably due to its large size preventing it from adequately transferring like smaller proteins. The consequence of these findings indicates if endogenous REV3L is expressed at very low levels in cells, then a majority of the protein will remain trapped in the gel and may never be visualized by immunoblot. This discovery may be a significant technical hurdle which must be overcome if one intends to study the endogenous protein. Second, the REV3L specific antibodies were unable to delineate an endogenous REV3L specific protein band in various normal and tumorigenic human cell lines regardless of knockdown using various *REV3L* shRNA retroviruses or a *REV3L* shRNA plasmid. Examination of mouse testis, heart and brain tissue yielded no discernable REV3L signal by immunoblot. Complicated by the above technical findings, a potential endogenous REV3L specific band in Maher's human foreskin fibroblast parental cell line compared to the REV3L anti-sense cell line could not be visualized. However, it was observed a robustly expressed band migrating at the same distance as the recombinant protein and this corresponded with the predicted molecular weight of REV3L. Further analysis by knockdown of endogenous REV3L using various shRNA retroviruses indicated suppression of endogenous *REV3L* transcript and possible knockdown in HeLa protein extracts. Unfortunately, without confirmation that the shRNA constructs were in fact knocking down endogenous REV3L protein, these studies remain

inconclusive. In order to verify whether the shRNA constructs could knock down REV3L transcript (and therefore recombinant REV3L protein), validation of the shRNA constructs in the inducible cell line was attempted. It was concluded that these REV3L shRNA retroviruses and plasmid were unable to knockdown the inducible REV3L overexpression cell line as determined by immunoprecipitation and immunoblot. The potential reasons for this may be due to the large amount of REV3L mRNA generated within the cell upon induction and an inability of REV3L shRNA to adequately suppress. Though a potentially valid explanation, it does not explain why protein levels are not even minimally suppressed compared to the parental clone containing the vector control shRNA. The REV3L suppressed cells were subjected to a second round of REV3L shRNA knockdown using a published plasmid reported to be able to suppress endogenous REV3L. Even with this second round of suppression, recombinant REV3L could not be knocked down as determined by immunoprecipitation and immunoblot. Therefore, it can only be concluded that the shRNA is unable to knock down the inducible REV3L expression cell line. Furthermore, REV3L mRNA is knocked down in the HeLa cell line, but remains unconfirmed for suppression of endogenous REV3L protein. The inability to detect REV3L protein in these cells has severely limited endogenous REV3L cell studies. Because of these results, the REV3L specific antibodies have been used to only detect recombinant REV3L as described in Chapters 3 and 4.

3.0 REV3L CLONING AND PROTEIN EXPRESSION

3.1 INTRODUCTION

A class of genes known as REV (or reversionless) were found to be involved with UV-induced mutagenesis in yeast *Saccharomyces cerevisiae* (102). It was later shown that the yeast gene, Rev3 was responsible for much of the UV-induced mutagenesis observed in S.cerevisiae (19). Yeast Rev3 cDNA encodes for a 173 kDa protein. Twenty years later, Lawrence's group identified that yeast Rev3 was a DNA polymerase capable of bypassing abasic site lesions (103). Work by other groups demonstrated that REV3L may work in conjunction with other polymerases *in vitro* to bypass a variety of different lesions that may be encountered in the cell (22-24). Extensive work has been done to try and find a human homologue to yeast Rev3. Various groups using different methods characterized two major human REV3L DNA homologues – one that encodes for a predicted 3,053 amino acid protein (82) and another that codes for a predicted 3,130 amino acid protein (69,75). Cloning and expression of the full-length human proteins are of extreme importance. However, due to the large size of both the cDNA and the protein, expression so far has been limited to only fragments. Our goal was the expression of the full-length 3,130 amino acid protein which would allow for analysis of REV3L function and its potential interaction partners. In order to study potential protein interaction (Chapter 4), the full-length human REV1 and REV7 was also cloned.

3.2 METHODS

3.2.1 Cloning full-length recombinant human REV3L

The full-length cDNA for human REV3L was acquired from Zhigang Wang (75). They constructed the plasmid in a modified pUC19M1 vector. In order to manipulate the large cDNA, REV3L was subcloned into pBluescript II KS+ in two parts (Figure 3.1A). REV3L-pUC19M1 was sequentially restriction enzyme digested first with XhoI and then with SalI. pBluescript II KS+ was digested with SalI and then alkaline phosphatase treated (Figure 3.1B). For REV3L, two fragments were generated, a 6146 bp piece and a 4345 bp piece designated fragments A and B, respectively. Single digestion of pBluescript linearized the vector. All three fragments were purified using a standard gel purification kit (Qiagen). Fragment A was ligated to dephosphorylated, linearized pBluescript II KS+. Ligation of Fragment A's XhoI site into the vector's SalI site destroyed the SalI RE site and created a new αTaqI site in exchange (Figure 3.1C). The ligated plasmid was transformed into DH5α library efficiency cells. Colonies were picked, restreaked on fresh LB/carbenicillin plates and inoculated into fresh LB/carbenicillin for mini-preps. DNA mini-prep isolations were done using the Wizard SV miniprep kit (Promega). Multiple rounds of diagnostic restriction enzyme digestions (PvuI, SalI, DraI and SapI) were used to confirm the correct integration of Fragment A into the vector backbone. Once orientation was confirmed, two clones were chosen and designated as pG^2-3 and pG^2-4. A maxi-prep was generated for pG^2-3. pG^2-3 was linearized with SalI and then treated with alkaline

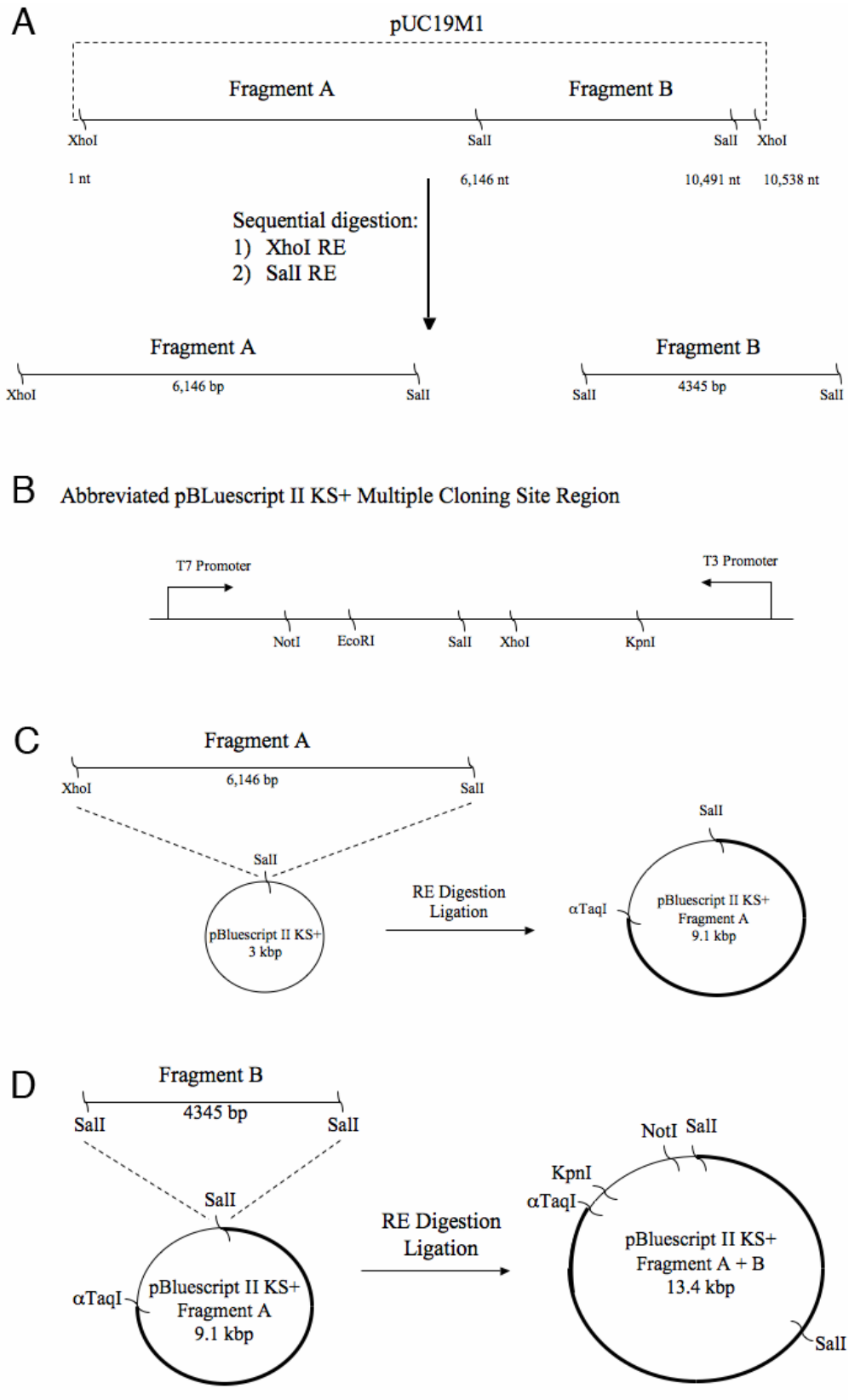
A
pUC19M1
Fragment A
Fragment B
XhoI
SalI
SalI
XhoI
1 nt
6,146 nt
10,491 nt
10,538 nt
Sequential digestion:
1) XhoI RE
2) SalI RE
Fragment A
6,146 bp
XhoI
SalI
Fragment B
4345 bp
SalI
SalI
B
Abbreviated pBLuescript II KS+ Multiple Cloning Site Region
T7 Promoter
T3 Promoter
NotI
EcoRI
SalI
XhoI
KpnI
C
Fragment A
6,146 bp
XhoI
SalI
SalI
pBluescript II KS+
3 kbp
RE Digestion
Ligation
SalI
αTaqI
pBluescript II KS+
Fragment A
9.1 kbp
D
Fragment B
4345 bp
SalI
SalI
SalI
αTaqI
pBluescript II KS+
Fragment A
9.1 kbp
RE Digestion
Ligation
NotI
SalI
KpnI
αTaqI
pBluescript II KS+
Fragment A + B
13.4 kbp
SalI

Figure 3.1 Scheme for subcloning hREV3L into pBluescript II KS+.

A. pUC19M1-hREV3L plasmid was acquired from Zhigang Wang (U. Kentucky). This plasmid was digested with restriction enzymes XhoI and SalI generating a 6146 bp and a 4345 bp fragment each. B. A diagram illustrating an abbreviated pBluescript II KS+ (pBlue2) multiple cloning site map. pBlue2 was linearized by SalI and then dephosphorylated by alkaline phosphatase. C. Fragment A was ligated into the linearized pBlue2 vector. Ligation of XhoI (Fragment A) to Sal I (vector) destroyed the XhoI site and created a new αTaqI site. D. pBlue2-Fragment A plasmid was linearized with SalI, alkaline phosphatase treated, gel purified and ligated to SalI digested, gel purified Fragment B.

phosphatase and gel purified. Fragment B was ligated to linearized pG^2-3 and transformed into DH5α max efficiency cells (Figure 3.1D). Potential colonies were selected and processed as described above and diagnostic restriction enyzme digestions (SalI, XhoI, SalI-XhoI, DraIII, BamHI, EcoRI-XhoI, BsaWI, BstXI) (NEB) were used to confirm the correct integration of Fragment B into the vector backbone (Figure 3.2). The restriction enzyme fragment sizes for SalI (9106, 4345 bp), XhoI (13,451 bp), SalI-XhoI (6151, 4345, 2955 bp), DraIII (6631, 3700, 3084, 36 bp), BamHI (4391, 3642, 2099, 1572, 1354, 393 bp), EcoRI-XhoI (10523, 2928 bp), BsaWI (7704, 4769, 831, 147 bp), and BstXI (10,650, 2801 bp) digested pBluescript II KS+-hREV3L plasmid were predicted using Vector NTI 9.0 (Invitrogen). Positive clones were submitted to the University of Pittsburgh DNA Sequencing Core facility in order to ascertain the subcloned REV3L cDNA did not have any mutations. A single plasmid was obtained and designated pG^2-5. A single base polymorphism (A→G) was detected in the original cDNA from Zhigang Wang (pUC19M1-hREV3L) which was not present in the Lawrence-Gibbs cDNA. This polymorphism changes amino acid 1796 from an aspartate to a serine.

With the cDNA in pBluescript II KS+, REV3L could be moved to the shuttle vector, pENTR1a, for use with the Invitrogen Gateway Expression System. REV3L cDNA was RE digested from pG^2-5 and subcloned into pENTR1a using RE's KpnI and NotI. This clone (pG^2-8) was not sequenced but was examined by multiple RE digestions (KpnI, NotI, KpnI-NotI,

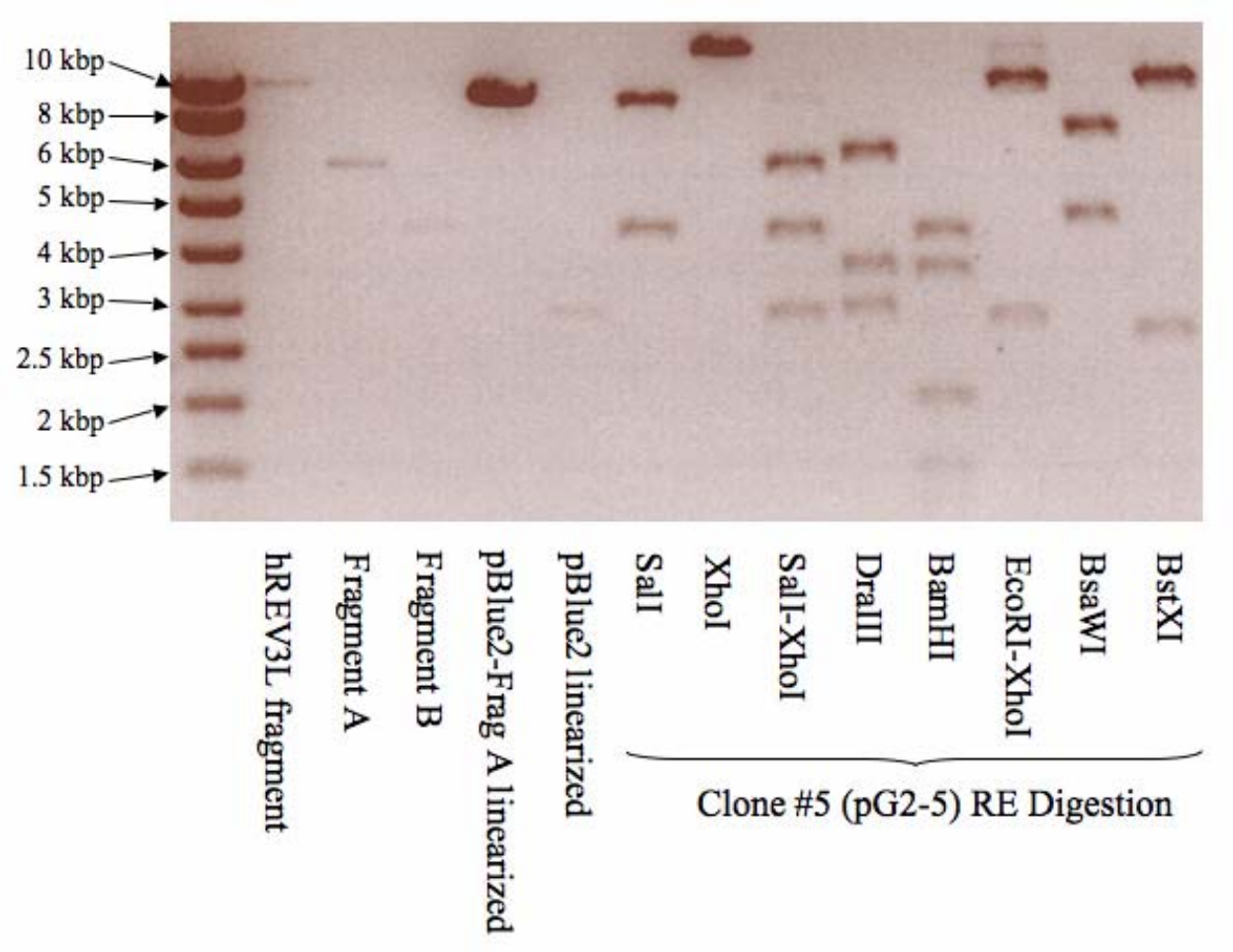

Figure 3.2 Diagnostic restriction enzyme digestion of pBluescript II (KS+)-hREV3L (pG2-5).

In order to confirm correct orientation of hREV3L in pBluescript II (KS+), 600 ng of plasmid was digested with multiple enzymes: SalI, XhoI, SalI-XhoI, DraIII, BamHI, EcoRI-XhoI, BsaWI, and BstXI for 5 hours in a 20 µl volume at the prescribed temperature recommended by NEB. The DNA samples was resolved on a 0.7% Tris-acetate EDTA agarose gel supplemented with ethidium bromide and run at 70 V for 1 hour.

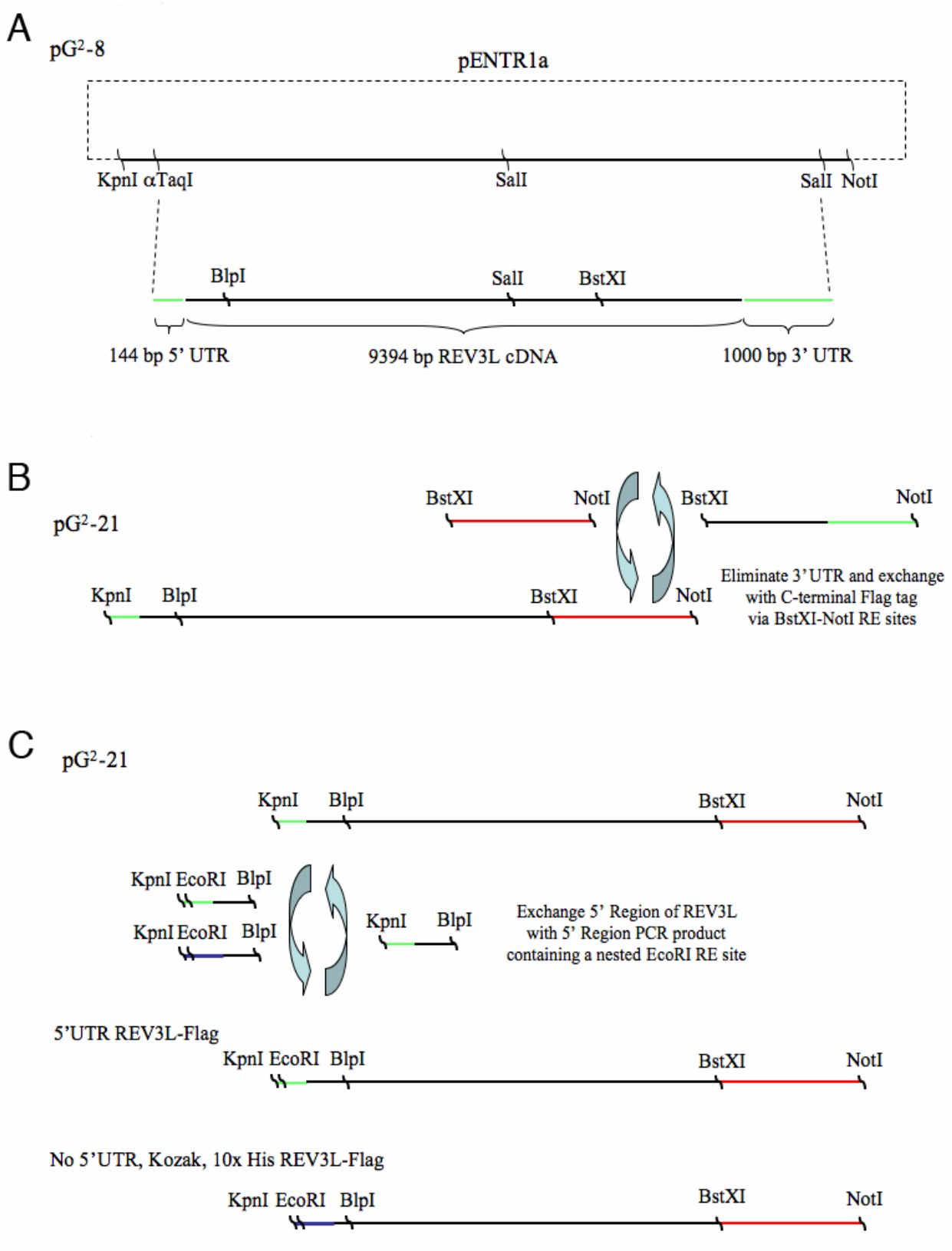
A
pG2-8
pENTR1a
KpnI αTaqI
SalI
SalI NotI
BlpI
SalI
BstXI
144 bp 5' UTR
9394 bp REV3L cDNA
1000 bp 3' UTR
B
pG2-21
BstXI
NotI
BstXI
NotI
KpnI
BlpI
BstXI
NotI
Eliminate 3'UTR and exchange
with C-terminal Flag tag
via BstXI-NotI RE sites
C
pG2-21
KpnI
BlpI
BstXI
NotI
KpnI EcoRI BlpI
KpnI EcoRI BlpI
KpnI
BlpI
Exchange 5' Region of REV3L
with 5' Region PCR product
containing a nested EcoRI RE site
5'UTR REV3L-Flag
KpnI EcoRI BlpI
BstXI
NotI
No 5'UTR, Kozak, 10x His REV3L-Flag
KpnI EcoRI BlpI
BstXI
NotI

Figure 3.3 Modification of the 5' and 3' region of hREV3L cDNA.

A. Diagram depicting pENTR1a-hREV3L (pG2-8). pG^2-8 was constructed by digesting pG^2-5 with KpnI and NotI (RE flanking hREV3L cDNA in the MCS) and ligating this fragment to KpnI-NotI digested pENTR1a. B. pG^2-8 was digested with BstXI-NotI removing part of hREV3L's polymerase domain and all of the 3' UTR. A PCR fragment coding for the removed polymerase domain portion and a C-terminal Flag tag was used to replace the original. C. Introducing an EcoRI restriction enzyme (RE) site into pG2-21 and pG2-25 for subcloning into the mammalian expression vector, pTSIGN. The REV3L 5' region of interest (5' UTR and no 5' UTR, Kozak, 10x His tag) containing a nested EcoRI RE site was generated by PCR. pG^2-21 and pG_2-25 were each digested with KpnI and BlpI and the PCR product for each was ligated, respectively, into both plasmids.

BamHI, SalI). All subsequent modifications to the REV3L cDNA was performed using the pG^2-8 plasmid (Figure 3.3A) as template.

The first modification to the parent pG^2-8 consisted of eliminating the 3' UTR and adding a C-terminal Flag tag. Refer to Figure 3.5a. First, a 1,799 bp PCR fragment was generated in a 25 μl PCR tube using 0.2 and 0.4 μM of the "no 3' UTR" Forward and "no 3' UTR – p5" Reverse primers, respectively, 1.25 U of Turbo Pfu (Strategene), 400 μM dNTP and 5 ng of pG^2-5 (Appendix). PCR fragments were gel purified, sequentially digested with BstXI (NEB), then with NotI (NEB) and finally gel purified. Gel purification was performed using a commercial kit (Qiagen). The vector was prepared by similarly sequentially digestion with BstXI and then with NotI generating two fragments, a 2,815 bp and a 10,014 bp. The vector was then alkaline phosphatase (Roche) treated and gel purified. The gel purified RE digested PCR product and linearized vector was ligated overnight at 16ºC using T4 DNA ligase (Strategene). Ligated plasmid was transformed into E.coli Stbl2 (Invitrogen) bacterial cells and plated on kanamycin resistant LB agar plates and grown at 30ºC overnight. Colonies were picked the next day, restreaked onto fresh plates and small-scale DNA minipreps cultures grown overnight at 30ºC, shaken at 225 RPM. DNA from mini preps was prepared using a commercial kit (Promega). Potential colonies were subjected to two rounds of diagnostic digestions (SalI and

BamHI) and then sent for sequence analysis. Correct plasmids were designated pG^2-21 and pG^2-22.

Using pG^2-21 as a backbone, the next modification was elimination of the 5'UTR and introduction of an optimized mammalian Kozak sequence. The optimized mammalian Kozak sequence, ***ACC ATG G*NN**, was described in an Invitrogen cloning catalogue (pENTR Manual) based on work by Marilyn Kozak (104-106). In order to eliminate the 5' UTR, a PCR product containing the optimized mammalian Kozak sequence and lacking the 5' UTR had to be generated. The no 5' UTR – p1 Forward primer and the no 5' UTR Reverse primer was used (Appendix A). The PCR product was gel purified and both the PCR product and pG^2-21 were digested with KpnI (NEB) and BlpI (NEB) sequentially. The vector was subsequently alkaline phosphatase treated and both the digested PCR product and plasmid were further gel purified. The gel purified DNA was then ligated overnight and transformed into Stbl2 cells and grown at 30ºC until the next day. Potential colonies were picked, restreaked on fresh kanamycin agar plates and inoculated into fresh LB-kanamycin and grown at 30ºC, overnight for DNA mini-preps the next day. Correct plasmid orientation was selected based on two diagnostic digestions (SalI and BamHI) and then sent for sequence analysis. Correct plasmids were designated pG^2-23 and pG^2-24.

Using pG^2-21 as a backbone, another modification was elimination of the 5'UTR and introduction of both an optimized mammalian Kozak sequence and a 10x His tag. In order to eliminate the 5' UTR, a PCR product containing the optimized mammalian Kozak sequence and 10x His tag minus the 5' UTR had to be generated. The no 5' UTR – p2 Forward primer and the no 5' UTR Reverse primer was used (Appendix A). The PCR product was gel purified and both the PCR product and pG^2-21 were RE digested with KpnI (NEB) and BlpI (NEB) sequentially.

The vector was subsequently alkaline phosphatase treated and both the digested PCR product and plasmid were further gel purified. The gel purified DNA was then ligated overnight and transformed into Stbl2 cells and grown at 30ºC until the next day. Potential colonies were picked, restreaked on fresh kanamycin agar plates and inoculated into fresh LB-kanamycin and grown at 30ºC, overnight for DNA mini-preps the next day. Correct plasmid orientation was selected based on two diagnostic digestions (SalI and BamHI) and then sent for sequence analysis. Correct plasmids were designated pG^2-25 and pG^2-26.

In order to subclone the modified REV3L cDNA into pTSIGN, an EcoRI site had to be engineered into the various REV3L-pENTR vectors. Refer Figure 3.3C. Using the parent vector, pG^2-8, two PCR fragments were generated. Both fragments contained an internalEcoRI site which would allow integration of the new PCR fragment into the existing pENTR vector by KpnI and BlpI. Once integrated, the full-length modified cDNA was digested by EcoRI and NotI for subcloning into a linearized EcoRI-NotI digested, dephosphorylated pTSIGN vector. Refer to Figure 3.4. In brief, "EcoRI insert, 5' UTR REV3L" fragment was PCR amplified using 0.2 μM of "5' End, (5' primer) EcoRI insertion Forward primer" and the "No 5'UTR, Reverse primer", 1.25 U of Turbo Pfu, 400 μM dNTP and 5 ng of pG^2-8. The EcoRI insert, "no 5'UTR, Kozak-10x His tag REV3L" fragment was PCR amplified using 0.4 μM of "No 5' UTR, Kozak+10x His Forward primer" and "No 5'UTR, Reverse primer", 1.25 U of Turbo Pfu, 400 μM dNTP and 5 ng of pG^2-25. Refer to Appendix for PCR amplification protocol and PCR primers. Both PCR fragments were gel purified and then digested using KpnI and BlpI. These fragments were gel purified and ligated into gel purified, linearized dephosphorylated pG^2-8 or pG^2-25. Fragments were ligated overnight at 16ºC using T4 DNA ligase (NEB) and transformed the next day into Stbl2 chemically competent bacteria (Invitrogen). Potential colonies were

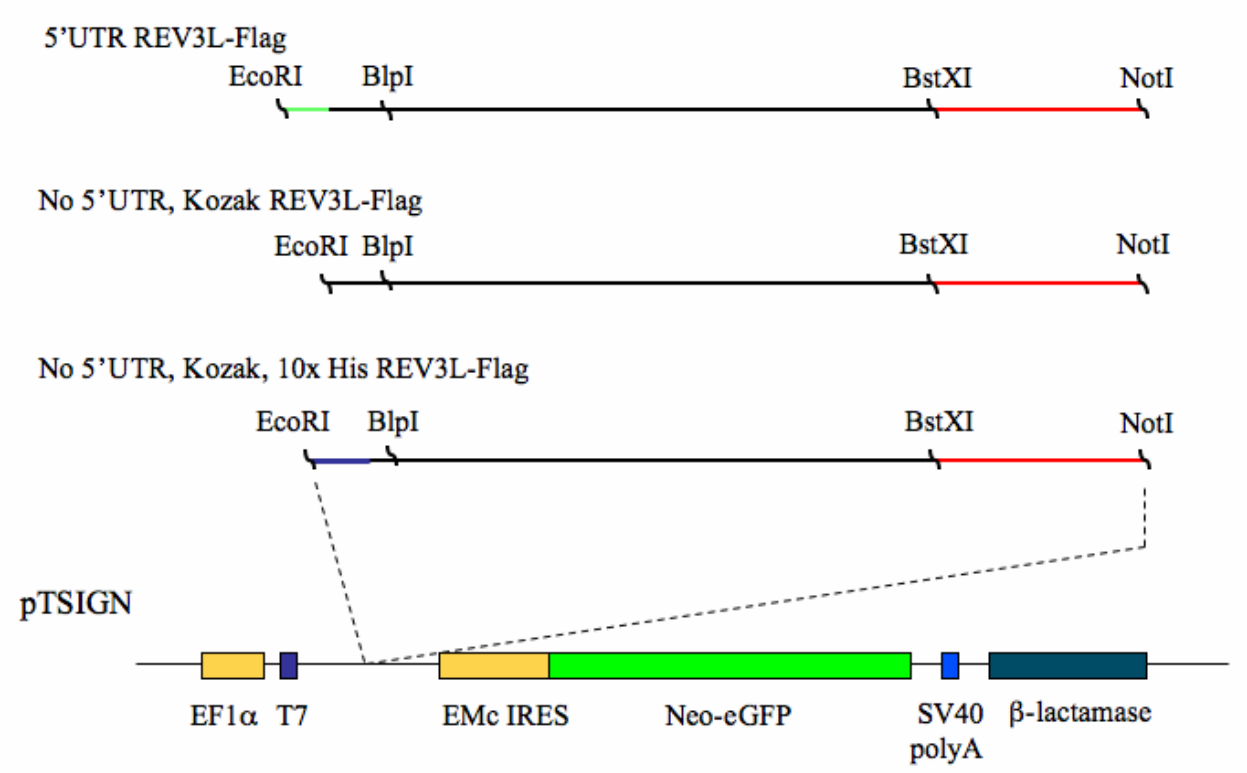

Figure 3.4 Subcloning of three modified hREV3L cDNA's from pENTR1a into the mammalian pTSIGN expression vector.

Subcloning of three modified hREV3L cDNA's from pENTR1a into the mammalian pTSIGN expression vector.

picked, restreaked on fresh kanamycin agar plates and inoculated into fresh LB-kanamycin and grown at 30ºC, overnight for DNA mini-preps the next day. Mini-prep DNA was linearized with EcoRI in order to determine integration of 5' Region PCR product. Potential clones were sent for sequence analysis. The two plasmids, one containing the modified 5' UTR and the other containing no 5'UTR with the 10x His, were both digested with EcoRI-NotI (NEB) simultaneously. Fragments were gel purified and ligated into gel purified, linearized EcoRI-NotI digested, dephosphorylated pTSIGN. Fragments were ligated overnight at 16ºC using T4 DNA ligase (NEB) and transformed the next day into Stbl2 chemically competent bacteria (Invitrogen) and plated onto LB carbenicillin agar plates. Next day, potential colonies were picked,

restreaked on fresh carbenicillin agar plates and inoculated into fresh LB-carbenicillin and grown at 30ºC, overnight for DNA mini-preps the next day. Correct plasmid orientation was selected based on multiple RE diagnostic digestions (PvuI, SapI, SalI-NotI, EcoRI) and then sent for sequence analysis.

The no 5'UTR-Kozak-REV3L-Flag modified cDNA was engineered in pENTR (pG^2-23) contained a nested EcoRI RE downstream of KpnI RE making lateral transfer to the pTSIGN vector simpler. pG^2-23was EcoRI-NotI (NEB) digested, gel purified (Qiagen) and subcloned directly into a linearized EcoRI-NotI digested, dephosphorylated pTSIGN backbone. Fragments were ligated overnight at 16ºC using T4 DNA ligase (NEB) and transformed the next day into Stbl2 chemically competent bacteria (Invitrogen) and plated onto LB carbenicillin agar plates. Next day, potential colonies were picked, restreaked on fresh carbenicillin agar plates and inoculated into fresh LB-carbenicillin and grown at 30ºC, overnight for DNA mini-preps the next day. Correct plasmid orientation was selected based on EcoRI-NotI RE diagnostic digestions and then sent for sequence analysis.

3.2.2 Cloning the REV3L Polymerase Domain Active-Site Mutant

Generating the REV3L polymerase domain active-site mutant was done by two-step PCR (107). Two critical residues in the active site of Region I, YG**DTD**S, of the REV3L polymerase domain were changed from aspartate to alanine residues (108). The first step was to generate the two overlapping fragments with the appropriate base substitutions. Refer to Appendix A for primer sequences used. Refer to Figure 3.5. Fragment A used PCR primers: "No 3' UTR Forward

primer (or p1)" and "Pol Dom Mutant p2 Reverse primer (or p2)" while Fragment B used PCR primers: "No 3' UTR – p5 (C-terminal Flag), Reverse primer (or p4)" and "Pol Dom Mutant p3 Forward primer (or p3). Refer to Appendix B for PCR protocols used to amplify both Fragment A and B. Fragment A was generated using 2.5 U of Turbo Pfu (Stratagene), 0.4 μM Forward and Reverse primers and 400 μM dNTP. Fragment B was generated using 2.5 U of Turbo Pfu (Stratagene), 0.2 μM of each primer, 400 μM dNTP and 5 ng of pTSIGN-REV3L-Flag tag. Once both fragments were generated and gel purified, the second step of PCR was initiated. Both PCR fragments were combined into one tube and PCR amplified. The combined A/B fragment was PCR amplified for 1 round using 2.5 U of Turbo Pfu and 400 μM dNTP at 72ºC for 4 minutes. Then, 0.4 μM Forward (p1) and Reverse primers (no 3' UTR – p5 Flag tag or p4) were added to the reaction and amplified. Refer to Appendix A and B for PCR primers and amplification protocol. pTSIGN-REV3L, His-Flag and the gel purified large PCR product were both digested using BstXI and NotI sequentially, gel purified and ligated together overnight using T4 DNA ligase. Plasmids were transformed into chemically competent Stbl2 cells and grown overnight at 30ºC on LB/carbenicillin plates. Potential colonies were picked, restreaked onto fresh LB agar/carbenicillin plates and fresh LB broth/carbenicillin was inoculated and grown overnight at 30ºC for DNA mini preps. Mini-prep DNA was made from 2 ml of bacteria and was processed using the Wizard SV mini prep kit (Promega). Potential REV3L polymerase domain active site mutant clones were analyzed by RE digestion using the single cutter, HaeII (NEB) which was not present in the wild type REV3L Polymerase Domain sequence. Digested products were run out on a 0.7% Tris-acetate, EDTA agarose gel (Molecular Biology Grade, Biorad) supplemented with 130 ng/ml of ethidium bromide. Gels were run at 80 V. Clones were confirmed by DNA sequencing.

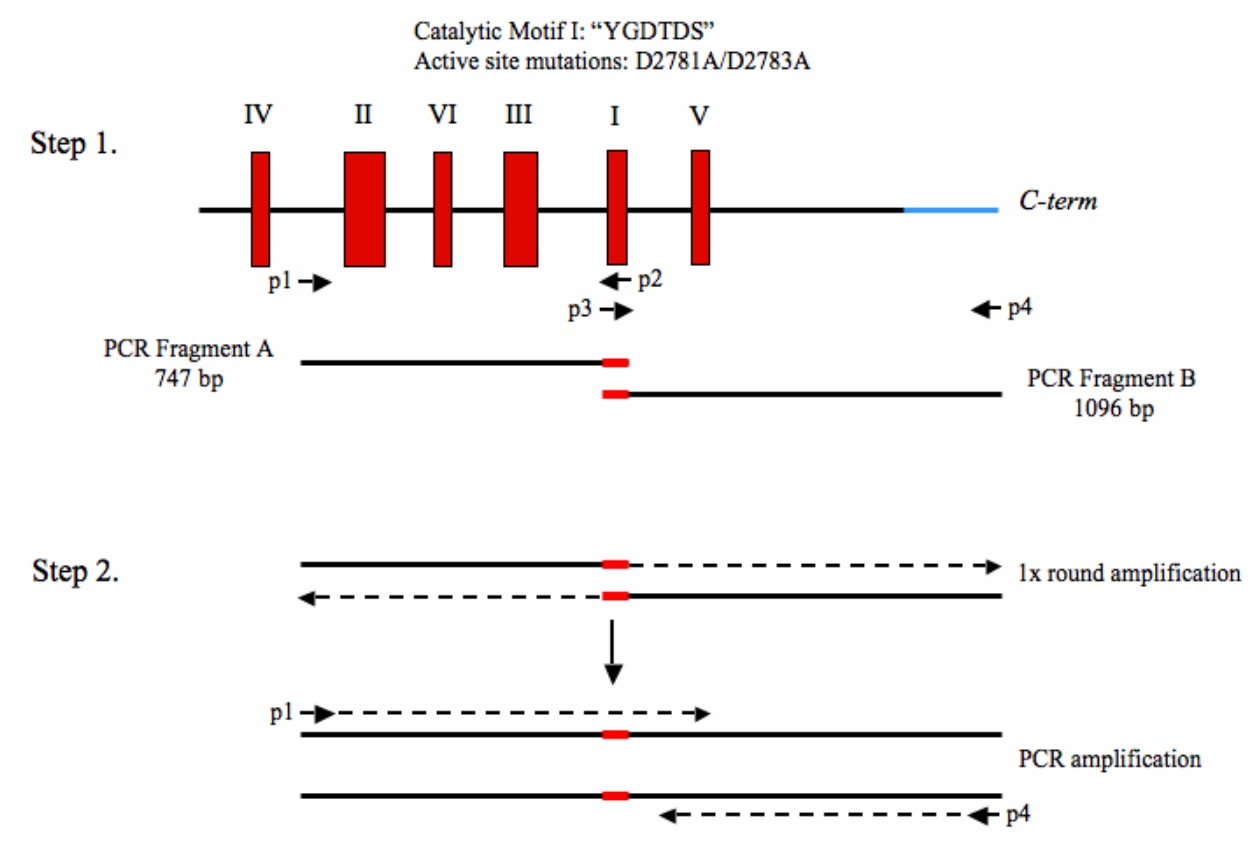

Figure 3.5 Diagram of two-step PCR method for generating REV3L polymerase domain active site mutant.

Two PCR fragments (Fragment A utilized primers, p1-p2, and Fragment B utilized primers, p3-p4) were generated with a corresponding overlap region containing the desired site for mutagenesis. Both fragments (A and B) were gel purified and recombined for a second round of PCR. The full-length polymerase domain fragment was PCR amplified using primers p1 and p4. The full-length active site mutant polymerase domain PCR product was RE digested with BstXI-NotI and exchanged with the same region in the no 5' UTR, Kozak, 10x His tag hREV3L-pTSIGN plasmid. Integration of the polymerase domain mutant was confirmed by RE digestion with HaeII. Potential plasmids were submitted for sequence verification.

3.2.3 Cloning Full-length Human REV1

The REV1 cDNA was acquired from Zhigang Wang (109). REV1 was modified to contain an N-terminal V5 tag and no C-terminal tag (Figure 3.6A). Because of difficulty with PCR

amplification with Turbo Pfu, Platinum Taq, high-fidelity (Invitrogen) was used for modification and subcloning REV1. The 50 µl PCR reaction contained 2 units of Platinum Taq, hi-fi, 400 µM dNTP's, 0.2 mM Forward and Reverse primers and 3.5 ng of the original REV1 cDNA. Refer to Appendix A and B for the Forward and Reverse PCR primer sequence and the PCR amplification protocol. The 3.827 kbp PCR product was gel purified using a commercial kit (Qiagen) and the PCR product and pTSIGN vector were sequentially digested with BstXI and then with NotI. Both digested products were gel purified using a commercial kit (Qiagen), ligated overnight at 16ºC and transformed the following day into Top10, One-shot max efficiency chemically competent cells (Invitrogen) and plated onto LB agar/carbenicillin plates. Potential colonies were picked, restreaked onto fresh LB agar/carbenicillin plates and fresh LB broth/carbenicillin was inoculated and grown overnight at 30ºC for DNA mini preps. Mini-prep DNA was made from 2 ml of bacteria and was processed using the Wizard SV mini prep kit (Promega). Potential REV1 DNA clones were subjected to multiple rounds of restriction enzyme diagnostic digestions using BamHI, HindIII, EcoRI and NotI. Digested products were run out on a 0.7% agarose gel (Molecular Biology Grade, Biorad) supplemented with 130 ng/ml of Ethidium Bromide made in 1x Tris-acetate, EDTA (Biorad) running buffer. Gels were run at 80 V. Potentials clones with correctly digested fragments were sequence confirmed.

3.2.4 Cloning Full-length Human REV7

The human REV7 cDNA was acquired from Richard Fishel (110). REV7 was modified in two major ways. One construct, REV7, His-Flag tag (REV7-HF) contained an N-terminal Flag tag

and a C-terminal 10x His tag while another construct, REV7, HA tag (REV7-HA), contained an N-terminal HA tag (Figure 3.6A). REV7-HF was PCR amplified using 2.5U of Turbo Pfu, 0.4 μM Forward and Reverse primers, and 400 μM dNTP. REV7-HA was PCR amplified using 2.5U of Turbo Pfu, 0.4 μM Forward and Reverse primers and 400 μM dNTP. Refer to Appendix A and B for primer sequences and PCR amplification protocol. PCR products were gel purified using a commercial kit (Qiagen). Gel purified PCR products and pTSIGN were EcoRI and NotI RE digested. The vector was alkaline phosphatase (Roche) treated and both digested products were further gel purified. Each PCR purified product was ligated to the linearized vector using T4 DNA ligase (NEB) at 16ºC overnight and transformed the following day into Top10, One-shot max efficiency chemically competent cells (Invitrogen) and plated onto LB agar/carbenicillin plates. Potential colonies were picked, restreaked onto fresh LB agar/carbenicillin plates and fresh LB broth/carbenicillin was inoculated and grown overnight at 30ºC for DNA mini preps. Mini-prep DNA was made from 2 ml of bacteria and was processed using the Wizard SV mini prep kit (Promega). Potential REV7 DNA clones were subjected to multiple rounds of RE diagnostic digestions using EcoRI-NotI, PvuI and BamHI for REV7-HF and EcoRI-NotI and SapI for REV7-HA. Digested products were run out on a 1% agarose gel (Molecular Biology Grade, Biorad) supplemented with 130 ng/ml of Ethidium Bromide made in 1x Tris-acetate, EDTA (Biorad) running buffer. Gels were run at 80 V. Potential clones with correctly digested fragments were confirmed by sequencing.

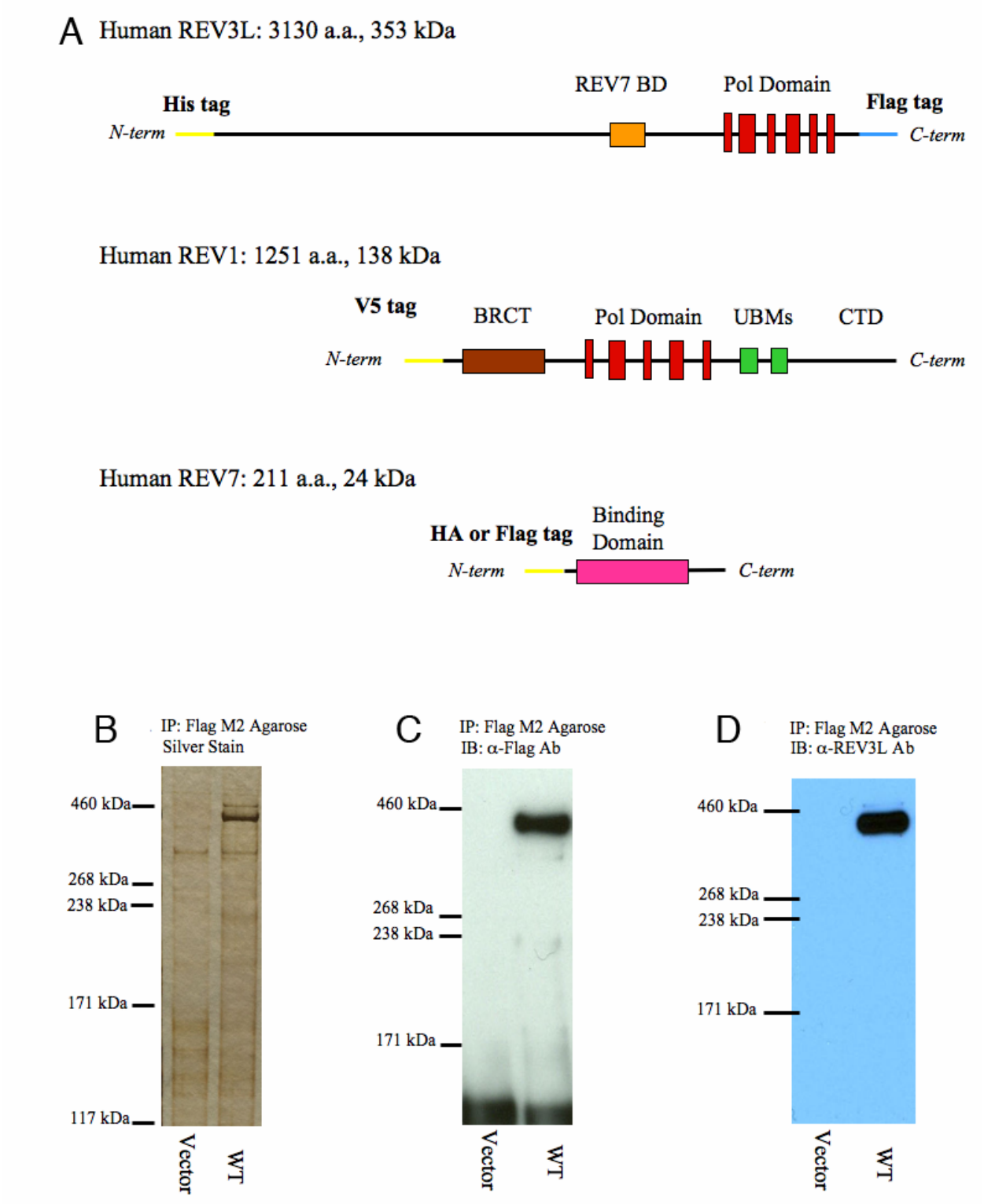
A
Human REV3L: 3130 a.a., 353 kDa
His tag
REV7 BD
Pol Domain
Flag tag
N-term
C-term
Human REV1: 1251 a.a., 138 kDa
V5 tag
BRCT
Pol Domain
UBMs
CTD
N-term
C-term
Human REV7: 211 a.a., 24 kDa
HA or Flag tag
Binding Domain
N-term
C-term
B
IP: Flag M2 Agarose
Silver Stain
460 kDa
268 kDa
238 kDa
171 kDa
117 kDa
Vector
WT
C
IP: Flag M2 Agarose
IB: α-Flag Ab
460 kDa
268 kDa
238 kDa
171 kDa
Vector
WT
D
IP: Flag M2 Agarose
IB: α-REV3L Ab
460 kDa
268 kDa
238 kDa
171 kDa
Vector
WT

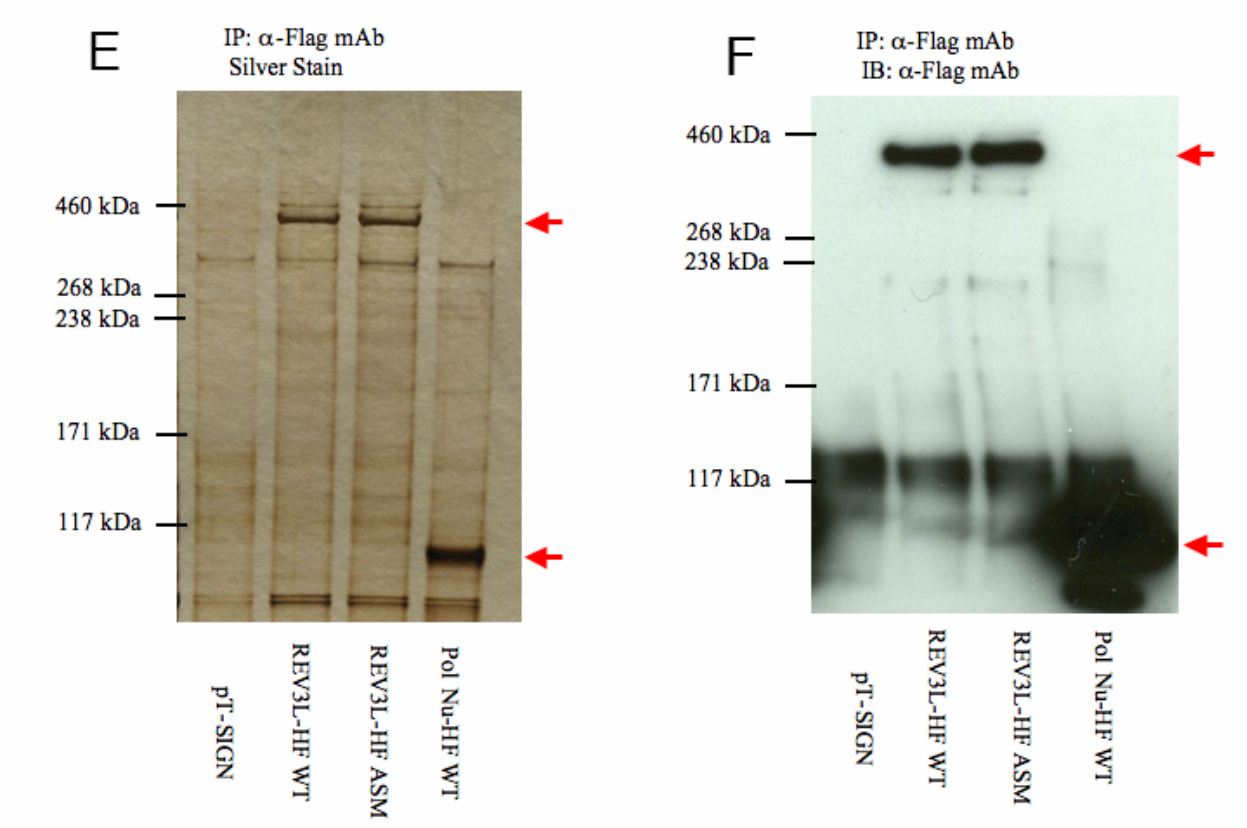

Figure 3.6 Expression and detection of recombinant human REV3L protein.

A. Silver stain of using Flag M2 agarose immunoprecipitated vector and Kozak-REV3L-Flag protein. B. Immunoblot with αFlag M2 mAb against Flag M2 agarose immunoprecipitated vector and Kozak-REV3L-Flag protein. C. Immunoblot with αN-terminal REV3L pAb against Flag M2 agarose immunoprecipitated vector and Kozak-REV3L-Flag protein. D. Silver stain of Flag M2 agarose immunoprecipitated REV3L-HF wild-type and active site mutant protein. E. Immunoblot with αFlag M2 mAb against Flag M2 agarose immunoprecipitated REV3L-HF wild-type and active site mutant protein.

3.2.5 Method for Expression and Detection of Recombinant Full-Length Human REV3L, REV1 and REV7 Using RIPA Lysis Buffer

Recombinant full-length human N-terminal 10x-His tag, C-terminal Flag tag REV3L (REV3L-HF) protein was expressed by transient transfection of human embryonic kidney (HEK) 293T cells (ATCC) with the plasmid, pT-SIGN-REV3L-HF, using FuGENE6 (Roche). Several cell

lines were tested before settling on HEK 293T. These cells were grown in Dulbecco's modified essential media (DMEM) supplemented with 10% fetal bovine serum (FBS) and 1% penicillin/streptomycin. 1.6 x10^6 cells were plated into 10 cm^2 dishes 18 hours before transfection or 2.5 x10^6 cells per 10 cm^2 dish were plated for transfection on the same day (allowing a minimum of 3 hours for the cells to adhere before transfection). For transfection, 400 µl of serum-free DMEM was aliquoted into a 2.2 ml eppendorf tube for each plate. 20 µl of FuGENE6 was added to each tube and then an appropriate amount of REV DNA was added to each tube (Table 2). Tubes were gently tapped to mix. The solution was incubated at RT for 1 hour in the dark before being added drop wise to each plate and grown for 48 hours before harvesting for immunoprecipitation. Media was removed and plates were washed with 5 ml of cold 1x PBS (Bio-Whittaker). 1 ml of 1x trypsin/EDTA (Bio-Wittaker) was added to each dish for 1 minute and then the sides tapped in order to unattach cells. Typsin/EDTA was inactivated with 4 ml of cold DMEM/10% FBS and similarly transfected groups (2 plates) were pooled into a 15 ml Falcon tube. The two plates were washed with an additional 5 ml of cold 1x PBS and this volume was added to the appropriate 15 ml tube. Cells were spun down at 1200 RPM (Sorvall Legend) for 2 minutes at 20ºC and the media eliminated. Cells were washed in 10 mls of cold 1x PBS and spun down at 1200 RPM's for 2 minutes at 20ºC and the 1x PBS wash aspirated. Cells were lysed using a modified RIPA lysis buffer containing hi-salt (Appendix C). For each plate equivalent, cells were lysed in 200 µl of modified RIPA lysis buffer by pipetting up and down and transferring the whole cell lysate to a 2.2 ml eppendorf tube and spinning down at 13,000 g's for 15 minutes at 4ºC using a table top centrifuge (Sorvall). The cleared lysate was then immunoprecipitated using 20 µl of Flag-M2 Agarose beads. Flag M2 Agarose beads were prepared by first washing an amount of beads in 5x bead volumes of 1x TBS to eliminate

glycerol and preservatives and then spun down at 2000 g's for 20 seconds. The beads were then activated in 5x bead volumes of 0.1 M Glycine, pH 3.0 and allowed to mix for 1 minute. The beads were washed 2x in 5x bead volumes of 1x TBS. The final wash involved resuspending the beads in lysis buffer (50 µl/20 µl of beads) and transferring ~55 µl of bead slurry to 1.5 ml screw cap eppendorf tubes by cutting a P200 pipette tip taking care not to disturb the pelleted beads. REV3L lysate was incubated in Flag M2 Agarose matrix for 5 hours at 4ºC on a rotary shaker. After 5 hours, beads were spun down at 2000 g's for 20 seconds, washed 3x in 20x bead volumes of lysis buffer and then boiled for 3 minutes in 30 µl of 2x SDS loading buffer. A similar method was used for expression and immunoprecipitation of other REV3L, REV1 and REV7 plasmids. Refer to Table 3. For immunoprecipitation of one 10 cm^2 plate equivalent of REV1 or REV7 transfected cells, 2 µl of anti-V5 (Invitrogen) or 1.5 µl anti-HA (ICRF) mAb were used, respectively. Antibody was allowed to interact with protein for 6 – 8 hours on a rotary shaker at 4ºC and then 30 µl (approximately 15 – 20 µl of packed beads) of recombinant ProteinG (Invitrogen) slurry was added to each tube. The ProteinG/mAb interaction was incubated for 3 hours on a rotary shaker at 4ºC. Beads were spun down at 2000 g's for 15 seconds and washed 3x in 20x bead volumes (~400 µl) of lysis buffer. Samples were boiled in 30 µl of 2x SDS loading buffer for 3 minutes and stored at -20ºC until ready to resolve by SDS-polyacrylamide gel electrophoresis.

Table 3. Masterlist for Plasmid Transfection and Protein Immunoprecipitation

Plasmid	FUGENE6	Amount of DNA (μg)	DMEM	Method of Immunoprecipitation	Amount of Antibody and Beads Used for 1x Plate
pT-SIGN	20 μl	4, 8 or 16	400 μl	Either Flag M2 Agarose, V5 or HA mAb with ProteinG	20 μl Flag M2 Agarose; 2 μl αV5 or 1.5 μl αHA with 20 μl ProteinG
pT-SIGN-hREV3L, Flag tag	20 μl	16	400 μl	Flag M2 Agarose	20 μl Flag M2 Agarose
pT-SIGN-hREV3L, His-Flag tag	20 μl	16	400 μl	Flag M2 Agarose	20 μl Flag M2 Agarose
pT-SIGN-hREV3L, His-Flag tag; Active-site Mutant	20 μl	16	400 μl	Flag M2 Agarose	20 μl Flag M2 Agarose
pT-SIGN-REV1, V5 tag	20 μl	8	400 μl	V5 mAb with ProteinG	2 μl αV5 with 20 μl ProteinG
pT-SIGN-REV1, V5 tag; G76R BRCT Mutant	20 μl	8	400 μl	V5 mAb with ProteinG	2 μl αV5 with 20 μl ProteinG
pT-SIGN-CTD(REV1), V5 tag	20 μl	8	400 μl	V5 mAb with ProteinG	2 μl αV5 with 20 μl ProteinG
pT-SIGN-REV7, His-Flag tag	20 μl	4	400 μl	Flag M2 Agarose	20 μl Flag M2 Agarose
pT-SIGN-REV7, HA tag	20 μl	8	400 μl	HA mAb with Protein G	1.5 μl αHA with 20 μl ProteinG
pT-SIGN-REV7 Binding Domain(REV3L), Flag tag	20 μl	8	400 μl	Flag M2 Agarose	20 μl Flag M2 Agarose
pT-SIGN-Polymerase Domain(REV3L), Flag tag	20 μl	8	400 μl	Flag M2 Agarose	20 μl Flag M2 Agarose
pcDNA3.0-HA-ubiquitin	**	0.6	**		
pcDNA3.0-ATM-Flag	6 μl	2	400 μl	Flag M2 Agarose	20 μl Flag M2 Agarose
**** supplement to existing transfection by adding 2 μl of a 0.3 μg/μl**					

3.2.6 Immunoblotting Full-length Human REV3L, REV1 and REV7

Full-length REV3L (353 kDa) protein was resolved using a commercial 10 well, NuPAGE 3-8% Tris-acetate gradient gels (Invitrogen) using their standard protocol with minimal changes. All components from this system were acquired from Invitrogen (Appendix D). 600 ml of 1x Tris-acetate SDS running buffer and 500 µl of antioxidant added to the middle chamber was used to resolve either one or two gels. Positive control samples consisted of REV1, REV3L or REV7 protein transiently transfected, harvested, immunoprecipitated and prepared on a separate day. A fraction of this material was loaded onto each gel to act as a sizing control for each experiment. The Prestained Himark Molecular Weight Standards (Invitrogen) was also used as another sizing marker. Gels were run for 100 – 120 minutes (depending on desired resolution) at 170 V. 500 ml of ddH_2O and 1x Tris-acetate transfer buffer (500 ml for transferring 1 – 2 gels, 1 L for transferring 3 – 4 gels) were chilled for a minimum of 1 hour. Once the gel(s) has finished resolving, remove gel cassette from apparatus and rinse apparatus under running water for about 2 – 3 minutes in order to eliminate excess SDS running buffer. Gel cassettes were cracked along the sides using a Flat-head screwdriver. The top cover of the gel cassette was removed and discarded. The base and the wells were cut off the gel leaving approximate 6.5 x 8 cm mini gel. For each gel, 0.45 µm PVDF membrane (Millipore) and two pieces of 3MM filter paper (Whatman) were cut to the dimensions of 7 x 9 cm. The PVDF membrane was pre-soaked in 100% MeOH and briefly rinsed in ddH_2O. Then, the membrane, two pieces of filter paper and 4x fiber pads in transfer buffer (done in a 1 ml tip box lid) were presoaked in transfer buffer thoroughly avoiding air bubbles. The transfer membrane sandwich within the semi-wet transfer

apparatus consisted of two soaked fiber pads, 3MM filter paper, gel, PVDF membrane, filter paper, and two more soaked fiber pads on top being mindful to avoid air bubbles. The remaining transfer buffer was poured into the sandwiched internal cartridge and chilled ddH_2O was added to the external portion of the gel box. Protein was transferred for 5 hours at 30 V. Membranes were blocked in 10% milk/1x PBS Tween20 (0.1%) (1x PBST(0.1)) for a minimum of 1 hour at RT with shaking or overnight at 4ºC with shaking.

Before incubating with primary antibody, cut the blocked PVDF membrane to the necessary dimensions. Resolved REV3L, REV1 and REV7 while using the Himark (Invitrogen) molecular weight standards should be cut using a fresh surgical razor blade as follows: above 460 kDa and below 238 kDa for REV3L, above 171 kDa and below 117 kDa for Rev1 and cut above 31 kDa and save the base of the membrane for REV7.

Flag immunoprecipitated REV3L was immunoblotted using either a mouse anti-Flag-M2 monoclonal antibody (Ab) or one of the chicken affinity-purified anti-REV3L specific polyclonal Abs (refer to Chapter 2). Membranes were incubated with primary Ab diluted in 10% milk/1x PBST(0.1) for 2 hours at RT with shaking or overnight at 4ºC with shaking. The membranes were washed 3x in 1x PBST(0.1) for 10 minutes each. Blots were then incubated for 30 minutes with a secondary Ab conjugated with HRP diluted in 10% milk/1x PBST(0.1). The blots were then washed 4x in 1x PBST(0.1) for 10 minutes each. Super Signal West Femto (Pierce) was the chemiluminescent kit used to detect REV3L. For primary and secondary Ab dilutions, refer to Table 2.

Transfection, expression, immunoprecipitation and immunoblotting of recombinant, full length REV1 and REV7 was performed similarly as described for REV3L. Refer to Table 3 and 2 for specific immunoprecipitation and immunoblotting conditions. Immunoblotting of

recombinant REV1 and REV7 was performed using either the Invitrogen NuPAGE system or Biorad Mini-cel system. When the NuPAGE system was used for REV7, the samples were run for a maximum of 52 minutes at 170 V in order to avoid running recombinant REV7 off the 3-8% Tris-acetate gel. When using the Biorad mini-cel system, REV1 and REV7 were resolved on 4-15% Tris-glycine gels run at 20 mAmps/gel for 80 minutes. Protein was transferred from gel to 0.45 μm PVDF membranes using a Biorad mini-cel transfer apparatus. Protein was transferred at 40 V for 4 hours in a 1x Tris-glycine (Biorad) and 20% methanol buffer. Membranes were similarly blocked in 10% milk/1x PBST(0.1) and similarly immunoblotted. Refer to Table 2 for primary and secondary Ab dilutions.

3.2.7 Silver Stain of Full-length Human REV3L, REV1 and REV7

Full-length human REV3L, REV1 or REV7 was resolved using a NuPAGE 3-8% Tris-acetate SDS-PAGE gel apparatus as described in the Immunoblotting protocol. After the gel has finished resolving, remove gel from cassette and briefly was in ddH_2O in a transparent plastic container. Gel was fixed for 30 minutes in fixative solution with gentle shaking. Refer to Appendix D for Silver Stain solutions. The gel was washed twice for 20 minutes in ddH_2O with gentle shaking. Gel was soaked in Sensitizer solution for 1 minute and rinsed 2x for 30 seconds in ddH_2O. The gel was then soaked in 0.1% silver nitrate solution for 10 minutes with gentle shaking. After 10 minutes, the gel was rinsed in ddH_2O followed by a brief rinse in Developing solution. Then, 100 ml of Developing solution was added and incubated gently shaking for 1 minute monitoring closely to ensure the gel did not overdevelop. The Developing solution was

inactivated by adding 5 ml of sodium citrate for every 100 ml of Developing solution. After 3 minutes of continued gentle shaking, the gel was transferred into fresh water to fully inactivate the reaction.

3.2.8 DNA Polymerase Activity Assay

REV3L, REV7, REV1 either alone or in combination were analyzed for DNA polymerase activity using a standard DEAE polymerase activity assay. Refer to Appendix E for all solutions and templates used. Catalytic DNA polymerase activity was determined by whether the protein of interest could incorporate nucleotides along either a calf-thymus DNA template or an oligo dT:poly dA DNA template. Polymerase reactions involving REV3L were performed using protein bound to Flag M2 Agarose derived from two different immunoprecipitation methods. The first method involved taking the proteins produced separately and then combining them into a reaction. REV1 and REV7 were produced in baculovirus by Dr. Birgitte Wittschieben and sequentially purified using Flag M2 Agarose and Ni-NTA and eluted. Stock solutions of both proteins were diluted down to 2 ng of REV1 and 0.68 ng of REV7 and were supplemented to REV3L for each reaction. The REV proteins either alone or in combination were assayed for polymerase activity. The second method involved assaying co-immunoprecipitated proteins REV1 and REV3L (Chapter 4) for polymerase activity.

In the first method, REV3L protein was harvested using a modified RIPA lysis buffer. Refer to Appendix C for buffer formulation. 293T cells were plated down at 1.8 x10^6 cells/dish – there were four plates per group. The next day, cells were transfected with 16 μg of wild type

or active-site mutant REV3L/plate. After 48 hours, cells were harvested similarly as described above with the following exception. The cells were washed and resuspended in modified RIPA lysis buffer, proceeded to cell lysis by passing cells through a 23 G needle up-and-down 10 times. Then, lysate was spun down at 13,000 g's for 15 minutes at 4ºC. REV3L was Flag immunoprecipitated as described above taking extreme precaution to avoid bubbles and foregoing boiling the beads in 2x SDS loading buffer after the 3rd wash. For the second method, refer to Chapter 4 for specifics on the Freeze-Thaw lysis method used to demonstrate a REV3L-REV1. For both methods, bead-protein slurry in 60 µl of lysis buffer was used. 15 µl of the total volume of the matieral was examined by silver stain to approximate amount of total protein in the reaction. For the polymerase activity assay, a 1:5:10 fmol ratio of REV3L:REV1:REV7 was used on a calf-thymus DNA template. REV1-V5 and REV7-HF was diluted in their elution buffer to a concentration of 2 ng and 0.68 ng. The final reaction buffer consisted of 33.8 mM Tris, pH 7.5; 3.6 mM KPO4; 22 mM KCl; 4.9% glycerol; 0.26% NP-40; 37.5 NaCl; 80 mg/ml BSA; 2 mM DTT; 8 mM MgCl2; 10 µM dNTP; 2.5 µg activated calf-thymus DNA; 0.13 mM EDTA; 3.75 µCi of α-^{32}P-dTTP; ~1 ng REV3L-HF protein (WT or ASM) (15 µl); ~2 ng REV1-V5 (4 µl); ~0.68 ng REV7-HF (0.4 µl); ~10 ng Pol Nu. Samples were incubated for 0, 30, 60 and 180 minutes at 37ºC. At the prescribed times, 15 µl was taken from the master reaction mix and inactivated in 1x Stop solution. After the time course was complete, 10 µl was taken from each inactivated reaction and spotted onto DEAE Sepharose and washed for 5 minutes, 3x in 0.5 M Na_2HPO_4 buffer. The DEAE paper was washed 2x for 1 minute in 100% EtOH and dried for 20 minutes in a chemical hood. The reaction mix was diluted 100x and 5 µl was spotted as a radioactive control. The DEAE paper was wrapped in Saran Wrap and exposed to the Fuji magnetic film for 10 minutes and total counts were measured using a Fuji PhosphoImager.

3.3 RESULTS

3.3.1 Expression of Recombinant Full-length Human REV3L

Multiple protein expression systems were used in an attempt to express full-length human REV3L. Attempts were made using various protein expression systems including bacterial, *in vitro* transcription and translation as well as baculovirus. Furthermore, N or C-terminal tags consisting of eGFP, Lumio tags (Invitrogen), and commercial affinity tags (His and Flag) were used to modify the REV3L cDNA. All three of these systems did not result in expression of the 353 kDa protein either from whole cell lysates or Flag immunoprecipitation from whole cell lysates, but were able to express other smaller control proteins (data not shown). Furthermore, use of the Invitrogen Gateway Recombination system allowed me to generate a REV3L C-terminal eGFP plasmid (data not shown). Transfection of multiple eGFP-tagged REV3L constructs into different cell lines did not produce any green cells (or protein) by visual inspection 48 hours post-transfection by eGFP fluorescence microscopy or by immunoblot (data not shown). Various transfection reagents including Superfect (Qiagen), Lipofectamine 2000 (Invitrogen), FuGENE6 (Roche), Lipofectin with Plus reagent (Invitrogen), Calcium Chloride (Amersham), Jetpei (Qbiogene) and Nucleofection – electroporation were all assessed to see if they could improve overall transfection efficiency using some of the above plasmids in HeLa, 293T and REV3L null MEFs. All the transfection reagents above were unable to transfect the various REV3L plasmids. An in-house designed vector, pTSIGN (ICRF) (Figure 3.4), was used

because it contained a unique internal ribosomal entry site (IRES) fused to a neomycin-eGFP downstream of its multiple cloning site/polylinker. Another unique feature of the pTSIGN plasmids was the E1α promoter. Many commercial plasmids contain a CMV promoter to drive transcription. Because of the size and potential toxicity of the REV3L protein, concern arose whether the CMV promoter was being inactivated by methylation. The advantage of using the E1α promoter is two-fold. First, it is a human promoter which allows for continuous gene expression and second, it does not become methylated and therefore inactivated. Another advantage of the pTSIGN plasmid is the downstream IRES-Neo-eGFP cassette which acts as a cellular indicator of full-length mRNA expression. In the plasmid, pTSIGN-REV3L, if the whole REV3L mRNA was expressed, then one would see eGFP expression by fluorescence microscopy. With the knowledge that full-length REV3L mRNA was being produced, it provided additional insight into whether the transfected cells were producing mRNA. This plasmid was a critical benchmark tool which allowed me to titrate the amount of REV3L plasmid necessary for successful transfection and potential REV3L expression in different human cell lines. After examining multiple cell lines (HeLa, REV3L disrupted murine embryonic fibroblasts (MEFs), IRF½ MEFs (Chang-Moore lab), XP12RO and 293T), only 293T cells were able to express REV3L mRNA. However, even among four different HEK 293T cell lines examined from different labs, the ability to express REV3L varied significantly in each. The 293T cell line which was finally settled upon was a generous gift from the Bakkenist lab (University of Pittsburgh) which they purchased directly from ATCC. In order to determine the optimal amount of FuGENE6 and pTSIGN-REV3L-Flag plasmid for transfection into 293T, a dose titration was performed between 2 – 32 μg of plasmid and a range of 2 μl to 36 μl of FuGENE6 was examined. Amounts of DNA greater than 20 μg began killing cells. After

extensive testing, a dose of 16 μg of REV3L plasmid per 10 cm^2 dish was settled upon because ~50% of 293T cells were green by fluorescence microscopy 48 hours post-transfection. REV3L protein expression was characterized by Flag immunoprecipitation and visualization by silver stain (Figure 3.6b) and by immunoblot with αFlag M2 (Figure 3.6c) and αREV3L N-terminal (Figure 3.6d) Abs. Migration of the REV3L protein on the gel runs around 400 kDa. However, the use of 16 μg of REV3L-HF active-site mutant irrespective of DNA quality always yielded a little less immunoprecipitated REV3L by silver stain (Figure 3.6e) and by αFlag mAb immunoblot (Figure 3.6f) compared to wild-type REV3L. Lane 4 in the silver stain and immunoblot corresponds to Polymerase Nu Flag-tagged protein expressed in the 293T-Rex Inducible cell system (Invitrogen) was similarly Flag immunoprecipitated followed by silver stain and immunoblot with an anti-Flag M2 mAb (Figure 3.6e and f). The 293T-Rex Inducible Pol Nu Flag-tagged expression cell line was developed by Dr. Birgitte Wittschieben.

3.3.2 Expression of Recombinant Full-length Human REV1 and REV7

Successful expression of both full-length REV1 and REV7 would provide a unique tool for use in polymerase activity assays as well as for immunoprecipitation studies. Human REV1 is a 138 kDa protein while human REV7 is a 24 kDa protein. Both proteins were cloned into and expressed using the pTSIGN vector. Using 8 μg of REV1-V5 plasmid, ~50% of transiently transfected cells were green 48 hours post-transfection. Using 4 μg of REV7-HF or 8 μg of REV7-HA, ~80 – 90% of transiently transfected cells were green 48 hours post-transfection.

REV1-V5, REV7-HF and REV7-HA expression was characterized by αV5, αFlag M2 Agarose and αHA immunoprecipitation and visualized by immunoblot, respectively (Figure 3.7A and B).

3.3.3 Testing the Influence of the 5' UTR in REV3L Expression

The 5' UTR of REV3L was predicted to influence translation of the gene. Comparison of two REV3L constructs, one with the intact 5' UTR with native mammalian Kozak sequence and another that removed the 5'UTR and contained an optimized mammalian Kozak sequence, was examined. Recombinant REV3L was not detected in either the input, input depleted or pellet fraction. However, a high molecular weight band corresponding to 400 kDa was detected in the Flag M2 agarose immunoprecipitation fraction of the REV3L transfected sample and not in the corresponding vector transfected sample (Feigure 3.8). There was no significant difference in the amount of protein produced indicated by Flag immunoprecipitation of the REV3L protein containing the 5' UTR hairpin stem-loop compared to the REV3L protein containing the optimized Kozak sequence.

3.3.4 DNA Polymerase Activity Assay

The REV1, REV3L and REV7 proteins were examined either individually or in combination with one another for polymerase catalytic activity. Comparison of polymerase activity on an oligo dT:poly dA DNA template for REV3L wild-type versus active site mutant did not

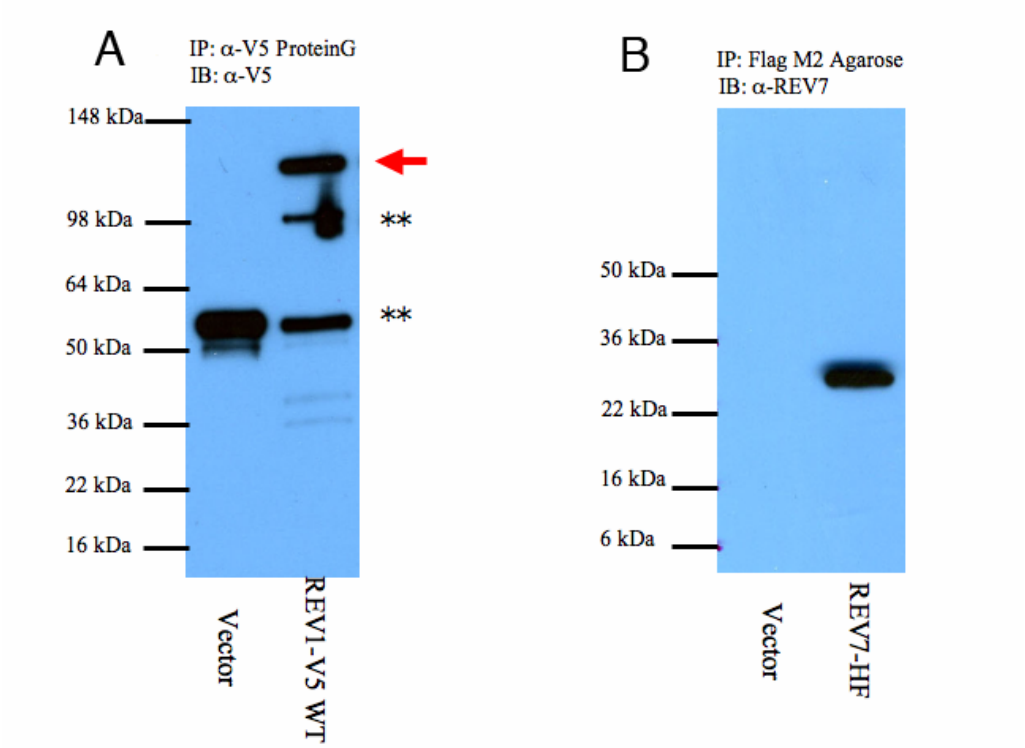

Figure 3.7 Expression and detection of human REV1-V5 and REV7-HF.

A. Immunoblot with αV5 mAb against αV5-ProteinG agarose immunoprecipitated vector and REV1-V5 protein (red arrow). Double asterisk denotes mouse immunoglobulin heavy chain (from V5 mAb) detected by goat anti-mouse secondary. B. Immunoblot with αREV7 pAb against Flag M2 agarose immunoprecipitated vector and REV7-HF protein.

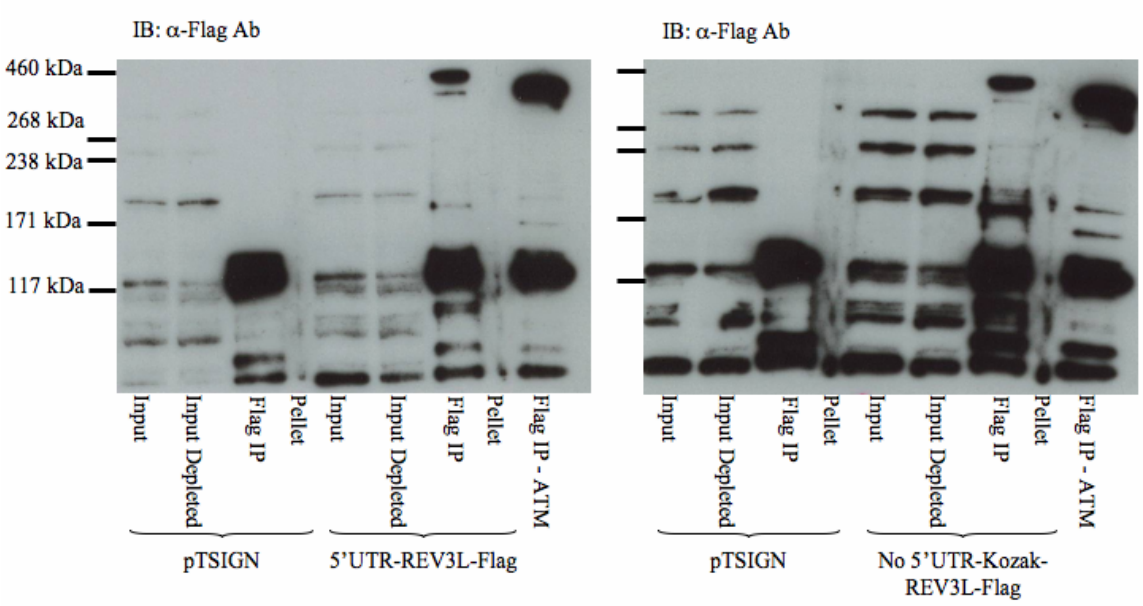

Figure 3.8 Translation with and without the 5' UTR of recombinant human REV3L-Flag protein.

Cells were transfected with either a 5' UTR-REV3L-Flag or a No 5' UTR-Kozak-REV3L-Flag pTSIGN plasmid into 293T and cells were harvested for protein using a hi-salt RIPA lysis buffer 48 hours post-transfection. Cell lysates were immunoprecipitated using Flag M2 agarose, boiled in 2x SDS loading buffer and resolved on a 3-8% Tris-acetate gel. Protein was transferred onto a 0.45 μm PVDF membrane and blotted with αFlag M2 Ab.

demonstrate significant activity above the vector control. Similarly, no significant DNA polymerase activity was observed for REV3L wild-type protein when baculovirus purified human REV7, REV3L's supposed interaction partner, or with human REV1 (Figure 3.9). An activated calf-thymus DNA template was chosen because it would more closely resemble what REV3L may actually encounter in a cell. What is special about activated calf-thymus compared to a poly dA DNA template is the use of all four nucleotides in the DNA template as well as the variable sized single-strand gaps which REV3L protein could potential incorporate nucleotides across. However, these results were the same when using an activated calf-thymus DNA template as was observed for the oligo dT:poly dA DNA template (Figure 3.10). The ability to co-immunoprecipitate a REV1-REV3L complex using the freeze-thaw lysis method provided an

alternative method for protein purification since an actual complex could be visualized by immunoblot. However, REV1 associated with either REV3L wild-type or active site mutant did not show any DNA polymerase activity above background on an activated calf-thymus DNA template (Figure 3.11). In contrast, the positive control polymerases, Klenow, exo– and Polymerase Nu proteins, had strong DNA polymerase catalytic activity on both DNA templates (Figure 3.9, 3.10 and 3.11). Commercial Klenow exo- protein was diluted from a stock protein solution while Polymerase Nu-Flag tagged protein was expressed from a 293T Rex Pol Nu inducible expression cell line, purified in the same way as the REV3L Flag-tagged wild type and active site mutant proteins and assayed similarly as above.

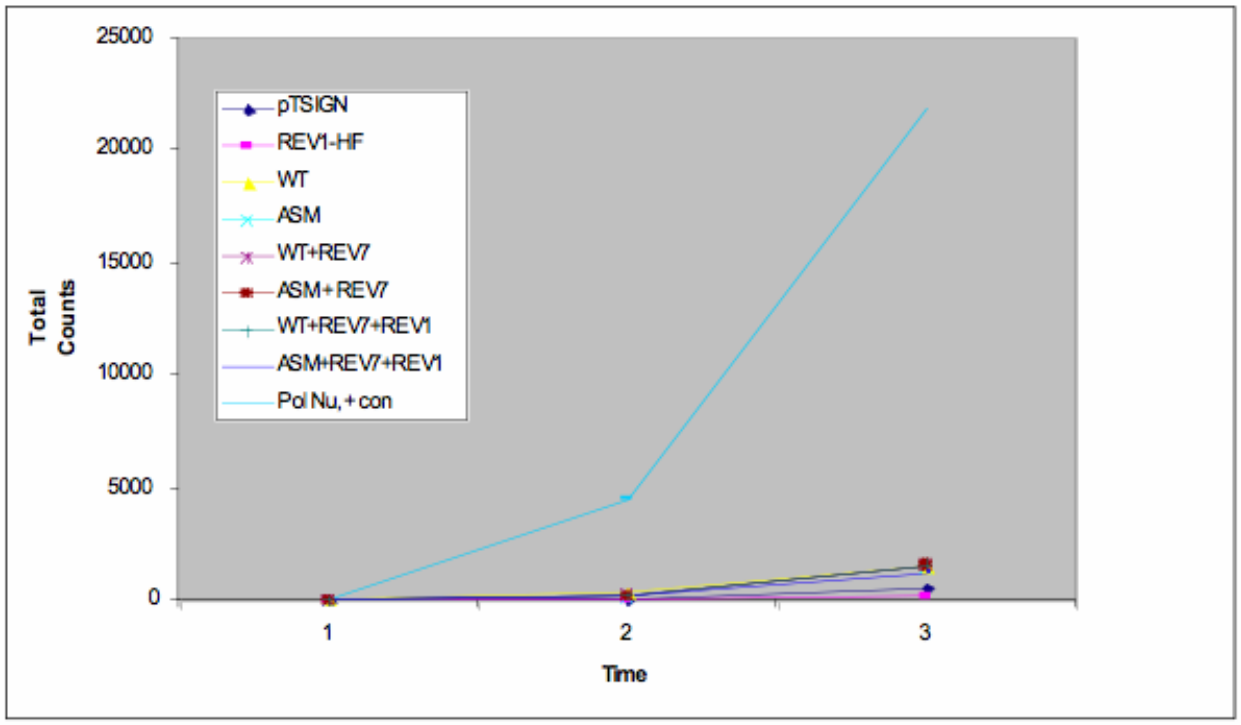

Figure 3.9 Examining recombinant REV3L's catalytic polymerase activity with REV7 and REV1 on an oligo dT:poly dA DNA template.

REV3L wild-type (WT) and active-site mutant (ASM) proteins were harvested from 293T cells transiently transfected 48 hours earlier using a modified RIPA lysis protocol. The proteins were Flag M2 agarose immunoprecipitated. 1 – 3 ng of WT and ASM REV3L protein bound to Flag M2 agarose was used per reaction. REV7 (0.68 ng) and REV1 (2 ng) produced in baculovirus and double purified over a Flag and His column were supplemented to each reaction as needed. Radionucleotide incorporation (α-^{32}P-dTTP) on an oligo dT:poly dA template by the proteins described above was measured over 0, 60, and 180 minutes. Pol Nu-Flag was used as a positive control and was prepared from a 293T Rex Pol Nu inducible expression cell line, purified in the same way as the REV3L Flag-tagged proteins and assayed similarly as above. Reactions were spotted on DEAE Sepharose filter paper and analyzed under a Fuji Phosphoimager.

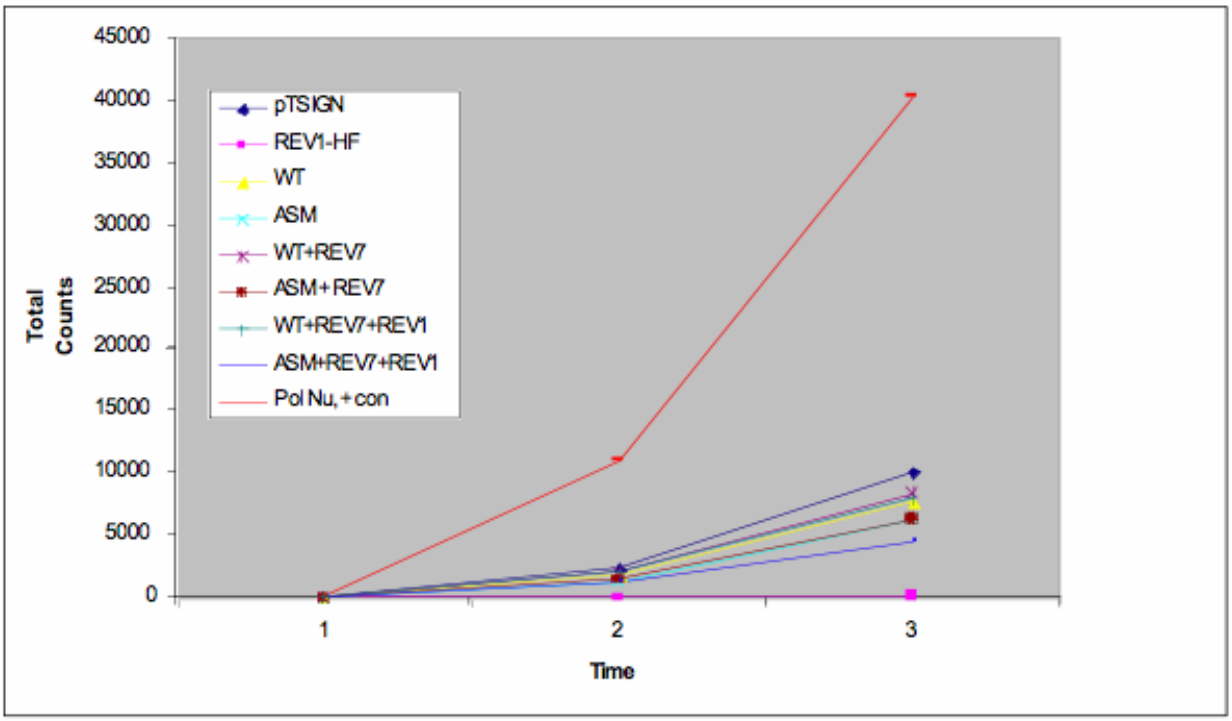

Figure 3.10 Testing for catalytic DNA polymerase activity of recombinant REV3L with REV7 and REV1 on an activated calf-thymus DNA template.

REV3L wild-type (WT) and active-site mutant (ASM) proteins were harvested from 293T cells transiently transfected 48 hours earlier using a modified RIPA lysis protocol. The proteins were Flag M2 agarose immunoprecipitated. 1 – 3 ng of WT and ASM REV3L protein bound to Flag M2 agarose was used per reaction. REV7 (0.68 ng) and REV1 (2 ng) produced in baculovirus and double purified over a Flag and His column were supplemented to each reaction as needed. Radionucleotide incorporation (α-^{32}P-dTTP) on an activated calf-thymus DNA template by the proteins described above was measured over 0, 60, and 180 minutes. Pol Nu-Flag was used as a positive control. Reactions were spotted on DEAE Sepharose filter paper and analyzed under a Fuji Phosphoimager.

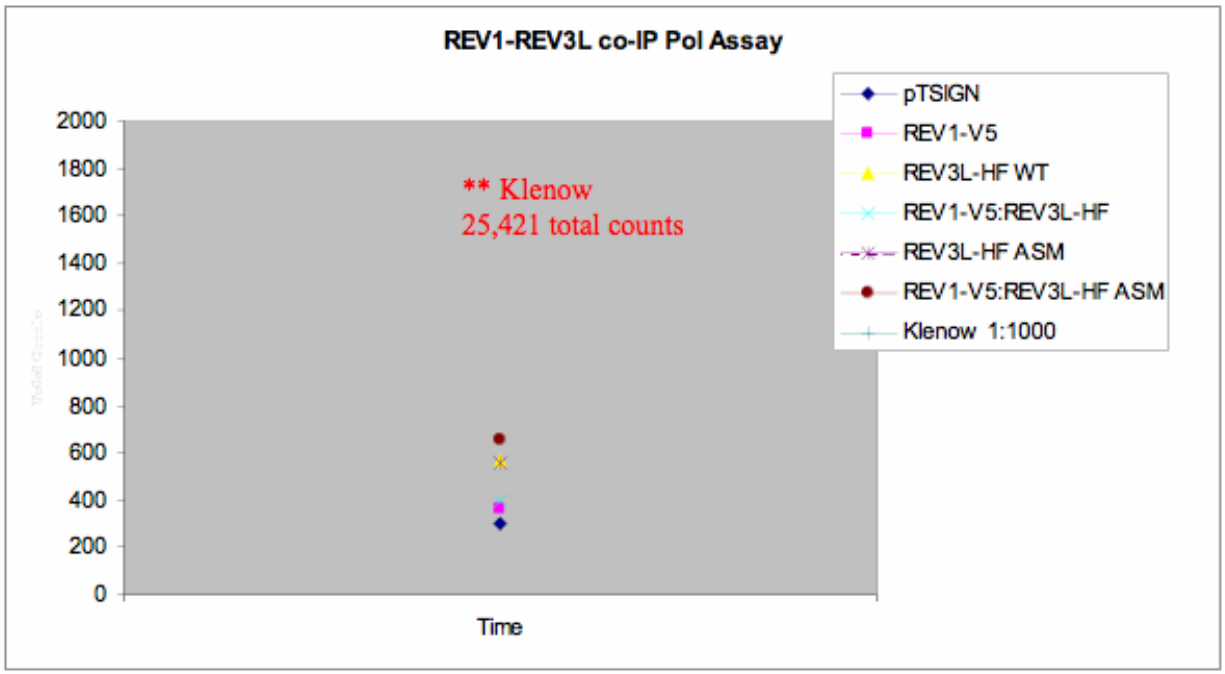

Figure 3.11 Examining recombinant Testing for catalytic DNA polymerase activity of recombinant REV3L with REV7 and REV1 on an activated calf-thymus DNA template.

REV1 was co-transfected with either REV3L wild-type (WT) or active-site mutant (ASM) proteins were harvested from 293T cells transiently transfected 48 hours earlier using a modified freeze-thaw lysis protocol (described in Chapter 4). The proteins were Flag M2 agarose immunoprecipitated and used directly in the polymerase assay. Radionucleotide incorporation (α-^{32}P-dTTP) on an activated calf-thymus DNA template by the proteins described above was measured over 0 and 180 minutes. The positive control DNA polymerase, Klenow, exo- was diluted 1:1000 and assayed similarly to the Flag immunoprecipitated REV3L-Flag tagged protein. Reactions were spotted on DEAE Sepharose filter paper and analyzed under a Fuji Phosphoimager.

3.4 DISCUSSION

3.4.1 Expression of Human Full-length REV3L

Multiple attempts to express full-length human REV3L have been made by many labs but were unsuccessfully as indicated by informal discussion with other investigators. The wide array of cells, expression vectors and systems and transfection reagents tested in my work confirm the extreme difficulty of trying to clone and express this large gene. There are many potential explanations for why REV3L expression initially was so poor compared to other similarly sized plasmids (ie. ATM-Flag). First, potential plasmid and FuGENE6 mediated toxicity was a concern. High quantities of plasmid or transfection reagent are inherently cytotoxic. This proved to be true when using either pTSIGN (vector control) or pTSIGN-REV3L-Flag total plasmid in amounts greater than 24 μg. There was no observed effect with increasing amounts of FuGENE6. Another concern was REV3L's large mRNA (~10 kbp). Such a large transcript may not be fully transcribed thus leading to poor protein expression. In order to determine whether or not full-length REV3L mRNA could be produced, the modified REV3L cDNA was subcloned into pT-SIGN. The unique IRES-Neo-eGFP cassette downstream of the polylinker allowed assessment of REV3L mRNA production. Knowing that the mRNA was produced did not address whether or not the mRNA could be translated into a stable, soluble protein. Poor protein expression could be due to REV3L being a toxic gene product. Rev3 biochemistry in yeast has demonstrated it to be a processive polymerase capable of potentially misincorporating

nucleotides across a DNA template either by itself or in conjunction with other translesion synthesis polymerases (21,22,24,68). Furthermore, *rev3* yeast cells have an overall decrease in spontaneous as well as damage-induced mutagenesis (111). The concern is that cells expressing REV3L for any lengthy period of time may undergo apoptosis due to genomic instability due to wide scale mutagenesis. However, this possibility was ruled out on multiple levels. First, there was no observed increase in cell death with the pTSIGN-REV3L-HF wild type or active site mutant transfected plasmids compared to the vector control plasmid alone. Second, there was no observed cytotoxic difference in the conditional expression REV3L-HF wild type and active site mutant 293T cell lines compared to the vector control cell line. Third, REV3L protein expression was further optimized using a low passage 293T cell line acquired from Dr. Bakkenist as well as further optimizing the quality of the plasmid maxi preps thereby easily doubling the amount of protein produced without causing any significant increase in cytotoxicity compared to the vector control transfected cells. For the first time, these results demonstrate that full-length human REV3L wild-type and active site mutant can be expressed in a transient transfection system.

3.4.2 Expression of Human Full-length REV1 and REV7

Cloning, transfection, expression, immunoprecipitation and immunoblotting of both REV1 and REV7 proteins were successful. Both the affinity tag specific Abs as well as commercial Abs were able to detect the recombinant proteins by immunoblot. However, it has been impossible to detect endogenous REV1 using the commercial Ab (Santa Cruz). Recent evidence indicates that

REV1 is cell cycle regulated in yeast and is predominantly expressed during G_2/M (54). However, cell cycle arrest and analysis of human whole cell and nuclear extracts for endogenous REV1 during that phase still do not detect REV1 using the commercial Ab (data not shown). These results are in stark contrast to REV7 which can be detected abundantly with the commercial antibody (Abcam) from whole cell extracts and shows no cell cycle mediated preference (data not shown).

3.4.3 5' UTR of Human REV3L

Endogenous REV3L mRNA contains a 5' UTR which has been predicted to form a stem-hairpin loop. Work by other groups indicate that stem-hairpin loops may effect translation and thereby limit the amount of available gene product in a cell (112,113). Because of REV3L potential mutagenic polymerase activity, it would be logical for a cell to maintain very low levels of the protein possibly sequestering it in another cellular compartment and recruiting it to DNA only when trying to bypass specific lesions (75). In contrast to this, work by Tagawa's group indicates that the mouse 5'UTR stem loop for a REV3L fragment cloned into a mammalian expression vector had enhanced translational efficiency compared to constructs lacking the 5' UTR stem loop (114). In order to determine whether the 5' UTR plays a role in full-length human REV3L expression, two plasmids were used to answer this question: pTSIGN-5' UTR-REV3L-Flag and pTSIGN-no 5'UTR-Kozak-10x His-REV3L-Flag. The results indicate that the human 5' UTR stem loop does not enhance full-length recombinant human REV3L expression

compared to a REV3L plasmid lacking the 5' UTR stem loop and possessing an optimized mammalian Kozak sequence (Figure 3.8).

3.4.4 DNA Polymerase Activity

Rev3 has been demonstrated in both yeast and *Drosophila* to have DNA polymerase activity (103,115). It remains unknown whether human REV3L has DNA polymerase activity on activated calf-thymus or on an oligo dT:poly dA DNA template and whether it can insert and extend from a mismatched primer template. Currently, all that is known about mammalian REV3L is that it plays a role in damage-induced mutagenesis and that disruption of the gene is embryonic lethal (68,116). Elucidating the function of mammalian REV3L is of extreme importance in order to understand what role it plays in translesion synthesis and cellular damage tolerance. Work done predominantly with the yeast protein has established that Rev3 either itself or in association with other translesion synthesis polymerases can insert a nucleotide opposite a non-coding lesion *in vitro* and then extend from this primer termini (103,117,118). Much of this has been demonstrated using either calf-thymus or single nucleotide DNA templates.

Expression and purification of full-length human REV3L wild-type and active-site mutant protein is a significant step towards attempting to delineate REV3L function. However, initial attempts at expression and purification did not yield any catalytic DNA polymerase activity above the vector control background on activated calf-thymus or oligo dT:poly dA DNA template compared to positive control polymerases Klenow fragment and Pol Nu. The lack of

polymerase activity observed could be explained by the following reasons. First and probably the most significant was the very small amounts of protein that were produced and therefore could be added to a total polymerase reaction. Approximately 0.25 – 0.5 ng of REV3L protein was used per reaction compared to Pol Nu which was 3 – 4 ng of protein per reaction. Currently, production of large quantities of REV3L protein is not feasible and therefore limits the amount of protein that can be used in each assay as well as limits the number of assay conditions that can be examined and may explain the lack of polymerase activity. Because of small quantities of protein being used as well as adding REV proteins purified separately from another system, association of the different REV proteins is probably suboptimal. Second, REV3L's large size may render the protein unstable and susceptible to degradation or proteolysis. Furthermore, the cell lysis method may have caused protein denaturation since a 23½ gauge needle was employed to open the cells. The shearing motion inherently generated bubbles regardless of how cautious the protein prep was made which could cause protein denaturation. Although, the positive control protein, Pol Nu, was expressed, purified and assayed similarly to the REV3L protein and possessed potent polymerase activity on both templates. Therefore, this would argue against the possibility that REV3L may be denatured or that the protein preparation using the modified RIPA lysis protocol was inadequate for the DNA polymerase assay.

It was discovered that when cells were co-transfected with REV1 and REV3L, the two polymeraseases were able to interact by immunoprecipitation when lysed using a freeze-thaw lysis method. This encouraged the re-examination of whether REV1 could enhance the catalytic activity of REV3L on a DNA template. The catalytic polymerase activity of REV3L WT or ASM either alone or complexed with REV1 was no better than the vector control. Again, the amount of protein harvested from these co-immunoprecipitations was small making it difficult to

test multiple polymerase activity conditions. Another possibility is the choice of assay conditions. Another concern is spotting polymerase reactions on DEAE Sepharose filter paper. This method may be too insensitive for detecting nucleotide incorporation compared to analysis on a sequencing gel. If mammalian Rev3L preferentially inserts or extends from certain nucleotides and not others, the use of calf-thymus DNA could both be a problem and a panacea since all four nucleotides are represented in the template and contain a variety of nucleotide combinations as well as varying single-strand gaps. Because yeast Rev3 does not have difficulty incorporating nucleotides over a variety of DNA templates, it was presumed the human REV3L would also be able to process over various DNA templates as well. However, if REV3L did possess a nucleotide restriction to its DNA polymerase catalysis, the use of a single nucleotide template with its corresponding oligo primer would remedy this problem in part. Again, the choice to use both templates and the DEAE Sepharose filter paper spotting method for determining REV3L catalytic polymerase activity was based on the notion that both yeast and *Drosophila* Rev3 could robustly incorporate and extend from primer termini. Unfortunately, the results from this indicate no detectable polymerase activity. One reason why catalytic activity above background was not detected could be due to inadequate REV3L protein quantities and not the templates chosen. Another potential explanation for lack of REV3L catalytic activity may be because REV3L requires proteins other than REV1 and REV7 for function. It has been recently shown that yeast Rev3 catalytic activity is enhanced with PCNA (15), although various other proteins along with PCNA may be required for mammalian REV3L activity. Co-immunoprecipitation of REV1-REV3L using the freeze-thaw lysis conditions may allow for immunoprecipitation of novel protein(s) to interact. However, because of the low yields of

protein, a method for increasing the amount of immunoprecipitated protein will need to be achieved in order to begin studying this possibility.

The question of REV3L's biochemical function remains an important question that can hopefully be unraveled by improving the amount of REV3L protein generated.

4.0 HUMAN REV1, REV3L AND REV7 EXPRESSION AND INTERACTION STUDIES

4.1 INTRODUCTION

Much of the understanding of vertebrate, particularly mammalian, Rev3 primarily stems from functional genetic studies in cells and mouse models (59,68,73,78,79,83). However, many attempts at trying to understand vertebrate Rev3 function at the biochemical level have been complicated by an inability to express and purify the full-length protein. Therefore, fundamental questions regarding possible binding partners of mammalian REV3L, covalent modification, or protein complex stabilization in the presence of DNA damage remain unanswered. In contrast, there is a much better understanding of REV1 in regards to potential interaction partners and biological function in cells.

Growing evidence indicates that Rev1 plays a role in coordinating various processes associated with translesion synthesis by interacting with various damage response proteins (26,52,89). Mouse and human REV1 have been shown to interact with the Y-family translesion synthesis polymerases and this interaction is mediated predominantly through the REV1 C-terminal domain (89,119). Furthermore, mouse REV1 is ubiquitinated and possesses ubiquitin binding domains. The ubiquitin binding domains can bind ubiquitinated PCNA, allowing for localization to damaged DNA (89). However, the biological function and localization of the

ubiquitination site on mammalian REV1 remains unknown. The first genetic characterization of the yeast Rev1 phenotype was described with the *rev1-1* mutant which demonstrated an increased sensitivity to UV irradiation and an overall decrease in damage-induced mutagenesis (17). Years later, characterization of the *rev1-1* mutant delineated the mutation at G193R of Rev1 which rendered cells unable to bypass a T-T (6-4) photoproduct (120). The homologous mouse Rev1 G76R BRCT point mutant was shown to have significantly diminished ability to bind PCNA (121). Deletion of the mouse *Rev1* BRCT domain conferred the same phenotype as the G76R point mutant. Recent work demonstrated that the G193R mutation in yeast prevents REV1 from associating with DNA double-strand breaks suggesting that REV1-PCNA is important for DSB resolution (40). Prakash's group has demonstrated that yeast Rev1 binds yeast Rev3/Pol zeta. This interaction requires the C-terminal domain of Rev1 and the polymerase domain of Rev3 (99). However, determining whether human REV1 and REV3L are able to interact and identifying what domains are responsible for this interaction have not been achieved.

This work demonstrates for the first time that full-length human REV3L interacts with human REV1 in co-immunoprecipitation studies. In order to identify the regions responsible for this interaction, various REV1 and REV3L fragments were generated. Whether DNA damage plays a role in stabilization of the protein(s) or enhances the protein-protein complex was also examined. Finally, it was determined whether covalent modification of REV1, REV3L and REV7 by ubiquitin could enhance the formation and/or stability of the REV1-REV3L complex.

4.2 METHODS

4.2.1 Cloning the REV1 and REV3L Fragments

Four REV3L fragments and two REV1 fragments corresponding to regions of the full-length proteins were PCR amplified and subcloned into the mammalian expression vector, pTSIGN. Three REV1 fragments were generated: the REV1ΔCTD (amino acids 1 – 1,111); C-terminal domain (CTD) #1 (amino acids 1,112 – 1251) and C-terminal domain #2 (1,166 – 1,251) (Figure 4.1). Platinum Taq, high-fidelity (Invitrogen) was used to PCR amplify all three fragments. Refer to Appendix A and B for primers and PCR protocols used to amplify the fragments. The REV1 CTD PCR fragment was initially gel purified using a commercial kit (Qiagen), then digested with BstXI (NEB) and NotI (NEB), and finally gel purified a second time. The REV1ΔCTD of REV1 PCR product was initially gel purified using a commercial kit, then digested with NheI (NEB) and NotI, and finally gel purified a second time. These doubly digested, gel purified PCR products were ligated using T4 DNA ligase (NEB) at 16ºC overnight to similarly doubly digested, gel purified pTSIGN vector. Next day, the ligated plasmids were transformed into Top10 chemically competent high-efficiency one-shot cells (Invitrogen) and plated out on LB agar/carbenicillin plates and grown overnight at 30ºC. Next day, bacterial colonies were picked using P200 pipette tips, restreaked out on fresh LB agar/carbenicillin plates and then inoculated into fresh LB/carbenicillin and grown overnight at 37ºC at 225 RPM's. Next day, 2 ml of each overnight bacterial colony growth was prepped for DNA using a commercial mini-prep kit (Promega). Correct plasmid orientation was determined by multiple restriction

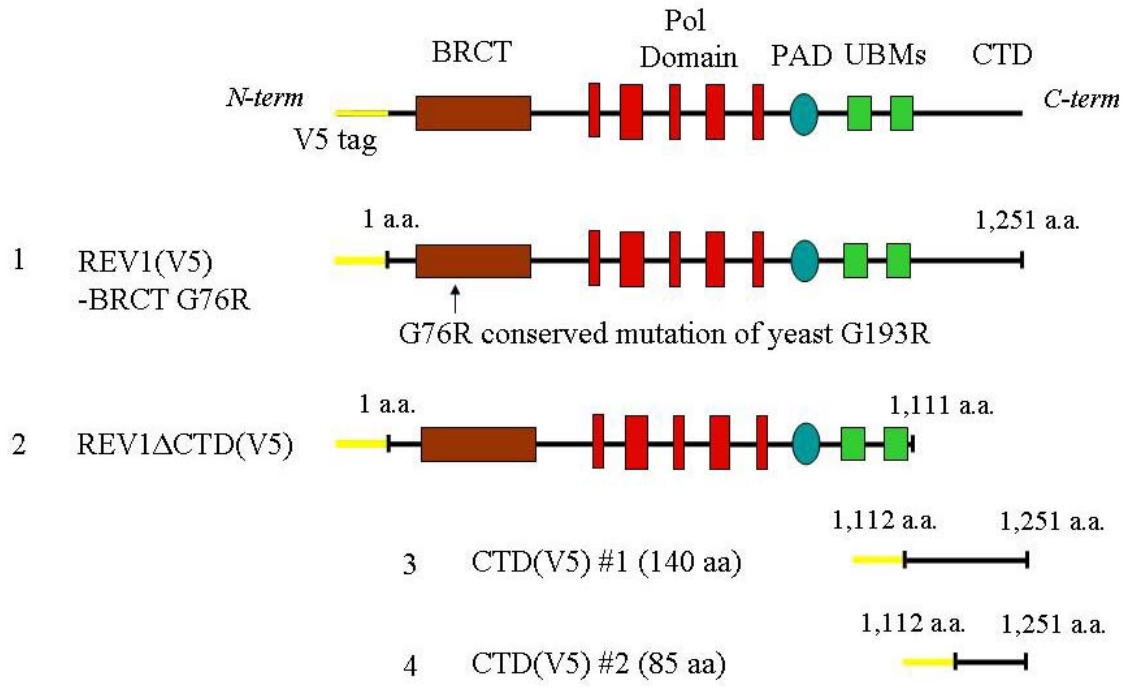

Figure 4.1 Diagram of full-length human REV1-V5 and corresponding REV1 G76R BRCT point mutant and REV1 fragments.

Construction of the REV1 G76R BRCT point mutant was done by site-directed mutagenesis using a commercial kit (Stratagene). The REV1 fragments were generated by PCR creating a 1,111 amino acid (1 – 1,111 a.a.) REV1ΔCTD fragment and two smaller C-terminal domain fragments, 140 and 85 amino acids (1,112 – 1,251 a.a. and 1,166 – 1251 a.a., respectively) each and subcloned into the mammalian expression vector, pTSIGN. Note that the residue numbers in parenthesis corresponds to the protein sequence derived from the endogenous protein and does not account for the 16 amino acids preceding the fragment which correspond to the mammalian Kozak sequence and the N-terminal V5 tag.

enzyme (RE) digestions (NheI-NotI and EcoRI for REV1ΔCTD; BstXI-NotI and EcoRI for CTD). Potential colonies were sequence analyzed for mutations.

Generation of the REV1 G76R BRCT point mutant was done by Dr. Birgitte Wittschieben using a commercial site-directed mutagenesis kit (Stratagene). Refer to her notes for PCR conditions, transformation and mini-prep isolation.

The four REV3L fragments corresponded to the Polymerase Delta homology domain, the Exon 13/KIAA domain, the REV7 Binding Domain and the Polymerase Domain. Refer to

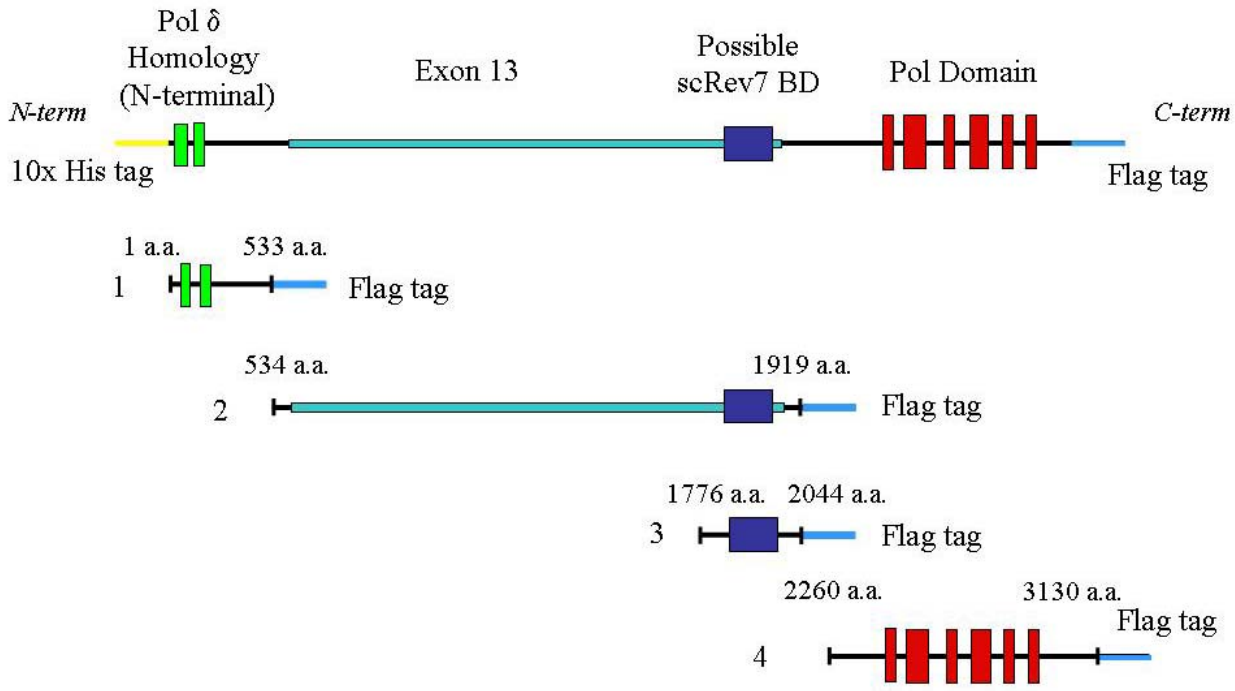

Figure 4.2 Diagram of full-length human REV3L-His-Flag (REV3L-HF) and corresponding REV3L-HF fragments.

Construction of the REV3L fragments was generated by PCR creating a 541 amino acid (1 – 533 a.a.) N-terminal domain fragment (1), a 1396 amino acid (534 – 1919 a.a.) KIAA/Exon 13 fragment (2), a 279 amino acid (1776 – 2044 a.a.) REV7 binding domain fragment (3) and a 881 amino acid (2260 – 3130 a.a.) Polymerase domain fragment (4). Note that the residue numbers in parenthesis corresponds to the protein sequence derived from the endogenous protein and does not account for the 2 amino acids preceding the fragment which correspond to the mammalian kozak sequence and the 8 amino acids at the end of each fragment which correspond to the C-terminal Flag tag. These four fragments were subcloned into the mammalian expression vector, pTSIGN.

Figure 4.2. Platinum Taq, high-fidelity was used to PCR amplify the REV7 Binding Domain and Polymerase Delta homology fragment. Refer to Appendix A and B for primers and PCR protocols used to amplify the fragments. Because of the timing, the remaining two fragments were cloned by an undergraduate assisting on the REV3L project. The two REV3L PCR fragments were initially gel purified using a commercial kit (Qiagen), then simultaneously digested with EcoRI (NEB) and NotI, and finally gel purified a second time. These doubly

digested, gel purified PCR products were ligated using T4 DNA ligase at 16ºC overnight to similarly doubly digested, gel purified pTSIGN vector. Next day, the ligated plasmids were transformed into Top10 chemically competent high-efficiency one-shot cells (Invitrogen) and plated out on LB agar/carbenicillin plates and grown overnight at 37ºC. Next day, bacterial colonies were picked using P200 pipette tips, restreaked out on fresh LB agar/carbenicillin plates and then inoculated into fresh LB/carbenicillin and grown overnight at 37ºC at 225 RPM's. Next day, 2 ml of each overnight bacterial colony growth was prepped for DNA using a commercial mini-prep kit (Promega). Correct fragment integration was determined first by digestions with EcoRI-NotI to excise the insert from the vector followed by subsequent RE digestions using EcoRV and SpeI for the KIAA/exon 13 plasmid; EcoRV for the Pol Delta homology plasmid, BstXI for the Pol Dom plasmid and EcoRI for the REV1ΔCTD plasmid. Potential colonies were sequence analyzed for verification.

The REV1ΔCTD, Polymerase Delta homology, Exon 13/KIAA and Polymerase Domain fragments either needed to be cloned or recloned because of point mutations. The design and method for engineering these four plasmids was conceived by the author, but executed by two undergraduates assisting on the protein interaction project. The REV1ΔCTD fragment will be generated by Jenny Kim while the remaining three REV3L fragments will be generated by Sharon Shung. These fragments will be amplified using Turbo Pfu polymerase.

4.2.2 Freeze-Thaw Lysis Method for REV1, REV3L, REV7 Co-immunoprecipitation

293T cells were plated at 2.5 x10^6 cells or at 1.6 x10^6 cells for transfection 2 hours or 18 hours later, respectively. Cells were single or co-transfected with 16 μg of REV3L-His-Flag (REV3L-HF) WT, 8 μg of REV1-V5 WT, REV1-V5 G76R BRCT point mutant, REV1 CTD or REV7-HA or with 4 μg of REV7-His-Flag (REV7-HF). For single, double and triple plasmid transfection, 20 μl, 40 μl and 60 μl of FuGENE6 were used. Refer to Table 3 for specifics. Cells were grown an additional 48 hours before harvesting in order to allow for protein production. Transfection efficiency was determined by eGFP expression (using IRES Neo-eGFP on pTSIGN). Expression with pTSIGN and visualization of eGFP fluorescence is an indication that the GOI is being transcribed since the IRES is downstream of GOI.

Media was aspirated from cells (on 10 cm dishes) and washed with cold 5 ml 1x PBS. Then, 1 ml of trypsin/EDTA was added to each 10 cm dish and allowed ~1 minute to trypsinize. Plates were shaken and the sides of the dish struck in order to detach cells. Trypsin was inactivated using 4 ml of media. For 2x 10 cm plates from the same group, the 2x 5 ml volumes were pooled in the same 15 ml Falcon tube. An extra 5 ml of 1x PBS (ice cold) was used to wash both plates and then this volume was added to the 15 ml Falcon for a total of ~15 ml. Cells were spun down in a table top centrifuge at 1200 RPMs for 2 minutes at 20ºC. Then, the cell pellet was washed with ice cold 1x PBS and spun down using the same conditions described above. Cells (equivalent of 2x plates, ~ 16 – 20 million cells) were resuspended in 400 μl of Freeze-Thaw lysis buffer (use 200 μl/plate). Cells were transferred into 2.2 ml eppendorf tubes and frozen in liquid nitrogen for 30 – 60 seconds or until the liquid was frozen through and then the tube was rapidly thawed in a 37ºC water bath. Cells were placed on ice and allowed to sit for

5 minutes. This freeze-thaw cycle was repeated 2x more times. The degree of cell lysis was determined by trypan blue exclusion. Lysed cells were spun down at 13,000 RPM at 4ºC for 15 minutes using a table top centrifuge (Sorval Legend). Supernatant was separated from pellet (whole cell lysate – WCL) and an aliquot or all of the supernatant was snap frozen in liquid nitrogen. The clarified supernatant can be used for immunoprecipitation or direct analysis by Western blot. In order to further analyze the contents of the remnant pellet, proceed to the insoluble chromatin protocol.

4.2.3 Chromatin Digestion

The pellet was resuspended in 200 µl (1/2 volume of Freeze-Thaw lysis buffer) of chromatin extract buffer. The pellet was gently resuspended using a P200 pipetteman trying to avoid generating bubbles. Once the cells were resuspended, 60 U's of S7 micrococcal nuclease (Roche) was added to 200 µl of chromatin extract buffer. The degree of chromatin digestion was determined empirically for each cell line. The method used for determining the degree of chromatin digestion was by mononucleosome DNA laddering on a 3% agarose gel/1x TAE. Chromatin was digested at 37ºC for 20 minutes (at 10 minutes, the pellet was pipetted up and down using a P200 pipetteman). Cells were spun down at 13,000 g's at 4ºC for 15 minutes. The clarified chromatin fraction was separated from the non-digested pellet and an aliquot or all of the chromatin fraction was snap frozen in liquid nitrogen along with the pellet remnant. The clarified chromatin fraction can be used for immunoprecipitatation or direct analysis by immunoblot.

4.2.4 Co-Immunoprecipitation of REV Protein Complex

The WCL (or chromatin fraction) was pre-cleared using 30 µl slurry of recombinant ProteinG agarose for 1 hour rotating on a rotary platform at 4ºC. In order to prepare 30 µl of bead slurry for pre-clearing the lysate, 90 µl of ProteinG agarose bead stock (Invitrogen) was washed with 300 µl of freeze-thaw lysis buffer. The beads were spun down at 2000 g's for 15 seconds and resuspended in 90 µl of lysis buffer. Then, 200 µl of WCL was added to the 30 µl of bead slurry followed by an additional 200 ul of Freeze-thaw lysis buffer (dilute by half). After 1 hour mixing, beads were spun down at 2000 RPMs at RT for 15 seconds. The pre-cleared WCL was filtered using a 1 ml Biorad spin filtration column. Then all of the pre-cleared material was pooled together before IP. 400 µl of WCL (equivalent of 1x plate) was IP per reaction. For Flag IP, each tube contained 20 µl of Flag M2 Agarose beads per 400 µl pre-cleared WCL. IP reactions were incubated for 5 hours at 4ºC with rotation. For αV5 or αHA immunoprecipitation, pre-cleared lysates were incubated for 6 hours with primary Ab and then 3 hours with ProteinG agarose (~30 µl of bead slurry) (use the same procedure described above for preparation of proteinG for pre-clearing). Beads were washed 3x with 400 µl of lysis buffer – cells were washed/resuspended for a minimum of 1 minute on ice before spinning down. Wash buffer was removed after each spin without disturbing the beads. After the final wash, beads were resuspended in 30 µl of 2x SDS loading buffer. Samples were resolved on a SDS-PAGE gel as described in Chapter 3.

4.2.5 Co-transfection of HA-ubiquitin and REV1, REV3L or REV7

Co-transfection of cells was performed as described above in the Freeze-Thaw lysis protocol with the following exceptions: 1) 0.6 μg of Ub-HA plasmid (generous gift from Dr. Yong Wan, University of Pittsburgh) was co-transfected with either REV1-V5, REV3L-HF or REV7-HF plasmid; 2) Co-transfected Ub-HA with either REV1, REV3L or REV7 was process cells using hi-salt RIPA lysis buffer (described in Chapter 3); 3) For triple co-transfected Ub-HA with both REV1 and REV3L, cells were processed using the freeze-thaw lysis method.

4.2.6 DNA Damage and Nocodazole Treatment of Transiently Transfected 293T Cells

Transiently transfected 293T cells grown in 10 cm^2 tissue culture plates were damaged with various DNA damaging agents for 30 to 90 minutes before harvesting cells for protein. For UV irradiation: Without changing their media, cells received a dose of 20 J/m^2 (0.5 J/m^2/sec) from a stationary 254 nm UVC source (40W bulb X-Series, Spectronics Corporations). After irradiation, mock treated and treated cells had their media aspirated and replaced with 5 ml of fresh DMEM/10% FBS with 1% pennicillin/streptomycin and were incubated at 37ºC in a humidified 5% CO_2 incubator until they were harvested. For ionizing radiation: Cells received 2 Gy of γ-IR delivered from a ^{137}Cesium source at an unattenuated dose rate of 4.28 Gy/min in a Shepherd Mark I Model 68 (J.L. Shepherd and Associates). Cells were incubated at 37ºC in a humidified 5% CO_2 incubator until they were harvested. For MMS and cisplatin: Cells received a final concentration of 0.5 mM MMS (generous gift from the Sobol lab) or 30 μg/ml cisplatin

diluted in DMEM. Mock treated cells only received DMEM. Cells were incubated at 37ºC in a humidified 5% CO_2 incubator until they were harvested. For experiments examining the whole cell lysate and chromatin fractions, cells were harvested 60 and 90 minutes post-DNA damage using the Freeze-thaw lysis method with chromatin digestion protocol described above. For experiments examining protein ubiquitination, cells were harvested 30 minutes post-DNA damage.

For G_2/M arrest of co-transfected 293T cells, cells were treated 18 hours before harvest with 100 ng/ml of nocodazole (Sigma) per 10 cm dish (10 ml total volume). After 18 hours, cells were examined under the microscope to determine percent number of rounded cells. Successful G_2/M enrichment was defined as ~95% rounded cells. Transfection efficiency was assessed by fluorescence microscopy. Cell harvest was modified from above. For two identical plates, 7.5 ml of media was collected from each plate and added to a single 15 ml Falcon tube and spun down at 1200 RPM's for 2 minutes at 20ºC. While cells spun down, forego the 1x PBS wash of each dish and proceed to detach cells using 1x trypsin/EDTA for 1 minute. Trypsin/EDTA was inactivated in 4 ml of media. Using the same 15 ml Falcon tube with the pelleted "floating" cells, the media was aspirated and the freshly trypsinized cells were added on top of the spun-down floating" cells and respun using the conditions described above. Each Falcon tube was washed with 10 ml of 1x PBS and spun down for 2 minutes at 1200 RPM's at 20ºC. These cells were processed using a Freeze-Thaw lysis as described above.

4.2.7 Proteasome Inhibitor Treatment of Transiently Transfected 293T Cells

Proteasome inhibitors were added to transiently transfected cells 5 hours (MG132) or 6 hours (ALLN) before harvesting for protein. Final concentration of each proteasome inhibitor was 20 μM M132 and 25 μM ALLN for each 10 cm plate. Preparation of MG132 and ALLN was difficult because of solubility issues. From a stock concentration of 5 mM MG132, 40 μl of stock was added to 40 μl of media and successively diluted in four complete cycles by adding the summed volume for the next dilution (ie. 80 μl of diluted MG132 to 80 μl of media, then 160 μl of dilute MG132 to 160 μl of media, etc) until a final volume of 960 μl was achieved. This volume was then added to a single plate. Proteasome inhibitor fractions for MG132 were prepared similarly for each plate. From a stock concentration of 50 mM ALLN, 5 μl was diluted in 20 μl of media. After mixing, another 50 μl was added and thoroughly mixed. Four successive additions of media (100 μl/ea) were used to further dilute ALLN. This total diluted solution was then added to a single plate. Proteasome inhibitor fractions for ALLN were prepared similarly for each plate.

4.3 RESULTS

4.3.1 REV1-REV3L Protein Interaction

In order to test for interaction between human REV1 and REV3L proteins, the recombinant human proteins were co-expressed in 293T cells. The cell lysate was immunoprecipitated and

resolved by SDS-PAGE. Protein interaction was then assessed by immunoblot. Initial attempts to combine purified proteins separately and in a modified RIPA lysis buffer (refer to chapter 3 DNA Polymerase Activity Method section) did not demonstrate a REV1-REV3L interaction by either Flag M2 agarose or αV5 immunoprecipitation. Since protein denaturation during purification was a concern, various lysis and purification methods were tested. Preparation of the protein according to a modified freeze-thaw lysis protocol allowed for co-immunoprecipitation of the REV1-REV3L complex by Flag M2 agarose (Figure 4.3A). It was discovered that REV1 prepared using the freeze-thaw lysis buffer non-specifically bound to both Flag M2 agarose and ProteinG agarose. However, when the lysate was extensively precleared using an excess amount of ProteinG, a majority of this non-specific REV1 interaction was lost. A faint band can still be observed in the REV1-V5 Flag M2 IP lane alone (Figure 4.3C). It appears that REV1 is sticky and binds non-specifically to the agarose matrix. To determine if the REV1-REV3L interaction was real, immunoprecipitation by αV5-ProteinG was performed. This demonstrated that REV3L can co-immunoprecipitate with REV1 (Figure 4.3B). Furthermore, the full-length REV3L active-site mutant can interact with full-length REV1 (Figure 4.3D).

In order to determine whether the BRCT domain point mutation G76R in REV1 plays a role in the REV1-REV3L interaction, the REV1 G76R mutant (REV1 Mut) was co-transfected with full-length REV3L (Figure 4.4A). REV1 Mut was no different compared to REV1 WT in its ability to interact with full-length REV3L (Figure 4.4B). In the presence or absence of 20 J/m^2 of UV irradiation, both wild type and mutant REV1 co-immunoprecipitated with REV3L as demonstrated by immunoblot (Figure 4.4C). Exposure of transiently co-transfected cells to UV-irradiation, MMS and CDDP did not enhance the REV1-REV3L

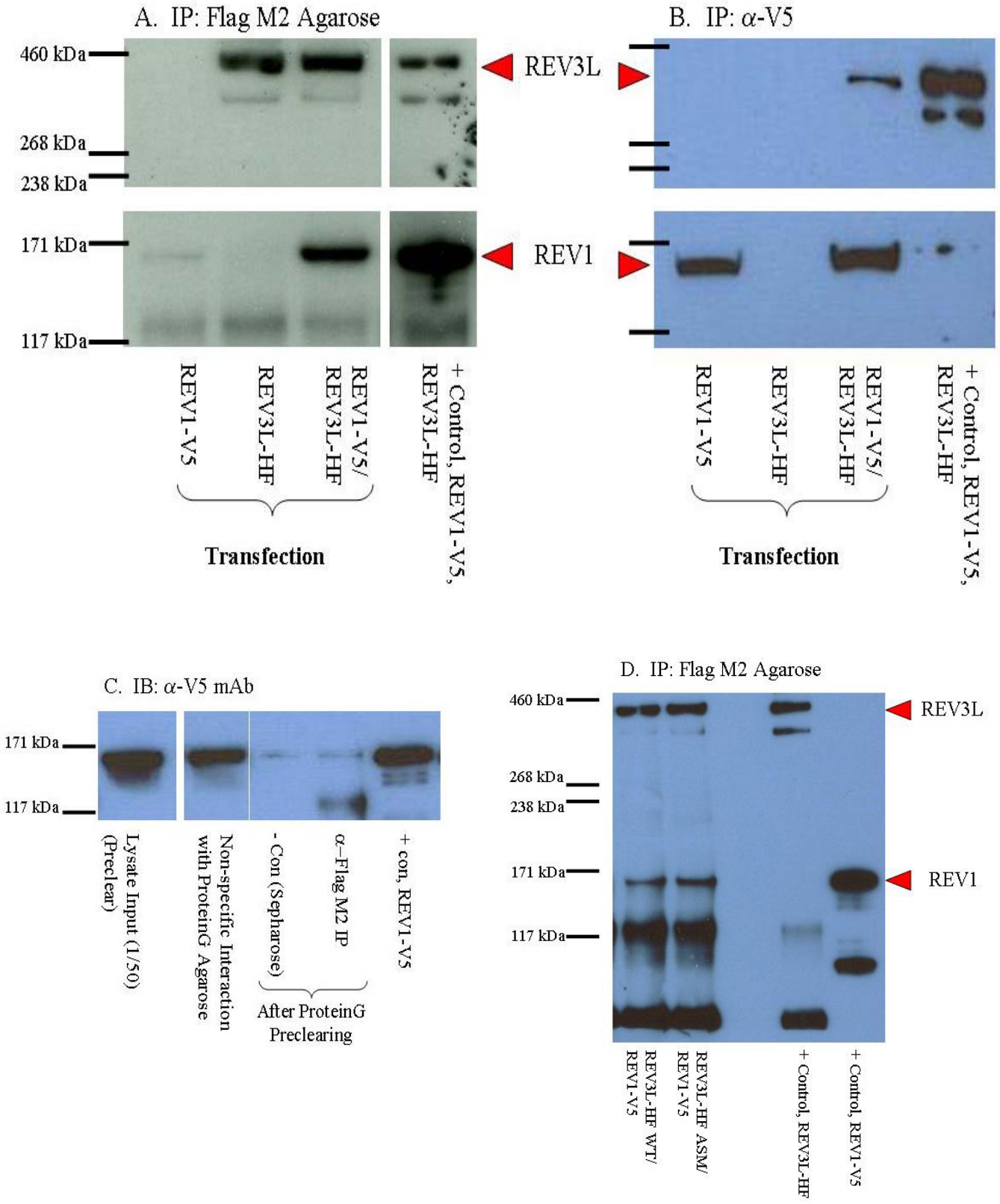
A. IP: Flag M2 Agarose
460 kDa
268 kDa
238 kDa
171 kDa
117 kDa
REV3L
REV1
REV1-V5
REV3L-HF
REV1-V5/ REV3L-HF
+ Control, REV1-V5, REV3L-HF
Transfection
B. IP: α-V5
REV1-V5
REV3L-HF
REV1-V5/ REV3L-HF
+ Control, REV1-V5, REV3L-HF
Transfection
C. IB: α-V5 mAb
171 kDa
117 kDa
Lysate Input (1/50) (Preclear)
Non-specific Interaction with ProteinG Agarose
- Con (Sepharose)
α–Flag M2 IP
After ProteinG Preclearing
+ con, REV1-V5
D. IP: Flag M2 Agarose
460 kDa
268 kDa
238 kDa
171 kDa
117 kDa
REV3L
REV1
REV3L-HF WT/ REV1-V5
REV3L-HF ASM/ REV1-V5
+ Control, REV3L-HF
+ Control, REV1-V5

Figure 4.3 Interaction of full-length human REV1 and REV3L by co-immunoprecipitation.

REV1-V5 and REV3L-HF plasmids were transiently transfected either individually or together into 293T cells 48 hours before harvesting. Cells were lysed by freeze-thaw. Pre-cleared lysates were immunoprecipitated (IP) either by Flag M2 agarose (A) or by αV5-ProteinG (B). IP samples were, resolved by SDS-PAGE and blotted with αREV3L N-term pAb (REV3L) and αV5 mAb (REV1) for Flag M2 agarose IP samples or blotted with αFlag M2 mAb (REV3L) and αREV1 pAb (REV1) for aV5 IP samples. C. Lysate (input), Lysate precleared on ProteinG beads and the ProteinG beads themselves were examined for relative amounts of non-specific REV1 interaction by αV5 mAb immunoblot. D. Immunoblot demonstrating co-immunoprecipitation of WT or polymerase domain active-site mutant (ASM) REV3L-HF with REV1-V5.

interaction by co-immunoprecipitation from whole cell lysates (Figure 4.4C and 4.5). There was no observed increase in the amount of endogenous REV7 co-immunoprecipitating with the recombinant REV1-REV3L complex (Figure 4.5). Transiently transfected REV1-REV3L in clarified whole cell extracts was examined in order to determine whether there was a change in REV1 or REV3L protein expression upon DNA damage. No change in protein expression or stabilization of recombinant REV1, REV3L or REV7 in either 60 μg of whole cell lysate protein or in 60 μg of chromatin extract protein regardless of DNA damage was observed (Figure 4.6). In order to determine whether DNA damage or cell cycle arrest could cause enrichment of a REV1-REV3L complex within the chromatin extract, cells were co-transfected with REV1-REV3L in the presence or absence of DNA damage or nocodazole. Nocodazole treated cells were assessed for arrest in G_2/M phase using FACS analysis. Approximately 90% of cells were arrested in G_2/M after 18 hours of nocodazole treatment compared to approximately 15% in non-treated cells. Cells were processed using a freeze-thaw lysis method and the whole cell lysate and chromatin fractions were co-immunoprecipitated and immunoblotted. There was no observed enrichment of the immunoprecipitated REV1-REV3L complex regardless of DNA damage (Figure 4.7A) or nocodazole treatment (Figure 4.7B).

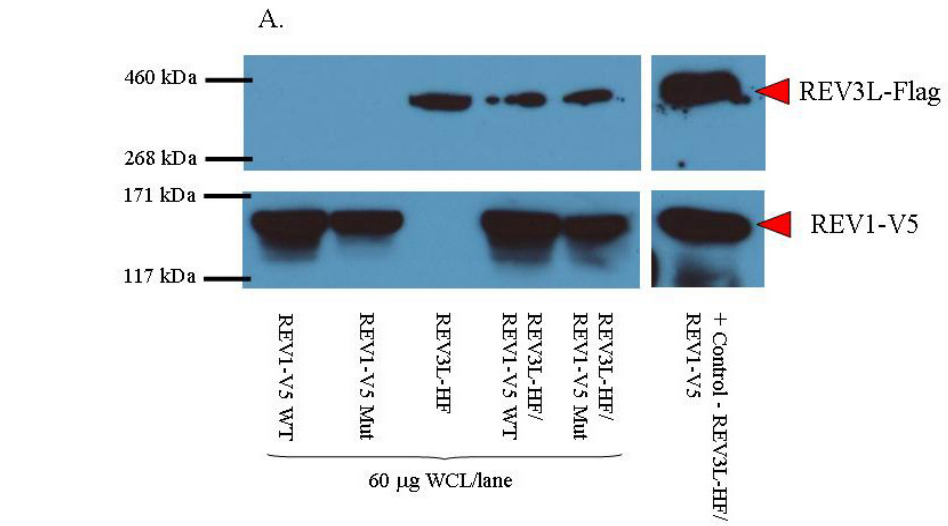
A.
460 kDa
268 kDa
171 kDa
117 kDa
REV3L-Flag
REV1-V5
REV1-V5 WT
REV1-V5 Mut
REV3L-HF
REV3L-HF/ REV1-V5 WT
REV3L-HF/ REV1-V5 Mut
60 µg WCL/lane
+ Control - REV3L-HF/ REV1-V5

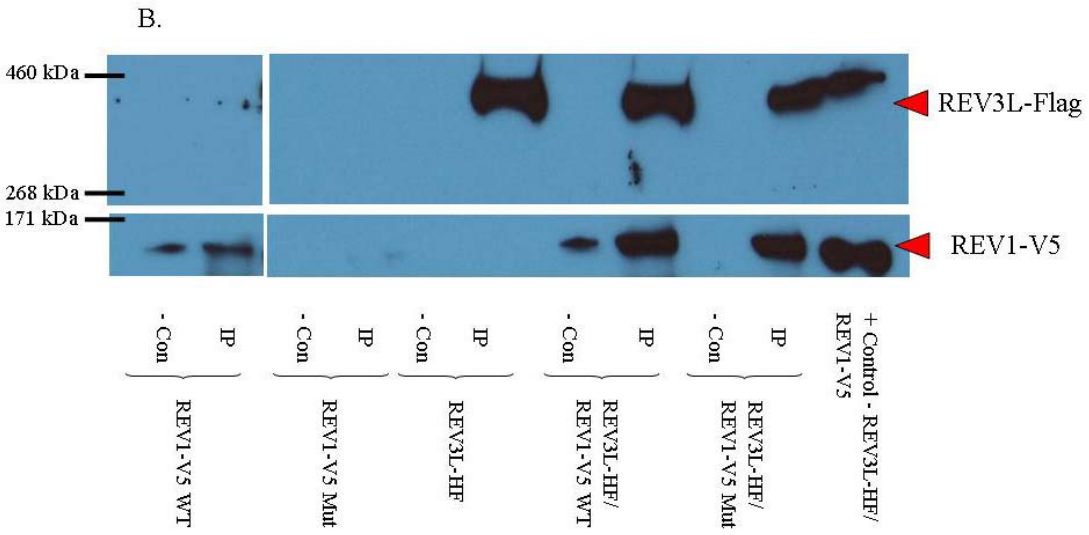
B.
460 kDa
268 kDa
171 kDa
REV3L-Flag
REV1-V5
- Con
IP
REV1-V5 WT
REV1-V5 Mut
REV3L-HF
REV3L-HF/ REV1-V5 WT
REV3L-HF/ REV1-V5 Mut
+ Control - REV3L-HF/ REV1-V5

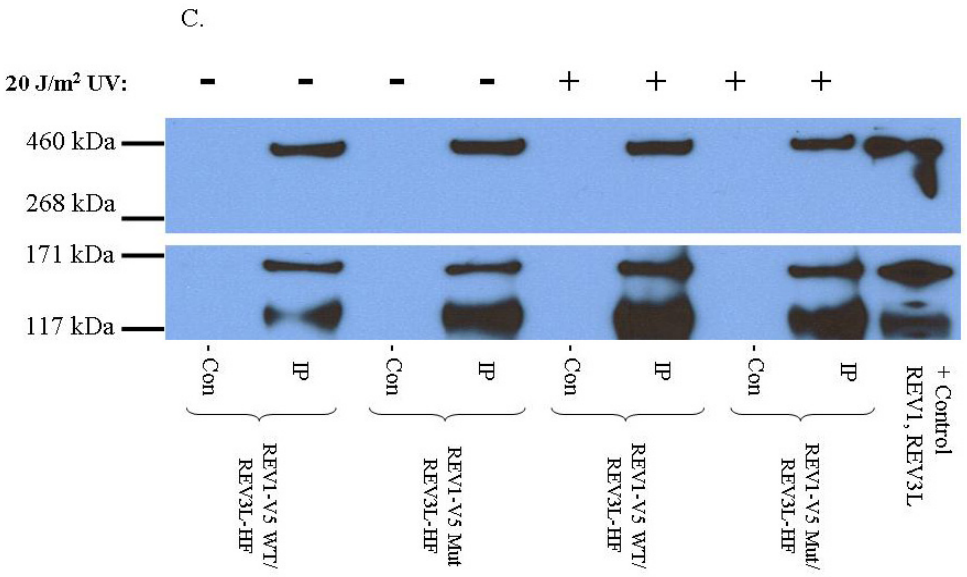

Figure 4.4 Full-length human REV3L interacts with REV1 WT or REV1 G76R BRCT point mutant (REV1 Mut) by co-immunoprecipitation.

REV1-V5 and REV3L-HF plasmids were transiently transfected either individually or together into 293T cells 48 hours before harvesting. Cells were lysed by freeze-thaw. A. 60 µg of whole cell lysate protein was resolved by SDS –PAGE and blotted with αREV3L N-term pAb and αV5 mAb (REV1). The positive control lane consisted of REV1 or REV3L protein prepared separately, immunoprecipitated from transiently transfected cells, and a fraction loaded to act as a sizing control for each gel. B. Pre-cleared lysates were immunoprecipitated (IP) by Flag M2 agarose or with negative control Sepharose beads. IP samples were washed, resolved by SDS-PAGE and blotted with αREV3L N-term pAb (REV3L) and αV5 mAb (REV1). C. Cells were UV irradiated with 20 J/m^2 1.5 hours before harvesting for protein. Cells were processed as described above for immunoblot.

4.3.2 REV1-REV7 Protein Interaction

In order to determine whether the recombinant human full-length REV1 and REV7 proteins were also able to interact with one another, these proteins were co-transfected into 293T cells. Protein interaction of REV1 and REV7 was demonstrated by immunoprecipitating cell lysates using αV5 or αHA and detected by immunoblot (Figure 4.8A). Similarly, REV7 interacted equally well with both the REV1 G67R mutant and the WT REV1 (Figure 4.8B).

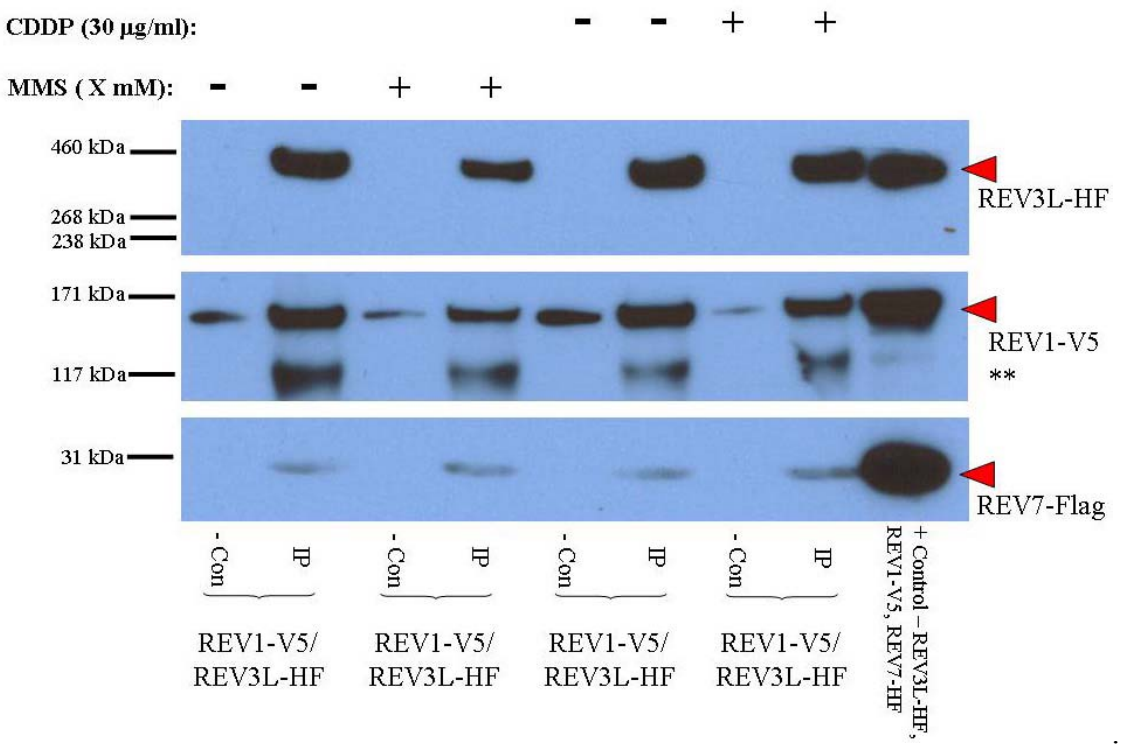

Figure 4.5 DNA damage and its effect on the human REV1-REV3L complex.

REV1-V5 and REV3L-HF plasmids were transiently transfected together into 293T cells 48 hours before harvesting. Cells were treated with 30 µg/ml of cisplatin or with 0.5 mM MMS 1.5 hours before harvesting for protein. Cells were lysed using freeze-thaw. Pre-cleared lysates were immunoprecipitated (IP) by Flag M2 agarose or with negative control Sepharose beads. IP samples were washed, resolved by SDS-PAGE and blotted with αREV3L N-term pAb, αV5 mAb (REV1) or αREV7 pAb. The double asterisk indicates a non-specific band corresponding to the IgG heavy chain detected from the Flag M2 agarose.

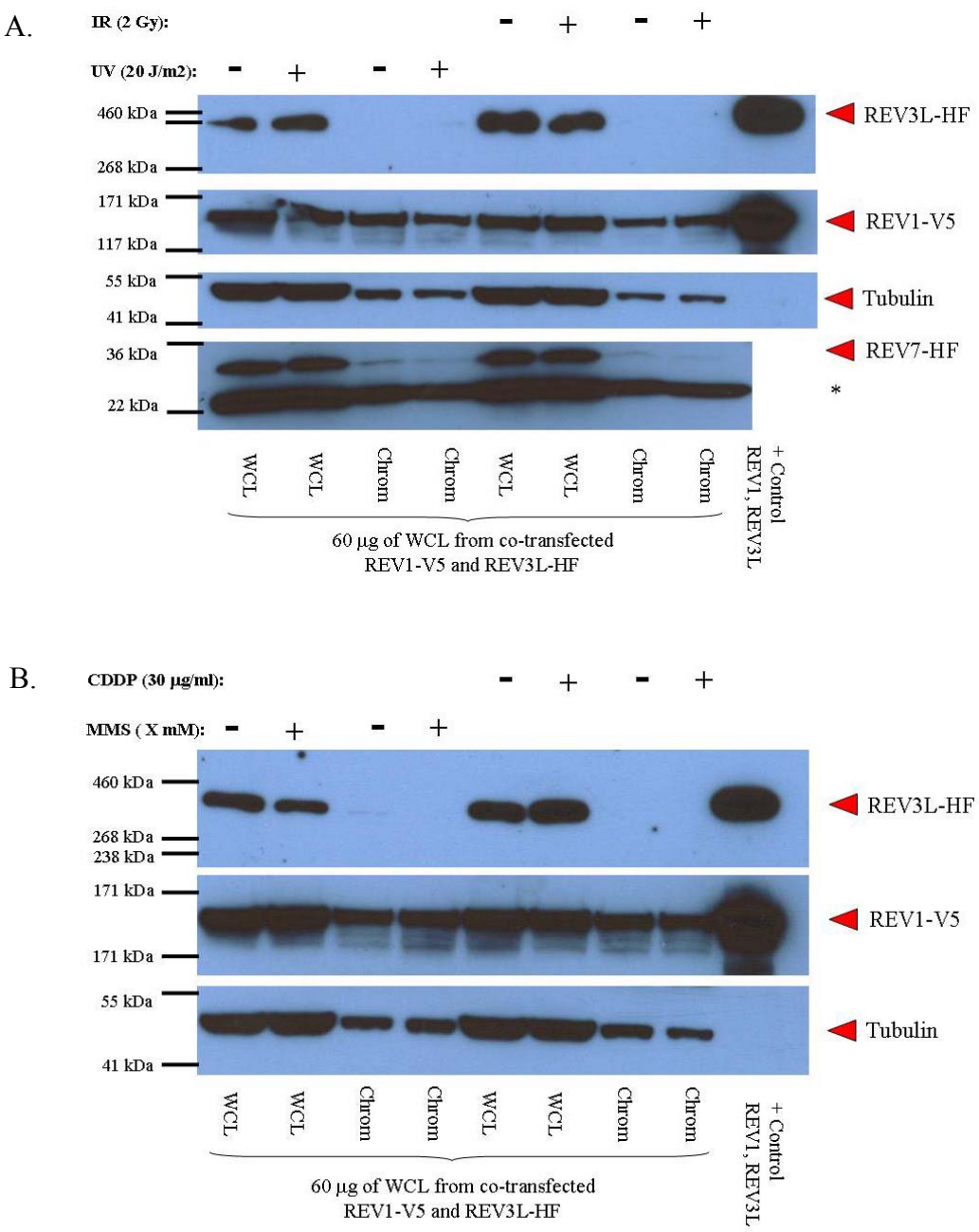

Figure 4.6 The effect of DNA damage on recombinant full-length human REV1 and REV3L.

REV1-V5 and REV3L-HF plasmids were transiently co-transfected into 293T cells 48 hours before harvesting. A. Cells were treated with 20 J/m2 of UV (254 nm) or 2 Gy of IR 1.5 hours before harvesting for protein. 60 µg of whole cell and chromatin lysate protein was resolved by SDS –PAGE and blotted with αREV3L N-term pAb, αV5 mAb (REV1), αREV7 pAb and αTubulin mAb. The single asterisk indicates endogenous REV7. B. Cells were treated with 30 µg/ml of cisplatin or with 0.5 mM MMS 1.5 hours before harvesting for protein. 60 µg of whole cell and chromatin lysate protein was resolved by SDS –PAGE and blotted with αREV3L N-term pAb, αV5 mAb (REV1) or αTubulin mAb. Tubulin was used as a loading control.

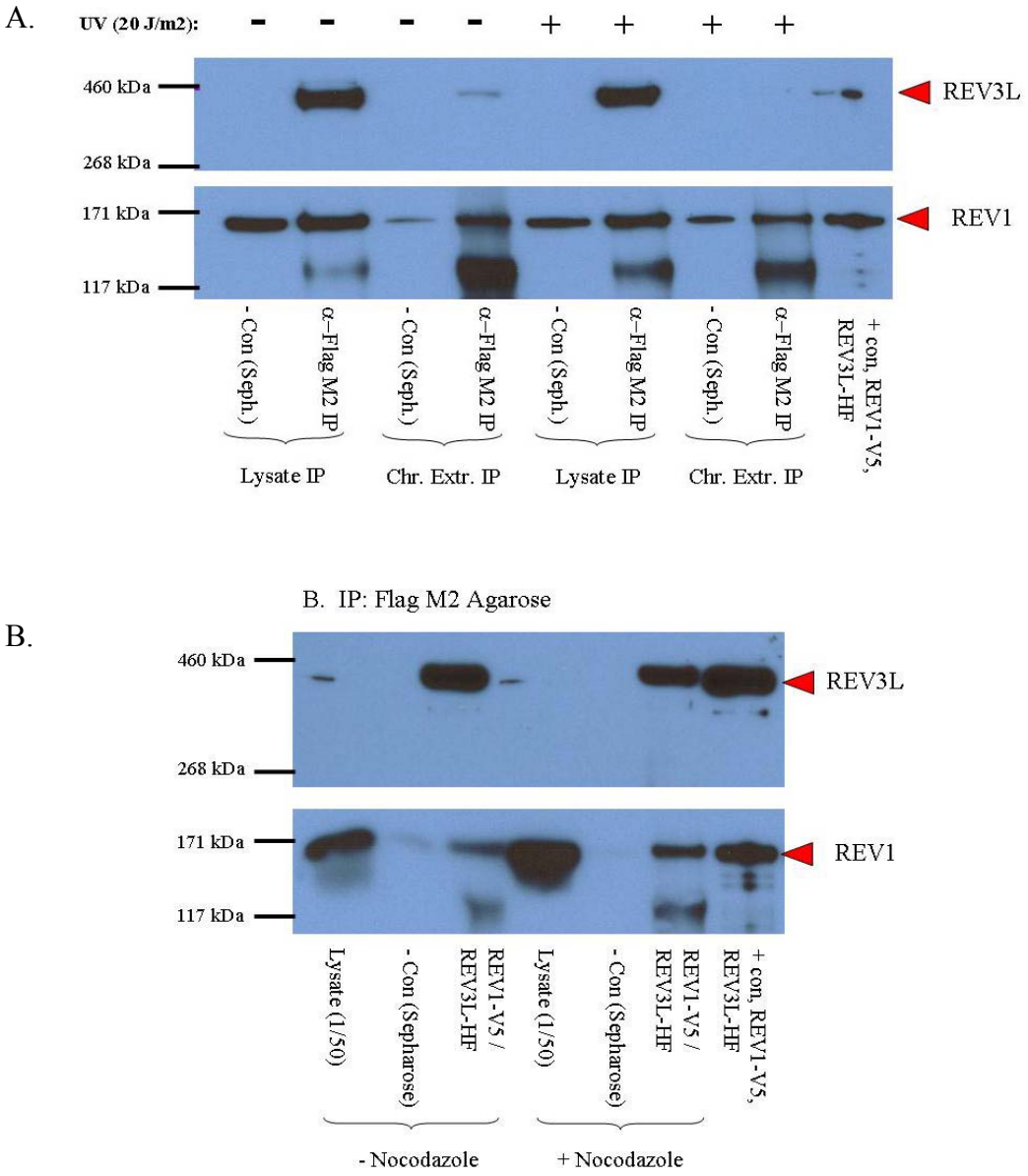

Figure 4.7 The effect of UV-irradiation and Nocodazole on REV1-REV3L interaction.

A. The effect of UV irradiation on the REV1-REV3L interaction was examined as followed. REV1-V5 and REV3L-HF plasmids were transiently co-transfected into 293T cells 48 hours before harvesting. 90 minutes before harvesting, cells were UV irradiated at 20 J/m^2. Cells were lysed using freeze-thaw and the insoluble pellet was further chromatin digested. Pre-cleared whole cell and chromatin lysates were immunoprecipitated by Flag M2 agarose, resolved by SDS-PAGE and immunoblotted with αREV3L N-term pAb (REV3L-HF) and αV5 mAb (REV1-V5). B. The effect of cell cycle arrest in G_2/M using nocodazole was examined as follows. REV1-V5 and REV3L-HF plasmids were transientlyco-transfected into 293T cells 48 hours before harvesting. 18 hours before cells were harvested, cells were treated with 100 ng/ml nocodazole. Cells were lysed using freeze-thaw. Pre-cleared lysates were immunoprecipitated by Flag M2 agarose, resolved by SDS-PAGE and immunoblotted with αREV3L N-term pAb (REV3L-HF) and αV5 mAb (REV1-V5).

Figure 4.7 The effect of UV-irradiation and Nocodazole on REV1-REV3L Interaction

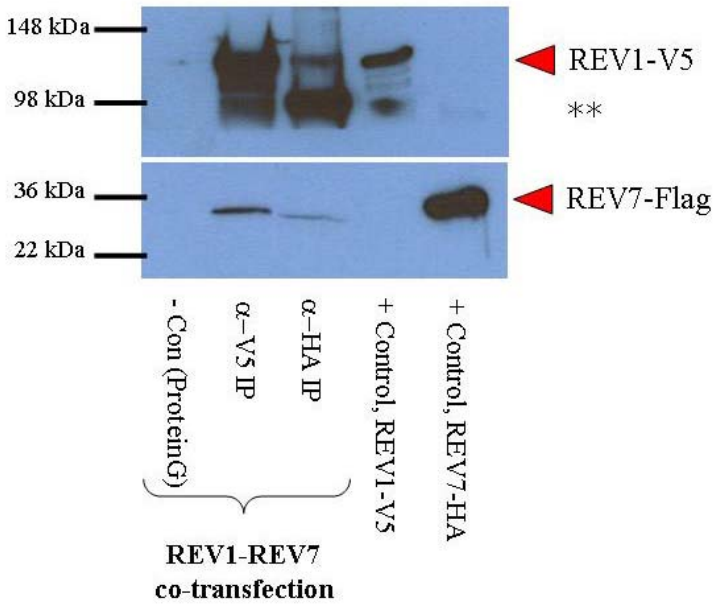

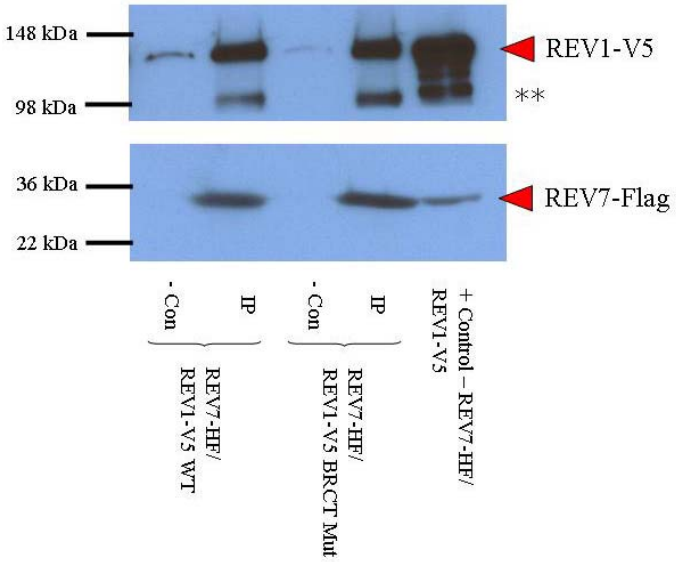

Figure 4.8 Full-length human REV1 WT and G76R BRCT point mutant interacts with REV7 by co-immunoprecipitation.

A. REV1-V5 and REV7-HA plasmids were transiently co-transfected into 293T cells 48 hours before harvesting. Cells were lysed using freeze-thaw. Pre-cleared lysates were immunoprecipitated (IP) either by αV5-ProteinG, αHA-ProteinG or ProteinG beads by itself (negative control). IP samples were washed, resolved by SDS-PAGE and blotted with either αREV7 pAb and αV5 mAb (REV1). Double asterisks indicate a non-specific band. A. REV1-REV7 interaction. B. REV1 wild type versus REV1 G76R mutant interaction with REV7.

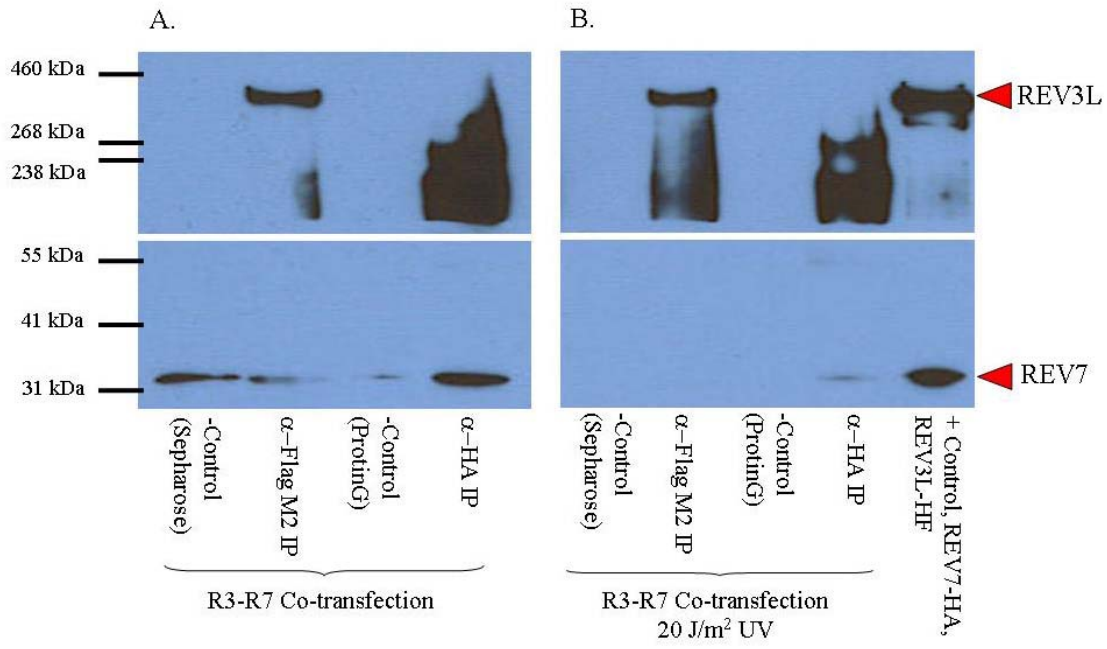

Figure 4.9 Full-length human REV3L does not interact with REV7 irrespective of UV damage.

REV3L-HF and REV7-HA plasmids were transiently co-transfected into 293T cells 48 hours before harvesting. Cells were lysed using freeze-thaw. Pre-cleared lysates were immunoprecipitated (IP) by Flag M2 agarose and with negative control Sepharose beads or with αHA-ProteinG and ProteinG beads by itself (negative control). IP samples were washed, resolved by SDS-PAGE and blotted with αREV7 pAb and αFlag mAb (REV3L).

4.3.3 REV3L-REV7 Protein Interaction

Co-transfection and purification of REV3L and REV7 using the freeze-thaw method did not reveal a protein-protein interaction in contrast to the REV1-REV3L interactions described above (Figure 4.9A). Furthermore, UV irradiation did not result in enhanced REV3L-REV7 interaction (Figure 4.9B). Co-immunoprecipitation of the REV1-REV3L complex was also examined in the presence or absence of DNA damage in order to determine whether endogenous REV7 interaction with REV1-REV3L could be observed. There was no observed interaction of

endogenous REV7 with co-immunoprecipitated REV1-REV3L from cells treated with cisplatin or MMS. The faint REV7 band observed after overexposure of the blot may be due to non-specific REV7 interaction with the Flag M2 agarose beads (Figure 4.5).

4.3.4 Expression of REV1 and REV3L Protein Fragments

In order to determine which domains are responsible for the human REV1-REV3L protein-protein interaction, fragments of REV1 and REV3L and the REV1 G76R point mutant (described above) were employed. C-terminal domain fragments of REV1 corresponding to its last 140 amino acids (CTD #1), or its last 85 amino acids (CTD #2), as well as a REV1 fragment lacking the last 140 amino acid (REV1ΔCTD) were generated (Figure 4.1). Transfection of 293T cells with 8 μg of REV1 G76R mutant DNA or the C-terminal domain (CTD #1) of REV1 followed by αV5-ProteinG immunoprecipitation demonstrated robust expression by αV5 mAb immunoblot (Figure 4.10). Using the same amount of DNA, the CTD #2, did not express as well as CTD #1 and overexposure was needed for detection (data not shown). Two base insertion mutations in REV1ΔCTD caused a +2 frameshift in the DNA sequence preventing protein expression. Therefore, the plasmid pTSIGN- REV1ΔCTD will need to be fixed or reconstructed.

The N-terminal Domain, Exon 13/KIAA Domain, REV7 Binding Domain, and the Polymerase Domain correspond to the four REV3L fragments (Figure 4.2). The REV7 Binding Domain fragment has been successfully cloned and sequenced. However, it has not yet been transfected and expressed in 293T cells. The polymerase domain has been successfully cloned and contains a single point mutation generated by PCR amplification in the 5' region of the gene.

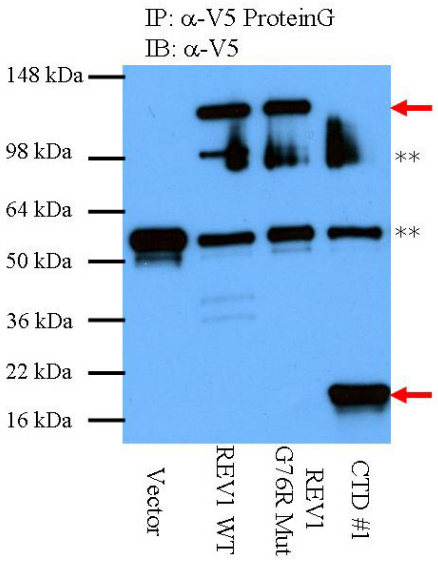

Figure 4.10 Expression and detection of REV1 G76R BRCT point mutant and REV1 CTD fragment.

REV1-V5 G76R BRCT point mutant and CTD fragment plasmids were transiently transfected individually into 293T cells and grown for 48 hours before harvesting. Cells were lysed using a freeze-thaw lysis method. Pre-cleared lysates were immunoprecipitated by αV5-ProteinG. Beads were washed, resolved by SDS-PAGE and blotted with αV5 mAb (REV1 and CTD). Double asterisk indicates a non-specific band.

A single experiment involving co-transfection of the polymerase domain and the REV1 plasmid has been attempted with the results described below. Furthermore, attempts are currently being made to reclone the 5' portion of the polymerase domain in order to eliminate the single mutation. The two remaining plasmids, exon 13/KIAA and N-terminal Domain, have been subcloned into pTSIGN and need to be sequence verified.

4.3.5 REV1 and REV3L Fragment Interaction with Full-length REV1 and REV3L

Using the fragments already generated, work has begun characterizing the domains potentially responsible for the REV1-REV3L interaction. Flag M2 agarose immunoprecipitation of co-transfected CTD#1 with full-length REV3L-HF demonstrated that the CTD#1 co-immunoprecipitates with REV3L as demonstrated by immunoblot (Figure 4.11). Because of the poor expression level of CTD#2, CTD#2 was not co-transfected with REV3L for this experiment. As expected, REV1 co-immunoprecipitated with REV3L. Similarly, CTD#1 interacted with REV7 by Flag immunoprecipitation as demonstrated by immunoblot (Figure 4.12). Transfection with REV1ΔCTD did not yield a product because of the +2 frameshift mutation in its sequence. Negative control (sepharose) results were negative for non-specific protein interaction for all transfected samples. Preliminary results examining Flag M2 agarose immunoprecipitated cell lysates co-transfected with the polymerase domain fragment with full-length REV1 indicated that REV1 interacted with the polymerase domain of REV3L. This is a single result and will need to be verified.

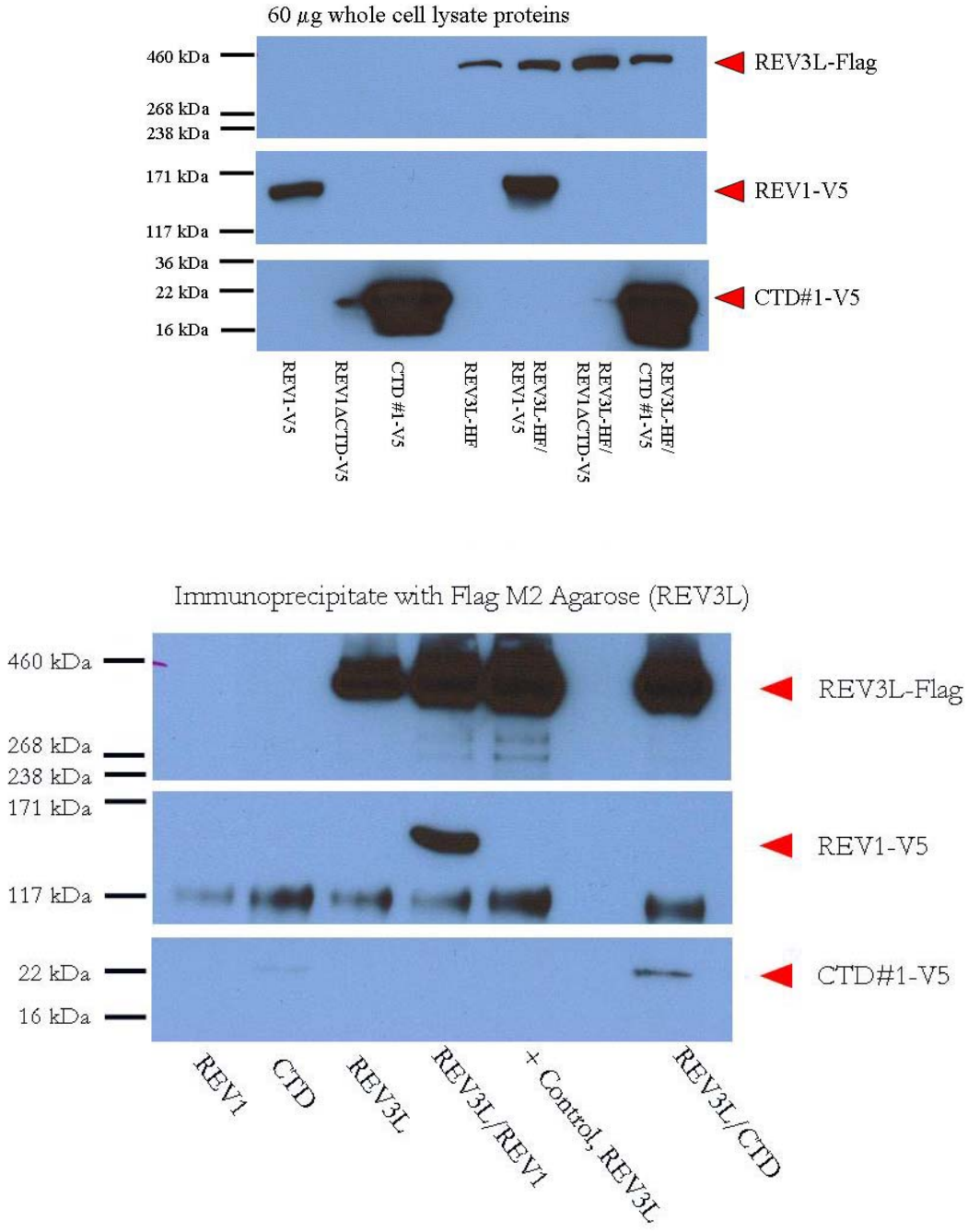

Figure 4.11 The CTD of REV1 interacts with full-length human REV3L.

REV1-V5, REV1ΔCTD, CTD and REV3L-HF plasmids were transiently transfected either individually or in pairs into 293T cells 48 hours before harvesting. Cells were lysed using freeze-thaw. A. 60 μg of whole cell lysate was resolved by SDS –PAGE and blotted with αREV3L N-term pAb and αV5 mAb (REV1, CTD). B. Pre-cleared lysates were immunoprecipitated (IP) by Flag M2 agarose or with negative control Sepharose beads. IP samples were washed, resolved by SDS-PAGE and blotted with αREV3L N-term pAb and αV5 mAb (REV1, CTD). Double asterisks indicate a non-specific band.

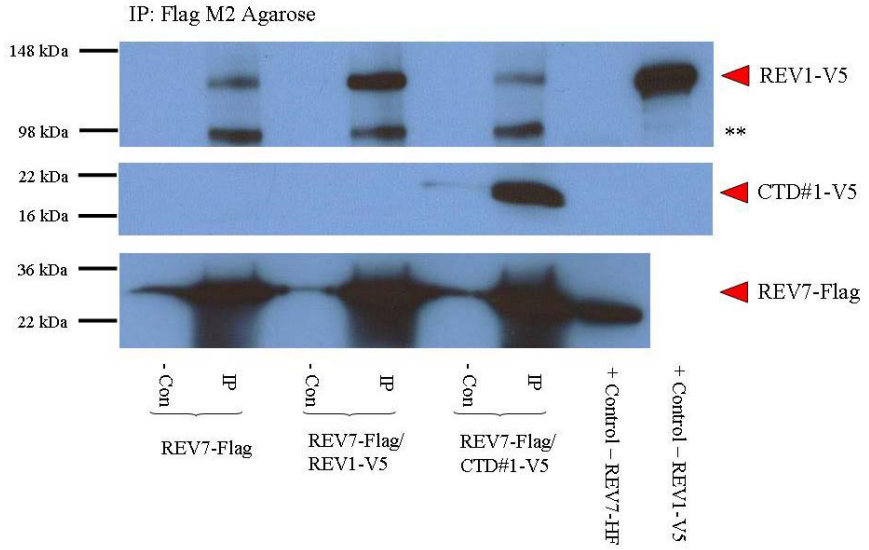

Figure 4.12 The CTD of REV1 interacts with full-length human REV7.

REV1-V5 and REV7-HF plasmids were transiently co-transfected into 293T cells 48 hours before harvesting. Cells were lysed using freeze-thaw. Pre-cleared lysates were immunoprecipitated using Flag M2 agarose beads or with Sepharose4B beads (negative control). IP samples were washed, resolved by SDS-PAGE and blotted with αREV7 pAb and αV5 mAb (REV1, CTD). Double asterisks indicate a non-specific band.

4.3.6 Ubiquitination of REV1, REV3L and REV7

The ubiquitination status of the REV proteins was examined by co-transfection with HA-Ub and the various REV plasmids followed by immunoblotting immunoprecipitated protein with a αHA mAb. Examination of REV3L ubiquitination by immunoblot indicates that REV3L is ubiquitinated and that this ubiquitination is UV-irradiation damage independent. Immunoblotting of recombinant REV1 indicated that the protein was ubiquitinated (Figure 4.14). The ubiquitination observed was also damage independent for UVC (20 J/m^2) for REV1 (Figure 4.14B). In order to identify the region of REV1 which becomes ubiquitinated, the CTD#1 was co-transfected with HA-ubiquitin. Three major forms were observed by immunoblot of co-

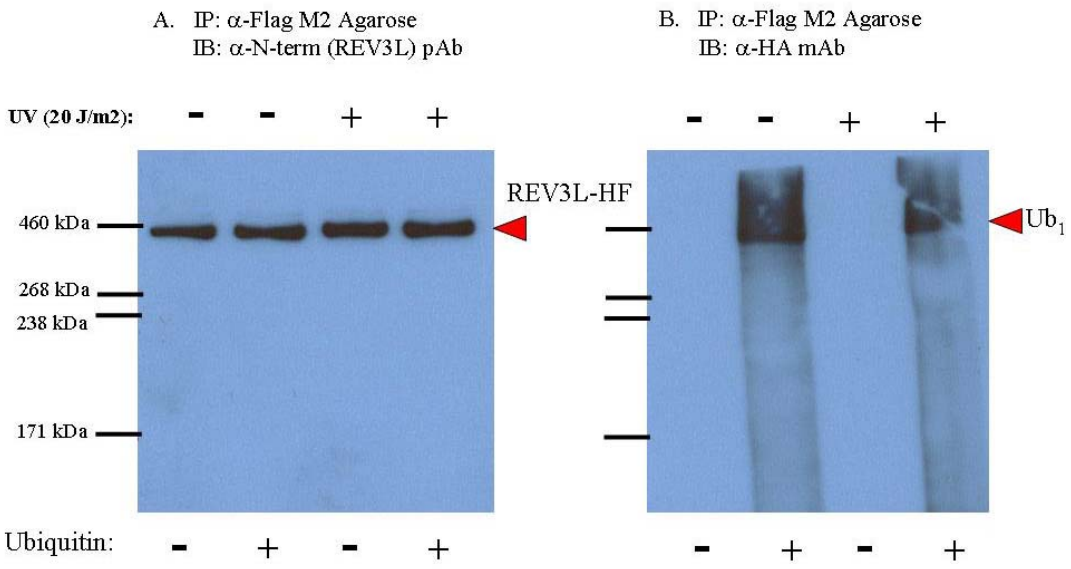

Figure 4.13 Ubiquitination of human REV3L.

REV3L-HF was transfected by itself or co-transfected with the Ubiquitin-HA plasmids into 293T cells 48 hours before harvesting. 30 minutes before cell harvest, cells were UVC (254 nm) irradiated with 20 J/m^2. Protein was harvested from cells using a hi-salt RIPA lysis method. Lysates were immunoprecipitated by Flag M2 agarose. IP samples were washed, resolved by SDS-PAGE and blotted with either: A. αREV3L N-term pAb (total REV3L-HF) or B. αHA mAb (Ub-REV3L-HF).

transfected CTD#1 with Ub-HA using αV5 mAb and αHA mAb. The non-ubiquitinated CTD#1 at 16-18 kDa, a band at 26-28 kDa for the mono-ubiquitinated form and the di-ubiquitinated form at 36-38 kDa was observed (Figure 4.14). For REV7, three forms were also observed. Using the REV7 polyclonal antibody, recombinant REV7 at 30 kDa, mono-ubiquitinated REV7 at 38–40 kDa, and another less distinct di-ubiquitinated band at 48–50 kDa which was partially obscured by the Ig heavy chain, were observed (Figure 4.15). These results will need to be confirmed by αHA IP for the HA-ubiquitinated REV

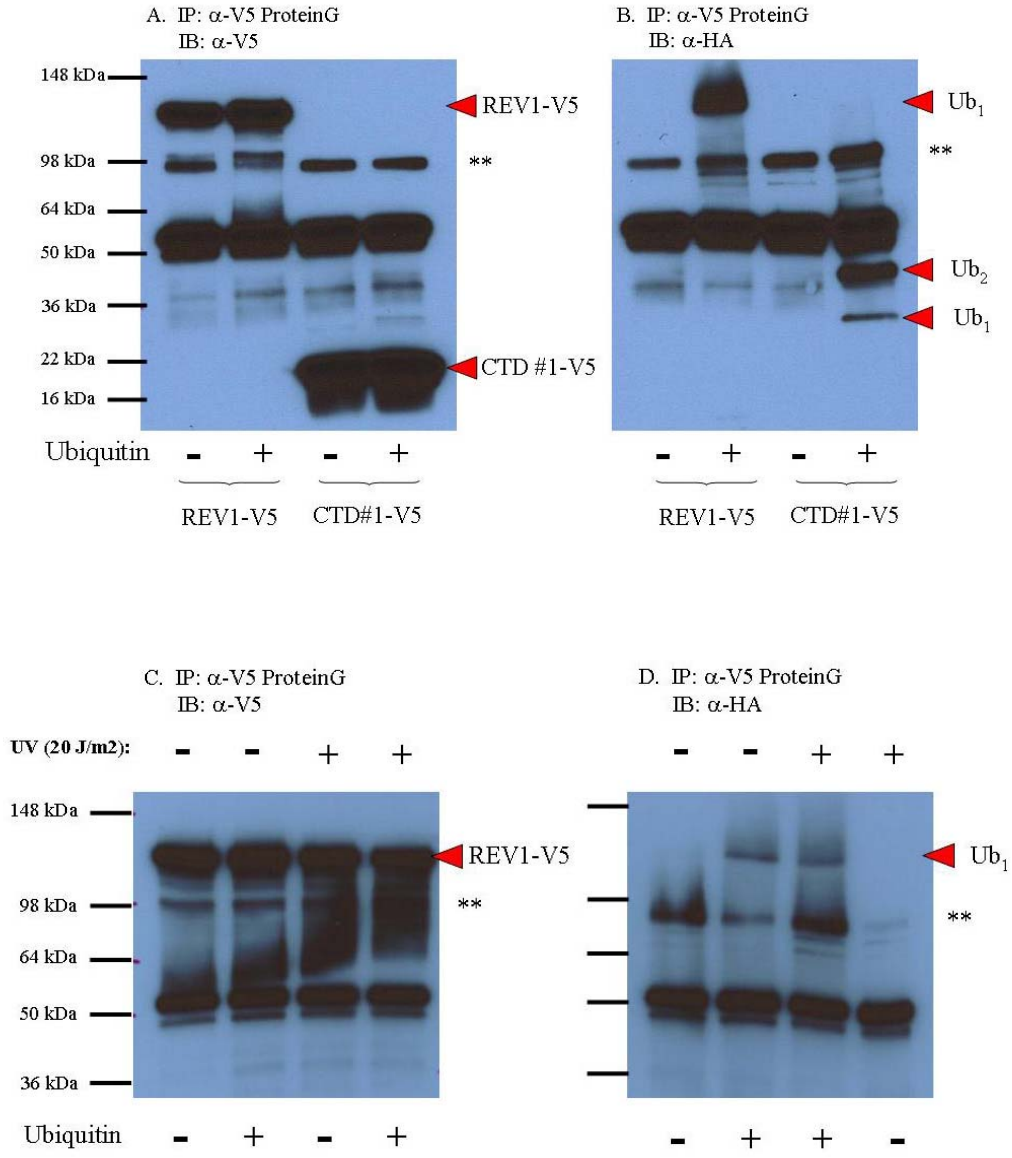

Figure 4.14 Ubiquitination of human REV1.

REV1-V5 or CTD#1-V5 were each transfected separately or co-transfected with the Ubiquitin-HA plasmids into 293T cells 48 hours before harvesting. 30 minutes before cell harvest, cells were UVC (254 nm) irradiated with 20 J/m^2. Protein was harvested from cells using a hi-salt RIPA lysis method. Lysates were immunoprecipitated by αV5-ProteinG agarose. IP samples were washed, resolved by SDS-PAGE and immunoblotted with either: A. αV5 mAb (total REV1-V5, total CTD-V5) or B. αHA mAb (Ub-REV1-V5, Ub-CTD-V5). REV1-V5 transfected, UV treated samples were similarly immunopreciptated, resolved and immunoblotted by either: C. αV5 mAb (total REV1-V5) or D. αHA mAb (Ub-REV1-V5).

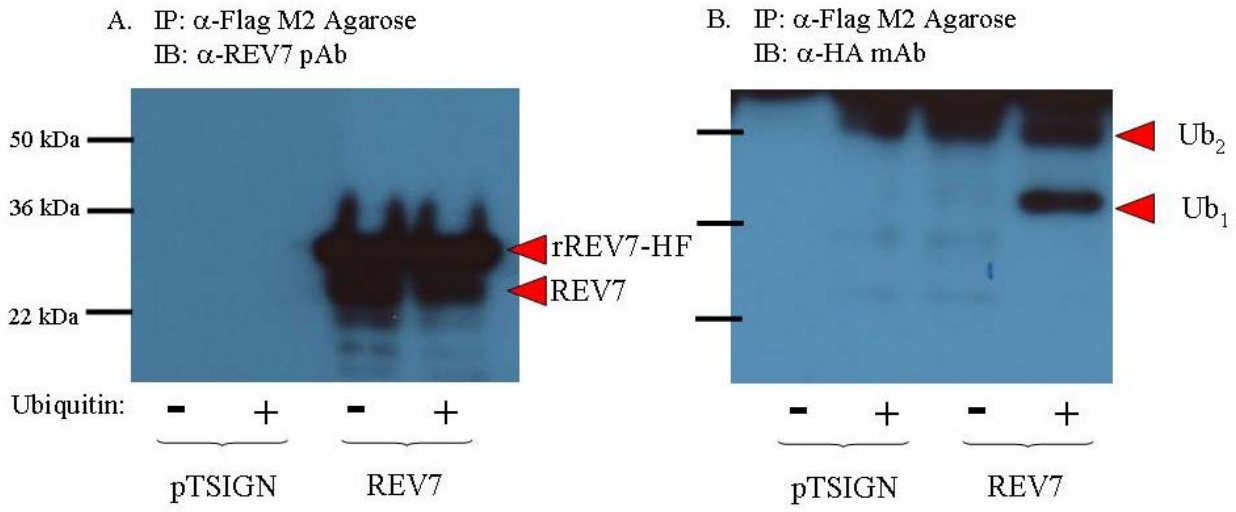

Figure 4.15 Ubiquitination of human REV7.

REV7-HF was transfected by itself or co-transfected with the Ubiquitin-HA plasmids into 293T cells 48 hours before harvesting. Protein was harvested from cells using a hi-salt RIPA lysis method. Lysates were immunoprecipitated by Flag M2 agarose. IP samples were washed, resolved by SDS-PAGE and blotted with αREV7 pAb and αHA mAb (Ub-REV7). A. The top arrow indicates recombinant REV7-HF while the bottom arrow indicates endogenous cellular REV7.

protein and immunoblotted for the respective protein. Furthermore, preliminary results that need to be repeated indicate that none of the REV proteins become significantly ubiquitinated upon UV irradiation.

In order to determine whether recombinant REV3L was proteasomally regulated, pT-SIGN-REV3L-HF wasvtransiently transfected into 293T cells and treated with proteasome inhibitors (either MG132 or ALLN) before harvesting for protein. Immunoprecipitation and immunoblot of REV3L-HF indicates that there is a slight increase in the amount of recombinant protein in the proteasome inhibitor-treated cells compared to the untreated cells (data not shown).

4.4 DISCUSSION

4.4.1 REV1-REV3L Protein Interaction

It has been demonstrated by transient transfection in yeast that full-length yeast Rev1 interacts with full-length yeast Rev3 alone or in complex with yeast Rev7 as Pol zeta (40,99). A growing body of evidence has emerged which describes mammalian REV1 interacting with various translesion synthesis polymerases. Most interactions have been localized predominantly to the C-terminal region of the protein (86,99,122). Murakumo has shown that human REV7 interacts with the C-terminal domain (amino acids 1130 – 1251) of human REV1. Similarly, Acharya has demonstrated that the yeast Rev1 C-terminal domain (amino acids 913 – 985) interacts with the polymerase domain of yeast Rev3 (amino acids 612 – 1377).

This thesis demonstrates for the first time that full-length human REV1 interacts with full-length human REV3L in co-immunoprecipitation experiments. Based on the literature, it was predicted that the C-terminal domain of REV1 and the polymerase domain of REV3L were responsible for the REV1-REV3L interaction observed. Preliminary evidence indicates that the C-terminal domain of human REV1 indeed plays a role in the REV1-REV3L interaction. The REV1ΔCTD fragment, currently being cloned, will help to determine whether the 140 amino acid C-terminal domain is the essential region required for the human REV1-REV3L interaction. If the REV1ΔCTD fragment does interact with REV3L, generation of other REV1 fragments and attempts to further delineate the essential polypeptide region(s) necessary for mediating the REV1-REV3L interaction will be needed. In a single experiment, the polymerase domain of

REV3L interacted with full-length human REV1. While this result needs to be confirmed, it does reinforce the prediction that the polymerase domain is important for the human REV1-REV3L interaction. The Pol Delta homology, Exon13/KIAA, and REV7 binding domain region will have to be co-expressed and immunoprecipitated with REV1 in order to determine the specificity of the REV1-REV3L interaction. It must be taken into consideration that co-expression of both recombinant REV1 and REV3L full-length and fragment proteins may force an artificial interaction which may not be biologically relevant due to the large amounts of protein generated from both plasmids. However, there are currently no methods or reagents available to study the endogenous protein-protein interaction. Therefore, future experiments will use the recombinant proteins to study this protein interaction. It would be especially worthwhile to examine whether REV1 or REV3L prepared separately, mixed together and immunoprecipitated can interact. This would allow competition experiments in which increasing amounts of purified REV1 CTD fragments would be added to the REV1-REV3L complex in an attempt to compete with full-length REV1 binding. Such experiments would help to confirm that the REV1 CTD is responsible for the REV1-REV3L interaction. Furthermore, determining the binding affinity of REV1-REV3L could be initiated using surface plasmon resonance in which excess REV1 could be flowed over the fixed REV3L protein. Although many more experiments are needed in order to more fully characterize the REV1-REV3L complex, these pioneering results provide a glimpse into this protein interaction.

To note, REV1-V5 has been observed to non-specifically interact with the agarose matrix. One reason for this is that potentially soluble, denatured REV1 protein is not associating with other proteins and has a high affinity to the negatively charged agarose. It is predicted that

the pre-clearance step removes the denatured protein without significantly affecting the soluble, correctly folded REV1 that is interacting with other proteins.

To further the understanding of what domains play a role in the REV1-REV3L complex, the REV1 G76R BRCT domain point mutant was generated. The homologous point mutant strain, yeast *rev1-1*, was first described by Lawrence's group as a mutant unable to bypass a T-T (6-4) UV photoproduct on transfected plasmids. The *rev1-1* mutant was identified as a Rev1 G193R point mutation (37). Further work characterized a homologous point mutation in mouse *REV1* as G76R located in the BRCT domain. Generation of a REV1 G76R BRCT point mutant mouse did not yield a significant phenotype. However, isolated embryonic stem cells carrying this mutation treated with UV irradiation demonstrated a decreased number of UV-induced mutations as well as an increased number of chromatid aberrations (39). This single point mutation was reported to disrupt the ability of mouse *REV1* to interact with PCNA by immunoprecipitation as well as diminish its ability to localize to the nucleus to form replication foci in the presence or absence of UV irradiation (121). It is predicted that a human REV1 BRCT point mutant would similarly be unable to bind PCNA. It was determined whether this human REV1 G76R point mutant would be able to form a stable REV1-REV3L complex. It was speculated that if the REV1-PCNA interaction was an important precursor step, diminished PCNA interaction with the BRCT mutant could result in diminished REV3L interaction with the REV1-BRCT mutant. These findings indicate that independent of DNA damage, REV3L can co-immunoprecipitate with both wild type and mutant REV1 as determined by immunoblot. These findings correspond to work done in yeast (40). Furthermore, the increased chromatid aberrations and decreased mutagenesis of the REV1 G76R BRCT mutant mouse embryonic stem cells is most likely not due to an inability to form a REV1-REV3L protein interaction.

The next step will be to determine whether the human REV1-REV3L protein complex can associate with damaged DNA *in vivo*. Yeast Rev1 and Pol zeta form a tripartite complex and can associate to double-strand breaks *in vivo* via chromatin immunoprecipitation (40). Based on these results, it was hypothesized that the human REV1 and REV3L will similarly co-localize at double-strand breaks. In order to determine this, it must first be determined whether human REV1 can interact with PCNA. If REV1 is found to interact with PCNA and this interaction is disrupted by the BRCT G76R point mutant, the next step would be to induce double-strand breaks using gamma irradiation and determine whether REV1, PCNA and REV3L can co-localize at the breaks using immunofluorescence. γH2-AX would be used as a control protein for double-strand break repair foci. These results would help to elucidate whether the REV1-REV3L protein complex is potentially involved in double-strand break repair (44). Evidence examining human REV3L indicates that it plays a role in extrachromosomal homologous recombination of platinated plasmids and therefore may play a role in homologous recombination.

Recent discoveries involving Rev1 indicated a unique regulation that may affect mammalian REV3L and REV7. Hanaoka's group found that HeLa cells synchronized in S phase and UV irradiated could enrich for Polymerase eta, Rad6, Rad18 and REV1 in the chromatin fractions. This indicated that association of translesion synthesis machinery could accumulate at stalled replication forks (119). Walker's group demonstrated that yeast Rev1 was predominantly expressed during G_2/M and thus challenged the traditional notion that translesion synthesis may be acting at replication forks within S phase (54). In order to understand whether DNA damage or cell cycle arrest could allow for enrichment of a human REV1-REV3L complex in chromatin, cells were transiently transfected with REV1 and REV3L and either treated with nocodazole or

UV irradiation. There was no observed enrichment of the REV1-REV3L complex in the chromatin fraction with either an 18 hour nocodazole treatment or with UV irradiation compared to mock treated samples. Furthermore, examination of whole cell and chromatin lysate protein from cells co-transfected with REV1 and REV3L and treated with various DNA damaging agents did not demonstrate enrichment for either REV1 or REV3L in the chromatin fraction. These results suggest that REV1-REV3L may be continuously engaged along the chromatin scanning for stalls in the replication machinery. One possibility is that expression and localization of both proteins to the chromatin may be a discrete event and examination of the complex may require combining nocodazole treatment with DNA damage simultaneously. This will need to be considered for future experiments since all the results described herein examined DNA damage and cell cycle arrest separately. Study of cell cycle or DNA damage regulation using recombinant REV1 or REV3L protein will not allow for examination of whether protein is upregulated transcriptionally or translationally. Furthermore, post-translational modification (ie. Ubiquitination or phosphorylation) leading to protein stabilization in overexpressed protein may not be discernable between treated and untreated cells. Small changes in the amount of endogenous REV1 and REV3L protein could lead to an increase in protein interaction or association to the chromatin fraction and may be highly significant. However, in contrast, slight changes in the amount of the recombinant protein could appear insignificant by immunoblot. Therefore, in order to better appreciate the REV1-REV3L interaction and whether post-translational modification may effect protein interaction, future studies will need to examine the degree of interaction (K_d) for REV1-REV3L in response to cell cycle arrest or DNA damage. Using surface plasmon resonance, recombinant REV3L or REV1 protein derived from treated and untreated cells could be bound to the surface matrix and its corresponding partner flowed

over the matrix in order to determine the change in binding affinity of REV1-REV3L due to cell cycle arrest and DNA damage.

4.4.2 REV1-REV7 Protein Interaction

Prior work in yeast and humans have demonstrated that the full-length REV1 and REV7 proteins interact with one another *in vitro* (50,87). The recombinant REV1 and REV7 proteins generated in the Wood lab similarly interact with one another by co-immunoprecipitation. Furthermore, the REV1 G76R BRCT point mutant does not affect the REV1-REV7 interaction which corresponds with Hirano's findings in yeast (40). Preliminary evidence indicates that the C-terminal domain of mammalian REV1 is responsible for interaction with REV7 which corresponds to observations made by the Fishel and Friedberg labs (86,122).

4.4.3 REV3L-REV7 Protein Interaction

Work done in yeast provided the first indication that Rev3 and Rev7 interact with one another to form a catalytically active DNA polymerase capable of inserting and extending from damaged DNA templates (21). Since then, various groups have demonstrated that yeast Rev3 interacted with Rev7 by co-immunoprecipitation (21,99). These results were further corroborated by work done in Fishel's group, which demonstrated that a fragment of human REV3L could interact with human REV7 by yeast-two hybrid and co-immunoprecipitation assays in Cos7 cells (86).

However, to date, verification of full-length human REV3L interaction with REV7 has not been demonstrated. Difficulty with cloning and expression of human REV3L has only allowed for examination of partial fragments by immunoprecipitation. The ability to express full-length human REV3L has enabled us to finally explore this question. However, the findings indicate that regardless of DNA damage, full-length human REV3L does not interact with REV7. This is contradictory to what has been described in the literature although many reasons may account for this. (86,99,122). Fishel's group demonstrated that the human REV3-8 fragment (corresponding to the REV7 binding domain) was responsible for the observed REV7 interaction by co-immunoprecipitation when prepared using a modified RIPA lysis buffer (86). In order to verify that the freeze-thaw lysis buffer could also co-immunoprecipitate Fishel's REV3-8 fragment (amino acid 1776 – 2044) and REV7, these expression plasmids will be generated and their interaction tested using the freeze-thaw lysis protocol. Full-length endogenous dmRev3 has been isolated which possesses catalytic polymerase activity. Sakaguchi's group demonstrated that a dmRev3 fragment could interact with dmRev7, but addition of dmRev7 had no effect on dmRev3's catalytic polymerase activity (57). These results correspond to our own in that addition of recombinant REV7 did not enhance the catalytic activity of REV3L on either an activated calf-thymus or oligo dT:polydA DNA template. Furthermore, a recently developed database, the Allen Mouse Brain Atlas, utilizes *in-situ* hybridization as a tool for localizing mRNA transcripts to the various regions of the mouse brain. This atlas indicates that *REV7* and *REV3L* transcripts do not co-localize to similar regions of the brain, in contrast to to *REV3L* and *REV1* which do co-localize. This suggests that REV7 may not interact with REV3L at the protein level. This lack of interaction may also be due to human REV3L being twice the size of its yeast counterpart. The increased size is due to exon 13 in REV3L which codes for a 1388

amino acid fragment containing both a KIAA 2022 homology region as well as the putative REV7 binding domain region (Figure 4.2). Currently, all *in vitro* protein interactions between REV3L and REV7 that have been described use human REV3L fragments which do not accurately reflect protein folding for the full-length protein. These REV3L fragments which are normally buried within the full-length protein may expose regions that are charged and potentially sticky thus explaining why the fragments interact but the full-length does not. Another reason may be that the REV7 binding domain is masked and only revealed in response to DNA damage or covalent modification. However, examination of three different DNA damaging agents, UV, cisplatin, and MMS, did not indicate that either endogenous or recombinant REV7 binds to REV3L.

Our observation that full-length recombinant REV3L does not interact with REV7 by no means suggests these proteins may not function in similar pathways in damage tolerance. Work by Fishel's group has demonstrated that human REV7 interacts with human MAD2, a gene involved in the spindle assembly checkpoint, and with a human REV3L fragment (1776 – 2445 a.a.). The specific region necessary for MAD2 interaction with REV3L is unknown, but is presumed to be mediated within the amino acid region 1776 – 2445 (88). Preliminary findings indicate that REV7 interacts with the human REV3-8 fragment (1776 – 2044 a.a.) – a fragment expressed by Fishel in HeLa cells and demonstrated to interact with recombinant REV7 by immunoprecipitation. However, lacking both the MAD2 Ab and cDNA, it is unknown whether MAD2 can interact with the REV3-8 fragment. These findings suggest that full length REV3L and REV7 alone may be insufficient to mediate a protein-protein interaction and that MAD2 may also be needed. Recent evidence indicates that suppression of human REV1, REV3L and REV7 in various tumor lines by shRNA lead to decreased cisplatin-induced homologous recombination

and diminished sister-chromatid exchange (44,46,123). These results suggest that all three translesion synthesis proteins may play a role in post-replication repair through homologous recombination. As to what role the REV proteins play either in a complex or individually in homologous recombination has yet to be determined.

4.4.4 Ubiquitination of the REV1, REV3L and REV7 Proteins

Because of the large size of human REV3L (353 kDa), post-translational modification of a protein by covalent modification offers an alternative level of regulation that does not require new protein synthesis. There is preliminary indication that REV3L may be phosphorylated. The significance as well as the location of this phosphorylation, however, remains unknown. Study of protein ubiquitination may be another form of covalent modification that regulates REV3L function. In multiple experiments, it is observed that the Flag immunoprecipitated recombinant REV3L may be ubiquitinated, possibly polyubiquitinated. Prior experiments examining the proteasome inhibitors MG132 and ALLN demonstrated a mild increase in recombinant REV3L compared to the untreated cells. This could suggest that overexpressed REV3L protein may be proteasomally regulated. However, another possibility is that this overexpressed recombinant protein may be ubiquitinated by the cell in order to eliminate the excess protein. Until the HA-tagged protein that has been immunoprecipitated can be validated by an alternative method, one possibility is that another high molecular weight protein is being ubiquitinated. In order to better understand whether REV3L is ubiquitinated, the individual REV3L fragments generated for the protein interaction study will need to be examined. More work will have to be done

characterizing the function of REV3L ubiquitination. However, these findings are nonetheless exciting and could provide clues to how REV3L is cellularly regulated.

Examination of REV1 and REV7 indicate that the proteins are ubiquitinated. Closer examination of the C-terminal domain of REV1 and REV7 indicate that these proteins are mono and di-ubiquitinated. Although the biological function of this modification remains unknown. One explanation is that this observed polyubiquitylation may be preparing the proteins for proteasomal degradation. Proteasomal regulation of human REV1 should also be examined since yeast Rev1 has been shown to be cell cycle regulated and is stabilized with proteasomal inhibitor treatment (54). This could be a potential explanation for the observed REV1 ubiquitination. Presuming that ubiquitination of the REV proteins may upregulate or activate the proteins in response to DNA damage, cells transiently transfected with ubiquitin and either REV1 or REV3L were UV irradiated and the degree of ubiquitination was qualitatively assessed by immunoblot. Interestingly, the amount of ubiquitinated REV1 and REV3L by immunoblot was independent of UV irradiation. These results suggest that the two recombinant REV proteins may be constitutively ubiquitinated. Similarly, there was no observed difference between the ubiquitinated and non-ubiquitinated forms of REV1 and REV3L when the complex was co-immunoprecipitated.

These results may not necessarily reflect the true biological function of the endogenous proteins. The lack of change in REV1 and REV3L ubiquitination status following DNA damage and protein interaction could be due to enhanced proteasomal degradation of the overexpressed recombinant protein in the cell. However, the finding that the C-terminal domain of REV1 is mono and di-ubiquitinated provides new direction for future study. One way to study potential biological function would be to examine proteasomal regulation through site-directed

mutagenesis. Another way would be to determine whether overexpression of the fragment in combination with a genotoxic stressor can cause increased cell sensitivity in a dominant negative fashion.

5.0 *REV3L* LACZ EXPRESSION STUDIES IN MICE

5.1 INTRODUCTION

REV3 is expressed in all vertebrate tissues. Studies of mouse and human mRNA derived from organs and analyzed by RT-PCR or by northern blot reveal REV3L transcript in every organ examined in both organisms (62,75,76). However, little information exists regarding whether expression occurs throughout the whole organ or is limited to only specific cells within a particular organ.

The expression of other translesion synthesis polymerases in mouse testis has already been characterized in detail. Using *in situ* hybridization and immunohistochemistry, Pol iota, kappa, nu and lambda were found to be expressed in the seminiferous tubule of the testis throughout different phases of spermatogenesis (124-126). Pol kappa expression was observed specifically in the pachytene cells of meiosis I and in post-meiotic round spermatids, and was not observed in the epididymus. Pol iota was found in early pachytene cells during meiosis I and in round and early elongating post-meiotic spermatids (124). Similarly, Pol lambda was shown to be expressed in late pachytene spermatocyctes and early round spermatids (126). Expression of Pol Nu was found predominantly in meiotic spermatocytes and in post-meiotic round spermatids and absent in almost all other cells of seminiferous tubule (125). The common process which unifies all these polymerases is not just their expression in the testis, but also a meiosis-specific

process known to generate double-strand breaks during DNA recombination. Identifying when and which cells express *Rev3L* transcript in mouse testis will help to elucidate what role REV3L may play in cellular proliferation, tolerance of endogenous DNA damage, and the double-strand break repair that occurs during meiotic recombination.

An example of tissue selective expression of *Rev3L* comes from examination of the Allen Mouse Brain Atlas, which demonstrates that the three *Rev* transcripts are expressed in certain portions of the brain (127). By *in situ* hybridization, *Rev1* and *Rev3L* transcript were strongly expressed in the regions of the hippocampus and dentate gyrus (DG), while *Rev7* transcript was not. In contrast, *Rev7* was expressed at higher relative levels in the thalamus. The implication of this finding is that *Rev1* and *REV3L* are required for cellular proliferation since this region of the brain is known to undergo neurogenesis.

Beyond the testis and brain, various groups have identified that *Rev3L* plays a role in immunologic diversity, as well as in embryonic development. Specifically in B-cells, *Rev3L* transcript is constituitively expressed and is important for Ig and *bcl-6* hypermutation (128). Initial characterization of *Rev3L* expression in mouse embryonic tissue was done by using an IRES-*lacZ-neo*^{r} targeting cassette to put a histochemical marker in the mouse *Rev3L* locus. The LacZ staining results demonstrated high levels of Rev3L expression in the somites at embryonic day 7.5. This expression expanded to other somites and mesoderm origin tissues such as the peri-optic mesenchyme and especially in and around the embryonic heart and lung buds (59). Expression appeared more widespread after embryonic day 11.5. However, corresponding studies in the adult mouse were not done.

Because so little is known about the biochemistry of Rev3L, methods are needed to explore and better understand its cellular function. The goals of this study were to identify

tissues and specific cell types in the adult mouse that express moderate to high levels of *Rev3L*, and determine if these cells are actively replicating and/or subject to genotoxic stress. A tool uniquely available to the Wood laboratory was used to accomplish these goals. These studies will provide insight into the cells or tissues that express high amounts of *Rev3L* in the adult mouse, suggesting which cell types require REV3L for proper function.

5.2 METHODS

5.2.1 *Rev3L* $^{+/-}$ *lacZ* Expression Mice

These mice were acquired from Dr. John Wittschieben from the Wood lab. In brief, disruption of the REV3L polymerase domain was done by targeted replacement using an IRES-*lacZ*-*neo*^{r}-SV40 polyA cassette in mouse ES cells which led to the generation of the *REV3L* heterozygous *lacZ* expression mouse described previously (59). Heterozygous cells expressing the disrupted transcript will allow for LacZ (beta-galactosidase) protein expression because of the IRES motif. The IRES (internal ribosomal entry site) is a nucleotide sequence which allows for translation initiation within an existing mRNA sequence. When tissues expressing LacZ (an E.coli derived β-galactosidase protein) are treated with the colorless compound, X-gal, β-galactosidase will cleave the substrate generating a compound that will stain tissues blue.

5.2.2 Organ Harvest from Euthanized Mice

Wild type and *Rev3L* $^{+/-}$ *lacZ* expression mice were euthanized using a CO_2 asphyxiation chamber. Organs dissected included the brain, thymus, heart, lungs, liver, pancreas, spleen, small and large intestines, testis, ovary, skin and quadracep skeletal muscle using standard mouse necropsy procedures. Under advisement from histologists, the brain was always harvested first because the tissue tended to break down faster and would become problematic upon tissue sectioning.

5.2.3 Frozen Tissue Preparation by OCT Method

In order to generate a very cold, flat metal surface to allow OCT (Tissue Tek, Sakura) to solidify (~20 – 30°C or below), a metal dish was embedded into an ice tray surrounded by dry ice. Pre-labeled disposable base molds (1.5 cm x 1.5 cm x 0.5 cm dish or 2.4 cm x 2.4 cm x 0.5 cm dish) were placed on the metal dish to cool down. For brain, testis and heart, these organs were coated in a layer of OCT creating the appearance of a soft gelatinous film surrounding the organ. These coated organs were then rapidly frozen in liquid nitrogen for 10, 8 and 8 seconds for each organ respectively. Using a clean razor blade for each organ, tissue pieces were sliced accordingly. The organs were sectioned into longitudinal and cross-sectional pieces and mounted on top of a thin layer of OCT in the base mold. Once the orientation of the tissue was established, more OCT was added on top until the mold was completely filled. The OCT freezes through solidly within 2 – 3 minutes. The tissue was allowed to sit on top of the metal container for another 5 –

10 minutes before transferring them into a plastic bag or other container and stored buried in dry ice. Until the OCT tissue blocks are ready for sectioning, they are stored long-term in a -80ºC freezer.

5.2.4 Sectioning OCT Tissue Blocks

Initial tissue blocks were submitted to UPMC Shadyside Pathology for sectioning. In order to speed up the sectioning time, I learned how to generate tissue slides for more rapid analysis. The necessary blocks were removed from -80ºC and temporarily stored on dry ice. Tissue blocks were cut using disposable microtome blades (02118 Teflon) (Surgipath Medical Industries) to 10 μm thickness using a cryotome (ThermoShandon) and mounted onto Superfrost Plus slides (Fisher) and allowed to air dry for approximately 15 minutes. Tissue sections were cut in the cryotome at -18 to -16°C. Slides to be immediately stained with X-gal were moved to a 4ºC refrigerator otherwise they were stored at -80ºC for later use.

5.2.5 LacZ Staining OCT Tissue Sections

Before use, slides were moved from -80ºC storage and then placed on a tin foil/ice surface to air dry. A circle was drawn around the mounted tissue using a PAP pen (Zymed). Tissue was fixed using a commercial Tissue Fixative solution (Chemicon) for 1.5 hours on a wet ice/tin foil base. Refer to Appendix F for all commercial solution formulations. The slides were rinsed briefly in

Rinse Solution A (Chemicon) at room temperature, then the slide were soaked in Rinse Solution A for 30 minutes. Slides were briefly rinsed in Rinse Solution B (Chemicon) at room temperature then soaked in Rinse Solution B for 5 minutes at room temperature. Tissue slides were drained and the circle reapplied using a PAP pen. X-gal stain solution (Chemicon) was added within the PAP circle containing tissue (X-Gal Stock solution (Chemicon) was mixed with Tissue Stain Base Solution in a 1:40 dilution) in the dark and incubated in a humidified chamber at 37ºC for a minimum of 8 hours (overnight was found to be optimal) avoiding tissue drying. The slides were rinsed in D-PBS (Chemicon) twice for 3 min each at RT. Slides were then counter stained with Nuclear Fast Red (Vector Labs) for 15 – 45 seconds depending on the tissue. All hematopoeitic tissue were counterstained for 15 seconds, all other tissue were counterstained for 30 – 45 seconds. Slides were washed under running water for 10 minutes. They were then dehydrated in two 95% EtOH washes for 30 seconds, each. Then, the slides were dehydration in two changes of 100% EtOH for 30 seconds. Finally, they were cleared in two changes of Xylene for 30 seconds each. Slides were coverslipped using Cytoseal (Richard Allen Scientific).

5.3 RESULTS

5.3.1 Expression of *Rev3L* in the Testis

β-galactosidase staining of heterozygous *Rev3L lacZ* expression tissue indicated that *Rev3L* transcript was found throughout the seminiferous tubule. Punctate blue staining specifically due to lacZ activity was observed in spermatogonia, 1º and 2º spermatocytes and in spermatozoa indicating the involvement of Rev3 in all stages of spermatogenesis (Figure 5.1A). The staining was not due to endogenous β-gal activity (Figure 5.1B). High Rev3L expression is also observed in the columnar epithelial of the epididymus and not within the lumen of the epididymus containing the spermatozoa (Figure 5.2A). This characteristic staining is not observed in the *REV3L* WT control mice (Figure 5.2B). These results represent two independent β-gal LacZ stainings from tissue taken from the same animal.

5.3.2 Expression of Rev3L in the Pulmonary, Cardiovascular, Gastrointestinal System

Rev3L-lacZ expression is observed in parts of the mouse heart. Extensive staining is observed in the ventricles (Figure 5.3A). Staining will need to be performed for the atrium. These results represent stains from three independent sections from three different mice. Further

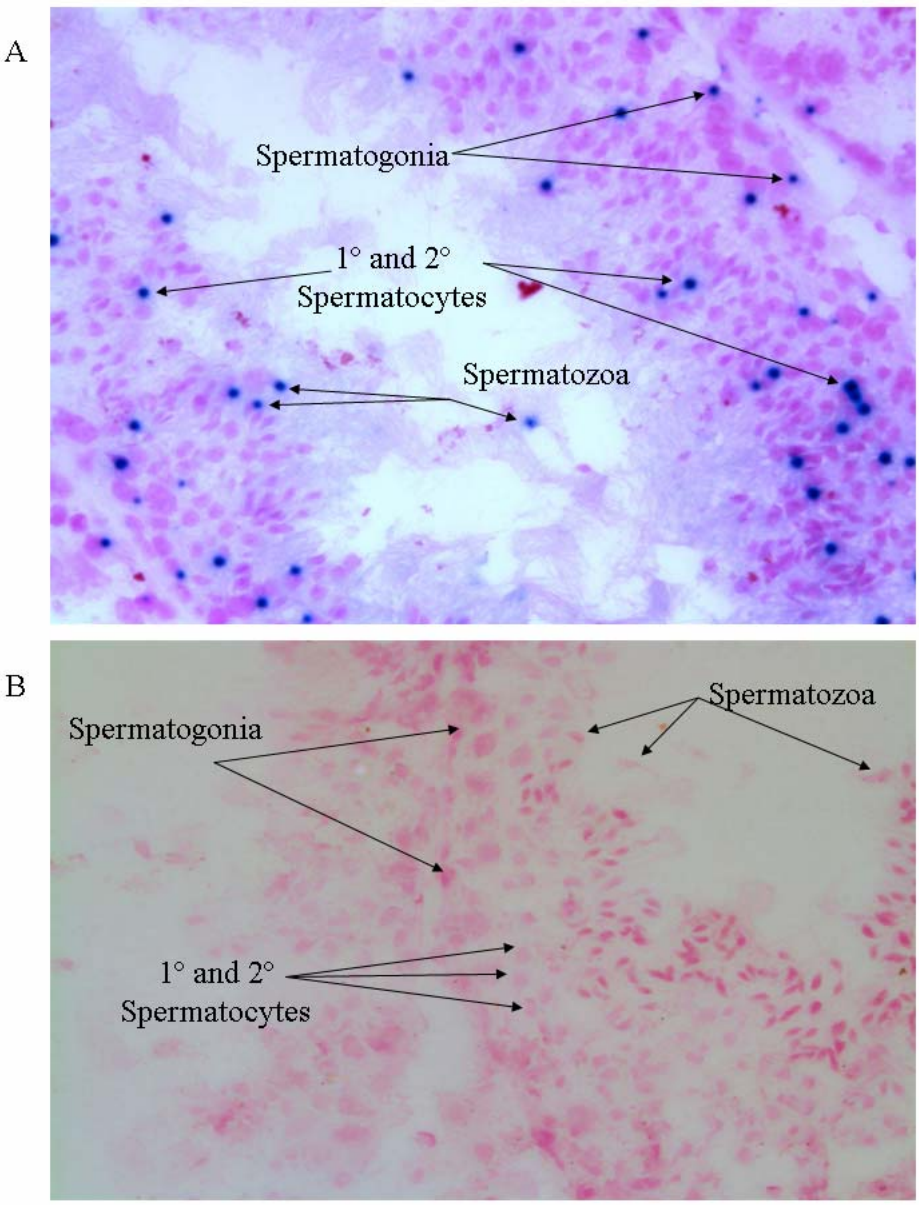

Figure 5.1 ***Rev3L*$^{+/-}$** ***lacZ*** **Expression in Mouse Seminiferous Tubule.**

A. Frozen OCT tissue blocks were sectioned at 10 μm. Tissue was fixed using the Chemicon fixative solution for 1.5 hours, stained with X-gal (1:40) solution overnight and counterstained with Nuclear Fast Red for 30 seconds. Punctate blue foci are distributed throughout all layers of the seminiferous tubule in the LacZ expression mouse and not in the wild-type mouse (B).

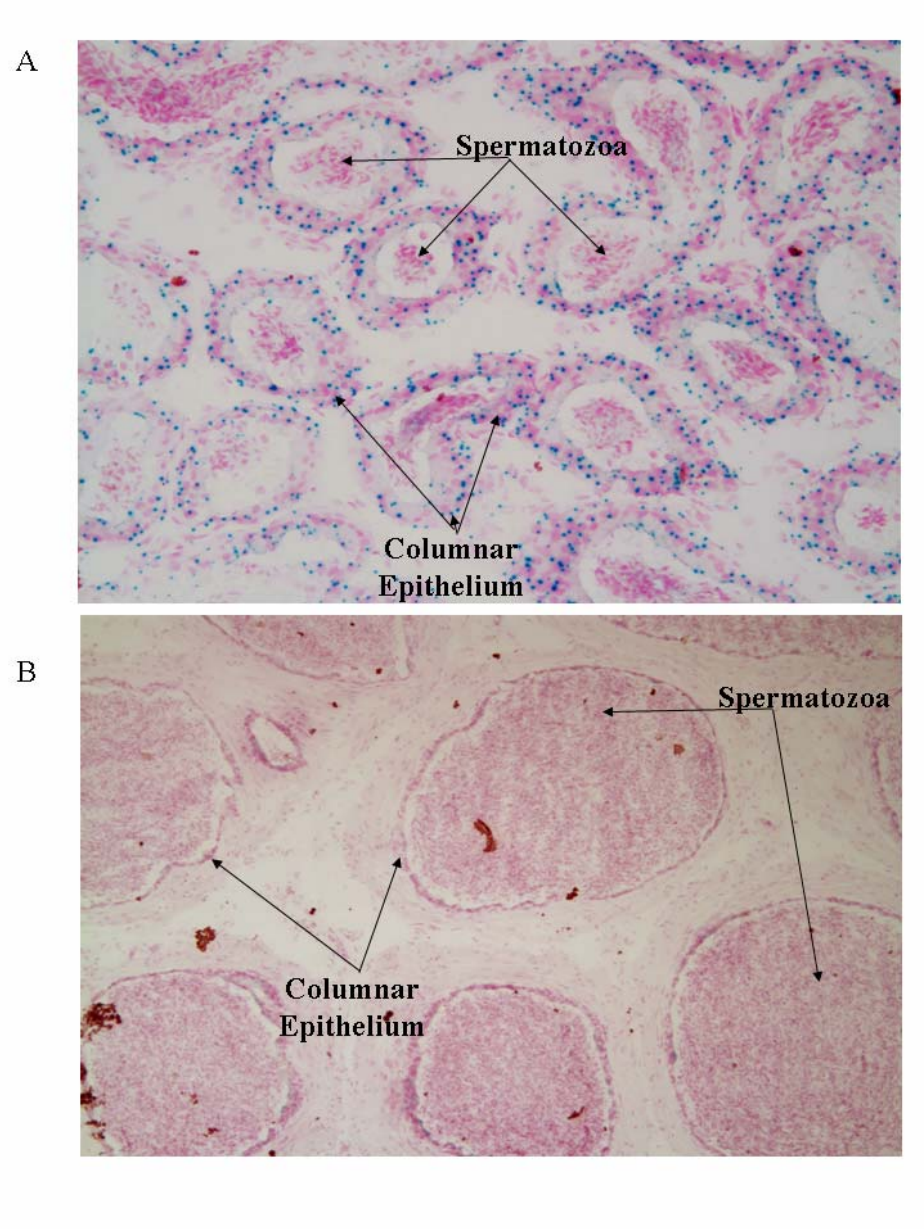

Figure 5.2 *Rev3L*$^{+/-}$ *lacZ* Expression in Mouse Epipdidymus.

A. Frozen OCT tissue blocks were sectioned at 10 μm. Tissue was fixed using the Chemicon fixative solution for 1.5 hours, stained with X-gal (1:40) solution overnight and counterstained with Nuclear Fast Red for 30 seconds. Punctate blue foci are distributed throughout the columnar epithelium in the LacZ expression mouse and not in the wild-type mouse (B). Expression is distinctly absent in the lumen containing the spermatozoa for both.

characterization of mouse abdominal aorta indicates that some LacZ expression is found localized outside of the musculature in the tunica adventitia (data not shown). Preliminary staining does not indicate *REV3L* LacZ staining in veins or venules (data not shown). The blood vessel results represent a single mouse stained for LacZ in a single experiment. Staining in bronchioles of the lung also demonstrate Rev3L expression within the smooth muscle and epithelia (Figure 5.4A). These results represent two independent β-gal stains from two different mice. The expression of REV3L LacZ foci throughout the small and large intestines remains localized in the circular and longitudinal smooth muscle layers and not in the epithelia or connective tissue associated with the microvilli (Figure 5.5A, C). These foci were not present in the WT mice. These results represent two independent β-gal stains from one mouse.

5.3.3 Lack of *REV3L* LacZ Expression in the Hematopoeitic System

Examination of the spleen, thymus, peyer's patch and bone marrow did not reveal LacZ expression. Multiple sections taken from multiple mice fixed and stained at different times indicate no LacZ expression, particularly within the thymus and spleen (Figure 5.6A and 5.7A). Examination of other sections containing spleenic blood did not indicate any further LacZ staining.

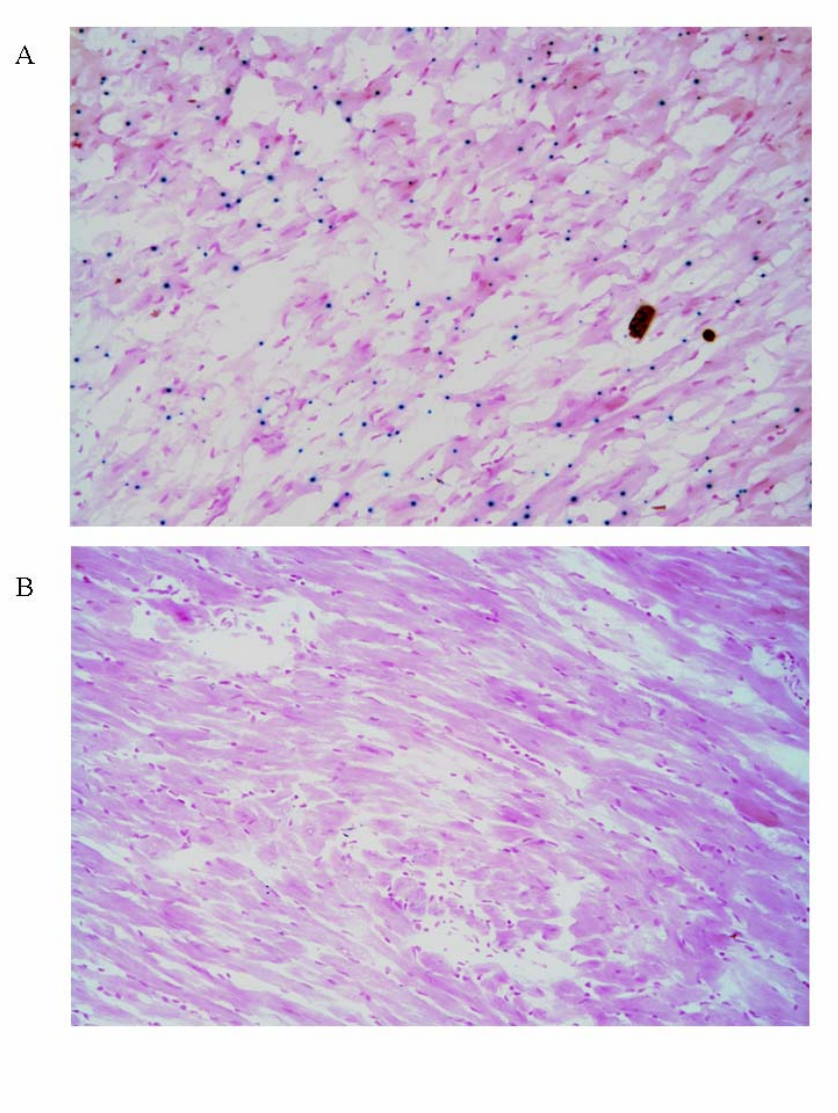

Figure 5.3 *Rev3L*$^{+/-}$ *lacZ* Expression in Mouse Cardiac Tissue.

A. Frozen OCT tissue blocks were sectioned at 10 μm. Tissue was fixed using the Chemicon fixative solution for 1.5 hours, stained with X-gal (1:40) solution overnight and counterstained with Nuclear Fast Red for 30 seconds. Punctate blue foci are widely distributed throughout the ventricle in the LacZ expression mouse and not in the wild-type mouse (B).

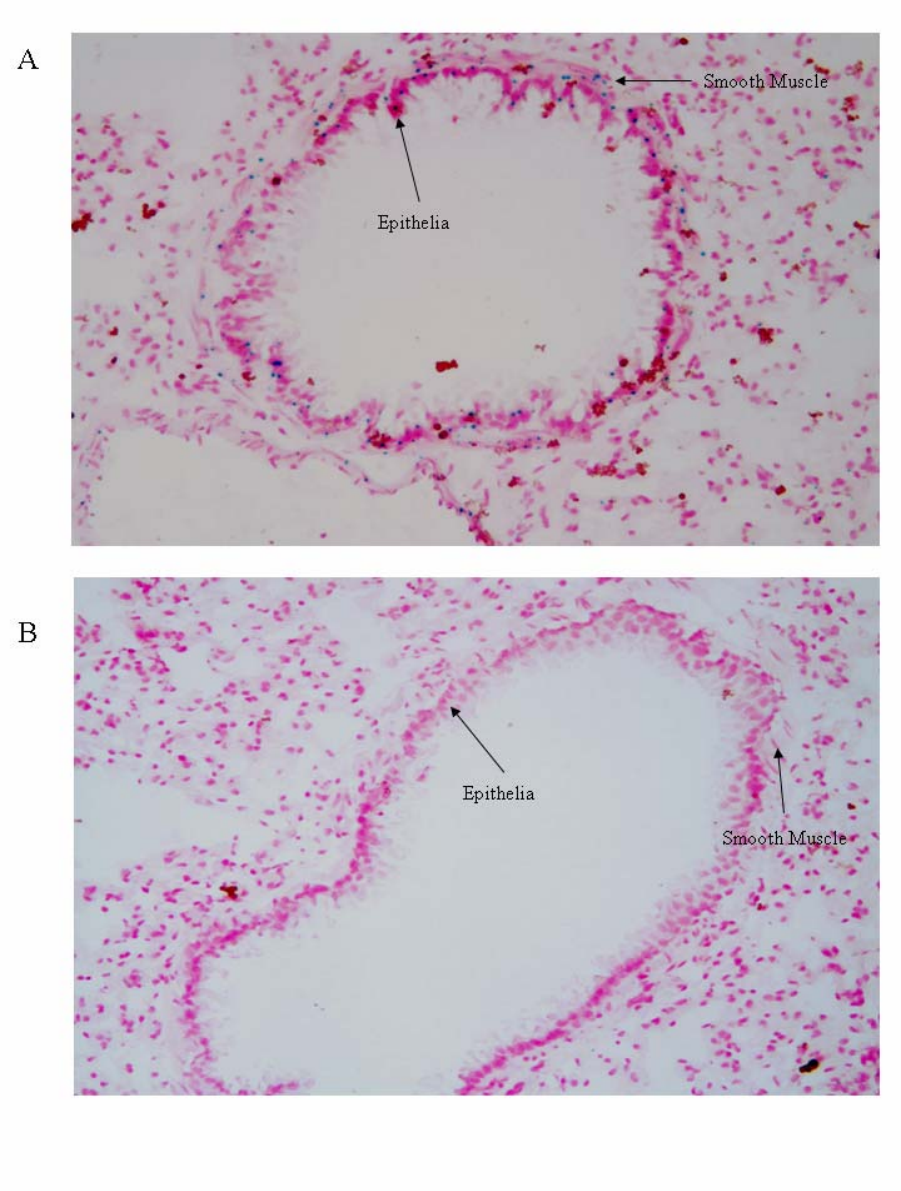

Figure 5.4 *Rev3L*$^{+/-}$ *lacZ* Expression in Mouse Terminal Bronchiole

Frozen OCT tissue blocks were sectioned at 10 μm. Tissue was fixed using the Chemicon fixative solution for 1.5 hours, stained with X-gal (1:40) solution overnight and counterstained with Nuclear Fast Red for 30 seconds. A. Punctate blue foci are widely distributed throughout the epithelia and smooth muscle of the terminal bronchiole in the LacZ expression mouse and not in the wild-type mouse (B).

A

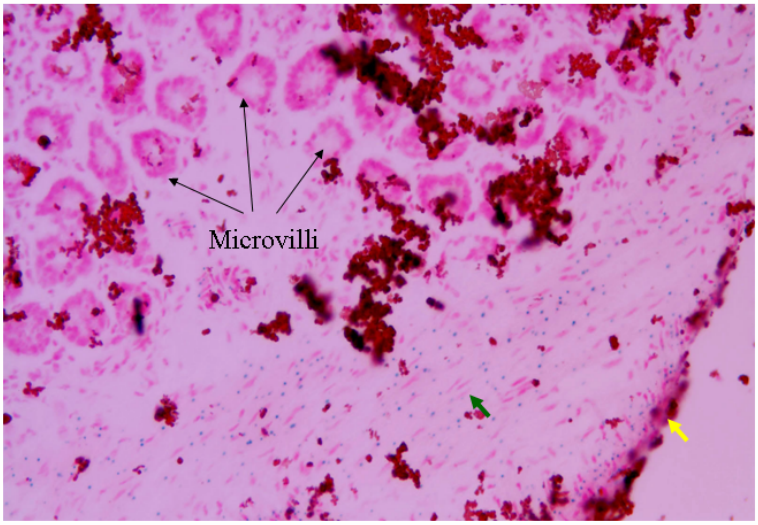

B

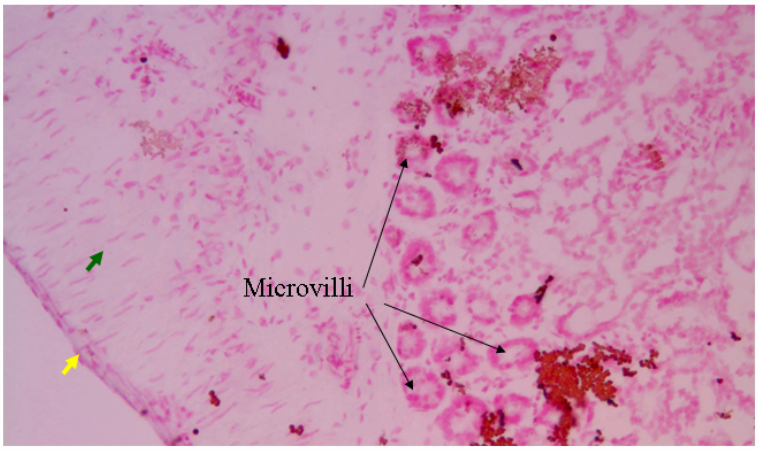

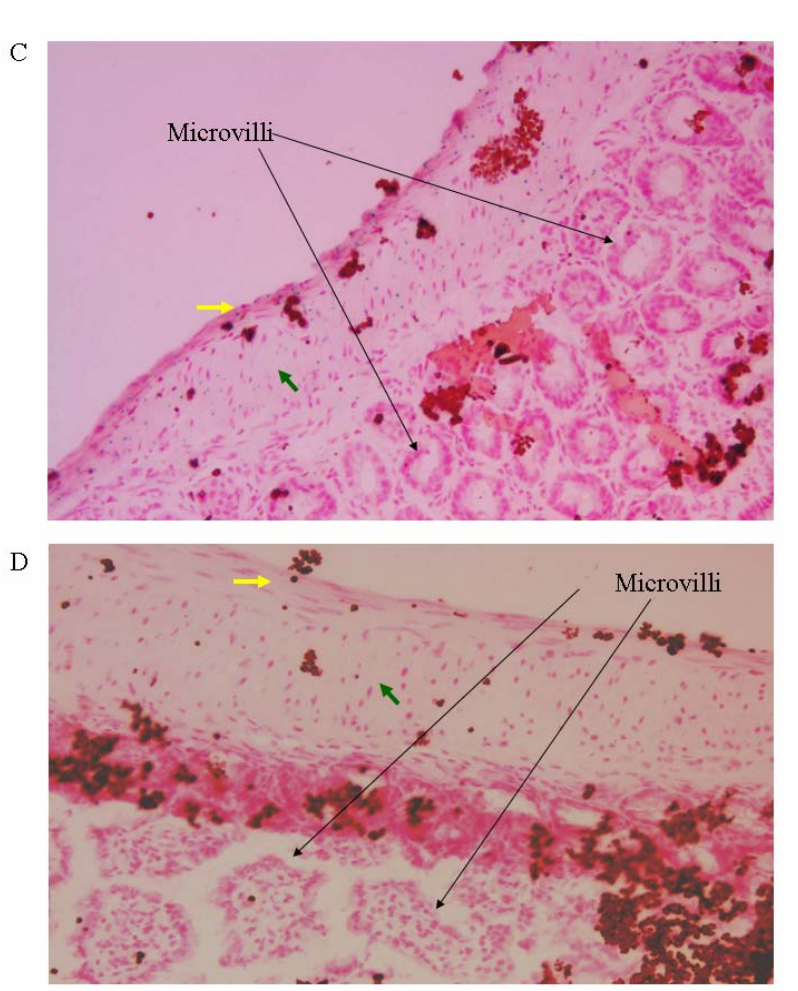

Figure 5.5 *Rev3L*$^{+/-}$ *lacZ* Expression in Mouse Small Intestine.

Frozen OCT tissue blocks were sectioned at 10 μm. Tissue was fixed using the Chemicon fixative solution for 1.5 hours, stained with X-gal (1:40) solution overnight and counterstained with Nuclear Fast Red for 30 seconds. Punctate blue foci are widely distributed throughout the smooth muscle of the duodenum (A) and ilium (C) in the LacZ expression mouse and not in the wild-type mice (B and D). Yellow arrows indicate the longitudinal smooth muscle and Green arrows indicate the circular smooth muscle.

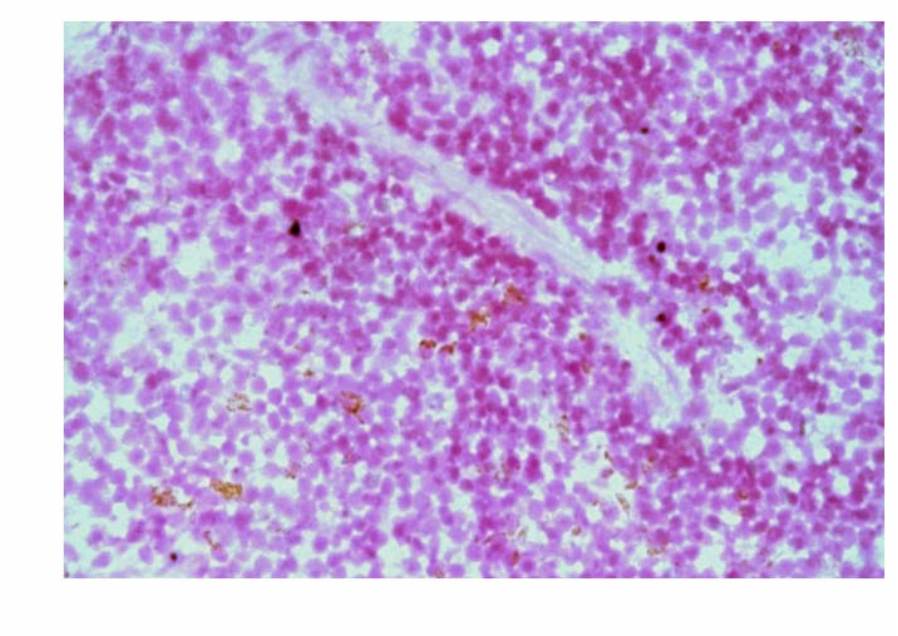

Figure 5.6 *Rev3L*$^{+/-}$ *lacZ* Expression in Mouse Spleen.

Frozen OCT tissue blocks were sectioned at 10 μm. Tissue was fixed using the Chemicon fixative solution for 1.5 hours, stained with X-gal (1:40) solution overnight and counterstained with Nuclear Fast Red for 30 seconds. Representative cross-section of spleen red pulp with a small arteriole. No observed punctate foci observed in multiple sections. Negative controls (wild type *REV3L* mouse spleen not shown) were also LacZ expression negative.

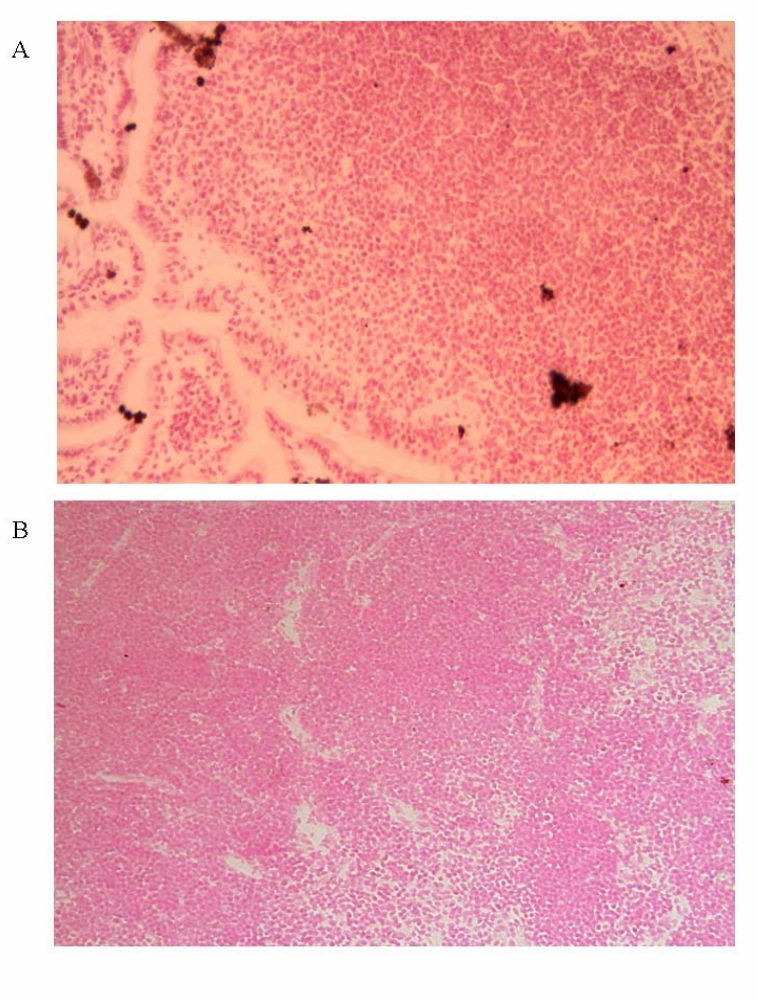

Figure 5.7 *Rev3L*$^{+/-}$ *lacZ* Expression in the Thymus and Peyer's Patch of the Ilium.

Frozen OCT tissue blocks were sectioned at 10 μm. Tissue was fixed using the Chemicon fixative solution for 1.5 hours, stained with X-gal (1:40) solution overnight and counterstained with Nuclear Fast Red for 30 seconds. A. Representative cross section of Peyer's Patch of the ilium taken from the LacZ expression mouse. B. Representative cross section of thymus from the LacZ expression mouse. Negative controls (wild type *Rev3L* mouse thymus and Peyer's patch were not shown) were also LacZ expression negative.

5.4 DISCUSSION

5.4.1 *REV3L* is Expressed Throughout the Testis

Multiple studies by other labs demonstrated high REV3L expression by northern blot and RT-PCR of total testis tissue in both mouse and human. The expression pattern of Rev3L in specific testis cells was determined by using a *Rev3L-lacZ* expression mouse. Many other translesion synthesis polymerases have been shown to be highly expressed in the testis and ovaries. However, their biochemical function is currently unknown. Some are presumed to play a role in recombination and double-strand break repair during meiosis (124-126). Expression of the translesion synthesis polymerases (iota, kappa, lambda and nu) was found in early, middle and late pachytene spermatocytes during meiosis I as well as in post-meiotic round spermatids by using *in situ* hybridization and immunohistochemistry (124-126). Through LacZ staining, blue foci were observed in all major cell types of the seminiferous tubule – spermatogonia, primary and secondary spermatocytes and spermatids. Although the meiotic stage in which Rev3L is expressed has not been characterized, it is apparent that it is expressed in primary and secondary spermatocytes which are involved in meiosis (Figure 5.1A). *In situ* hybridization will be needed in order to determine when during meiosis Rev3L is required.. The expression of *Rev3L* in these tissues could indicate repair of double-strand breaks associated with meiotic recombination. REV3L is involved in damage-induced mutagenesis (68) and may function not only in double-strand break repair but also in generating DNA mutations which would be important for inducing

genetic diversity in organisms. Furthermore, the lack of expression in the mature spermatozoa may indicate a diminished requirement for REV3L. In contrast, REV3L appears to be highly expressed in the columnar epithelia of the epididymus potentially indicating that the musculature and the epithelial cells have an increased demand for REV3L. Perhaps its requirement in translesion synthesis is greater here because of the highly oxidative environment (129).

5.4.2 *REV3L* LacZ Expression in the Pulmonary, Cardiovascular and Gastrointestinal System

Expression of *REV3L* LacZ in the cardiovascular system has potential implications. REV3L is an essential gene believed to function by bypassing stalled replication forks during cell replication. Disruption of the gene leads to a significantly growth retarded mouse fetus and eventual midgestational embryonic death (59-61). The fact that Rev3L is expressed in the mouse cardiac ventricle and the muscular and epithelial lining of the pulmonary tree, both high oxygen consumption organs, suggest that Rev3L plays a role in tolerating free-radical DNA damage. Furthermore, these results are similar to the embryonic LacZ expression which demonstrated Rev3L expression in the heart (59). Nitric oxide, a potent free radical involved in inflammation and vascular signaling, can associate with superoxide radical to form peroxynitrous acid. This agent can damage DNA bases and cause single strand breaks (1). Recent evidence indicates that Rev3 is required in yeast and DT-40 chicken cells for bypass of free radical DNA damage caused by reactive oxygen and nitric oxide (63,130). Single-strand DNA breaks can be converted to double-strand breaks by multiple mechanisms (i.e. DNA replication). Growing evidence in yeast indicates that Rev3 protein, through Rev1, associates to double-strand breaks and plays a role in

double-strand break repair (40,41). Loss of *REV3L* in such a highly oxidative organ could quickly lead to cellular dysfunction and death. To a lesser degree, β-gal staining was also found throughout the smooth musculature of the intestines, again suggesting the importance of *Rev3L* in tolerating oxidative damage either due to oxidative respiration or through nitric oxide signaling. Interestingly, the microvilli of the small intestines do not appear to express high levels of REV3L. This finding is curious because of the high turnover rate of GI epithelia cells (every 24 – 48 hours). This would suggest that high levels of *Rev3L* are not critical for general cell proliferation as once thought. Perhaps the protein plays a more specialized role in tolerating high levels of DNA damage caused by reactive oxygen and nitric oxide.

Disruption of the *Rev3L* gene leads to murine embryonic lethality, and widescale LacZ expression driven by the endogenous *Rev3L* promoter in fetal mesenchymal tissue demonstrates the the importance of this gene in development. However, *Rev3L* may not be important for proliferation or damage tolerance in some tissues of the adult organism. Unpublished work from the Wood lab indicates that some cells require *Rev3L* more than others. Conditional *Rev3L* null mice generated using a MMTV Cre-lox system has shown that hematopoetic cells were not viable without Rev3L. In contrast, epithelial cells are viable and *Rev3L* null dermal fibroblasts were able to be established and grown in culture. These findings suggest that after embryonic development, certain adult tissue may have a greater requirement for *Rev3L* over others.

Our observation that *Rev3L* expression as a function of LacZ expression is detectable in non-proliferating musculature (cardiac and smooth muscles of the lungs and intestines) and not in other organs will need to be confirmed using an alternative method such as *in situ* hybridization. Findings in the embryonic *Rev3L*$^{+/-}$ and *Rev3L*$^{-/-}$*-lacZ* mice demonstrate lacZ staining in fetal mesenchymal tissue around the terminal lung bud, heart and gut. These results

are substantiated by our own findings in the adult *Rev3L*$^{+/-}$*-lacZ* mice. It is speculate that REV3L in these tissues may be necessary for tolerating double-strand breaks generated from oxidative damage. There is some genetic evidence which indicates that yeast Rev3 may play a role in both non-homologous end-joining (NHEJ) and microhomology mediated end joining (MMEJ) – both are recombinational repair pathways employed in non-proliferating cells (42,43). NHEJ uses Ku, a protein which binds to ends of double-strand breaks, and requires less than five nucleotides of microhomology in order to mediate double-strand break repair. MMEJ is Ku independent and often requires between 5 – 20 nucleotides of microhomology in order to mediate repair (43). The role of these two repair processes in non-replicating cells could allow for repair of DNA double-strand breaks as a result of oxidative stress and could explain why *Rev3L-lacZ* expression is observed in muscle.

5.4.3 Lack of *REV3L* LacZ Expression in the Hematopoeitic System

Prior studies examining the thymus and spleen demonstrate expression of REV3L mRNA by northern blot and by RT-PCR. Examination of human and mouse normal and tumor tissues indicate that REV3L transcript is present in almost all tissue (74-76). The lack of β-gal staining in the various hematopoeitic tissues does not mean lack of *REV3L* expression. Expression of the gene may be at much lower amounts in these tissues. Casali's group indicated that mouse *REV3L* mRNA is constituitively expressed and Rev3L has been shown to act in somatic hypermutation – a very specific time in antibody generation (79). Expression in these tissues may also be at a lower level compared to other more highly oxidative tissue which could require

Rev3L continuously. This may indicate that LacZ staining in these experiments could have a threshold for detection. Unless there are a minimum number of transcripts available for sufficient translation of LacZ, it may not be detectable in these tissues. Potentially staining thicker tissue sections or whole mounts may allow detection. Although highly unlikely, a false negative result could arise if the IRES-*Rev3L-lacZ-neo*^{r} message was unstable in hematopoetic cells. A secondary method, such as *in-situ* hybridization, will help to confirm the *REV3L-lacZ* staining observed.

6.0 CONCLUSIONS

6.1 NOVEL REAGENTS FOR STUDYING HUMAN FULL-LENGTH REV3L

For many years, an understanding of human REV3L came only from limited functional genetic studies. This dearth of knowledge about REV3L resulted from a lack of essential reagents needed to study its protein biochemistry. Therefore, many basic questions regarding the function of REV3L and its interaction partners remained unanswered. As described in Chapters 2 and 3, reagents that have now been successfully generated include a recombinant full-length affinity-tagged human REV3L protein and multiple affinity-purified human REV3L antibodies. These reagents now provide the field of DNA damage tolerance with a unique set of tools for the study of human REV3L biochemistry.

To note, the ability to clone and express the REV3L cDNA has provided the opportunity to study whether the 5' UTR hairpin-loop can regulate REV3L expression. There are many future applications for the full-length human REV3L expression construct which will be discussed further below. Two important areas involve identification of novel protein interactions associated with REV3L as well as determination of whether REV3L is in fact a DNA polymerase capable of bypassing DNA lesions. The antibodies are advantageous because they can robustly detect the full-length recombinant protein, a finding that cannot be claimed for any

commercial anti-REV3L antibody. The unmet applications of the affinity-purified antibodies include immunoprecipitation, immunohistochemistry and immunofluorescence of either the endogenous or recombinant REV3L protein. These reagents may provide a better understanding regarding the cellular expression of REV3L and may also help to identify novel protein interaction partners.

6.2 TISSUE EXPRESSION STUDIES

6.2.1 Rev3L Expression in the Testis

Several translesion synthesis DNA polymerases are highly expressed during spermatogenesis, particularly during meiosis (124-126). The cellular proliferation and DNA metabolism that occurs during meiosis can generate both nucleotide base damage and double-strand breaks. Many translesion synthesis DNA polymerases are expressed during different stages of meiosis in the testis and are thought to bypass these lesions in a mutagenic fashion (124-126). Our hypothesis is that REV3L plays a role in spermatogenesis. Using the *Rev3L* LacZ expression mouse, characterization of the testis and epididymus demonstrated blue staining throughout the seminiferous tubule of the testis and the columnar epithelia of the epididymus, but not within the lumen of the epididymus (Figure 5.1A, 5.2A). *Rev3L* expression as measured by β-gal staining was observed in the spermatogonia, the primary and secondary spermatocytes and the spermatids. The precise stage of meiosis has not been defined in spermatocytes.

However, the observation that it is present in both primary and secondary spermatocytes indicates that REV3L plays a role in meiosis and spermatogenesis.

Our data show that *Rev3L* is expressed throughout the seminiferious tubules and suggests that it ,too, is involved in meiosis. Human fibroblast cell lines expressing *Rev3L* anti-sense RNA and treated with cisplatin, BPDE or UV irradiation experience diminished damage-induced mutagenesis and extrachromosomal recombination, indicating the importance of *Rev3L* in mutagenic repair and recombination (44,81). Error-prone translesion synthesis may serve the dual role of facilitating bypass at stalled replication forks with the added benefit of contributing to evolutionary mutagenesis during this process (131). REV3L is important for the bypass and extension of many types of DNA lesions which take place in an error-prone fashion (11). Diminished somatic hypermutation in immune system development as seen in *Rev3L* antisense knockdown mice suggests the importance of REV3L in controlled mutagenesis (79) and illustrates how REV3L may play a role in meiosis.

6.2.2 *Rev3L* Expression in the Musculature

The literature indicates that vertebrate Rev3 is important for tolerating many types of DNA damage (45,47,63,78). Findings in embryos suggest that many tissue types (neuronal, heart, lung and intestine) require *Rev3L* during embryogenesis to survive and to allow for correct development (59). In order to better understand what role REV3L may play in adult tissue, varous tissues in adult mice were examined. Extensive Rev3L-promoter driven LacZ staining was observed in the cardiac ventricle, the terminal bronchioles of the lung, and the smooth

musculature of the intestines. In the lung, both the epithelia and the smooth muscle scored positive for Rev3L expression (Figure 5.4A). In the intestines, expression was observed in both the longitudinal and circular smooth muscle layers but not in the epithelia of the microvilli (Figure 5.5A and C). For the cardiac ventricle, staining was observed throughout the musculature (Figure 5.3A). Blue staining was also observed in the musculature of the abdominal aorta.

What is the meaning of this expression in muscle tissues? Prior work examining the LacZ expression pattern of *Rev3L* in embryonic mouse sections demonstrated a high level of staining that initially appeared in the somites. Staining spread later in development and, by day 11.5, was observed throughout the mesenchymal tissue with emphasis in the heart and developing aorta, the lung bud and the fourth branchial arch (59). H & E staining of murine *Rev3L*$^{-/-}$ cardiac myocytes and gut mesenchyme demonstrated degenerating or disordered growth compared to *Rev3L*$^{+/-}$ embryos (59). These embryonic findings are in line with the present experimental observations in the adult mouse where *Rev3L*-promoter driven LacZ staining was observed in these tissues. There are many reasons for why REV3L may be critical for both embryogenesis and the adult organism. The time at which Rev3L expression is observed in embryogenesis corresponds with an increasing need for oxidative metabolism. Furthermore, the adult musculature acts as a receiver (smooth muscle and cardiac) as well as a conduit (blood vessel smooth muscle and bronchioles) for oxygen use and transport. One possible explanation is that mouse REV3L protein is critical for damage tolerance caused by endogenous genotoxic agents such as hydroxyl radicals or peroxynitrite causing base damage or strand breaks (1,132). A recent investigation of chicken DT40 B-cells disrupted for *Rev3* demonstrated an increased sensitivity to both hydrogen peroxide and nitric oxide (63,65). Nitric oxide is a potent signal

transduction molecule involved in vascular relaxation. Nitric oxide byproducts, such as peroxynitrite in vascular and cardiac cells, can diffuse into cells causing DNA damage (1) and perhaps REV3L is particularly important for processing this DNA damage in such tissues.

6.2.3 Future Direction for the *Rev3L LacZ* Expression Mice

Our results demonstrate that Rev3L is expressed in the smooth muscle of lung and intestine, the cardiac ventricle and the cells of the testis. The next step is to apply immunohistochemical analysis in order to determine what specific cell types are expressing β-gal. This will provide a context of how Rev3L is functioning in the cell (ie. tolerating oxidative stress, meiotic recombination, or cellular proliferation).

Another area of interest is whether tissue specific *Rev3L* expression increases in a p53-dependent manner in response to DNA damage. In a recent paper, chromatin immunoprecipitation and quantitative RT-PCR demonstrated that the *Rev3L* promoter contains a p53 binding element, and that the *Rev3L* transcript is upregulated in a p53-dependent fashion in response to treatment with adriamycin (133). Characterization of genes upregulated with the seizure-inducing drug pentylenetetrazol identified *Rev3L* mRNA in the adult mouse brain (134). The mechanism of action of pentylenetetrazol is thought to be due to generation of oxidative radicals in the cell. These findings, in combination with preliminary results characterizing sections of the adult mouse brain by LacZ staining, indicate that *Rev3L* is expressed in the brain and may be important for tolerating oxidative damage. One avenue of investigation would be to examine $p53^{+/+}$ and $p53^{-/-}$, heterozygous *Rev3L* LacZ expression mice treated with gamma

irradiation. The intestines, heart, spleen, bone marrow and brain would be examined for LacZ expression, and results confirmed using *in situ* hybridization. The findings from this study would help to determine whether *Rev3L* is upregulated in a p53 dependent damage response to gamma irradiation. It is possible that these organs require REV3L for tolerance of DNA damage.

6.3 THE REV3L-REV1 PROTEIN INTERACTION

6.3.1 Characterizing the Domains

Evidence in yeast supports an interaction between the full-length Rev1-Rev3/Pol zeta proteins (26,40). However, the only work that has been done to date with the human REV proteins involves work with fragments. The field has been stymied for some time because many groups have been unable to generate either the full-length human REV3L protein or a REV3L-specific antibody. Our hypothesis is that full-length human REV3L can interact with REV1 and REV7. The work accomplished in this dissertation demonstrates successful expression, purification and immunoprecipitation of the full-length human REV3L protein. Furthermore, it has been demonstrated for the first time that full-length REV3L and full-length human REV1 can interact with one another by co-immunoprecipitation. It was also observed that the human full-length REV1 and REV7 proteins interact. However, no interaction was observed between the full-length REV3L protein and REV7. The REV1-REV7 interaction has been demonstrated with

both the yeast and human proteins by other groups (50,135). To note, in contrast to studies peformed by Kamiya et al., in which 3 μg of REV7 and 24 μg of REV1 was required to demonstrate an interaction by immunoprecipitation, an interaction has been demonstrated here using only nanogram quantities.

The lack of interaction between full length human REV3L and REV7 is somewhat surprising, but may be attributed to several factors. First, all the work done on the invertebrate and vertebrate proteins attempting to demonstrate a Rev3-Rev7 interaction has been done using fragments (57,86,88). Use of partial proteins could lead to non-specific interactions. Second, *in situ* hybridization demonstrates that mouse *Rev3L* and *Rev7* mRNA are not expressed in the same sections of the brain. Their expression occurs in the hippocampus and thalamus, respectively. In contrast, REV1 does co-localize with REV3L by *in situ* hybridization (127). Studies by Sakaguchi et al. further support a possible independence of Rev3 and Rev7 function. They found that *Drosophila* Rev3 had polymerase activity independent of Rev7 – suggesting that Rev7, though able to bind a *Drosophila* Rev3 fragment, was unnecessary for *Drosophila* DNA polymerase zeta processivity (57). Although contrasting with the yeast results, these findings in mouse and *Drosophila* may suggest an evolutionarily divergent path in which Rev7 is involved with damage tolerance and translesion synthesis, but not Rev3 function. Third, there is a significant difference in protein size of mammalian REV3L (3130 amino acids) compared to yeast Rev3 (1504 amino acids). The lack of REV7 interaction with human REV3L may be due to the protein folding or masking of a vestigial yeast Rev7 binding domain found in full-length REV3L. Finally, attempts to enhance an interaction by DNA damage as well as co-expression of all three REV proteins simultaneously have not facilitated formation of a REV3L-REV7 interaction. Taken together, these factors do not definitively rule out the possibility of a REV3L-

REV7 interaction, but suggest that REV3L may not require REV7 for biological function. A recent paper examining multiple nasopharyngeal carcinoma cell lines suppressed for REV7 demonstrate increased sensitivity to cisplatin and gamma irradiation. These cells also experienced an increased number of chromosomal aberrations and a decreased rate of mutagenesis and sister chromatid exchange (71). Studies done on REV1 and REV3L knockdown cell lines demonstrate a diminished frequency of homologous recombination and an increased sensitivity to cisplatin (44,46). These results suggest that REV7, REV1 and REV3L function in homologous recombination and postreplication repair together. However, full characterization of this interaction remains incomplete.

The experiments described here have begun to delineate the protein domains of REV1 and REV3L responsible for the protein-protein interactions. The results indicate that the 140 amino acid C-terminal domain region of REV1 can interact with full-length human REV3L and with REV7. Further results indicate that the polymerase domain of REV3L interacts with full-length REV1. The human protein fragment results corroborate the published yeast data which demonstrates that the 72 amino acid C-terminal domain of yeast Rev1 interacts with the polymerase domain (amino acid 612 – 1377) of Rev3 (26). There was no difference in REV3L interaction with a REV1 G76R BRCT domain point mutant compared to wild type REV1. There was also no difference observed between the interaction of REV1 wild type or mutant with REV7. These results suggest that the point mutant has no effect on the ability of REV1 to co-immunoprecipitate with either REV3L or REV7. These results reflect what is known regarding the yeast homologs (40). Unpublished observations from the Wood lab indicate that the 140 amino acid C-terminal domain of REV1 interacts with endogenous human Pol iota and kappa by immunoprecipitation. Furthermore, data indicate that the last 100 amino acid C-terminal domain

of mouse Rev1 is responsible for interacting with mouse REV7 as well as Pol iota, eta and kappa (89). The findings in this thesis substantiate these results.

6.3.2 Future Direction Regarding the REV1-REV3L Protein Interaction Studies

The first follow-up experiments should examine the remaining REV1 (REV1ΔCTD) and REV3L (N-terminal, Exon 13/KIAA and yeast Rev7 binding domain) fragments to determine whether they can interact with their corresponding full-length partners. Only then can a more complete understanding of the protein domains necessary for mediating the REV1-REV3L interaction be achieved.

Based on the observed interactions, it is tempting to speculate that human REV3L associates with REV1 on double-strand breaks after DNA damage. It has been shown in two independent yeast studies that Rev1 associates with Rev3/Pol zeta (26,40). Using a system which allowed for the generation of a single double-strand break (HO-endonuclease acting at an *ADH4* locus) in yeast, Sugimoto and Hirano demonstrated that Rev1 associated with double-strand breaks using chromatin immunoprecipitation. Furthermore, the binding of REV1 to the strand break required a functional REV1 BRCT domain as well as phosphorylation by Mec1 (the yeast ATR homolog) (40). In another study, Mec1 phosphorylated Rev1 in a DNA damage dependent fashion and this phosphorylation was necessary for the protein to interact with chromosomes. In the absence of damage, phosphorylation of Rev1 was greatest in G_2/M and minimal during G_1/S. These effects were mediated by Mec1 (55), which suggests that Rev1 is phosphorylated in order to bind to double-strand breaks. However, it remains unknown whether

human REV1 is similarly phosphorylated. Growing evidence indicates that the DNA damage sensors ATM and ATR are interconnected in their response to replication fork stress and double-strand breaks (136) and if human REV1 is phosphorylated, it may be due to one of these damage response kinases.

Another possible avenue to explore is determining whether association of human REV1 with double-strand breaks is phosphorylation-dependent. My preliminary results suggest that REV3L is phosphorylated. The biological significance of this covalent modification remains unknown but may suggest a form of regulation coordinating protein-protein interaction (i.e. REV1-REV3L), perhaps during a specific phase in the cell cycle or in response to DNA damage. The next step would be to determine whether both REV1 and REV3L are phosphorylated and to begin characterization of which domain(s) becomes phosphorylated using the protein fragments generated in the protein interaction study. Identifying the domain that is phosphorylated can provide insight for more targeted site-directed mutagenesis. Based on the outcome of these results, one could then determine whether or not phosphorylation plays a role in the REV1-REV3L protein interaction. If so, it can further be determined whether phosphorylation is due to ATM or ATR and if this phosphorylation is cell cycle-dependent or modulated in response to DNA damage. Using ChIP in combination with ATM and ATR specific inhibitors, as well as the REV1 G67R BRCT point mutant, it can now be determined whether REV1 interacts with double-strand breaks in human cells. Specific DNA damaging agents that cause single and double-strand breaks could then be examined, so that a potential role for REV1 (and REV3L) in tolerance of DNA strand breaks can be delineated.

6.3.3 Covalent Modification and Possible Regulation of the Human REV Proteins

This work demonstrates that recombinant REV1, REV3L and REV7 are ubiquitinated when co-transfected with an HA-tagged ubiquitin expression plasmid. Mono and di-ubiquitination of the 140 amino acid C-terminal domain of REV1 and full-length REV7 were observed. The biological effect of REV protein ubiquitination remains unknown. One possibility is that it affects regulation of the protein in response to damage. Another is that it prepares the protein for proteasomal degradation. Ubiquitination is capable of playing a regulatory role as seen in the evolutionarily conserved Rad6-Rad18 pathway. This ubiquitin ligase complex has been shown to ubiquitinate PCNA when initiating postreplication repair (12). The functional consequence of this ubiquitination has been demonstrated with Pol eta. In response to DNA damage by UVC, PCNA becomes ubiquitinated, enhancing the affinity of Pol eta for this protein and thereby recruiting it to the site of a DNA lesion for bypass (14). Furthermore, a recent discovery in yeast and mammalian cells indicates that the Y-family polymerases possess ubiquitin binding motifs (UBM) which have an affinity for ubiquitin and ubiquitinated-PCNA (33-35). Work with mouse REV1 has also shown an enhanced interaction with mono-ubiquitinated PCNA and this interaction was mediated by REV1 UBMs. It is presumed that UBMs may bind ubiquitinated molecules other than PCNA. One possibility is that these UBMs may facilitate protein-protein interactions between REV1 and REV3L or REV1 and REV7.

The observed ubiquitination might also be related to proteasomal degradation. Removal of the REV proteins could minimize spontaneous mutagenesis in a cell. Data indicate that yeast Rev1 is cell cycle regulated. Its mRNA and protein expression peak during G_2/M and are

minimal throughout G_1/S (54). Treatment with proteasome inhibitors prevents Rev1 degradation in the cell (correspondence with the Walker lab). If human REV1 is similarly regulated by the cell cycle, the observed mono and di-ubiquitination of the C-terminal domain of REV1 may be a signal for REV1 proteasomal degradation. However, the ubiquitination observed on the C-terminal domain of REV1 may not mediate this process. Therefore the REV1ΔCTD should also be examined for mono and polyubiquitination. There are two ways to test whether this ubiquitination is associated with degradation as opposed to being associated with a regulatory pathway. One way would be to use a K48R-ubiquitin to prevent polyubiquitylation, and the other is to use proteasome inhibitors to see if REV1 and/or its C-terminal domain can be stabilized. This same analysis can be performed for REV3L and REV7. Using the four REV3L fragments generated from the interaction study, work can begin to determine which REV3L fragment becomes ubiquitinated. Prior experiments in which cells expressing recombinant full-length human REV3L were treated with either ALLN or MG132 revealed a slight increase in the amount of REV3L protein suggesting that the recombinant protein may be proteasomally regulated. In yeast, the Rev7 and Rev3 proteins apparently remain constant throughout the cell cycle (54). In contrast, the findings reported herein could be attributed to the fact that the protein was exogenously overexpressed. To note, there does not appear to be a qualitative difference in the amount of ubiquitinated versus non-ubiquitinated REV1-REV3L complex by immunoprecipitation, suggesting that ubiquitination does not regulate REV1-REV3L interaction.

6.4 CONCLUSION

Our understanding of the biochemistry and function of mammalian REV3L has been severely limited due to the lack of necessary reagents to address fundamental questions. This dissertation focused first on the generation of these necessary reagents. Two affinity purified antibodies generated against the N-terminal domain of human REV3L and the yeast Rev7 binding domain were both able to detect the recombinant full-length human REV3L protein (Chapter 2). A recombinant full-length human REV3L expression construct containing dual His-Flag affinity tags was successfully cloned, and the protein was expressed, immunoprecipitated and detected by immunoblot. A polymerase domain active-site mutant was also generated to study DNA polymerase activity. Furthermore, recombinant full-length human REV1 and REV7 proteins were also generated to study potential protein interactions (Chapter 3). Our hypothesis was that REV3L could interact with REV1 and/or with REV7. It was found that full-length REV3L interacts with full-length REV1 but does not interact with full-length REV7. Furthermore, the REV1 interaction with REV3L is mediated by the C-terminal domain of REV1 and potentially by the polymerase domain of REV3L. Finally, all three REV proteins were found to be ubiquitinated (Chapter 4). Our second hypothesis was that organs with highly proliferative tissue require Rev3L. In order to understand what tissues and cell types expressed REV3L, transgenic mice containing a targeted IRES-*Rev3L-lacZ-neo*^{r} disruption construct recombined into the *Rev3L* locus were examined. Interestingly, non-proliferative tissue such as muscle from cardiac ventricle, the terminal bronchiole of the lung and the small intestine were found to express Rev3L, but no expression was observed in lymphoid tissue (Chapter 5).

Future biochemical studies will further characterize the protein domains responsible for the REV1-REV3L interaction, the effect of DNA damage on the DNA-REV1-REV3L interaction and the possible regulatory role of ubiquitination on REV1, REV3L and REV7. Future animal studies will examine whether tissue specific *Rev3L* expression is elevated in a p53-dependent manner in response to DNA damage.

Appendix

Appendix A. PCR Primer Sequences

REV3L PCR Primers for Epitope Fragment Generation

Alt Splice Forward primer:
GTC TCC ATG GCT ATG TTT TCA GTA AGG ATA GTG ACT

Alt Splice Reverse primer:
GTG CCG CTC GAG TTA TTA ATG GTG ATG GTG ATG GTG ATG GTG ATG GTG ACT TTC TGG CTG CTG TCC

N-terminal Forward primer:
GTC ACC ATG GCA ATG GCA TTC AGT ATC GAC AGA G

N-terminal Reverse primer:
GTG CCG CTC GAG TTA TTA ATG GTG ATG GTG ATG GTG ATG GTG ATG GTG TCT CTG GGA CAT CAC CAA ACT

Conserved Domain Forward primer:
AAT CAA TCC ATA TGG GGA CGT TAG AAA CTG AGC AG

Conserved Domain Reverse primer:
TAA TCG CTC GAG TTA TTA TTA TTT ATT TGT CTG ATT TCG TTT GTT C

REV7 Binding Domain Forward primer:
AAT CAA TCG CAT ATG ACT CCT GAT AGT TCA CCA AGA TCT ACT

REV7 Binding Domain Reverse primer:
TAA TCG CTC GAG TTA TTA TTA CCT GGG CTT TTC TGG TAC ATC

Polymerase Domain Forward primer:
GAC TAC TCA CAT ATG TTA CTT ATT AGA TCT GGA ATT ACA GGA CTC

Polymerase Domain Reverse primer:
TAA TCG CTC GAG TTA TTA TTA GCC ATA TAC AAC CCT AGC CC

RT-PCR Primers for Amplifying Human Genomic REV3L

Human REV3hu-F Forward primer:
CAT GCA TTG AGG TTG GCG ATA GT

Human REV3hu-R Reverse primer:
CAG AAG GAG CCA GTA TTT GAT GCG

Human GAPDH Forward primer:
GGT CGG AGT CAA CGG ATT TGG TCG

Human GAPDH Reverse primer:
GTG GTG AAG CAG GCG TCG GAG G

REV3L shRNA Sequences (SBI)

shRNA #1:
GAC CTT GGA ACG AGC TAT TAA ACT GG

shRNA #2:
GCC AGC ATA CAA GAC TTT ATC TTT GC

shRNA #3:
CCC GAG TAA ATA GAG AAT TGT CCA AG

Modifying the C-terminal end of REV3L

No 3' UTR Forward primer:
CTG ATT GGG AAA ACC AGT GA

No 3' UTR – p5 (C-terminal Flag), Reverse primer:
AAG GAC AAG GCG GCC GCA TGA GCT CTT ATT ACT TGT CGT CAT CGT CTT TGT AGT CAA ACT GGT CTA ATA ACT GCC GGA GAT ATG

Modifying the N-terminal end of REV3L

No 5' UTR – p1 (Mam Kozak only) Forward primer:
ATG ATG CGG GGT ACC GTA GAA TTC GCA CCA TGG TTT CAG TAA GGA TAG TGA C

No 5'UTR – p2 (Mam Kozak and 10x His tag) Forward primer:

ATG ATG CGG GGT ACC GTA GAA TTC GCA CCA TGG TTC ATC ACC ATC ACC ATC ACC ATC ACC ATC ACT CAG TAA GGA TAG TGA CTG CAG ACT AC

No 5'UTR, Reverse primer:
TTT GTC TTT GTG AAC TTC TAC CAT

Inserting an EcoRI RE Site into the Existing REV3L-pENTR Clones

5' End, (5' primer) EcoRI insertion Forward primer:
ATG ATG ATG GGT ACC GAA TTC GGG CCC CCC CTC GAG GTC

No 5' UTR, Kozak+10x His Forward primer:
ATG ATG CGG GGT ACC GAA TTC ACC ATG GTT CAT CAC CAT CAC CAT CAC CAT CAC CAT CAC TCA GTA AGG ATA GTG ACT GCA GAC TAC

No 5'UTR, Reverse primer (same as above):
TTT GTC TTT GTG AAC TTC TAC CAT

2-Step PCR, REV3L Active Site Mutant

No 3' UTR Forward primer (or p1):
CTG ATT GGG AAA ACC AGT GA

Pol Dom Mutant p2 Reverse primer (or p2):
ACT GGC AGT GGC GCC ATA TAC AAC CCT AGC CCC CCA TTT

Pol Dom Mutant p3 Forward primer (or p3):
TAT GGC GCC ACT GCC AGT ATG TTT GTG CTA CTG AAA GGA

No 3' UTR – p5 (C-terminal Flag), Reverse primer (or p4):
AAG GAC AAG GCG GCC GCA TGA GCT CTT ATT ACT TGT CGT CAT CGT CTT TGT AGT CAA ACT GGT CTA ATA ACT GCC GGA GAT ATG

Cloning Recombinant Human REV1-V5

REV1 (5' primer) Forward primer:
ATG ATG CCA ACA CAC TGG ACC ATG GGT AAG CCT ATC CCT AAC CCT CTC CTC GGT CTC GAT TCT ACG AGG CGA GGT GGA TGG AGG AAG CGA GCT

REV1 (3' primer) Reverse primer:
CAT CAT GCG GCC GCT TAT GTA ACT TTT AAT GTG CTT CCA TAA

Cloning Recombinant Human REV7-HF and REV7-HA

REV7-N-Flag-EcoRI (5' primer) Forward primer:
CGG CTA GAA TTC ACC ATG GAC TAC AAA GAC GAT GAC GAC AAG ACC ACG CTC ACA CGA CAA GAC

REV7 Cloning primer (3' end with 10x His tag) Reverse primer:
CGG CTA GGT ACC GCG GCC GCT CAG TAGA TGG TGA TGG TGA TGG TGA TGG TGA TG

REV7 EcoRI-N-term HA tag Forward primer:
CGG CTA GAA TTC ACC ATG GCC TAT CCA TAT GAC GTC CCT GAC TCT GCC ACC ACG CTC ACA CGA CAA GAC

REV7, no C-term tag (3' primer) Reverse primer:
CAT CAT CGC GGC CGC TCA GCT GCC TTT ATG AGC GCG CTC

REV3L Fragment PCR Primers

Polymerase Delta Homology Forward primer:
ATG ATG GAA TTC ACC ATG GCA TCA GTA AGG ATA GTG ACT GCA GAC T

Polymerase Delta Homology Reverse primer:
CAT CAT GCG GCC GCT TAC TTG TCG TCA TCG TCT TTG TAG TCG TCA CTA TTT TCA TCT GCA GTT CC

KIAA/exon 13 Forward primer:
ATG ATG GAA TTC ACC ATG GCA AAT CCA TTG AAC AAT GAA AAT TCT AGA

KIAA/exon 13 Reverse primer:
CAT CAT GCG GCC GCT TAC TTG TCG TCA TCG TCT TTG TAG TCG GGC TTT TCT GGT ACA TCA GAA GGA TTA CT

REV7 Binding Domain Forward primer:
ATG ATG GAA TTC ACC ATG GCA AGA TTG AAT AGG AGT TCA GTA AGC AAA G

REV7 Binding Domain Reverse primer:
CAT CAT GCG GCC GCT TAC TTG TCG TCA TCG TCT TTG TAG TCA TCT GGG TTA ACT GAA GAG CTA AAG TTC TC

Polymerase domain Forward primer:
ATG ATG GAA TTC ACC ATG GCA CCA CAG AAA GAA ACT TCT CAG ATT GAT

Polymerase domain Reverse primer:

CAT CAT GCG GCC GCT TAC TTG TCG TCA TCG TCT TTG TAG TCA AAC TGG TCT AAT AAC TGC CG

REV1 Fragment PCR Primers

REV1ΔCTD Forward primer (hREV1-N-term V5 tag primer – NheI):
ATG ATG GCT AGC ACC ATG GGT AAG CCT ATC CCT AAC CCT CTC CTC GGT CTC GAT TCT ACG AGG CGA GGT GGA TGG AGG AAG CGA GCT

REV1ΔCTD Reverse primer (REV1-V5 CTD R' primer):
CAT CAT GCG GCC GCT TAC TGG GGA CTG CCA CAG GCC CC

CTD#1 Forward primer (REV1 CTD F' primer):
ATG ATG CCA ACA CAC TGG ACC ATG GGT AAG CCT ATC CCT AAC CCT CTC CTC GGT CTC GAT TCT ACG AAG TTA ATT GAT GGG TTT CTA AAA CAT G

CTD#1 Reverse primer (3' primer – hREV1 – no C-term tag):
CAT CAT GCG GCC GCT TAT GTA ACT TTT AAT GTG CTT CCA TAA

CTD#2 Forward primer (REV1-V5 CTD F primer #2):
ATG ATG CCA ACA CAC TGG ACC ATG GGT AAG CCT ATC CCT AAC CCT CTC CTC GGT CTC GAT TCT ACG GAT GTG AAG ACC TTG CTC AGA GAA TG

CTD#2 Reverse primer (3' primer – hREV1 – no C-term tag):
CAT CAT GCG GCC GCT TAT GTA ACT TTT AAT GTG CTT CCA TAA

Appendix B. PCR Protocols

PCR Amplification protocol for Alternative Splice and REV7 Binding Domain fragments

1) 94ºC	2 min
2) 94ºC	30 sec
3) 54ºC	30 sec
4) 72ºC	1 min
5) goto #2	5x cycles
6) 94ºC	30 sec
7) 52ºC	30 sec
8) 72ºC	1 min
9) goto #6	25 cycles
10) 72ºC	2 min
11) 0.1ºC/sec to 16ºC	
12) 16ºC	forever

PCR Amplification protocol for N-terminal, Conserved Region and Polymerase Domain fragment

1) 94ºC	2 min
2) 94ºC	30 sec
3) 54ºC	30 sec
4) 72ºC	3 min
5) goto #2	5x cycles
6) 94ºC	30 sec
7) 52ºC	30 sec
8) 72ºC	3 min
9) goto #6	25 cycles
10) 72ºC	4 min
11) 0.1ºC/sec to 16ºC	
12) 16ºC	forever

RT-PCR Amplification Protocol for Human REV3L

1) 94ºC	2 min
2) 94ºC	30 sec
3) 55ºC	30 sec
4) 68ºC	1 min
5) goto #2	35x cycles
6) 68ºC	2 min
7) 0.1ºC/sec to 16ºC	
8) 16ºC	forever

RT-PCR Amplification Protocol for Human GAPDH

1) 94ºC 2 min
2) 94ºC 30 sec
3) 55ºC 30 sec
4) 68ºC 1 min
5) goto #2 25x cycles
6) 68ºC 2 min
7) 0.1ºC/sec to 16ºC
8) 16ºC forever

PCR Protocol for amplifying "no 3' UTR, C-terminal Flag-tag"

1) 94ºC 2 min
2) 94ºC 30 sec
3) 45ºC 45 sec
4) 72ºC 5 min
5) go to #2 5x cycles
6) 94ºC 30 sec
7) 48ºC 45 sec
8) 72ºC 5 min
9) go to #6, 30x
10) 72ºC 5 min
11) 0.1ºC/sec to 16ºC
12) 16ºC forever

PCR Protocol for Generating EcoRI Insert into 5' end of REV3L

1) 94ºC 2 min
2) 94ºC 30 sec
3) 45ºC 45 sec
4) 72ºC 5 min
5) go to #2 5x cycles
6) 94ºC 30 sec
7) 48ºC 45 sec
8) 72ºC 5 min
9) go to #6, 30x
10) 72ºC 5 min
11) 0.1ºC/sec to 16ºC
12) 16ºC forever

PCR Protocol for Generating Fragment A and Fragment B (2-step PCR)

Fragment A PCR Protocol

1) 94ºC 2 min
2) 94ºC 30 sec
3) 48ºC 45 sec
4) 72ºC 4 min
5) go to #2 30x cycles
6) 72ºC 4 min
7) 0.1ºC/sec to 16ºC
8) 16ºC forever

Fragment B PCR Protocol

1) 94ºC 2 min
2) 94ºC 30 sec
3) 45ºC 45 sec
4) 72ºC 4 min
5) go to #2 35x cycles
6) 72ºC 4 min
7) 0.1ºC/sec to 16ºC
8) 16ºC forever

Fragment A/B PCR protocol

1) 94ºC 2 min
2) 94ºC 30 sec
3) 45ºC 45 sec
4) 72ºC 4 min
5) go to #2 4x cycles
6) 94ºC 30 sec
7) 48ºC 45 sec
8) 72ºC 4 min
9) go to #6, 29x
10) 72ºC 4 min
11) 0.1ºC/sec to 16ºC
12) 16ºC forever

PCR Protocol for Generating REV1-V5

1) 94ºC 2 min
2) 94ºC 30 sec
3) 55ºC 30 sec
-1ºC/cycle
4) 68ºC 5 min
5) go to #2 9x cycles
6) 94ºC 30 sec
7) 55ºC 45 sec
8) 68ºC 5 min
9) go to #6, 20x
10) 68ºC 5 min
11) 0.1ºC/sec to 16ºC
12) 16ºC forever

PCR Protocol for Generating REV7-HF and REV7-HA

1) 94ºC 2 min
2) 94ºC 30 sec
3) 45ºC 45 sec
4) 72ºC 4 min
5) go to #2 35x cycles
6) 72ºC 4 min
7) 0.1ºC/sec to 16ºC
8) 16ºC forever

CTD#1, #2 and REV7 Binding Domain PCR Fragment

1) 94ºC 2 min
2) 94ºC 30 sec
3) 55ºC 30 sec
4) 68ºC 1 min
5) go to #2 5x cycles
6) 94ºC 30 sec
7) 55ºC 30 sec
8) 68ºC 1 min
9) go to #6, 20x
10) 68ºC 2 min
11) 0.1ºC/sec to 16ºC
12) 16ºC forever

Polymerase Domain and REV1ΔCTD PCR Fragment

1) 94ºC 2 min
2) 94ºC 30 sec
3) 48ºC 45 sec
4) 68ºC 3 min
5) go to #2 9x cycles
6) 94ºC 30 sec
7) 50ºC 45 sec
8) 68ºC 3 min
9) go to #6, 20x
10) 68ºC 4 min
11) 0.1ºC/sec to 16ºC
12) 16ºC forever

Appendix C. Lysis Buffers

Native lysis buffer

50 mM NaH_2PO_4, pH 8.0
300 mM NaCl
10 mM imidazole

Supplement with:
- 5 μM Pepstatin A
- 5 μM Chymostatin
- 5 μM Leupeptin
- 5 μM AEBSF
- 10 μl IC3 (Calbiochem) / 10 ml of lysis buffer
- 1 mg/ml of lysozyme

TEDM Buffer (500 ml)
50 mM Tris-HCl, pH 8.0
2 mM EDTA
Supplement with:
- 0.1 mM DTT
- 1 mM β-mercaptoethanol
- 100 μM AEBSF (two part addition)
- 0.05% Sodium deoxycholate

TE Wash Buffer (500 ml)
50 mM Tris-HCl, pH 8.0
2 mM EDTA

Hi-salt RIPA Lysis Buffer

50 mM Tris HCl, pH 7.4
400 mM NaCl
0.25% Sodium deoxycholate
1% NP-40
1 mM EDTA

Supplement with:
- 1 mM NaF
- 1 mM Na3VO4
- 5 μM Pepstatin A
- 5 μM Chymostatin
- 5 μM Leupeptin
- 10 μl IC3 (Calbiochem)/ 10 ml of lysis buffer

Mouse Tissue Extract Buffer

50 mM Tris HCl, pH 7.4
150 mM NaCl
0.1% NP-40
5% glycerol
Add 100 μl 0.5 M EDTA (final: 5 mM)

Hypotonic Buffer
10 mM Tris-HCl (pH 7.3)
10 mM KCl
1.5 mM $MgCl_2$
10 mM β-mercaptoethanol
1 μM AEBSF

Micrococcal nuclease buffer
20 mM Tris-HCl (pH 7.5)
100 mM KCl
2 mM $MgCl_2$
1 mM $CaCl_2$
0.3 M sucrose
0.1% Triton X-100

Extraction Buffer
15 mM Tris-HCl (pH 7.3)
1 mM EDTA
0.4 M NaCl
1 mM $MgCl_2$
10% glycerol
10 mM β-mercaptoethanol
1 μM AEBSF

Supplement all lysis buffers with:
- 5 μM Leupeptin
- 5 μM Chymostatin
- 5 μM Pepstatin A
- IC3 (10 μl inhibitor / 10 ml buffer)
- Add 60 U of S7 micrococcal nuclease per 200 μl nuclease buffer

Freeze Thaw Lysis Buffer
1) 20 mM HEPES, pH 7.6
2) 150 mM NaCl
3) 10% glycerol
4) 0.1% Tween20
5) No EDTA, add 20 ul/10ml buffer
6) No DTT, add 10 ul/10 ml buffer

Supplement with:
- 1 mM NaF
- 1 mM Na3VO4
- 5 μM Pepstatin A
- 5 μM Chymostatin
- 5 μM Leupeptin
- 10 μl IC3 (Calbiochem)/ 10 ml of lysis buffer

Appendix D. Gel Purification and Protein Analysis

Self-Casted <u>mini</u> SDS polyacrylamide gels using a glass plates and casting mounts from Biorad

10% SDS polyacrylamide gels	**1x gel**	**2x gel**
1) 30% Acrylamide/Bis Solution, 29:1 (3.3% crosslink) (Biorad)	1.7 ml	3.3 ml
1.5 M Tris, pH 8.8	1.3 ml	2.5 ml
2) 10% SDS (Sigma)	0.05 ml	0.1 ml
3) 10% NH_4HSO_4 (Sigma)	0.05 ml	0.1 ml
4) TEMED (Biorad)	0.002 ml	0.004 ml
5) ddH_2O	1.9 ml	4.0 ml

12% SDS polyacrylamide gels	**1x gel**	**2x gel**
1) 30% Acrylamide/Bis Solution, 29:1 (3.3% crosslink) (Biorad)	2 ml	4 ml
1.5 M Tris, pH 8.8	1.3 ml	2.5 ml
2) 10% SDS (Sigma)	0.05 ml	0.1 ml
3) 10% NH_4HSO_4 (Sigma)	0.05 ml	0.1 ml
4) TEMED (Biorad)	0.002 ml	0.004 ml
5) ddH_2O	1.6 ml	3.3 ml

15% SDS polyacrylamide gels	**1x gel**	**2x gel**
1) 30% Acrylamide/Bis Solution, 29:1 (3.3% crosslink) (Biorad)	2.5 ml	5 ml
1.5 M Tris, pH 8.8	1.3 ml	2.5 ml
2) 10% SDS (Sigma)	0.05 ml	0.1 ml
3) 10% NH_4HSO_4 (Sigma)	0.05 ml	0.1 ml
4) TEMED (Biorad)	0.002 ml	0.004 ml
5) ddH_2O	1.1 ml	2.3 ml

5% Stacking Gel Column	**1x gel**
1) 30% Acrylamide/Bis Solution, 29:1 (3.3% crosslink) (Biorad)	330 µl
1 M Tris, pH 6.8	500 µl
2) 10% SDS (Sigma)	20 µl
3) 10% NH_4HSO_4 (Sigma)	20 µl
4) TEMED (Biorad)	5 µl
5) ddH_2O	1150 µl

Biorad System

- Prestained SeeBlue2 Plus Molecular Weight Standards (Invitrogen)
- Biorad Gel Apparatus
- Biorad Transfer Apparatus
- 2x fresh Blotting fiber pads
- Biorad 10x Tris-Glycine SDS Running Buffer
- Biorad 10x Tris-Glycine Transfer Buffer
- Biorad Tris-Glycine 4 – 15% gradient gels, 10 and 12 well pre-cast
- 0.45 mm PVDF membrane (Millipore)
- 3 mm chromatography paper (Whatman)

1x Running Buffer

1) 25 mM Tris, pH 8.3
2) 192 mM Glycine
3) 0.1% SDS

1x Transfer Buffer

1) 25 mM Tris, pH 8.3
2) 192 mM Glycine
3) 20% MeOH

Coomassie Brilliant Blue Solution

1) 0.25 g Coomassie dye/100 ml solution
2) 40% MeOH
3) 10% Acetic acid
4) 50% ddH_2O

Membrane Wash Solution (1x PBS 0.1% Tween20)

1) 11.9 mM PO_4^{3-}
2) 137 NaCl
3) 2.7 mM KCl
4) 0.1% Tween20

Blocking Buffer Solution (10% milk or 5% normal goat serum in 1x PBS 0.1% Tween20)

1) 10% milk, dry nonfat OR 5% normal goat serum
2) 11.9 mM PO_4^{3-}
3) 137 NaCl
4) 2.7 mM KCl
5) 0.1% Tween20

Self-casted large-scale SDS polyacrylamide gels using a glass plates and casting mounts from Biorad

10% SDS polyacrylamide gels

1) 30% Acrylamide/Bis Solution, 29:1 (3.3% crosslink) (Biorad)	17 ml
2) 1.5 M Tris, pH 8.8	13 ml
3) 10% SDS (Sigma)	0.5 ml
4) 10% NH_4HSO_4 (Sigma)	0.5 ml
5) TEMED (Biorad)	0.05 ml
6) ddH_2O	19 ml

15% SDS polyacrylamide gels

1) 30% Acrylamide/Bis Solution, 29:1 (3.3% crosslink) (Biorad)	25 ml
2) 1.5 M Tris, pH 8.8	13 ml
3) 10% SDS (Sigma)	0.5 ml
4) 10% NH_4HSO_4 (Sigma)	0.5 ml
5) TEMED (Biorad)	0.05 ml
6) ddH_2O	11 ml

5% Stacking Gel Column

1) 30% Acrylamide/Bis Solution, 29:1 (3.3% crosslink) (Biorad)	2.48 ml
2) 1 M Tris, pH 6.8	3.75 ml
3) 10% SDS (Sigma)	150 µl
4) 10% NH_4HSO_4 (Sigma)	150 µl
5) TEMED (Biorad)	10 µl
6) ddH_2O	8.63 ml

Invitrogen NuPAGE System

- Prestained Highmark Molecular Weight Standards (Invitrogen)
- NuPAGE Gel Apparatus
- NuPAGE Transfer Apparatus
- 4x fresh Blotting fiber pads
- NuPAGE 20x Tris-Acetate SDS Running Buffer
- NuPAGE 20x Tris-Acetate Transfer Buffer
- NuPAGE Tris-Acetate 3 – 8% gradient gels
- NuPAGE Antioxidant
- 0.45 mm PVDF membrane (Millipore)
- 3 mm chromatography paper (Whatman)

1x NuPAGE Tris-Acetate Running Buffer Composition (600 ml)

1) 50 mM Tricine, pH 8.24
2) 50 mM Tris base
3) 0.1% SDS

1x NuPAGE Tris-Acetate Transfer Buffer Composition (500 ml)

1) 25 mM Bicine, pH 7.2
2) 25 mM Bis-Tris (free-base)
3) 1 mM EDTA
4) 20% MeOH
5) 500 µl of Antioxidant

Solutions for Silver Stain

Fixative Solution (200 ml) (made fresh for each experiment)

1) Methanol (80 ml)
2) 37% soln Formaldehyde (73 ml)
3) ddH_2O (43 ml)

Sensitizer Solution

1) 0.02% sodium thiosulfate
2) 500 ml ddH_20

Silver Nitrate Solution (100 ml) (made fresh for each experiment)

1) 0.1% silver nitrate
2) 100 ml ddH_2O

Developing Solution (1000 ml) (made fresh for each experiment)

1) Sodium carbonate (30 g)
2) 37% soln Formaldehyde (1.35 ml)
3) Sodium thiosulfate (4 mg)

2.3 M Sodium Citrate

88.4 g/200 ml

Appendix E. Buffers and Modified RIPA Lysis Buffer for Polymerase Activity Assay

Polymerase Activity Assay

5x EDBG buffer
100 mM Tris-HCl, pH 7.5
400 ug/ml DNAse free BSA
40 mM DTT
20% Glycerol

1x Stop solution
40 mM EDTA
2% Na-PPi

Enzyme Dilution Buffer
100 mM K_2HP0_4, pH 6.5
10 mM β-mercaptoethanol
10% glycerol

REV1, REV7 Elution Buffer
50 mM KPO4, pH 8.0
300 mM KCl
5% glycerol
0.1% NP40

Activated Calf-Thymus DNA
10 mM Tris-HCl
1 mM EDTA

Modified RIPA lysis buffer
50 mM Tris-HCl, pH 7.4
150 mM NaCl
10% glycerol
0.25% NP40

Supplemented with:
- 10 µl of IC3 (Calbiochem)/10 ml of lysis buffer
- 10 µl of Pepstatin A, Chymostatin, and Leupeptin(all Sigma)

Appendix F. Chemicon Solutions for LacZ Tissue Staining

Fixative Solution

1) EGTA	1.9 g/L
2) $MgSO_4$-$7H_2O$	0.492 g/L
3) Paraformaldehyde	40ml/L
4) Rest in Phosphate Buffered Saline	

Tissue Rinse Solution A

1) EGTA	1.9 g/L
2) $MgCl_2$-$6H_2O$	0.406 g/L
3) Rest in Phosphate Buffered Saline	

Tissue Rinse Solution B

1) $MgCl_2$-$6H_2O$	0.406 g/L
2) Sodium Deoxycholate	0.1 g/L
3) Nonidet P-40	0.200ml/L
4) Rest in Phosphate Buffered Saline	

Tissue Base Stain Solution

1) $MgCl_2$-$6H_2O$	0.406 g/L
2) $K_3Fe(CN)_6$	1.645 g/L
3) $K_4Fe(CN)_6$	2.110 g/L
4) Deoxycholate	0.1 g/L
5) Nonidet P-40	0.2ml/L
6) Rest in Phosphate Buffered Saline	

X-gal Stock Solution

References

1. Friedberg, E.C., Walker, G.C., Siede, W., Wood, R.D., Schultz, R.A. and Ellenberger, T. (2006) *DNA Repair and Mutagenesis, 2nd Ed*. Second ed. American Society for Microbiology, Washington, D.C.

2. Hoeijmakers, J.H. (2001) Genome maintenance mechanisms for preventing cancer. *Nature*, **411**, 366-374.

3. Wang, T.S. (1991) Eukaryotic DNA polymerases. *Annual review of biochemistry*, **60**, 513-552.

4. Woodgate, R. (1999) A plethora of lesion-replicating DNA polymerases. *Genes & development*, **13**, 2191-2195.

5. Friedberg, E.C., Wagner, R. and Radman, M. (2002) Specialized DNA polymerases, cellular survival, and the genesis of mutations. *Science*, **296**, 1627-1630.

6. Hickson, I.D. (2003) RecQ helicases: caretakers of the genome. *Nature reviews*, **3**, 169-178.

7. Johnson, R.E., Kondratick, C.M., Prakash, S. and Prakash, L. (1999) hRAD30 mutations in the variant form of xeroderma pigmentosum. *Science*, **285**, 263-265.

8. Berneburg, M. and Lehmann, A.R. (2001) Xeroderma pigmentosum and related disorders: defects in DNA repair and transcription. *Advances in genetics*, **43**, 71-102.

9. Matsuda, T., Bebenek, K., Masutani, C., Hanaoka, F. and Kunkel, T.A. (2000) Low fidelity DNA synthesis by human DNA polymerase-eta. *Nature*, **404**, 1011-1013.

10. Watts, F.Z. (2006) Sumoylation of PCNA: Wrestling with recombination at stalled replication forks. *DNA Repair (Amst)*, **5**, 399-403.

11. Prakash, S., Johnson, R.E. and Prakash, L. (2005) Eukaryotic translesion synthesis DNA polymerases: specificity of structure and function. *Annual review of biochemistry*, **74**, 317-353.

12. Ulrich, H.D. (2005) The RAD6 pathway: control of DNA damage bypass and mutagenesis by ubiquitin and SUMO. *Chembiochem*, **6**, 1735-1743.

13. Lehmann, A.R., Niimi, A., Ogi, T., Brown, S., Sabbioneda, S., Wing, J.F., Kannouche, P.L. and Green, C.M. (2007) Translesion synthesis: Y-family polymerases and the polymerase switch. *DNA Repair (Amst)*, **6**, 891-899.

14. Kannouche, P.L. and Lehmann, A.R. (2004) Ubiquitination of PCNA and the polymerase switch in human cells. *Cell cycle (Georgetown, Tex*, **3**, 1011-1013.

15. Garg, P., Stith, C.M., Majka, J. and Burgers, P.M. (2005) Proliferating cell nuclear antigen promotes translesion synthesis by DNA polymerase zeta. *J Biol Chem*, **280**, 23446-23450.

16. Barbour, L. and Xiao, W. (2003) Regulation of alternative replication bypass pathways at stalled replication forks and its effects on genome stability: a yeast model. *Mutat Res*, **532**, 137-155.

17. Lemontt, J.F. (1971) Mutants of Yeast Defective in Mutation Induced by Ultraviolet Light. *Genetics*, **68**, 21-33.

18. Lawrence, C.W., Nisson, P.E. and Christensen, R.B. (1985) UV and chemical mutagenesis in rev7 mutants of yeast. *Mol Gen Genet*, **200**, 86-91.

19. Lawrence, C.W. and Christensen, R.B. (1979) Ultraviolet-induced reversion of cyc1 alleles in radiation-sensitive strains of yeast. III. rev3 mutant strains. *Genetics*, **92**, 397-408.

20. Lawrence, C.W., O'Brien, T. and Bond, J. (1984) UV-induced reversion of his4 frameshift mutations in rad6, rev1, and rev3 mutants of yeast. *Mol Gen Genet*, **195**, 487-490.

21. Nelson, J.R., Lawrence, C.W. and Hinkle, D.C. (1996) Thymine-thymine dimer bypass by yeast DNA polymerase zeta. *Science*, **272**, 1646-1649.

22. Johnson, R.E., Washington, M.T., Haracska, L., Prakash, S. and Prakash, L. (2000) Eukaryotic polymerases iota and zeta act sequentially to bypass DNA lesions. *Nature*, **406**, 1015-1019.

23. Haracska, L., Unk, I., Johnson, R.E., Johansson, E., Burgers, P.M., Prakash, S. and Prakash, L. (2001) Roles of yeast DNA polymerases delta and zeta and of Rev1 in the bypass of abasic sites. *Genes & development*, **15**, 945-954.

24. Nelson, J.R., Lawrence, C.W. and Hinkle, D.C. (1996) Deoxycytidyl transferase activity of yeast REV1 protein. *Nature*, **382**, 729-731.

25. Haracska, L., Prakash, S. and Prakash, L. (2003) Yeast DNA polymerase zeta is an efficient extender of primer ends opposite from 7,8-dihydro-8-Oxoguanine and O6-methylguanine. *Molecular and cellular biology*, **23**, 1453-1459.

26. Acharya, N., Johnson, R.E., Prakash, S. and Prakash, L. (2006) Complex formation with Rev1 enhances the proficiency of Saccharomyces cerevisiae DNA polymerase zeta for mismatch extension and for extension opposite from DNA lesions. *Mol Cell Biol*, **26**, 9555-9563.

27. Johnson, R.E., Haracska, L., Prakash, S. and Prakash, L. (2001) Role of DNA polymerase zeta in the bypass of a (6-4) TT photoproduct. *Mol Cell Biol*, **21**, 3558-3563.

28. Kelman, Z. (1997) PCNA: structure, functions and interactions. *Oncogene*, **14**, 629-640.

29. Friedberg, E.C., Lehmann, A.R. and Fuchs, R.P. (2005) Trading places: how do DNA polymerases switch during translesion DNA synthesis? *Mol Cell*, **18**, 499-505.

30. Broomfield, S., Hryciw, T. and Xiao, W. (2001) DNA postreplication repair and mutagenesis in Saccharomyces cerevisiae. *Mutat Res*, **486**, 167-184.

31. Lehmann, A.R. (2003) Replication of damaged DNA. *Cell cycle (Georgetown, Tex*, **2**, 300-302.

32. Hochegger, H., Sonoda, E. and Takeda, S. (2004) Post-replication repair in DT40 cells: translesion polymerases versus recombinases. *Bioessays*, **26**, 151-158.

33. Guo, C., Tang, T.S., Bienko, M., Parker, J.L., Bielen, A.B., Sonoda, E., Takeda, S., Ulrich, H.D., Dikic, I. and Friedberg, E.C. (2006) Ubiquitin-binding motifs in REV1 protein are required for its role in the tolerance of DNA damage. *Mol Cell Biol*, **26**, 8892-8900.

34. Bienko, M., Green, C.M., Crosetto, N., Rudolf, F., Zapart, G., Coull, B., Kannouche, P., Wider, G., Peter, M., Lehmann, A.R. *et al.* (2005) Ubiquitin-binding domains in Y-family polymerases regulate translesion synthesis. *Science*, **310**, 1821-1824.

35. Wood, A., Garg, P. and Burgers, P.M. (2007) A Ubiquitin-binding Motif in the Translesion DNA Polymerase Rev1 Mediates Its Essential Functional Interaction with Ubiquitinated Proliferating Cell Nuclear Antigen in Response to DNA Damage. *J Biol Chem*, **282**, 20256-20263.

36. Lawrence, C.W. and Christensen, R.B. (1978) Ultraviolet-induced reversion of cyc1 alleles in radiation-sensitive strains of yeast. I. rev1 Mutant strains. *Journal of molecular biology*, **122**, 1-21.

37. Nelson JR, G.P., Nowicka AM, Hinkle DC, Lawrence CW. . (2000) Evidence for a second function for Saccharomyces cerevisiae Rev1p. *Mol Microbiol*, **37**, 549-554.

38. Guo, C., Sonoda, E., Tang, T.S., Parker, J.L., Bielen, A.B., Takeda, S., Ulrich, H.D. and Friedberg, E.C. (2006) REV1 protein interacts with PCNA: significance of the REV1 BRCT domain in vitro and in vivo. *Mol Cell*, **23**, 265-271.

39. Jansen, J.G., Tsaalbi-Shtylik, A., Langerak, P., Calleja, F., Meijers, C.M., Jacobs, H. and de Wind, N. (2005) The BRCT domain of mammalian Rev1 is involved in regulating DNA translesion synthesis. *Nucleic Acids Res*, **33**, 356-365.

40. Hirano, Y. and Sugimoto, K. (2006) ATR homolog Mec1 controls association of DNA polymerase zeta-Rev1 complex with regions near a double-strand break. *Curr Biol*, **16**, 586-590.

41. Holbeck, S.L. and Strathern, J.N. (1997) A role for REV3 in mutagenesis during double-strand break repair in Saccharomyces cerevisiae. *Genetics*, **147**, 1017-1024.

42. Chen, C.C., Motegi, A., Hasegawa, Y., Myung, K., Kolodner, R. and D'Andrea, A. (2006) Genetic analysis of ionizing radiation-induced mutagenesis in Saccharomyces cerevisiae reveals TransLesion Synthesis (TLS) independent of PCNA K164 SUMOylation and ubiquitination. *DNA Repair (Amst)*, **5**, 1475-1488.

43. Lee, K. and Lee, S.E. (2007) Saccharomyces cerevisiae Sae2- and Tel1-Dependent Single-Strand DNA Formation at DNA Break Promotes Microhomology-Mediated End Joining. *Genetics*, **176**, 2003-2014.

44. Wu, F., Lin, X., Okuda, T. and Howell, S.B. (2004) DNA polymerase zeta regulates cisplatin cytotoxicity, mutagenicity, and the rate of development of cisplatin resistance. *Cancer Res*, **64**, 8029-8035.

45. Sonoda, E., Okada, T., Zhao, G.Y., Tateishi, S., Araki, K., Yamaizumi, M., Yagi, T., Verkaik, N.S., van Gent, D.C., Takata, M. ***et al.*** (2003) Multiple roles of Rev3, the catalytic subunit of polzeta in maintaining genome stability in vertebrates. *Embo J*, **22**, 3188-3197.

46. Okuda, T., Lin, X., Trang, J. and Howell, S.B. (2005) Suppression of hREV1 expression reduces the rate at which human ovarian carcinoma cells acquire resistance to cisplatin. *Molecular pharmacology*, **67**, 1852-1860.

47. Lin, X., Trang, J., Okuda, T. and Howell, S.B. (2006) DNA polymerase zeta accounts for the reduced cytotoxicity and enhanced mutagenicity of cisplatin in human colon carcinoma cells that have lost DNA mismatch repair. *Clin Cancer Res*, **12**, 563-568.

48. Zhang, N., Liu, X., Li, L. and Legerski, R. (2007) Double-strand breaks induce homologous recombinational repair of interstrand cross-links via cooperation of MSH2, ERCC1-XPF, REV3, and the Fanconi anemia pathway. *DNA Repair (Amst)*.

49. Shen, X., Jun, S., O'Neal, L.E., Sonoda, E., Bemark, M., Sale, J.E. and Li, L. (2006) REV3 and REV1 play major roles in recombination-independent repair of DNA interstrand cross-links mediated by monoubiquitinated proliferating cell nuclear antigen (PCNA). *J Biol Chem*, **281**, 13869-13872.

50. Acharya N, H.L., Johnson RE, Unk I, Prakash S, Prakash L. . (2005) Complex formation of yeast Rev1 and Rev7 proteins: a novel role for the polymerase-associated domain. *Mol Cell Biol*, **25**, 9734-9740.

51. D'Souza, S. and Walker, G.C. (2006) Novel role for the C terminus of Saccharomyces cerevisiae Rev1 in mediating protein-protein interactions. *Mol Cell Biol*, **26**, 8173-8182.

52. Tissier, A., Kannouche, P., Reck, M.P., Lehmann, A.R., Fuchs, R.P. and Cordonnier, A. (2004) Co-localization in replication foci and interaction of human Y-family members, DNA polymerase pol eta and REVl protein. *DNA Repair (Amst)*, **3**, 1503-1514.

53. Lopes, M., Foiani, M. and Sogo, J.M. (2006) Multiple mechanisms control chromosome integrity after replication fork uncoupling and restart at irreparable UV lesions. *Mol Cell*, **21**, 15-27.

54. Waters LS, W.G. (2006) The critical mutagenic translesion DNA polymerase Rev1 is highly expressed during G(2)/M phase rather than S phase. *Proc Natl Acad Sci U S A*, **103**, 8971-8976.

55. Sabbioneda, S., Bortolomai, I., Giannattasio, M., Plevani, P. and Muzi-Falconi, M. (2007) Yeast Rev1 is cell cycle regulated, phosphorylated in response to DNA damage and its binding to chromosomes is dependent upon MEC1. *DNA Repair (Amst)*, **6**, 121-127.

56. Eeken, J.C., Romeijn, R.J., de Jong, A.W., Pastink, A. and Lohman, P.H. (2001) Isolation and genetic characterisation of the Drosophila homologue of (SCE)REV3, encoding the catalytic subunit of DNA polymerase zeta. *Mutat Res*, **485**, 237-253.

57. Takeuchi, R., Oshige, M., Uchida, M., Ishikawa, G., Takata, K., Shimanouchi, K., Kanai, Y., Ruike, T., Morioka, H. and Sakaguchi, K. (2004) Purification of Drosophila DNA polymerase zeta by REV1 protein-affinity chromatography. *The Biochemical journal*, **382**, 535-543.

58. Takeuchi, R., Ruike, T., Nakamura, R., Shimanouchi, K., Kanai, Y., Abe, Y., Ihara, A. and Sakaguchi, K. (2006) Drosophila DNA polymerase zeta interacts with recombination repair protein 1, the Drosophila homologue of human abasic endonuclease 1. *J Biol Chem*, **281**, 11577-11585.

59. Wittschieben, J., Shivji, M.K., Lalani, E., Jacobs, M.A., Marini, F., Gearhart, P.J., Rosewell, I., Stamp, G. and Wood, R.D. (2000) Disruption of the developmentally regulated Rev3l gene causes embryonic lethality. *Curr Biol*, **10**, 1217-1220.

60. Esposito, G., Godindagger, I., Klein, U., Yaspo, M.L., Cumano, A. and Rajewsky, K. (2000) Disruption of the Rev3l-encoded catalytic subunit of polymerase zeta in mice results in early embryonic lethality. *Curr Biol*, **10**, 1221-1224.

61. Bemark, M., Khamlichi, A.A., Davies, S.L. and Neuberger, M.S. (2000) Disruption of mouse polymerase zeta (Rev3) leads to embryonic lethality and impairs blastocyst development in vitro. *Curr Biol*, **10**, 1213-1216.

62. Van Sloun, P.P., Romeijn, R.J. and Eeken, J.C. (1999) Molecular cloning, expression and chromosomal localisation of the mouse Rev3l gene, encoding the catalytic subunit of polymerase zeta. *Mutat Res*, **433**, 109-116.

63. Wu, X., Takenaka, K., Sonoda, E., Hochegger, H., Kawanishi, S., Kawamoto, T., Takeda, S. and Yamazoe, M. (2006) Critical roles for polymerase zeta in cellular tolerance to nitric oxide-induced DNA damage. *Cancer Res*, **66**, 748-754.

64. Mizutani, A., Okada, T., Shibutani, S., Sonoda, E., Hochegger, H., Nishigori, C., Miyachi, Y., Takeda, S. and Yamazoe, M. (2004) Extensive chromosomal breaks are induced by tamoxifen and estrogen in DNA repair-deficient cells. *Cancer Res*, **64**, 3144-3147.

65. Okada, T., Sonoda, E., Yoshimura, M., Kawano, Y., Saya, H., Kohzaki, M. and Takeda, S. (2005) Multiple roles of vertebrate REV genes in DNA repair and recombination. *Mol Cell Biol*, **25**, 6103-6111.

66. Zheng, H., Wang, X., Warren, A.J., Legerski, R.J., Nairn, R.S., Hamilton, J.W. and Li, L. (2003) Nucleotide excision repair- and polymerase eta-mediated error-prone removal of mitomycin C interstrand cross-links. *Mol Cell Biol*, **23**, 754-761.

67. Wang, X., Peterson, C.A., Zheng, H., Nairn, R.S., Legerski, R.J. and Li, L. (2001) Involvement of nucleotide excision repair in a recombination-independent and error-prone pathway of DNA interstrand cross-link repair. *Mol Cell Biol*, **21**, 713-720.

68. Li, Z., Zhang, H., McManus, T.P., McCormick, J.J., Lawrence, C.W. and Maher, V.M. (2002) hREV3 is essential for error-prone translesion synthesis past UV or benzo[a]pyrene diol epoxide-induced DNA lesions in human fibroblasts. *Mutat Res*, **510**, 71-80.

69. Gibbs PE, W.X., Li Z, McManus TP, McGregor WG, Lawrence CW, Maher VM. . (2000) The function of the human homolog of Saccharomyces cerevisiae REV1 is required for mutagenesis induced by UV light. *Proc Natl Acad Sci U S A*, **97**, 4186-4191.

70. Lin, X., Okuda, T., Trang, J. and Howell, S.B. (2006) Human REV1 modulates the cytotoxicity and mutagenicity of cisplatin in human ovarian carcinoma cells. *Molecular pharmacology*, **69**, 1748-1754.

71. Cheung, H.W., Chun, A.C., Wang, Q., Deng, W., Hu, L., Guan, X.Y., Nicholls, J.M., Ling, M.T., Chuan Wong, Y., Tsao, S.W. *et al.* (2006) Inactivation of human MAD2B in nasopharyngeal carcinoma cells leads to chemosensitization to DNA-damaging agents. *Cancer Res*, **66**, 4357-4367.

72. Kajiwara, K., J, O.W., Sakurai, T., Yamashita, S., Tanaka, M., Sato, M., Tagawa, M., Sugaya, E., Nakamura, K., Nakao, K. *et al.* (2001) Sez4 gene encoding an elongation subunit of DNA polymerase zeta is required for normal embryogenesis. *Genes Cells*, **6**, 99-106.

73. Van Sloun, P.P., Varlet, I., Sonneveld, E., Boei, J.J., Romeijn, R.J., Eeken, J.C. and De Wind, N. (2002) Involvement of mouse Rev3 in tolerance of endogenous and exogenous DNA damage. *Mol Cell Biol*, **22**, 2159-2169.

74. J, O.W., Kajiwara, K., Kawamura, K., Kimura, M., Miyagishima, H., Koseki, H. and Tagawa, M. (2002) An essential role for REV3 in mammalian cell survival: absence of REV3 induces p53-independent embryonic death. *Biochemical and biophysical research communications*, **293**, 1132-1137.

75. Lin, W., Wu, X. and Wang, Z. (1999) A full-length cDNA of hREV3 is predicted to encode DNA polymerase zeta for damage-induced mutagenesis in humans. *Mutat Res*, **433**, 89-98.

76. Kawamura, K., J, O.W., Bahar, R., Koshikawa, N., Shishikura, T., Nakagawara, A., Sakiyama, S., Kajiwara, K., Kimura, M. and Tagawa, M. (2001) The error-prone DNA polymerase zeta catalytic subunit (Rev3) gene is ubiquitously expressed in normal and malignant human tissues. *International journal of oncology*, **18**, 97-103.

77. Zander, L. and Bemark, M. (2004) Immortalized mouse cell lines that lack a functional Rev3 gene are hypersensitive to UV irradiation and cisplatin treatment. *DNA Repair (Amst)*, **3**, 743-752.

78. Wittschieben, J.P., Reshmi, S.C., Gollin, S.M. and Wood, R.D. (2006) Loss of DNA polymerase zeta causes chromosomal instability in mammalian cells. *Cancer Res*, **66**, 134-142.

79. Diaz, M., Verkoczy, L.K., Flajnik, M.F. and Klinman, N.R. (2001) Decreased frequency of somatic hypermutation and impaired affinity maturation but intact germinal center formation in mice expressing antisense RNA to DNA polymerase zeta. *J Immunol*, **167**, 327-335.

80. Ross, A.L. and Sale, J.E. (2006) The catalytic activity of REV1 is employed during immunoglobulin gene diversification in DT40. *Molecular immunology*, **43**, 1587-1594.

81. Diaz, M., Watson, N.B., Turkington, G., Verkoczy, L.K., Klinman, N.R. and McGregor, W.G. (2003) Decreased frequency and highly aberrant spectrum of ultraviolet-induced mutations in the hprt gene of mouse fibroblasts expressing antisense RNA to DNA polymerase zeta. *Mol Cancer Res*, **1**, 836-847.

82. Morelli, C., Mungall, A.J., Negrini, M., Barbanti-Brodano, G. and Croce, C.M. (1998) Alternative splicing, genomic structure, and fine chromosome localization of REV3L. *Cytogenetics and cell genetics*, **83**, 18-20.

83. Gibbs, P.E., McGregor, W.G., Maher, V.M., Nisson, P. and Lawrence, C.W. (1998) A human homolog of the Saccharomyces cerevisiae REV3 gene, which encodes the catalytic subunit of DNA polymerase zeta. *Proc Natl Acad Sci U S A*, **95**, 6876-6880.

84. Wong, S.W., Wahl, A.F., Yuan, P.M., Arai, N., Pearson, B.E., Arai, K., Korn, D., Hunkapiller, M.W. and Wang, T.S. (1988) Human DNA polymerase alpha gene expression is cell proliferation dependent and its primary structure is similar to both prokaryotic and eukaryotic replicative DNA polymerases. *Embo J*, **7**, 37-47.

85. Murakumo, Y. (2002) The property of DNA polymerase zeta: REV7 is a putative protein involved in translesion DNA synthesis and cell cycle control. *Mutat Res*, **510**, 37-44.

86. Murakumo, Y., Ogura, Y., Ishii, H., Numata, S., Ichihara, M., Croce, C.M., Fishel, R. and Takahashi, M. (2001) Interactions in the error-prone postreplication repair proteins hREV1, hREV3, and hREV7. *J Biol Chem*, **276**, 35644-35651.

87. Masuda Y, O.M., Masuda K, Kamiya K. (2003) Structure and enzymatic properties of a stable complex of the human REV1 and REV7 proteins. *J Biol Chem*, **278**, 12356-12360.

88. Murakumo, Y., Roth, T., Ishii, H., Rasio, D., Numata, S., Croce, C.M. and Fishel, R. (2000) A human REV7 homolog that interacts with the polymerase zeta catalytic subunit hREV3 and the spindle assembly checkpoint protein hMAD2. *J Biol Chem*, **275**, 4391-4397.

89. Guo, C., Fischhaber, P.L., Luk-Paszyc, M.J., Masuda, Y., Zhou, J., Kamiya, K., Kisker, C. and Friedberg, E.C. (2003) Mouse Rev1 protein interacts with multiple DNA polymerases involved in translesion DNA synthesis. *Embo J*, **22**, 6621-6630.

90. Lin, W., Xin, H., Zhang, Y., Wu, X., Yuan, F. and Wang, Z. (1999) The human REV1 gene codes for a DNA template-dependent dCMP transferase. *Nucleic acids research*, **27**, 4468-4475.

91. Masuda, Y. and Kamiya, K. (2002) Biochemical properties of the human REV1 protein. *FEBS letters*, **520**, 88-92.

92. Masuda, Y., Takahashi, M., Tsunekuni, N., Minami, T., Sumii, M., Miyagawa, K. and Kamiya, K. (2001) Deoxycytidyl transferase activity of the human REV1 protein is closely associated with the conserved polymerase domain. *J Biol Chem*, **276**, 15051-15058.

93. Murakumo Y, M.S., Yamaguchi M, Ichihara M, Takahashi M. (2006) Analyses of ultraviolet-induced focus formation of hREV1 protein. *Genes Cells*, **11**, 193-205.

94. Cahill, D.P., da Costa, L.T., Carson-Walter, E.B., Kinzler, K.W., Vogelstein, B. and Lengauer, C. (1999) Characterization of MAD2B and other mitotic spindle checkpoint genes. *Genomics*, **58**, 181-187.

95. Zhang, L., Yang, S.H. and Sharrocks, A.D. (2007) Rev7/MAD2B links c-Jun N-terminal protein kinase pathway signaling to activation of the transcription factor Elk-1. *Mol Cell Biol*, **27**, 2861-2869.

96. Chen, J. and Fang, G. (2001) MAD2B is an inhibitor of the anaphase-promoting complex. *Genes & development*, **15**, 1765-1770.

97. Rechkoblit, O., Zhang, Y., Guo, D., Wang, Z., Amin, S., Krzeminsky, J., Louneva, N. and Geacintov, N.E. (2002) trans-Lesion synthesis past bulky benzo[a]pyrene diol

epoxide N2-dG and N6-dA lesions catalyzed by DNA bypass polymerases. *J Biol Chem*, **277**, 30488-30494.

98. Guo, D., Wu, X., Rajpal, D.K., Taylor, J.S. and Wang, Z. (2001) Translesion synthesis by yeast DNA polymerase zeta from templates containing lesions of ultraviolet radiation and acetylaminofluorene. *Nucleic Acids Res*, **29**, 2875-2883.

99. Acharya N, J.R., Prakash S, Prakash L. (2006) Complex Formation with Rev1 Enhances the Proficiency of Saccharomyces cerevisiae DNA Polymerase Zeta for Mismatch Extension and for Extension Opposite from DNA Lesions. *Molecular and Cellular Biology*, **26**, 9555 - 9563.

100. Biologicals, N. (2006), *Catalog Number: H00005980-A01*, Novus Biologicals, Inc.

101. Zhu, F., Jin, C.X., Song, T., Yang, J., Guo, L. and Yu, Y.N. (2003) Response of human REV3 gene to gastric cancer inducing carcinogen N-methyl-N'-nitro-N-nitrosoguanidine and its role in mutagenesis. *World J Gastroenterol*, **9**, 888-893.

102. Lawrence, C.W. and Christensen, R. (1976) UV mutagenesis in radiation-sensitive strains of yeast. *Genetics*, **82**, 207-232.

103. Nelson JR, L.C., Hinkle DC. (1996) Thymine-thymine dimer bypass by yeast DNA polymerase zeta. *Science*, **272**, 1646-1649.

104. Kozak, M. (1991) An analysis of vertebrate mRNA sequences: intimations of translational control. *The Journal of cell biology*, **115**, 887-903.

105. Kozak, M. (1990) Evaluation of the fidelity of initiation of translation in reticulocyte lysates from commercial sources. *Nucleic Acids Res*, **18**, 2828.

106. Kozak, M. (1987) At least six nucleotides preceding the AUG initiator codon enhance translation in mammalian cells. *Journal of molecular biology*, **196**, 947-950.

107. Ho, S.N., Hunt, H.D., Horton, R.M., Pullen, J.K. and Pease, L.R. (1989) Site-directed mutagenesis by overlap extension using the polymerase chain reaction. *Gene*, **77**, 51-59.

108. Copeland, W.C. and Tan, X. (1995) Active site mapping of the catalytic mouse primase subunit by alanine scanning mutagenesis. *J Biol Chem*, **270**, 3905-3913.

109. Lin W, X.H., Zhang Y, Wu X, Yuan F, Wang Z. (1999) The human REV1 gene codes for a DNA template-dependent dCMP transferase. *Nucleic Acids Res*, **27**, 4468-4475.

110. Murakumo Y, R.T., Ishii H, Rasio D, Numata S, Croce CM, Fishel R. (2000) A human REV7 homolog that interacts with the polymerase zeta catalytic subunit hREV3 and the spindle assembly checkpoint protein hMAD2. *J Biol Chem*, **275**, 4391-4397.

111. Pavlov YI, S.P., Kunkel TA. (2001) In vivo consequences of putative active site mutations in yeast DNA polymerases alpha, epsilon, delta, and zeta. *Genetics*, **159**, 47-64.

112. Kozak, M. (1986) Influences of mRNA secondary structure on initiation by eukaryotic ribosomes. *Proc Natl Acad Sci U S A*, **83**, 2850 - 2854.

113. Pelletier J, S.N. (1985) Insertion mutagenesis to increase secondary structure within the 5' noncoding region of a eukaryotic mRNA reduces translational efficiency. *Cell*, **40**, 515 - 526.

114. Kawamura K, O.-w.J., Bahar R, Koshikawa N, et al. (2001) The error-prone polymerase zeta cataytic subunit (Rev3) gene is ubiquithously expressed in normal and malignant human tissues. *Internation Journal of Oncology*, **18**, 97 - 103.

115. Takeuchi R, O.M., Uchida M, Ishikawa G, Takata K, Shimanouchi K, Kanai Y, Ruike T, Morioka H, Sakaguchi K. (2004) Purification of Drosophila polymerase zeta by REV1 protein-affinity chromatography. *Biochem J*, **382**, 535 - 543.

116. Wittschieben JP, R.S., Gollin SM, Wood RD. . (2006) Loss of DNA polymerase zeta causes chromosomal instability in mammalian cells. *Cancer Res*, **66**, 134-142.

117. Johnson RE, W.M., Haracska L, Prakash S, and Prakash L. (2000) Eukaryotic polymerases i and z act sequentially to bypass DNA lesions. *Nature*, **406**, 1015 - 1019.

118. Gibbs PE, M.J., Woodgate R, and Lawrence CW. (2005) The Relative Roles in Vivo of Saccharomyces cerevisiae Pol h, Pol z, Rev1 Protein
and Pol32 in the Bypass and Mutation Induction of an Abasic Site, T-T (6-4) Photoadduct and T-T cis-syn Cyclobutane Dimer. *Genetics*, **169**, 575 - 582.

119. Yuasa, M.S., Masutani, C., Hirano, A., Cohn, M.A., Yamaizumi, M., Nakatani, Y. and Hanaoka, F. (2006) A human DNA polymerase eta complex containing Rad18, Rad6 and Rev1; proteomic analysis and targeting of the complex to the chromatin-bound fraction of cells undergoing replication fork arrest. *Genes Cells*, **11**, 731-744.

120. Nelson, J.R., Gibbs, P.E., Nowicka, A.M., Hinkle, D.C. and Lawrence, C.W. (2000) Evidence for a second function for Saccharomyces cerevisiae Rev1p. *Mol Microbiol*, **37**, 549-554.

121. Guo C, S.E., Tang TS, Parker JL, Bielen AB, Takeda S, Ulrich HD, Friedberg EC. . (2006) REV1 protein interacts with PCNA: significance of the REV1 BRCT domain in vitro and in vivo. *Mol Cell*, **23**, 265-271.

122. Guo C, F.P., Luk-Paszyc MJ, Masuda Y, Zhou J, Kamiya K, Kisker C, Friedberg EC. (2003) Mouse Rev1 protein interacts with multiple DNA polymerases involved in translesion DNA synthesis. *EMBO J*, **22**, 6621-6630.

123. Cheung HW, C.A., Wang Q, Deng W, Hu L, Guan XY, Nicholls JM, Ling MT, Chuan Wong Y, Tsao SW, Jin DY, Wang X. (2006) Inactivation of human MAD2B in nasopharyngeal carcinoma cells leads to chemosensitization to DNA-damaging agents. *Cancer Res*, **66**, 4357-4367.

124. Velasco-Miguel, S., Richardson, J.A., Gerlach, V.L., Lai, W.C., Gao, T., Russell, L.D., Hladik, C.L., White, C.L. and Friedberg, E.C. (2003) Constitutive and regulated expression of the mouse Dinb (Polkappa) gene encoding DNA polymerase kappa. *DNA Repair (Amst)*, **2**, 91-106.

125. Marini, F., Kim, N., Schuffert, A. and Wood, R.D. (2003) POLN, a nuclear PolA family DNA polymerase homologous to the DNA cross-link sensitivity protein Mus308. *J Biol Chem*, **278**, 32014-32019.

126. Garcia-Diaz, M., Dominguez, O., Lopez-Fernandez, L.A., de Lera, L.T., Saniger, M.L., Ruiz, J.F., Parraga, M., Garcia-Ortiz, M.J., Kirchhoff, T., del Mazo, J. *et al.* (2000) DNA polymerase lambda (Pol lambda), a novel eukaryotic DNA polymerase with a potential role in meiosis. *Journal of molecular biology*, **301**, 851-867.

127. Allen-Institute. (2007) In Institute, A. (ed.).

128. Zan, H., Komori, A., Li, Z., Cerutti, A., Schaffer, A., Flajnik, M.F., Diaz, M. and Casali, P. (2001) The translesion DNA polymerase zeta plays a major role in Ig and bcl-6 somatic hypermutation. *Immunity*, **14**, 643-653.

129. Fujii, J., Iuchi, Y., Matsuki, S. and Ishii, T. (2003) Cooperative function of antioxidant and redox systems against oxidative stress in male reproductive tissues. *Asian journal of andrology*, **5**, 231-242.

130. Kow, Y.W., Bao, G., Minesinger, B., Jinks-Robertson, S., Siede, W., Jiang, Y.L. and Greenberg, M.M. (2005) Mutagenic effects of abasic and oxidized abasic lesions in Saccharomyces cerevisiae. *Nucleic Acids Res*, **33**, 6196-6202.

131. Laan, R., Baarends, W.M., Wassenaar, E., Roest, H.P., Hoeijmakers, J.H. and Grootegoed, J.A. (2005) Expression and possible functions of DNA lesion bypass proteins in spermatogenesis. *International journal of andrology*, **28**, 1-15.

132. Lindahl, T. and Wood, R.D. (1999) Quality control by DNA repair. *Science*, **286**, 1897-1905.

133. Krieg AJ, H.E., Giaccia AJ. (2006) Functional analysis of p53 binding under differential stresses. *Mol Cell Biol*, **26**, 7030-7045.

134. Kajiwara, K., Nagawawa, H., Shimizu-Nishikawa, S., Ookuri, T., Kimura, M. and Sugaya, E. (1996) Molecular characterization of seizure-related genes isolated by differential screening. *Biochemical and biophysical research communications*, **219**, 795-799.

135. Masuda, Y., Ohmae, M., Masuda, K. and Kamiya, K. (2003) Structure and enzymatic properties of a stable complex of the human REV1 and REV7 proteins. *J Biol Chem*, **278**, 12356-12360.

136. Hurley, P.J. and Bunz, F. (2007) ATM and ATR: components of an integrated circuit. *Cell cycle (Georgetown, Tex*, **6**, 414-417.